Universiteit Antwerpen

Faculty of Medicine and Health Sciences
Center for Oncological Research

Unraveling the biology of inflammatory breast cancer through multi-omics approaches.

Thesis submitted for the degree of Doctor of Medical Sciences at the University of Antwerp to be defended by

CHARLOTTE RYPENS

Prof. Steven Van Laere, PhD
Dr. Luc Dirix, MD, PhD

Antwerpen, 2023

EXAMINATION COMMITTEE

Promotors
Prof. Dr. Steven Van Laere, University of Antwerp
Dr. Luc Dirix, GZA Hospitals – Sint Augustinus

Internal jury members
Prof. Dr. Loeys Bart, University of Antwerp, Antwerp University Hospital
Prof. Dr. Vanden Berghe Wim, University of Antwerp

External jury members
Prof. Dr. Berditchevski Fedor, University of Birmingham
Prof. Dr. Schröder Carolien, The Netherlands Cancer Institute, University Medical Center Groningen

Table of contents

ABBREVIATIONS

aCGH	array comparative genomic hybridization
AGA	actionable genetic alterations
AJCC	American Joint Committee on Cancer
BL	basal-like
CNA	copy number aberration
CNV	copy number variation
CPM	count per million
CS	Connectivity Score
CTC	circulating tumor cell
DEG	differentially expressed gene
DPM	differentiation predictor model
ECM	extracellular matrix
EMT	epithelial-to-mesenchymal transition
ER	estrogen receptor
FBS	fetal bovine serum
FDR	false discovery rate
FFPE	formalin-fixed, paraffin-embedded
GEP	gene expression pattern
GMM	gene module memberships
GSEA	gene set enrichment analysis
HER2	human epidermal growth factor receptor 2
HR	hormone receptor
HRD	homologous recombination deficiency
IBC	inflammatory breast cancer
IBC-IC	Inflammatory Breast Cancer International Consortium
IHC	immunohistochemistry
IM	immunomodulatory
IPPON	Integrated Personalized and Precision Oncology Network
LABC	locally advanced breast cancer
LAP	latency-associated peptide
LAR	luminal androgen receptor
LBM	luminal/basal/mesenchymal
MET	mesenchymal to epithelial transition
MSL	mesenchymal stem–like
NGS	next generation sequencing
nIBC	non-IBC
NOTCH	neurogenic locus notch homolog protein
ORA	Overrepresentation analysis
PCA	principal component analysis
PCR	polymerase chain reaction
PMN	Proximal MYC Network

PPES	Protein chemistry, Proteomics and Epigenetic Signaling
PPI	protein-protein interaction
PR	progesterone receptor
PTK	thyrosine kinase
SMAD	mothers against decapentaplegic
SNP	single nucleotide polymorphism
SNV	single nucleotide variant
STK	serine/threonine Kinase
TAM	tumor-associated macrophages
TCRU	Translational Cancer Research Unit
TGFβ	transforming growth factor beta
TIME	tumor immune microenvironment
TMB	tumor mutational burden
TME	tumor microenvironment
TNBC	triple negative breast cancer
UHCA	unsupervised hierarchical clustering analysis
WES	whole exome sequencing
WGCNA	weighted gene co-expression network analysis
WGS	whole genome sequencing
WIBC	World IBC consortium

GENERAL INTRODUCTION

Breast cancer

Breast cancer is the most frequently diagnosed cancer in women worldwide, accounting for almost a third of all cancer diagnoses in Belgium in 2018. Breast cancer has a relatively good prognosis, with 5-year relative survival rates of 91.1% in females. However, prognosis depends strongly on the stage of disease and histopathological features at time of diagnosis, with survival rates ranging from 28% in patients with stage IV disease up to 99% in patients with stage I disease (https://kankerregister.org/).

Breast cancer is a heterogenous disease for which classification systems are used to identify high and low risk patients. The most used system is the TNM classification system in which a breast tumor is classified according to the size of the primary tumor and whether cancer cells invaded nearby tissue (T-stage), the status of lymph node involvement (N-stage) and the presence of metastases in distant organs (M-stage). An important feature of normal breast tissue is that the growth of breast cells is controlled by hormones, mostly estrogen and progesterone, by interaction with their receptors. Based on the expression of these receptors, determined by immunohistochemistry (IHC), breast tumors are categorized in three major clinical subtypes i.e. estrogen receptor (ER)/progesterone receptor (PR)-positive/Human Epidermal growth factor Receptor 2 (HER2)-negative tumors, HER2-positive tumors (either ER-positive or ER-negative) and triple negative breast cancer (TNBC). These markers determine which patients are likely to respond to targeted therapies, such as hormone therapy (e.g. Tamoxifen) and anti-HER2 therapy (e.g. Trastuzumab).

This model thus works well for prognostic determinations, and even though it lacks any molecular value, gene expression studies confirm the prominent role of these three proteins in the classification and treatment of breast cancer. Systematic reviews of the gene expression pattern in breast cancer have revealed five intrinsic molecular subtypes that roughly reflect the histological subtypes described above. Luminal A and luminal B breast cancers are both hormone-receptor positive (ER and/or PR positive), however differ in HER2 tumors impedes on the use of hormone and HER2-directed and Ki67 expression. Luminal A breast cancers are HER2 negative and have low levels of the protein Ki67, which reflects their overall good prognosis. Luminal B tumors can be HER2 positive in combination with high levels of Ki67, resulting in a slightly worse prognosis. HER2-enriched tumors are characterized by HER2 expression in combination with the absence of hormone receptor (HR) expression (i.e. ER, PR). These tumors tend to grow faster than luminal A and luminal B tumors and can have a worse prognosis, but they are often treated successfully with targeted therapies against the HER2 protein. Normal-like breast cancers have a gene expression profile resembling normal breast tissue and have a prognosis that is slightly worse as compared to patients diagnosed

with Luminal A-type breast cancer. The final category of breast cancers are the TNBCs that have a gene expression profile resembling basal myoepithelial cells and are therefore often termed Basal-like breast cancer. This type of cancer is often diagnosed in women with BRCA1 gene mutations and is associated with poor disease prognosis, amongst others by the fact that the lack of both HR and HER2 expression in these therapies [1-3]. In 2011, the group of Lehmann et al. identified six TNBC subtypes displaying unique gene expression profiles thereby recognizing that also the TNBC is heterogeneous in nature. The subtypes classify TNBC based on 2 basal-like (BL1 and BL2), an immunomodulatory (IM), a mesenchymal (M), a mesenchymal stem–like (MSL), and a luminal androgen receptor (LAR) gene expression patterns [4].

Table 1: Overview of the ten integrative clusters described by Curtis et al. [5] as a novel molecular stratification of breast cancer, taking into account the impact of somatic CNAs on the transcriptome.

Integrative cluster	Features
IntClust 1	Enriched for luminal B cancers 17q23/20q cis-acting aberrations
IntClust 2	ER-positive subgroup High mortality rate Cis-acting aberrations in the 11q13/14 region (several driver genes)
IntClust 3	Predominantly luminal A tumors Low genomic instability Marked by a paucity of copy number and cis-acting alterations
IntClust 4	ER+ and ER- tumors and varied intrinsic subtypes Marked by a paucity of copy number and cis-acting alterations
IntClust 5	HER2-amplified cancers regardless of ER status
IntClust 6	Enriched for luminal B cancers 8p12 cis-acting aberrations
IntClust 7	Primarily composed of luminal A tumors 16p gain/16q loss High frequency of 8q amplification
IntClust 8	Primarily composed of luminal A tumors 1q gain/16q loss
IntClust 9	Enriched for luminal B cancers 8q cis-acting aberrations/20q amplifications
IntClust 10	Majority of basal tumors Most instable at the genomic level Characteristic cis-acting alterations (5 loss/8q gain/10p gain/12p gain)

Although these classifications are well accepted and commonly adopted in breast cancer research, it should be noted that alternative subtyping schemes exist, amongst others the ten integrative clusters named IntClust 1 to 10, based on combined copy number variation (CNV) and gene expression profiles [5]. Table 1 gives an overview of the features for each integrative cluster, particularly in relation to the above-described intrinsic subtypes and HR and HER2 expression levels.

These InClust subtypes were shown to be associated with distinct patterns of survival and response to neoadjuvant chemotherapy, where IntClusts 3, 4, 7 and 8 have the best prognosis, IntClusts 1, 6 and 9 have an intermediate prognosis, and IntClusts 2, 5 and 10 a poor prognosis. Although these ten IntClust subtypes of breast cancer show characteristic patterns of association with traditional clinicopathological variables such as histological type, tumor grade, receptor status, and lymphocytic infiltration, no IntClust can be adequately identified by these variables alone. Hence, the addition of genomic stratification using the IntClust classification system has the potential to enhance the biological relevance of the current clinical evaluation and facilitate genome-guided therapeutic strategies [6].

In addition, it has been shown that by classifying breast tumors into the IntClust subtypes, important differences in recurrence rates have become apparent that could again, not be inferred optimally from standard clinical information and were obscured in the IHC and PAM50 subtypes alone. Especially the identification of the subset of ER-positive patients who have a high risk of recurrence up to 20 years after diagnosis may help to determine whether women who are relapse free five years after diagnosis might benefit from extended endocrine therapy or other interventions to improve late outcomes. These ER-positive subgroups could also benefit from new treatment strategies since an enrichment targetable CNAs was observed [7].

Inflammatory breast cancer

One of the most aggressive types of locally advanced breast cancer (LABC), inflammatory breast cancer (IBC), is rare (less then 5% of new diagnoses) but nonetheless responsible for a disproportionally high amount of breast-cancer related deaths. At time of diagnosis, virtually all patients have lymph node metastases and approximately 30% of patients have metastases in distant organs (vs. 6-10% in non-IBC). Five metastatic organs, bone, brain, liver, lung and distant lymph nodes account for more than 90% of all metastatic IBC patients. Bone is the most common metastatic organ accounting for 57-60%, which is comparable with nIBC (65-70%). IBC has lung/pleural effusion metastasis around 21–29% and approximately 6-15% of IBC develop brain metastasis [8, 9]. Compared to nIBC, brain metastases occur in around 10–30% [10-13]. Dependencies on molecular subtypes have been reported, with the

highest percentage of bone metastasis found in the HR+/HER2− subtype. Lung metastases occur significantly more often in HR−/HER2− IBC, and liver and brain metastases are significantly more often found in HER2-enriched (HR−/HER2+) tumors [8, 9, 14].

By consequence of the high incidence of distant metastasis, survival rates are poor. Studies have shown that among patients with stage III breast cancer, IBC is associated with a worse prognosis compared to nIBC [15, 16], with an overall survival of 4.75 years versus 13.40 years respectively. This holds true for stage IV disease and is underscored by a shorter overall survival time of 2.27 years vs. 3.40 years [17]. This may be accounted for by the fact that IBC is enriched for more aggressive breast cancer subtypes such as TNBC, HER2+ and Luminal B (Table 2).

Table 2: Frequency of molecular subtypes in IBC and nIBC [10, 14, 18-20].

Phenotype	HR	HER2	TNBC
IBC	30%	40%	30%
nIBC	60%-80%	25%	10%-15%

The reasons to study IBC are manifold. First, the high fraction of breast cancer-related mortality in combination with the fact that IBC is more prevalent amongst younger women, results in a significant loss in life-years [21]. Second, due to limited numbers of preclinical models and pretreatment patient samples, biological knowledge is lagging, and no IBC-specific treatment options exist. Together, these reasons imply that IBC has the potential to become a major global health problem within the next few years, particularly since it is observed that incidence is rising. Unfortunately, few risk factors have been associated with IBC such as African American race, and high body mass index [22]. Also, smoking, breast feeding and age at first pregnancy (≥26) may be associated with specific IBC subtypes [23]. Finally, IBC is the quintessential model for poor prognosis breast cancer, implying that insights in IBC are deemed to also have implications for non-IBC (nIBC) biology. Therefore, a more profound understanding of IBC biology is warranted.

 At present, no histological criteria exist to distinguish IBC from nIBC. The current definition of IBC stated by the American Joint Committee on Cancer (AJCC) describes IBC as "a clinical-pathologic entity characterized by diffuse erythema and edema (peau d'orange) involving a third or more of the breast." (https://cancerstaging.org/). In 2011, an international expert panel on inflammatory breast cancer has developed guidelines on the management of IBC and reported the following consensus diagnostic criteria: (i) rapid onset of breast erythema, edema and/or peau d'orange, and/or warm

breast, with or without an underlying palpable mass, (ii) duration of history of no more than 6 months, (iii) erythema occupying at least one-third of the breast, and (iv) pathological confirmation of invasive carcinoma [24]. Hence, diagnosis is primarily based on clinical criteria of rapidly developing symptoms of 'inflammation', combined with pathological confirmation via tissue biopsy of invasive disease. The specific symptomatology translates in IBC being assigned to a separate category in the TNM classification system (i.e. T4d). The explosive clinical course with an abrupt onset of symptoms is relevant as it distinguishes IBC from LABC, which can have the same clinical appearance but represents a longstanding and often neglected disease state. In addition, instead of a lump, IBC frequently presents with a diffuse growth pattern throughout the breast. This in combination with its typical 'inflamed' presentation often results in IBC being misdiagnosed as a benign mastitis leading to a delay in the recognition of IBC and in the onset of appropriate therapy [22].

A frequent histopathological feature associated with IBC is the presence of numerous cancer cell clusters, hereafter termed tumor emboli, in the dermal and parenchymal lymph vessels. These tumor emboli clog the drainage of the breast and are presumably responsible for part of the clinical presentation of IBC. Although the presence of tumor emboli is not accepted as a true diagnostic criterium for IBC, approximately 75% of patients with IBC present with tumor emboli and their presence confirms the diagnosis [22]. Tumor emboli thus appear to be integral to IBC biology and are hypothesized to contribute to metastatic dissemination and to local disease spreading by intravascular growth and self-metastasis. The latter may provide a mechanistic basis for the diffuse histological growth pattern associated with IBC. With respect to the genesis of tumor emboli, two hypotheses have been put forward: A. Encircling lymphovasculogenesis (passive dissemination); or B. lymphovascular infiltration (active dissemination) by cancer cells [25, 26]. Van der Auwera and colleagues reported elevated lymphatic endothelial cell proliferation in IBC compared to nIBC, consistent with the conclusion that lymphangiogenesis is highly active in IBC [27]. This observation lends credit to the hypothesis of encircling lymphovasculogenesis, which is corroborated by Mahooti and colleagues describing encircling lymphovasculogenesis in IBC to short-circuit some of the steps of the metastatic process leading to early dissemination [26] and offering an explanation to the high frequency of lymph node metastases present in patients with IBC at diagnosis.

Molecular profiling of IBC

Since the late eighties of previous century, researchers have been trying to unravel the biology of IBC using immunohistochemistry (IHC) and mRNA expression-based studies. One of the primary observations made by Kleer and colleagues was the unexpected

overexpression of E-Cadherin in IBC in the primary tumor, in the tumor emboli and in the metastases [28]. In the context of the aggressive nature of IBC, this molecular feature seems paradoxical given the established role of E-cadherin as a metastasis suppressor in a variety of cancers. For example, E-Cadherin expression is lost in nIBC during metastatic dissemination secondary to epithelial-to-mesenchymal transition (EMT). However, an unexpected role for E-cadherin in breast cancer progression is now becoming evident. Tomlinson and colleagues revealed that E-cadherin expression is responsible for the compactness of the tumor emboli in IBC and enables cancer cells invading collectively as clusters into the lymphatics [29]. It has been demonstrated that cancer cell clusters are more efficient in forming metastases than single cancer cells, possibly due to the survival benefit experienced by cancer cells in clusters over single cells when entering the circulation and encountering non-adherent conditions. Experiments with dominant negative forms E-cadherin revealed that the invasive potential of IBC cells was attenuated [30], corroborating the role for E-cadherin in IBC progression [31].

In addition to E-Cadherin, several additional molecular changes have been associated with IBC, including overexpression of EGFR and ErbB2 [32-34], loss of LIBC (WISP3) and overexpression of RhoC GTPase [35], strong MUC1 expression [36], increased angiogenesis [27, 37], overexpression of eIF4GI [38], and TIG1/Axl expression [39]. However, validation in independent data series for many of these molecules often failed [40]. In contrast, the frequent upregulation of NF-κB-related genes in IBC [41], and the presence of a stem cell phenotype [42-44], have been observed by several independent research groups and was linked to XIAP overexpression, stress response mechanisms, and MAPK activation downstream of EGFR and HER2 overexpression [45-48].

In order to obtain a more unbiased picture of the biology of IBC, several genome-wide gene expression studies have been performed since 2004 (Table 3). Overall, it was demonstrated that an IBC specific expression profile can be defined but results differed substantially in terms of the individual genes that are differentially expressed, which may be caused by confounding variables that differ between the various studies such as the predominance of the Basal-like and HER2 enriched subtypes in IBC. Additional limitations such as small sample numbers due to limited tissue availability and leading to limited statistical power, differences in the treatment status of the investigated samples and different study designs have hampered the success rate of these studies.

Therefore, in 2013, the Inflammatory Breast Cancer International Consortium (IBC-IC) launched a project to perform an integrated analysis of various data sets, vouching for a total of 137 IBC samples all adhering to a uniform case definition, to redefine the

molecular profile of IBC. Importantly, using this data set, it was possible the distinguish IBC-specific from molecular subtype confounded differences, which proofed to have a major impact on the outcome of the analysis [19]. The existence of a molecular basis for IBC was confirmed, however, with the side note that only 3% of the global gene expression differences between IBC and nIBC are intrinsic to IBC tumor cells. Referring to these genes, a molecular-independent IBC specific 79-gene signature was identified that discriminates between IBC and nIBC patient samples. Translation of this gene signature into biological concepts showed that the IBC biology is shaped by specific immune and TGFβ response programs. It was suggested that TGFβ signaling is attenuated in IBC, which is surprising given the importance of TGFβ signaling in metastatic progression in several cancer types [49-51]. **A better understanding of how TGFβ signaling contributes to the biology of IBC is therefore crucial.**

Table 3: Overview of all gene expression studies in IBC.

Group	IBC	nIBC	Platform	Genes	Major conclusions	REF
Bertucci et al.	37	44	cDNA microarray	8000	A signature containing 109 genes was identified	[52]
Bieche et al.	36	22	PCR	538	27 genes were differentially expressed	[53]
Bertucci et al.	37	44	cDNA microarray	8000	IBC comprises all molecular subtypes	[54]
*Van Laere et al.**	16	18	cDNA microarray	9600	756 differentially expressed genes enriched for NFkB targets	[41]
*Van Laere et al.**	16	18	cDNA microarray	9600	IBC is predominantly Basal-like/HER2-enriched	[55]
Nguyen et al.	13	12	Affymetrix	>20K	Hyperproliferative phenotype of IBC	[56]
Dressmann et al.	14	23	Affymetrix	>20K	Stromal gene signature of 22 genes	[57]
Van Laere et al.	19	40	Affymetrix	>20K	Platform independent validation of earlier results	[48]
Boersma et al.	15	35	Affymetrix	>20K	Strong expression differences in stroma	[58]
Iwamoto et al.	25	57	Affymetrix	>20K	Weak expression differences across subtypes	[59]
Woodward et al.	20	20	Affymetrix	>20K	131 differentially expressed genes	[60]
Van Laere et al.	137	252	Affimetrix	>20K	Subtype-independent IBC signature of 79 genes related to inflammation and TGFβ signaling	[19]
Zare et al.	66	83	Mixed/public data	>20K	Signature of 59 genes on micro-dissected samples	[61]
Rypens et al.	10	22	Affimetrix	>20K	Validation of IBC signature on preclinical models and identification of MYC activation	[62]
Richard et al.	110	169	Affimetrix	>20K	Increased AURKA mRNA expression	[63]

* Studies were performed on the same patient series
** Studies were performed on the same patient series

Genomic analysis of IBC

The clinical utility of previous observations in IBC has been limited. Since the adoption of precision oncology strategies based on profiles of genomic aberrations, a more recent approach is to explore the hypothesis that the molecular profile of IBC is a reflection of underlying genomic alterations. An overview of all studies performed today, and their major findings is listed in Table 4.

Overall, many actionable genetic alterations have been reported, however with a low frequency and without identification of IBC-specific driver genes. Regardless, mutations in TP53, PIK3CA and ERBB2 genes have been repeatedly observed in IBC, but these are most likely reflective of the different molecular breast cancer subtypes that are represented in IBC (i.e., Basal-like, Luminal-type and HER2-enriched respectively). Notably, an increased tumor mutational burden (TMB) has been repeatedly observed in IBC relative to nIBC. More recently, a study investigating germline mutations in a series containing more than 500 patient samples showed frequent mutations in DNA repair genes [64]. Regardless, the success rate in defining a genomic profile of IBC based on these studies is limited, which can be explained by the small patient series, the inclusion of both untreated primary tumors and post-treated relapses, and the limited number of genes that was tested in all studies. Furthermore, only a few studies made a direct comparison of the genomic portraits between IBC and nIBC, without stratification upon molecular subtypes. Given these limitations, **a more comprehensive analysis of the genomic landscape of IBC is warranted and detection of IBC-specific actionable genetic alterations could be crucial to improve systemic treatment.**

IBC and the tumor immune microenvironment

Evidence is emerging that the tumor immune microenvironment (TIME) has a significant contribution to the unique biological features associated with IBC. Not only the importance of the tumor stroma has been reported in IBC [18, 58, 65], but many publications also underline a prominent role of different immune cells in the TME of IBC [66-69]. Together, components of the TME dynamically interact to create a unique microenvironment that promotes the aggressive intrinsic features of IBC, such as stemness and the high metastatic potential [18]. For example, tumor-associated macrophages (TAMs) are a well-studied cell type in the TME of IBC. IBC is characterized by high infiltration of macrophages that under the influence of IBC tumor cells are polarized into tumor-promoting, immune-suppressing M2 macrophages [70].

Table 4: Overview of all genomic studies performed in IBC. TMB – mutational burden, NGS – next generation sequencing, SNV – single nucleotide variant, SNP – single nucleotide polymorphism, CNV – copy number variation, CNA - copy number aberration

Group	IBC	nIBC	Variants	Platform	#Genes	Major conclusions	REF
Ross et al.	53	0	SNV	Illumina	195/225	TP53, MYC, PIK3CA, ERBB2, FGFR1, BRCA2, and PTEN mutations	[71]
Hamm et al.	17	0	SNV	Illumina	225	TP53, PIK3CA and ERBB2 mutations and increased TMB	[68]
Goh et al.	26 13	0	SNV CNA	Illumina	WES	HER2-positive IBC: frequent TP53 mutations and a high TMB	[72]
Matsuda et al.	24	376	SNV	Illumina	46/50	TP53, PIK3CA and ERBB2 mutations and increased TMB	[73]
Liang et al.	156	197	SNV	Illumina	91	Increased MB and mutations in NOTCH and DNA repair genes	[74]
Rana et al.	501	0	SNP	Illumina	242	Frequent germline mutations in DNA repair genes	[64]
Faldoni et al.	24	0	SNV CNA	Illumina	105	Frequent gains of MYC and MDM4 genes, and loss of TP53 and RB1 genes, high homologous recombination deficiency scores	[75]
Bertucci et al.	101	2351	SNV, CNV	Mixed	756	Increased MB and mutations in NOTCH and DNA repair chromatin remodeling genes	[76]
Winn et al.	19	0	SNV	Illumina	93	Frequent mutations in TP53, PMS2, MRE11, RB1, BRCA1, PTEN, AR	[77]
Li et al.	22	23	SNV, CNV, CV	Illumina	WG	Frequent complex structural germline variants, lower clonality, TGFβ alterations	[78]
Gong et al.	32	0	SNV	Illumina	93	Frequent germline and somatic alterations in DNA repair genes	[79]
Luo et al.	6	0	SNV	Illumina	WES	Frequent mutations in KMT2C, PTEN and FBXW7 potential IBC driver genes	[80]
Richard et al.	34	602	SNV, CNA	Illumina	505	Frequent ERBB2, AURKA, PPM1D, FGFR1 amplifications, TP53 and PIK3CA mutations and increased TMB	[63]

These macrophages secrete chemotactic cytokines (TNFα, IL8 and IL10) that can enhance dissemination and metastasis of IBC tumor cells [81] and further contribute to the cancer stem-like, mesenchymal, and aggressive nature of IBC by secretion of high levels of IL-8 and GRO chemokines [82]. The specific modulation of tumor microenvironment in IBC is also exemplified by the fact that higher levels of PD-L1 expression, both at mRNA [57] and protein [54] level, were noted as compared nIBC despite the fact that the number of tumor infiltrating lymphocytes in both types of breast cancer are similar. Expression analysis of IBC samples with high PD-L1 mRNA levels suggest PD-L1 overexpression is reflective of immune exhaustion following a potent anti-tumor immune response. At present, the mechanisms and the chain of events that orchestrate the interactions between cancer cells and immune cells in IBC remain elusive, but the importance hereof to understand IBC biology and the implication for immunotherapy is increasingly being recognized.

Preclinical models

Despite the significant role of the tumor microenvironment in IBC biology, a lot of research is performed to investigate tumor intrinsic features of IBC. Breast cancer cell lines, organoids and xenografts are widely used to dissect breast cancer biology and develop new therapeutic approaches. These preclinical models have the advantage of the relative ease of pharmacologic and genetic manipulation. In contrast, it remains a question how accurate these models recapitulate key features of human tumors, particularly due to the lack of the stromal component. This also has consequences in translating observations from preclinical models (e.g. the response of cell lines to certain therapeutic drugs) into clinical practice.

Several preclinical models of IBC have been reported in the past: SUM149, SUM190, KPL4, MDA-IBC1, MDA-IBC3, FC-IBC-01, FC-IBC-02A, TJ-IBC-04, TJ-IBC-09, UA-IBC-01, Mary-X, and WIBC-9. However, not all these models are widely used or have been extensively characterized. Table 5 provides an overview of all preclinical models, their ER/HER2 expression and extra information if available. The SUM149, FC-IBC-01, FC-IBC-02, TJ-IBC-04, WIBC-9 and MARY-X are classified as triple negative, based on the absent expression of ER, PR and HER2. The remaining models SUM190, KPL4, MDA-IBC3, TJ-IBC-09, and UA-IBC-01 express the HER2 oncogene, and the MDA-IBC1 cell line expresses ER. The lack of luminal IBC models reflects the overrepresentation of the more aggressive, ER negative, subtypes in IBC compared to nIBC. Many of the IBC preclinical models are commonly used by the IBC research community without considering their representativity. Therefore, **a comprehensive evaluation of the molecular characteristics of all inflammatory breast cancer (IBC) preclinical models and**

to what extend these models recapitulate the molecular characteristics of IBC observed clinically is essential.

Table 5: Overview all IBC preclinical models available.

Model	HR	HER2	Other characteristics	REF
SUM149	Negative	Negative	Expression of CK8, CK18 and CK19 Strong EGFR expression Metastasis to multiple sites	[83-85]
SUM190	Negative	Positive	Expression of CK8, CK18 and CK20 CCND1 amplification Metastasis primarily to lung	[83-85]
KPL4	Negative	Positive	Absence of EGFR expression Lack of E-cadherin expression	[85, 86]
MDA-IBC3	Negative	Positive	Metastasis to the lung	[85, 87]
Mary-X	Negative	Negative	E-cadherin-positive lymphovascular emboli Metastasis primarily to the lung Increased Notch3 signaling ALDH1 positivity EGFR expression	[88]
FC-IBC-01	Negative	Negative	E-cadherin-positive lymphovascular emboli EGFR expression	[85]
FC-IBC-02	Negative	Negative	E-cadherin-positive lymphovascular emboli EGFR expression Metastasis to multiple sites Expression of stem cell markers	[89, 90]
WIBC09	Negative	Negative	Vascular mimicry and vasculogenesis	[18, 37, 91]
UA-IBC-01	Negative	Positive	NA	[62]
TJ-IBC-04	Negative	Negative	NA	[62]
TJ-IBC-09	Negative	Positive	NA	[62]
MDAIBC1	Positive	Negative	Lack of E-cadherin expression WISP3 protein expression	[18, 92]

Transforming growth factor beta signaling

Transforming growth factor beta (TGF-β) is a pleiotropic cytokine, consisting of three isoforms, TGF-β1, TGF-β2 and TGF-β3, that binds to members of the TGF-β receptor family. TGF-β is involved in tissue homeostasis by regulation of many cellular processes, such as proliferation, differentiation, migration, survival, and immunity.

Although TGF-β synthesis and expression of its receptors are widespread, activation is localized to sites where TGF-β is released from latency. Inactive TGF-β is stored in the extracellular matrix (ECM) as a latent complex with its furin-cleaved prodomain, called

the latency-associated peptide (LAP), hindering binding of TGF-β with its receptor. The LAP-TGF-β complex binds to latent TGF-β-binding proteins (LTBP1–LTBP4), which can then be processed further to release active TGF-β [93, 94]. In its active form, TGF-β binds to a TGF-βR receptor complex, consisting of type I (TGFβRI) and type II (TGFβRII) serine-threonine kinase receptors, which allows TGF-βRII to phosphorylate TGFβRI, and subsequently induce a signaling cascade to the nucleus [95].

In the canonical pathway, the receptor regulated Smad proteins (R-Smads; Smad2 and Smad3) are recruited and phosphorylated. These R-Smads shuttle between the cytoplasm and the nucleus in the basal state, but also during TGF-β signaling as a mechanism to monitor receptor activity [96]. Upon activation, they form heteromeric complexes with Smad4 and translocate to the nucleus. Continuous TGF-β receptor activity is a prerequisite for the R-Smads to remain phosphorylated, and for R-Smad/Smad4 complexes to persist in the nucleus [97]. In the nucleus the complex will bind several DNA-binding transcription factors, co-repressors, and co-activators to regulate transcription of target genes (Figure 1; [98]). Thus, R-Smads in the nucleus are being continuously dephosphorylated and dissociate from complexes with Smad4. The inactivated Smads are then exported back to the cytoplasm, whereafter rapid rephosphorylation takes place, as long as the receptors remain active. The reactivated R-Smads form again a complex with Smad4 and relocalise to the nucleus [97]. Important to note is that SMAD4 is not required for the movement of activated R-Smads into the nucleus itselves, but it is an essential member to trigger most TGF-β family gene responses [93].

Smad6 and mainly Smad7 act as inhibitory Smads that mediate a negative feedback loop in the TGF-β pathway. Smad7 recruits Smad ubiquitin regulatory factor (Smurf) proteins to mediate ubiquitination-mediated proteasomal degradation of TGFβRI [99], while Smad6 can interfere with the phosphorylation of Smad2 and the subsequent heteromerization with Smad4, but does not inhibit the activity of Smad3 [100].

Besides the canonical pathway, non-canonical signaling cascades induced by TGF-β exist that can activate several signaling molecules, such as various mitogen-activated protein kinases (MAPKs; ERK, JNK and p38 MAPK), PI3K/AKT, Rho-like GTPases and TRAF 4/6 (Figure 1; [98]). Both TGF-β canonical and non-canonical signaling cascades can occur simultaneously through the crosstalk of core pathway components and combined utilization of SMAD/non-SMAD transcription factors [98].
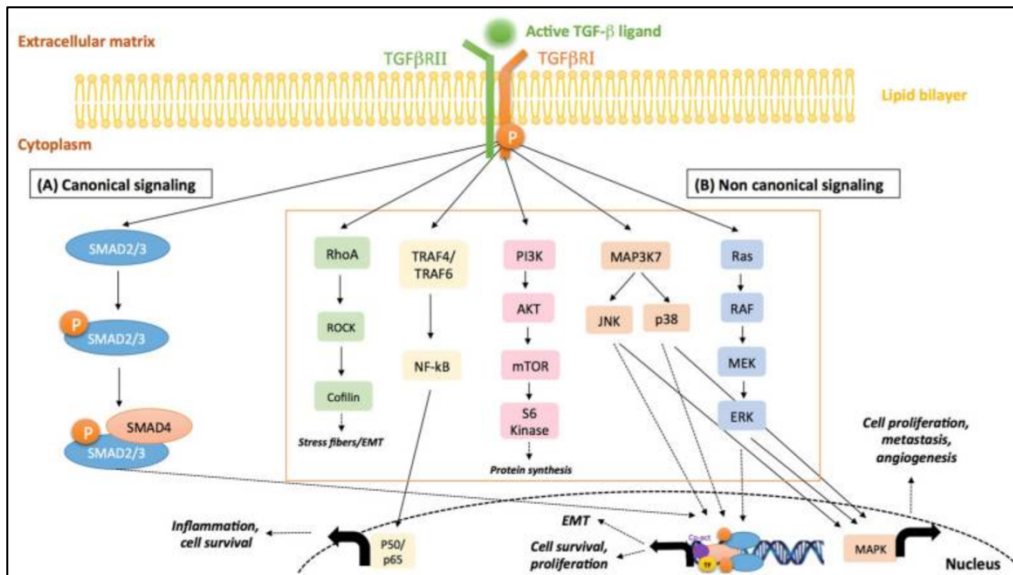
Figure 1: Schematic overview of canonical and non-canonical TGF-β signaling pathways. (A) In the canonical signaling pathway, TGF-β ligands bind to TGFβRII, which in turn activates TGFβRI. TGFβRI-regulated SMAD2/3 proteins are phosphorylated and form complexes with SMAD4, initiating a number of biological processes through transcriptional regulation of target genes. (B) In the non-canonical signaling pathways, the TGF-β receptor complex transmits its signal through other factors, such as the mitogen-activated protein kinases (MAPKs), phosphatidylinositide 3-kinase (PI3K), TNF receptor-associated factor 4/6 (TRAF4/6) and Rho family of small GTPases. Figure reprinted from [98].

The TGF-β paradox

TGF-β has long captured the interest of the biomedical field because of its pleiotropic roles in development an adult physiology, and its involvement in many malfunctions such as cancer when dysregulated. TGF-β has a dual nature in the context of cancer, functioning both as a tumor suppressor in pre-malignant cells and as a tumor promoter in malignant cells by supporting cell proliferation, differentiation, angiogenesis, epithelial-to-mesenchymal transition (EMT), metastasis, immune infiltration, evasion of immune surveillance, regulation of apoptosis, and drug resistance [93].

The mechanism underlying this dual role involves TGF-β effects in both the tumor cells and the supporting TME. First, suppression of genomic instability [101] and induction of cytostasis [95] are protective responses induced by TGF-β in tumor cells. In addition, a tumor-suppressive cytokine and chemokine profile in the tumor microenvironment is also maintained by TGF-β [102, 103]. However, during disease progression, activation

of oncogenic pathways in the tumor can dominate the tumor-suppressive responses to TGF-β and can also initiate pro tumorigenic responses such as induction of the EMT [104]. In addition, excessive tumor-derived TGF-β in the TME of advanced tumors can affect several cell types, such as stromal fibroblasts, endothelial cells and immune cells, to produce a favorable environment for tumor growth, invasion and metastasis, can disrupt antitumor immune surveillance, and promote angiogenesis [95, 104].

TGF-β and breast cancer

Already in 1987, TGF-β was found to be implicated in mammary epithelial development. Silberstein et al. demonstrated rapid regression of advancing endbuds in the mammary gland after implanting TGF-β-containing pellets [105]. Later, it was shown that TGF-β1 acts as a tumor suppressor in breast cancer by inducing growth inhibition [106] and the first data demonstrating tumor-promoting functions were reported by Gorska et al. who showed that tumor cell-specific TGF-β signaling promotes tumor cell invasion [107]. Many other studies have provided considerable support for a dual role for TGF-β in breast cancer [108, 109]. Overall, in early-stage breast cancer, TGF-β inhibits tumor cell cycle progression, and consequently suppresses tumor progression. During the course of mammary tumorigenesis, breast cancer cells uncouple TGF-β signaling from regulation of cell cycle progression and actively use TGF-β for the acquisition and development of metastatic phenotypes, in part through its ability to stimulate EMT in tumor cells [110, 111]. TGF-β has also been shown to acts as an important mediator of metastasis in breast cancer to specific organ sites, amongst others by enhancing the extravasation of breast cancer cells into the lung parenchyma [95] and supporting the development of breast cancer metastasis to bone [112]. On the other hand, some studies demonstrate persistent tumor-suppressive effects of TGF-β even in late-stage metastatic breast disease [113, 114]. Together, these data demonstrate that TGF-β signaling in breast cancer development and progression is elusive with evidence pointing at tumor-promoting and suppressive effects both in early and late stages of the disease.

The role of TGF-β in cancer cell migration

Metastasis is the primary cause of cancer morbidity and mortality and is estimated to be responsible for about 90% of cancer deaths. It is a complex process that involves a series of sequential and interrelated steps [115], which is associated with cancer cells that alter their shape as well as their attachment to other cells and to the extracellular matrix (ECM) [116]. The interaction with the TME is crucial to allow cells to disseminate and eventually colonize other tissues. A myriad of signaling molecules contribute to metastatic behavior, including mediators of the TGF-β signaling pathway.

TGF-β signaling is a potent inducer of EMT by increasing the expression of mesenchymal markers, such as N-cadherin and vimentin, and in parallel, reducing expression of epithelial markers, such as E-cadherin. The acquired mesenchymal phenotype results in enhanced migratory activity, extracellular matrix (ECM) production, invasiveness, and elevated resistance to apoptosis [117]. During EMT, cells lose their specialized cell-cell contacts and polarity, after which a migratory behavior is acquired allowing invasion in the surrounding tissue. Metastatic colonization of secondary sites by cancer cells then involves a reverse process, called mesenchymal to epithelial transition (MET) [118].

Although several signaling pathways have been implicated in TGFβ-induced EMT (such as PI3K/AKT [119], RhoA [120, 121] and p38 MAPK [122, 123]), SMAD signaling seems to be indispensable [123, 124]. Various studies have explored the roles of different Smad proteins in EMT. Overexpression of ectopic SMAD2/4 or SMAD3/4 was shown to induce or enhance EMT in NMuMG cells [125, 126] and the prominent role for SMAD3 in EMT was further corroborated in renal tubular cells [127]. Also, it was shown that the small GTPase RAC1B inhibits TGF-β1-induced cell motility in human PANC1 and MDA-MB-231 cells by blocking the function of SMAD3 [128]. In contrast, several studies have demonstrated an EMT suppressive function for SMAD2. SMAD2 ablation in keratinocytes leads to increased EMT and accelerates skin tumor formation, as a result of increased SMAD3/4 binding to the Snail promotor [129]. In a study by the group of Ju et al., SMAD2 ablation in hepatocytes leads to the spontaneous induction of mesenchymal features characteristic of EMT, and an increased migration rate [130]. These results all point towards SMAD3 as a main factor for EMT, while SMAD2 is not. In 2010, the group of Kohn et al. indeed reports that murine Smad3, but not Smad2, is necessary for TGFβ-induced EMT responses, whereas both murine Smad2 and Smad3 can support TGFβ-induced invasion [131]. Interestingly, it was described earlier that expression of activated murine Smad2 alone stimulates spindle tumor cell invasion, but that for an overt change from epithelial to mesenchymal cell type, additional factors were required, i.e. elevated murine H-ras levels [132].

Similarly to Smad3, murine Smad4 was also shown to be necessary for EMT. Knockdown of SMAD4 potently inhibits TGFβ-induced EMT and subsequent bone metastasis of NMuMG cells [133] and resulted in inhibition of EMT in hepatocytes [134]. In line with this, a study in a pancreatic cell line has shown that Smad4 is essential for TGFβ-induced down-regulation of E-cadherin, an essential step in EMT [135] and intact SMAD4 facilitates EMT and TGFβ-dependent growth in pancreatic ductal adenocarcinomas [136].

Collective migration

The migration of single cells is the best-studied mechanism of cell motility and is known to contribute to migration of tumor cells facilitating metastasis, amongst other through EMT. A second migratory strategy is collective migration during which intercellular cohesion is preserved. Collective migration is characterized by the capacity of cancer cells to remain interconnected by stable cell-cell junctions, and to move collectively, as sheets, through the extracellular matrix (ECM). This process requires a high level of intercellular coordination, whereby the migrating cells display polarity and the leading cells form an invasive front [117].

Recently, it was shown that partial EMT enables collective migration of cells as clusters of circulating tumor cells (CTCs) or tumor emboli and these clusters exhibit increased metastatic potential as compared to single CTCs [137, 138]. During partial EMT, cells that are transitioning between epithelial and mesenchymal phenotypes can retain some features of both phenotypes and hence, reach a hybrid epithelial/mesenchymal (E/M) phenotype. Thanks to the unique combination of these properties, cancer cells gain the capacity to move collectively as clusters or sheets [139]. One of the adhesion molecules that is lost during EMT, but preserved in a hybrid phenotype, is E-cadherin. As indicated before, E-cadherin is long assumed to be a metastasis suppressor because loss of the protein's expression enables cancer cells to migrate individually leading to subsequent dissemination [140]. However, several studies now report that E-cadherin plays a more complex role in certain types of cancers and actually promotes cell migration. For example, in ovarian cancer cells, E cadherin was shown to be indispensable for Rho GTPase-regulated cell migration [141]. In addition, E-Cadherin positive mammary 4T1 cancer cells that are highly invasive, move while remaining loosely inter-connected by E-cadherin-mediated membrane tethers [117]. More recently, Padmanaban and colleagues reported on a positive role for E-cadherin in metastasis resulting from the enhancement of cell survival. The same authors demonstrated that genes involved in TGF-β signaling, including SMAD2/3, are upregulated after E-cadherin loss [142]. These results are interesting in context of two papers, in which it was shown that carcinoma cells use TGF-β signaling to drive single cell migration but migrate collectively in the absence of TGF-β signaling [143, 144], therefore linking TGF-β and collective migration through E-cadherin expression. In addition, as collectively invading cancer cells also appear to favor lymphatic over hematogenous dissemination [144], this mechanism provides a functional explanation for the formation of E-cadherin positive tumor emboli, which are characteristic of IBC.

References

1. Perou CM, Sorlie T, Eisen MB, van de Rijn M, Jeffrey SS, Rees CA, Pollack JR, Ross DT, Johnsen H, Akslen LA et al: Molecular portraits of human breast tumours. Nature 2000, 406(6797):747-752.

2. Sorlie T, Perou CM, Tibshirani R, Aas T, Geisler S, Johnsen H, Hastie T, Eisen MB, van de Rijn M, Jeffrey SS et al: Gene expression patterns of breast carcinomas distinguish tumor subclasses with clinical implications. Proc Natl Acad Sci U S A 2001, 98(19):10869-10874.

3. Dai X, Li T, Bai Z, Yang Y, Liu X, Zhan J, Shi B: Breast cancer intrinsic subtype classification, clinical use and future trends. Am J Cancer Res 2015, 5(10):2929-2943.

4. Lehmann BD, Bauer JA, Chen X, Sanders ME, Chakravarthy AB, Shyr Y, Pietenpol JA: Identification of human triple-negative breast cancer subtypes and preclinical models for selection of targeted therapies. J Clin Invest 2011, 121(7):2750-2767.

5. Curtis C, Shah SP, Chin SF, Turashvili G, Rueda OM, Dunning MJ, Speed D, Lynch AG, Samarajiwa S, Yuan Y et al: The genomic and transcriptomic architecture of 2,000 breast tumours reveals novel subgroups. Nature 2012, 486(7403):346-352.

6. Mukherjee A, Russell R, Chin SF, Liu B, Rueda OM, Ali HR, Turashvili G, Mahler-Araujo B, Ellis IO, Aparicio S et al: Associations between genomic stratification of breast cancer and centrally reviewed tumour pathology in the METABRIC cohort. NPJ Breast Cancer 2018, 4:5.

7. Rueda OM, Sammut SJ, Seoane JA, Chin SF, Caswell-Jin JL, Callari M, Batra R, Pereira B, Bruna A, Ali HR et al: Dynamics of breast-cancer relapse reveal late-recurring ER-positive genomic subgroups. Nature 2019, 567(7748):399-404.

8. Wang Z, Chen M, Pan J, Wang X, Chen XS, Shen KW: Pattern of distant metastases in inflammatory breast cancer - A large-cohort retrospective study. J Cancer 2020, 11(2):292-300.

9. Chainitikun S, Saleem S, Lim B, Valero V, Ueno NT: Update on systemic treatment for newly diagnosed inflammatory breast cancer. J Adv Res 2021, 29:1-12.

10. Kai M, Kogawa T, Liu DD, Fouad TM, Kai K, Niikura N, Hsu L, Willey JS, Theriault RL, Valero V et al: Clinical characteristics and outcome of bone-only metastasis in inflammatory and noninflammatory breast cancers. Clin Breast Cancer 2015, 15(1):37-42.

11. Wang Y, Ye F, Liang Y, Yang Q: Breast cancer brain metastasis: insight into molecular mechanisms and therapeutic strategies. Br J Cancer 2021, 125(8):1056-1067.

12. Chen W, Hoffmann AD, Liu H, Liu X: Organotropism: new insights into molecular mechanisms of breast cancer metastasis. NPJ Precis Oncol 2018, 2(1):4.

13. Uemura MI, French JT, Hess KR, Liu D, Raghav K, Hortobagyi GN, Arun BK, Valero V, Ueno NT, Alvarez RH et al: Development of CNS metastases and survival in patients with inflammatory breast cancer. Cancer 2018, 124(11):2299-2305.

14. van Uden DJP, van Maaren MC, Strobbe LJA, Bult P, van der Hoeven JJ, Siesling S, de Wilt JHW, Blanken-Peeters C: Metastatic behavior and overall survival according to breast cancer subtypes in stage IV inflammatory breast cancer. Breast Cancer Res 2019, 21(1):113.

15. Low JA, Berman AW, Steinberg SM, Danforth DN, Lippman ME, Swain SM: Long-term follow-up for locally advanced and inflammatory breast cancer patients treated with multimodality therapy. J Clin Oncol 2004, 22(20):4067-4074.

16. Dawood S, Ueno NT, Valero V, Woodward WA, Buchholz TA, Hortobagyi GN, Gonzalez-Angulo AM, Cristofanilli M: Differences in survival among women with stage III inflammatory and noninflammatory locally advanced breast cancer appear early: a large population-based study. Cancer 2011, 117(9):1819-1826.

17. Fouad TM, Kogawa T, Liu DD, Shen Y, Masuda H, El-Zein R, Woodward WA, Chavez-MacGregor M, Alvarez RH, Arun B et al: Overall survival differences between patients with inflammatory and noninflammatory breast cancer presenting with distant metastasis at diagnosis. Breast Cancer Res Treat 2015, 152(2):407-416.

18. Lim B, Woodward WA, Wang X, Reuben JM, Ueno NT: Inflammatory breast cancer biology: the tumour microenvironment is key. Nat Rev Cancer 2018, 18(8):485-499.

19. Van Laere SJ, Ueno NT, Finetti P, Vermeulen P, Lucci A, Robertson FM, Marsan M, Iwamoto T, Krishnamurthy S, Masuda H et al: Uncovering the molecular secrets of inflammatory breast cancer biology: an integrated analysis of three distinct affymetrix gene expression datasets. Clin Cancer Res 2013, 19(17):4685-4696.

20. Bertucci F, Rypens C, Finetti P, Guille A, Adelaide J, Monneur A, Carbuccia N, Garnier S, Dirix P, Goncalves A et al: NOTCH and DNA repair pathways are more frequently targeted by genomic alterations in inflammatory than in non-inflammatory breast cancers. Mol Oncol 2019.

21. Woodward WA: Inflammatory breast cancer: unique biological and therapeutic considerations. Lancet Oncol 2015, 16(15):e568-576.

22. Robertson FM, Bondy M, Yang W, Yamauchi H, Wiggins S, Kamrudin S, Krishnamurthy S, Le-Petross H, Bidaut L, Player AN et al: Inflammatory breast cancer: the disease, the biology, the treatment. CA Cancer J Clin 2010, 60(6):351-375.

23. Atkinson RL, El-Zein R, Valero V, Lucci A, Bevers TB, Fouad T, Liao W, Ueno NT, Woodward WA, Brewster AM: Epidemiological risk factors associated with inflammatory breast cancer subtypes. Cancer Causes Control 2016, 27(3):359-366.

24. Dawood S, Merajver SD, Viens P, Vermeulen PB, Swain SM, Buchholz TA, Dirix LY, Levine PH, Lucci A, Krishnamurthy S et al: International expert panel on inflammatory breast cancer: consensus statement for standardized diagnosis and treatment. Ann Oncol 2011, 22(3):515-523.

25. Van der Auwera I, Van den Eynden GG, Colpaert CG, Van Laere SJ, van Dam P, Van Marck EA, Dirix LY, Vermeulen PB: Tumor lymphangiogenesis in inflammatory breast carcinoma: a histomorphometric study. Clin Cancer Res 2005, 11(21):7637-7642.

26. Mahooti S, Porter K, Alpaugh ML, Ye Y, Xiao Y, Jones S, Tellez JD, Barsky SH: Breast carcinomatous tumoral emboli can result from encircling lymphovasculogenesis rather than lymphovascular invasion. Oncotarget 2010, 1(2):131-147.

27. Van der Auwera I, Van Laere SJ, Van den Eynden GG, Benoy I, van Dam P, Colpaert CG, Fox SB, Turley H, Harris AL, Van Marck EA et al: Increased angiogenesis and lymphangiogenesis in inflammatory versus noninflammatory breast cancer by real-time reverse transcriptase-PCR gene expression quantification. Clin Cancer Res 2004, 10(23):7965-7971.

28. Kleer CG, van Golen KL, Braun T, Merajver SD: Persistent E-cadherin expression in inflammatory breast cancer. Mod Pathol 2001, 14(5):458-464.

29. Tomlinson JS, Alpaugh ML, Barsky SH: An intact overexpressed E-cadherin/alpha,beta-catenin axis characterizes the lymphovascular emboli of inflammatory breast carcinoma. Cancer Res 2001, 61(13):5231-5241.

30. Dong HM, Liu G, Hou YF, Wu J, Lu JS, Luo JM, Shen ZZ, Shao ZM: Dominant-negative E-cadherin inhibits the invasiveness of inflammatory breast cancer cells in vitro. J Cancer Res Clin Oncol 2007, 133(2):83-92.

31. Rodriguez FJ, Lewis-Tuffin LJ, Anastasiadis PZ: E-cadherin's dark side: possible role in tumor progression. Biochim Biophys Acta 2012, 1826(1):23-31.

32. Guerin M, Gabillot M, Mathieu MC, Travagli JP, Spielmann M, Andrieu N, Riou G: Structure and expression of c-erbB-2 and EGF receptor genes in inflammatory and non-inflammatory breast cancer: prognostic significance. Int J Cancer 1989, 43(2):201-208.

33. Cabioglu N, Gong Y, Islam R, Broglio KR, Sneige N, Sahin A, Gonzalez-Angulo AM, Morandi P, Bucana C, Hortobagyi GN et al: Expression of growth factor and chemokine receptors: new insights in the biology of inflammatory breast cancer. Ann Oncol 2007, 18(6):1021-1029.

34. Masuda H, Zhang D, Bartholomeusz C, Doihara H, Hortobagyi GN, Ueno NT: Role of epidermal growth factor receptor in breast cancer. Breast Cancer Res Treat 2012, 136(2):331-345.

35.   van Golen KL, Davies S, Wu ZF, Wang Y, Bucana CD, Root H, Chandrasekharappa S, Strawderman M, Ethier SP, Merajver SD: A novel putative low-affinity insulin-like growth factor-binding protein, LIBC (lost in inflammatory breast cancer), and RhoC GTPase correlate with the inflammatory breast cancer phenotype. Clin Cancer Res 1999, 5(9):2511-2519.

36. Alpaugh ML, Tomlinson JS, Kasraeian S, Barsky SH: Cooperative role of E-cadherin and sialyl-Lewis X/A-deficient MUC1 in the passive dissemination of tumor emboli in inflammatory breast carcinoma. Oncogene 2002, 21(22):3631-3643.

37. Shirakawa K, Kobayashi H, Heike Y, Kawamoto S, Brechbiel MW, Kasumi F, Iwanaga T, Konishi F, Terada M, Wakasugi H: Hemodynamics in vasculogenic mimicry and angiogenesis of inflammatory breast cancer xenograft. Cancer Res 2002, 62(2):560-566.

38. Silvera D, Arju R, Darvishian F, Levine PH, Zolfaghari L, Goldberg J, Hochman T, Formenti SC, Schneider RJ: Essential role for eIF4GI overexpression in the pathogenesis of inflammatory breast cancer. Nat Cell Biol 2009, 11(7):903-908.

39. Wang X, Saso H, Iwamoto T, Xia W, Gong Y, Pusztai L, Woodward WA, Reuben JM, Warner SL, Bearss DJ et al: TIG1 promotes the development and progression of inflammatory breast cancer through activation of Axl kinase. Cancer Res 2013, 73(21):6516-6525.

40. Lerebours F, Bieche I, Lidereau R: Update on inflammatory breast cancer. Breast Cancer Res 2005, 7(2):52-58.

41. Van Laere S, Van der Auwera I, Van den Eynden GG, Fox SB, Bianchi F, Harris AL, van Dam P, Van Marck EA, Vermeulen PB, Dirix LY: Distinct molecular signature of

inflammatory breast cancer by cDNA microarray analysis. Breast Cancer Res Treat 2005, 93(3):237-246.

42. Xiao Y, Ye Y, Yearsley K, Jones S, Barsky SH: The lymphovascular embolus of inflammatory breast cancer expresses a stem cell-like phenotype. Am J Pathol 2008, 173(2):561-574.

43. Charafe-Jauffret E, Ginestier C, Iovino F, Tarpin C, Diebel M, Esterni B, Houvenaeghel G, Extra JM, Bertucci F, Jacquemier J et al: Aldehyde dehydrogenase 1-positive cancer stem cells mediate metastasis and poor clinical outcome in inflammatory breast cancer. Clin Cancer Res 2010, 16(1):45-55.

44. Van Laere S, Limame R, Van Marck EA, Vermeulen PB, Dirix LY: Is there a role for mammary stem cells in inflammatory breast carcinoma?: a review of evidence from cell line, animal model, and human tissue sample experiments. Cancer 2010, 116(11 Suppl):2794-2805.

45. Aird KM, Ghanayem RB, Peplinski S, Lyerly HK, Devi GR: X-linked inhibitor of apoptosis protein inhibits apoptosis in inflammatory breast cancer cells with acquired resistance to an ErbB1/2 tyrosine kinase inhibitor. Mol Cancer Ther 2010, 9(5):1432-1442.

46. Arora J, Sauer SJ, Tarpley M, Vermeulen P, Rypens C, Van Laere S, Williams KP, Devi GR, Dewhirst MW: Inflammatory breast cancer tumor emboli express high levels of anti-apoptotic proteins: use of a quantitative high content and high-throughput 3D IBC spheroid assay to identify targeting strategies. Oncotarget 2017, 8(16):25848-25863.

47. Evans MK, Brown MC, Geradts J, Bao X, Robinson TJ, Jolly MK, Vermeulen PB, Palmer GM, Gromeier M, Levine H et al: XIAP Regulation by MNK Links MAPK and NFkappaB Signaling to Determine an Aggressive Breast Cancer Phenotype. Cancer Res 2018, 78(7):1726-1738.

48. Van Laere SJ, Van der Auwera I, Van den Eynden GG, van Dam P, Van Marck EA, Vermeulen PB, Dirix LY: NF-kappaB activation in inflammatory breast cancer is associated with oestrogen receptor downregulation, secondary to EGFR and/or ErbB2 overexpression and MAPK hyperactivation. Br J Cancer 2007, 97(5):659-669.

49. Ikushima H, Miyazono K: TGFbeta signalling: a complex web in cancer progression. Nat Rev Cancer 2010, 10(6):415-424.

50. Massague J: TGFbeta signalling in context. Nat Rev Mol Cell Biol 2012, 13(10):616-630.

51. Wakefield LM, Hill CS: Beyond TGFbeta: roles of other TGFbeta superfamily members in cancer. Nat Rev Cancer 2013, 13(5):328-341.

52. Bertucci F, Finetti P, Rougemont J, Charafe-Jauffret E, Nasser V, Loriod B, Camerlo J, Tagett R, Tarpin C, Houvenaeghel G et al: Gene expression profiling for molecular characterization of inflammatory breast cancer and prediction of response to chemotherapy. Cancer Res 2004, 64(23):8558-8565.

53. Bieche I, Lerebours F, Tozlu S, Espie M, Marty M, Lidereau R: Molecular profiling of inflammatory breast cancer: identification of a poor-prognosis gene expression signature. Clin Cancer Res 2004, 10(20):6789-6795.

54. Bertucci F, Finetti P, Rougemont J, Charafe-Jauffret E, Cervera N, Tarpin C, Nguyen C, Xerri L, Houlgatte R, Jacquemier J et al: Gene expression profiling identifies molecular subtypes of inflammatory breast cancer. Cancer Res 2005, 65(6):2170-2178.

55. Van Laere SJ, Van den Eynden GG, Van der Auwera I, Vandenberghe M, van Dam P, Van Marck EA, van Golen KL, Vermeulen PB, Dirix LY: Identification of cell-of-origin breast tumor subtypes in inflammatory breast cancer by gene expression profiling. Breast Cancer Res Treat 2006, 95(3):243-255.

56. Nguyen DM, Sam K, Tsimelzon A, Li X, Wong H, Mohsin S, Clark GM, Hilsenbeck SG, Elledge RM, Allred DC et al: Molecular heterogeneity of inflammatory breast cancer: a hyperproliferative phenotype. Clin Cancer Res 2006, 12(17):5047-5054.

57. Dressman HK, Hans C, Bild A, Olson JA, Rosen E, Marcom PK, Liotcheva VB, Jones EL, Vujaskovic Z, Marks J et al: Gene expression profiles of multiple breast cancer phenotypes and response to neoadjuvant chemotherapy. Clin Cancer Res 2006, 12(3 Pt 1):819-826.

58. Boersma BJ, Reimers M, Yi M, Ludwig JA, Luke BT, Stephens RM, Yfantis HG, Lee DH, Weinstein JN, Ambs S: A stromal gene signature associated with inflammatory breast cancer. Int J Cancer 2008, 122(6):1324-1332.

59. Iwamoto T, Bianchini G, Qi Y, Cristofanilli M, Lucci A, Woodward WA, Reuben JM, Matsuoka J, Gong Y, Krishnamurthy S et al: Different gene expressions are associated with the different molecular subtypes of inflammatory breast cancer. Breast Cancer Res Treat 2011, 125(3):785-795.

60. Woodward WA, Krishnamurthy S, Yamauchi H, El-Zein R, Ogura D, Kitadai E, Niwa S, Cristofanilli M, Vermeulen P, Dirix L et al: Genomic and expression analysis of

microdissected inflammatory breast cancer. Breast Cancer Res Treat 2013, 138(3):761-772.

61. Zare A, Postovit LM, Githaka JM: Robust inflammatory breast cancer gene signature using nonparametric random forest analysis. Breast Cancer Res 2021, 23(1):92.

62. Rypens C, Bertucci F, Finetti P, Robertson F, Fernandez SV, Ueno N, Woodward WA, Van Golen K, Vermeulen P, Dirix L et al: Comparative transcriptional analyses of preclinical models and patient samples reveal MYC and RELA driven expression patterns that define the molecular landscape of IBC. NPJ Breast Cancer 2022, 8(1):12.

63. Richard F, De Schepper M, Maetens M, Leduc S, Isnaldi E, Geukens T, Van Baelen K, Nguyen HL, Vermeulen P, Van Laere S et al: Comparison of the genomic alterations present in tumor samples from patients with metastatic inflammatory versus non-inflammatory breast cancer reveals AURKA as a potential treatment target. Breast 2023.

64. Rana HQ, Sacca R, Drogan C, Gutierrez S, Schlosnagle E, Regan MM, Speare V, LaDuca H, Dolinsky J, Garber JE et al: Prevalence of germline variants in inflammatory breast cancer. Cancer 2019, 125(13):2194-2202.

65. Chai F, Liang Y, Zhang F, Wang M, Zhong L, Jiang J: Systematically identify key genes in inflammatory and non-inflammatory breast cancer. Gene 2016, 575(2 Pt 3):600-614.

66. Van Berckelaer C, Rypens C, van Dam P, Pouillon L, Parizel M, Schats KA, Kockx M, Tjalma WAA, Vermeulen P, van Laere S et al: Infiltrating stromal immune cells in inflammatory breast cancer are associated with an improved outcome and increased PD-L1 expression. Breast Cancer Res 2019, 21(1):28.

67. Reddy SM, Reuben A, Barua S, Jiang H, Zhang S, Wang L, Gopalakrishnan V, Hudgens CW, Tetzlaff MT, Reuben JM et al: Poor Response to Neoadjuvant Chemotherapy Correlates with Mast Cell Infiltration in Inflammatory Breast Cancer. Cancer Immunol Res 2019, 7(6):1025-1035.

68. Hamm CA, Moran D, Rao K, Trusk PB, Pry K, Sausen M, Jones S, Velculescu VE, Cristofanilli M, Bacus S: Genomic and Immunological Tumor Profiling Identifies Targetable Pathways and Extensive CD8+/PDL1+ Immune Infiltration in Inflammatory Breast Cancer Tumors. Mol Cancer Ther 2016, 15(7):1746-1756.

69. Arias-Pulido H, Cimino-Mathews A, Chaher N, Qualls C, Joste N, Colpaert C, Marotti JD, Foisey M, Prossnitz ER, Emens LA et al: The combined presence of CD20 + B cells

and PD-L1 + tumor-infiltrating lymphocytes in inflammatory breast cancer is prognostic of improved patient outcome. Breast Cancer Res Treat 2018, 171(2):273-282.

70. Wolfe AR, Trenton NJ, Debeb BG, Larson R, Ruffell B, Chu K, Hittelman W, Diehl M, Reuben JM, Ueno NT et al: Mesenchymal stem cells and macrophages interact through IL-6 to promote inflammatory breast cancer in pre-clinical models. Oncotarget 2016, 7(50):82482-82492.

71. Ross JS, Ali SM, Wang K, Khaira D, Palma NA, Chmielecki J, Palmer GA, Morosini D, Elvin JA, Fernandez SV et al: Comprehensive genomic profiling of inflammatory breast cancer cases reveals a high frequency of clinically relevant genomic alterations. Breast Cancer Res Treat 2015, 154(1):155-162.

72. Goh G, Schmid R, Guiver K, Arpornwirat W, Chitapanarux I, Ganju V, Im SA, Kim SB, Dechaphunkul A, Maneechavakajorn J et al: Clonal Evolutionary Analysis during HER2 Blockade in HER2-Positive Inflammatory Breast Cancer: A Phase II Open-Label Clinical Trial of Afatinib +/- Vinorelbine. PLoS Med 2016, 13(12):e1002136.

73. Matsuda N, Lim B, Wang Y, Krishnamurthy S, Woodward W, Alvarez RH, Lucci A, Valero V, Reuben JM, Meric-Bernstam F et al: Identification of frequent somatic mutations in inflammatory breast cancer. Breast Cancer Res Treat 2017, 163(2):263-272.

74. Liang X, Vacher S, Boulai A, Bernard V, Baulande S, Bohec M, Bieche I, Lerebours F, Callens C: Targeted next-generation sequencing identifies clinically relevant somatic mutations in a large cohort of inflammatory breast cancer. Breast Cancer Res 2018, 20(1):88.

75. Faldoni FLC, Villacis RAR, Canto LM, Fonseca-Alves CE, Cury SS, Larsen SJ, Aagaard MM, Souza CP, Scapulatempo-Neto C, Osorio C et al: Inflammatory Breast Cancer: Clinical Implications of Genomic Alterations and Mutational Profiling. Cancers (Basel) 2020, 12(10).

76. Bertucci F, Rypens C, Finetti P, Guille A, Adelaide J, Monneur A, Carbuccia N, Garnier S, Dirix P, Goncalves A et al: NOTCH and DNA repair pathways are more frequently targeted by genomic alterations in inflammatory than in non-inflammatory breast cancers. Mol Oncol 2020, 14(3):504-519.

77. Winn JS, Hasse Z, Slifker M, Pei J, Arisi-Fernandez SM, Talarchek JN, Obeid E, Baldwin DA, Gong Y, Ross E et al: Genetic Variants Detected Using Cell-Free DNA from Blood and Tumor Samples in Patients with Inflammatory Breast Cancer. Int J Mol Sci 2020, 21(4).

78. Li X, Kumar S, Harmanci A, Li S, Kitchen RR, Zhang Y, Wali VB, Reddy SM, Woodward WA, Reuben JM et al: Whole-genome sequencing of phenotypically distinct inflammatory breast cancers reveals similar genomic alterations to non-inflammatory breast cancers. Genome Med 2021, 13(1):70.

79. Gong Y, Nagarathinam R, Arisi MF, Gerratana L, Winn JS, Slifker M, Pei J, Cai KQ, Hasse Z, Obeid E et al: Genetic Variants and Tumor Immune Microenvironment: Clues for Targeted Therapies in Inflammatory Breast Cancer (IBC). Int J Mol Sci 2021, 22(16).

80. Luo R, Chong W, Wei Q, Zhang Z, Wang C, Ye Z, Abu-Khalaf MM, Silver DP, Stapp RT, Jiang W et al: Whole-exome sequencing identifies somatic mutations and intratumor heterogeneity in inflammatory breast cancer. NPJ Breast Cancer 2021, 7(1):72.

81. Mohamed MM, El-Ghonaimy EA, Nouh MA, Schneider RJ, Sloane BF, El-Shinawi M: Cytokines secreted by macrophages isolated from tumor microenvironment of inflammatory breast cancer patients possess chemotactic properties. Int J Biochem Cell Biol 2014, 46:138-147.

82. Valeta-Magara A, Gadi A, Volta V, Walters B, Arju R, Giashuddin S, Zhong H, Schneider RJ: Inflammatory Breast Cancer Promotes Development of M2 Tumor-Associated Macrophages and Cancer Mesenchymal Cells through a Complex Chemokine Network. Cancer Res 2019, 79(13):3360-3371.

83. Ignatoski KM, Ethier SP: Constitutive activation of pp125fak in newly isolated human breast cancer cell lines. Breast Cancer Res Treat 1999, 54(2):173-182.

84. Forozan F, Veldman R, Ammerman CA, Parsa NZ, Kallioniemi A, Kallioniemi OP, Ethier SP: Molecular cytogenetic analysis of 11 new breast cancer cell lines. Br J Cancer 1999, 81(8):1328-1334.

85. Robertson FM BF, Finetti P, Marsan M, Fernandez S, Ueno NT: Gene expression profiling of preclinical models for Inflammatory Breast Cancer emphasizes the role of the tumor microenvironment in IBC biology. J Clin Exp Pathol 2012, 2(5).

86. Kurebayashi J, Otsuki T, Tang CK, Kurosumi M, Yamamoto S, Tanaka K, Mochizuki M, Nakamura H, Sonoo H: Isolation and characterization of a new human breast cancer cell line, KPL-4, expressing the Erb B family receptors and interleukin-6. Br J Cancer 1999, 79(5-6):707-717.

87. Klopp AH, Lacerda L, Gupta A, Debeb BG, Solley T, Li L, Spaeth E, Xu W, Zhang X, Lewis MT et al: Mesenchymal stem cells promote mammosphere formation and decrease E-cadherin in normal and malignant breast cells. PLoS One 2010, 5(8):e12180.

88. Alpaugh ML, Tomlinson JS, Shao ZM, Barsky SH: A novel human xenograft model of inflammatory breast cancer. Cancer Res 1999, 59(20):5079-5084.

89. Wurth R, Tarn K, Jernigan D, Fernandez SV, Cristofanilli M, Fatatis A, Meucci O: A Preclinical Model of Inflammatory Breast Cancer to Study the Involvement of CXCR4 and ACKR3 in the Metastatic Process. Transl Oncol 2015, 8(5):358-367.

90. Fernandez SV, Robertson FM, Pei J, Aburto-Chumpitaz L, Mu Z, Chu K, Alpaugh RK, Huang Y, Cao Y, Ye Z et al: Inflammatory breast cancer (IBC): clues for targeted therapies. Breast Cancer Res Treat 2013, 140(1):23-33.

91. Lacerda L, Woodward WA: Models of Inflammatory Breast Cancer. In: Inflammatory Breast Cancer: An Update. 1 edn. Edited by Ueno NT, Fink T: Springer Netherlands; 2012: 139-150.

92. Hall CS, Debeb BG, Xu W, Ueno NT, Reuben JM, Robertson F, Lucci A, Buchholz TA, Hortobagyi GN, Cristofanilli M et al: Novel inflammatory breast cancer cell line, MDA-IBC-1 expresses and secretes WISP3, a putative tumor suppressor in inflammatory breast cancer. Cancer Research 2009, 69(2).

93. David CJ, Massague J: Contextual determinants of TGFbeta action in development, immunity and cancer. Nat Rev Mol Cell Biol 2018, 19(7):419-435.

94. Taylor AW: Review of the activation of TGF-beta in immunity. J Leukoc Biol 2009, 85(1):29-33.

95. Siegel PM, Massague J: Cytostatic and apoptotic actions of TGF-beta in homeostasis and cancer. Nat Rev Cancer 2003, 3(11):807-821.

96. Inman GJ, Nicolas FJ, Hill CS: Nucleocytoplasmic shuttling of Smads 2, 3, and 4 permits sensing of TGF-beta receptor activity. Mol Cell 2002, 10(2):283-294.

97. Nicolas FJ, De Bosscher K, Schmierer B, Hill CS: Analysis of Smad nucleocytoplasmic shuttling in living cells. J Cell Sci 2004, 117(Pt 18):4113-4125.

98. Costanza B, Umelo IA, Bellier J, Castronovo V, Turtoi A: Stromal Modulators of TGF-beta in Cancer. J Clin Med 2017, 6(1).

99. Jung SM, Lee JH, Park J, Oh YS, Lee SK, Park JS, Lee YS, Kim JH, Lee JY, Bae YS et al: Smad6 inhibits non-canonical TGF-beta1 signalling by recruiting the deubiquitinase A20 to TRAF6. Nat Commun 2013, 4:2562.

100. Imamura T, Takase M, Nishihara A, Oeda E, Hanai J, Kawabata M, Miyazono K: Smad6 inhibits signalling by the TGF-beta superfamily. Nature 1997, 389(6651):622-626.

101. Glick AB, Weinberg WC, Wu IH, Quan W, Yuspa SH: Transforming growth factor beta 1 suppresses genomic instability independent of a G1 arrest, p53, and Rb. Cancer Res 1996, 56(16):3645-3650.

102. Bierie B, Chung CH, Parker JS, Stover DG, Cheng N, Chytil A, Aakre M, Shyr Y, Moses HL: Abrogation of TGF-beta signaling enhances chemokine production and correlates with prognosis in human breast cancer. J Clin Invest 2009, 119(6):1571-1582.

103. Cheng N, Bhowmick NA, Chytil A, Gorksa AE, Brown KA, Muraoka R, Arteaga CL, Neilson EG, Hayward SW, Moses HL: Loss of TGF-beta type II receptor in fibroblasts promotes mammary carcinoma growth and invasion through upregulation of TGF-alpha-, MSP- and HGF-mediated signaling networks. Oncogene 2005, 24(32):5053-5068.

104. Sato M, Kadota M, Tang B, Yang HH, Yang YA, Shan M, Weng J, Welsh MA, Flanders KC, Nagano Y et al: An integrated genomic approach identifies persistent tumor suppressive effects of transforming growth factor-beta in human breast cancer. Breast Cancer Res 2014, 16(3):R57.

105. Silberstein GB, Daniel CW: Reversible inhibition of mammary gland growth by transforming growth factor-beta. Science 1987, 237(4812):291-293.

106. Pierce DF, Jr., Gorska AE, Chytil A, Meise KS, Page DL, Coffey RJ, Jr., Moses HL: Mammary tumor suppression by transforming growth factor beta 1 transgene expression. Proc Natl Acad Sci U S A 1995, 92(10):4254-4258.

107. Gorska AE, Jensen RA, Shyr Y, Aakre ME, Bhowmick NA, Moses HL: Transgenic mice expressing a dominant-negative mutant type II transforming growth factor-beta receptor exhibit impaired mammary development and enhanced mammary tumor formation. Am J Pathol 2003, 163(4):1539-1549.

108. Moses H, Barcellos-Hoff MH: TGF-beta biology in mammary development and breast cancer. Cold Spring Harb Perspect Biol 2011, 3(1):a003277.

109. Bierie B, Moses HL: Gain or loss of TGFbeta signaling in mammary carcinoma cells can promote metastasis. Cell Cycle 2009, 8(20):3319-3327.

110. Tang B, Vu M, Booker T, Santner SJ, Miller FR, Anver MR, Wakefield LM: TGF-beta switches from tumor suppressor to prometastatic factor in a model of breast cancer progression. J Clin Invest 2003, 112(7):1116-1124.

111. Galliher AJ, Schiemann WP: Beta3 integrin and Src facilitate transforming growth factor-beta mediated induction of epithelial-mesenchymal transition in mammary epithelial cells. Breast Cancer Res 2006, 8(4):R42.

112. Yin JJ, Selander K, Chirgwin JM, Dallas M, Grubbs BG, Wieser R, Massague J, Mundy GR, Guise TA: TGF-beta signaling blockade inhibits PTHrP secretion by breast cancer cells and bone metastases development. J Clin Invest 1999, 103(2):197-206.

113. Forrester E, Chytil A, Bierie B, Aakre M, Gorska AE, Sharif-Afshar AR, Muller WJ, Moses HL: Effect of conditional knockout of the type II TGF-beta receptor gene in mammary epithelia on mammary gland development and polyomavirus middle T antigen induced tumor formation and metastasis. Cancer Res 2005, 65(6):2296-2302.

114. Kohn EA, Yang YA, Du Z, Nagano Y, Van Schyndle CM, Herrmann MA, Heldman M, Chen JQ, Stuelten CH, Flanders KC et al: Biological responses to TGF-beta in the mammary epithelium show a complex dependency on Smad3 gene dosage with important implications for tumor progression. Mol Cancer Res 2012, 10(10):1389-1399.

115. Seyfried TN, Huysentruyt LC: On the origin of cancer metastasis. Crit Rev Oncog 2013, 18(1-2):43-73.

116. Hanahan D, Weinberg RA: Hallmarks of cancer: the next generation. Cell 2011, 144(5):646-674.

117. Elisha Y, Kalchenko V, Kuznetsov Y, Geiger B: Dual role of E-cadherin in the regulation of invasive collective migration of mammary carcinoma cells. Sci Rep 2018, 8(1):4986.

118. Xu J, Lamouille S, Derynck R: TGF-beta-induced epithelial to mesenchymal transition. Cell Res 2009, 19(2):156-172.

119. Xu W, Yang Z, Lu N: A new role for the PI3K/Akt signaling pathway in the epithelial-mesenchymal transition. Cell Adh Migr 2015, 9(4):317-324.

120. Wang Q, Yang X, Xu Y, Shen Z, Cheng H, Cheng F, Liu X, Wang R: RhoA/Rho-kinase triggers epithelial-mesenchymal transition in mesothelial cells and contributes to the pathogenesis of dialysis-related peritoneal fibrosis. Oncotarget 2018, 9(18):14397-14412.

121. Ungefroren H, Witte D, Lehnert H: The role of small GTPases of the Rho/Rac family in TGF-beta-induced EMT and cell motility in cancer. Dev Dyn 2018, 247(3):451-461.

122. Bakin AV, Rinehart C, Tomlinson AK, Arteaga CL: p38 mitogen-activated protein kinase is required for TGFbeta-mediated fibroblastic transdifferentiation and cell migration. J Cell Sci 2002, 115(Pt 15):3193-3206.

123. Yu L, Hebert MC, Zhang YE: TGF-beta receptor-activated p38 MAP kinase mediates Smad-independent TGF-beta responses. EMBO J 2002, 21(14):3749-3759.

124. Itoh S, Thorikay M, Kowanetz M, Moustakas A, Itoh F, Heldin CH, ten Dijke P: Elucidation of Smad requirement in transforming growth factor-beta type I receptor-induced responses. J Biol Chem 2003, 278(6):3751-3761.

125. Piek E, Moustakas A, Kurisaki A, Heldin CH, ten Dijke P: TGF-(beta) type I receptor/ALK-5 and Smad proteins mediate epithelial to mesenchymal transdifferentiation in NMuMG breast epithelial cells. J Cell Sci 1999, 112 (Pt 24):4557-4568.

126. Valcourt U, Kowanetz M, Niimi H, Heldin CH, Moustakas A: TGF-beta and the Smad signaling pathway support transcriptomic reprogramming during epithelial-mesenchymal cell transition. Mol Biol Cell 2005, 16(4):1987-2002.

127. Sato M, Muragaki Y, Saika S, Roberts AB, Ooshima A: Targeted disruption of TGF-beta1/Smad3 signaling protects against renal tubulointerstitial fibrosis induced by unilateral ureteral obstruction. J Clin Invest 2003, 112(10):1486-1494.

128. Ungefroren H, Otterbein H, Wellner UF, Keck T, Lehnert H, Marquardt JU: RAC1B Regulation of TGFB1 Reveals an Unexpected Role of Autocrine TGFbeta1 in the Suppression of Cell Motility. Cancers (Basel) 2020, 12(12).

129. Hoot KE, Lighthall J, Han G, Lu SL, Li A, Ju W, Kulesz-Martin M, Bottinger E, Wang XJ: Keratinocyte-specific Smad2 ablation results in increased epithelial-mesenchymal transition during skin cancer formation and progression. J Clin Invest 2008, 118(8):2722-2732.

130. Ju W, Ogawa A, Heyer J, Nierhof D, Yu L, Kucherlapati R, Shafritz DA, Bottinger EP: Deletion of Smad2 in mouse liver reveals novel functions in hepatocyte growth and differentiation. Mol Cell Biol 2006, 26(2):654-667.

131. Kohn EA, Du Z, Sato M, Van Schyndle CM, Welsh MA, Yang YA, Stuelten CH, Tang B, Ju W, Bottinger EP et al: A novel approach for the generation of genetically modified mammary epithelial cell cultures yields new insights into TGFbeta signaling in the mammary gland. Breast Cancer Res 2010, 12(5):R83.

132. Oft M, Akhurst RJ, Balmain A: Metastasis is driven by sequential elevation of H-ras and Smad2 levels. Nat Cell Biol 2002, 4(7):487-494.

133. Deckers M, van Dinther M, Buijs J, Que I, Lowik C, van der Pluijm G, ten Dijke P: The tumor suppressor Smad4 is required for transforming growth factor beta-induced epithelial to mesenchymal transition and bone metastasis of breast cancer cells. Cancer Res 2006, 66(4):2202-2209.

134. Kaimori A, Potter J, Kaimori JY, Wang C, Mezey E, Koteish A: Transforming growth factor-beta1 induces an epithelial-to-mesenchymal transition state in mouse hepatocytes in vitro. J Biol Chem 2007, 282(30):22089-22101.

135. Takano S, Kanai F, Jazag A, Ijichi H, Yao J, Ogawa H, Enomoto N, Omata M, Nakao A: Smad4 is essential for down-regulation of E-cadherin induced by TGF-beta in pancreatic cancer cell line PANC-1. J Biochem 2007, 141(3):345-351.

136. Bardeesy N, Cheng KH, Berger JH, Chu GC, Pahler J, Olson P, Hezel AF, Horner J, Lauwers GY, Hanahan D et al: Smad4 is dispensable for normal pancreas development yet critical in progression and tumor biology of pancreas cancer. Genes Dev 2006, 20(22):3130-3146.

137. Aceto N, Bardia A, Miyamoto DT, Donaldson MC, Wittner BS, Spencer JA, Yu M, Pely A, Engstrom A, Zhu H et al: Circulating tumor cell clusters are oligoclonal precursors of breast cancer metastasis. Cell 2014, 158(5):1110-1122.

138. Jolly MK, Boareto M, Debeb BG, Aceto N, Farach-Carson MC, Woodward WA, Levine H: Inflammatory breast cancer: a model for investigating cluster-based dissemination. NPJ Breast Cancer 2017, 3:21.

139. Jolly MK, Boareto M, Huang B, Jia D, Lu M, Ben-Jacob E, Onuchic JN, Levine H: Implications of the Hybrid Epithelial/Mesenchymal Phenotype in Metastasis. Front Oncol 2015, 5:155.

140. Pecina-Slaus N: Tumor suppressor gene E-cadherin and its role in normal and malignant cells. Cancer Cell Int 2003, 3(1):17.

141. Haraguchi M, Fukushige T, Kanekura T, Ozawa M: E-cadherin loss in RMG-1cells inhibits cell migration and its regulation by Rho GTPases. Biochem Biophys Rep 2019, 18:100650.

142. Padmanaban V, Krol I, Suhail Y, Szczerba BM, Aceto N, Bader JS, Ewald AJ: E-cadherin is required for metastasis in multiple models of breast cancer. Nature 2019, 573(7774):439-444.

143. Matise LA, Palmer TD, Ashby WJ, Nashabi A, Chytil A, Aakre M, Pickup MW, Gorska AE, Zijlstra A, Moses HL: Lack of transforming growth factor-beta signaling promotes collective cancer cell invasion through tumor-stromal crosstalk. Breast Cancer Res 2012, 14(4):R98.

144. Giampieri S, Manning C, Hooper S, Jones L, Hill CS, Sahai E: Localized and reversible TGFbeta signalling switches breast cancer cells from cohesive to single cell motility. Nat Cell Biol 2009, 11(11):1287-1296.

CHAPTER 1: The role of TGFß signaling in IBC

Inflammatory breast cancer cells are characterized by abrogated TGFβ1-dependent cell motility and SMAD3 activity.

Abstract

Purpose: Inflammatory breast cancer (IBC) is an aggressive form of breast cancer with elevated metastatic potential, characterized by tumor emboli in dermal and parenchymal lymph vessels. This study has investigated the hypothesis that TGFβ signaling is implicated in the molecular biology of IBC.

Methods: TGFβ1-induced cell motility and gene expression patterns were investigated in three IBC and three non-IBC (nIBC) cell lines. Tissue samples from IBC and nIBC patients were investigated for the expression of nuclear SMAD2, SMAD3 and SMAD4. SMAD protein levels were related to gene expression data.

Results: TGFβ1-induced cell motility was strongly abrogated in IBC cells (P = 0.003). Genes differentially expressed between IBC and nIBC cells post TGFβ1 exposure revealed attenuated expression of SMAD3 transcriptional regulators, but overexpression of MYC target genes in IBC. IBC patient samples demonstrated a near absence of SMAD3 and -4 expression in the primary tumor compared to nIBC patient samples (P < 0.001) and a further reduction of staining intensity in tumor emboli. Integration of gene and protein expression data revealed that a substantial fraction of the IBC signature genes correlated with SMAD3 and these genes are indicative of attenuated SMAD3 signaling in IBC.

Conclusions: We demonstrate attenuated SMAD3 transcriptional activity and SMAD protein expression in IBC, together with obliterated TGFβ1-induced IBC cell motility. The further reduction of nuclear SMAD expression levels in tumor emboli suggests that the activity of these transcription factors is involved in the metastatic dissemination of IBC cells, possibly by enabling collective invasion after partial EMT.

Background

Inflammatory breast cancer (IBC) is a rare and aggressive form of locally advanced breast cancer characterized by fast local spread and dissemination of cancer cells. Almost all patients have lymph node metastases and one third of patients have metastases in distant organs at the time of diagnosis. IBC accounts for a disproportionally high fraction of breast cancer-related mortality [1]. Combined with a high prevalence in younger women, this results in a significant loss in life-years far greater than expected based solely upon the IBC incidence of 2-5% of all breast cancers. Furthermore, the number of new diagnoses is increasing without clear cause and specific treatments are lacking due to a limited understanding of IBC biology. It is increasingly evident that IBC is a distinct and significant subtype of breast cancer which warrants specific, dedicated research.

An important indication of IBC is the presence of numerous tumor emboli in dermal and parenchymal lymph vessels. These E-Cadherin positive cancer cell clusters appear to be integral to IBC pathology [2,3]. The physical obstruction of draining lymph vessels by tumor emboli induces clinical symptoms often associated with IBC such as swelling of the breast. Intravascular growth of tumor emboli may account for the fast, local spread, and typical diffuse growth pattern, or self-metastasis, associated with IBC. Tumor emboli thus seem to be key for disease progression.

The existence of a molecular basis for IBC was confirmed in 2013 when the World IBC consortium (WIBCC) reported a 79-gene signature that discriminates between IBC and non-IBC (nIBC) patient samples [4]. Translating this gene signature into molecular concepts suggested that the biology of IBC is shaped by specific TGFβ and immune response programs. The aim of the present study was to gain a better understanding of how TGFβ signaling contributes to the biology of IBC.

Methods

A detailed description of all methods is provided in supplementary data (Additional file 1).

Cell culture, cell motility assay and wound healing assays

Three IBC cell lines: KPL4, SUM190 and SUM149 and 3 nIBC cell lines: MDA-MB-231, MDA-MB-436 and MCF7 were used. The cell motility inducing effect of 11 chemokines and growth factors as well as fetal bovine serum (FBS) as positive control was evaluated using the xCELLigence RTCA DP instrument (ACEA Biosciences) according to manufacturer's instructions. A Chemoattractant dilution series: 10 µg/mL - 1 µg/mL - 100 ng/mL - 10 ng/mL was used to calculate a concentration for 50% of maximal effect

(EC50) for each chemoattractant. Classical would healing assays were performed to validate the TGFβ1-induced cell motility responses of all six cell lines.

RNA-sequencing and data analysis

All IBC and nIBC cell lines were treated with 5ng/ml TGFβ1 for 1hr, 4hrs and 14hrs. RNA-sequencing was performed using stranded cDNA libraries on a HiSeq2000 system. Reads were mapped to the reference genome (hg19) using TopHat 2.0 [5] and Bowtie2.0 [6]. Genes with count per million (CPM) values greater than 1 in at least 3 samples were included for further analysis. CPM values for each of the untreated controls were used to classify the cell lines according to the luminal-, basal-, mesenchymal-classification system. Global expression themes in the data set were evaluated using principal component analysis (PCA). Differential gene expression analysis was performed on the 2log-transformed CPM values using the BioConductor package *limma,* accounting for the molecular subtypes and other confounding sources of gene expression variation. Finally, to translate lists of differentially expressed genes into biological concepts related to pathway and transcriptional activities, the online tool EnrichR was used (http://amp.pharm.mssm.edu/Enrichr). Since this is an exploratory analysis and to increase statistical power, GSEA was performed using lists of genes significant at a nominal, uncorrected level of 5%.

Immunohistochemistry (IHC)

IHC was performed on 5μm formalin-fixed, paraffin-embedded (FFPE) tissue sections from 76 IBC patients and 152 nIBC patients collected at the GZA Hospitals Sint-Augustinus (Wilrijk, Belgium). Qualitative evaluation was performed by two independent pathologists. A total score was calculated by multiplying proportion with intensity. Nuclear staining in the cancer cells, both in the primary tumor and tumor emboli was scored according to proportion of tumor cells (%) and intensity of staining, being either negative (0), weak (1), medium (2) or strongly (3) positive. A total score was calculated by multiplying proportion with intensity.

Affymetrix data analysis

Gene expression data from two publicly available series of patients with and without IBC obtained from Antwerp (E-MTAB-1006) and Marseille (E-MTAB-1547) were analyzed as described before [4]. To integrate gene and SMAD protein expression data, pairwise Pearson correlation coefficients were calculated between the gene expression and SMAD protein expression data and correlation patterns were investigated for genes belonging to the IBC signature [4] as well as for genes exhibiting a differential response to 4 hours of TGFβ1 treatment in IBC and nIBC cells. Lists of differentially

expressed genes between samples from patients with and without IBC were investigated for enrichment of SMAD3 and MYC target genes identified from the cell line experiment using gene set enrichment analysis (GSEA).

Statistics

Relationships between two categorical variables were analyzed using classical Chi-Square or Fisher's Exact tests where appropriate. Relationships between two continuous variables were analyzed using Spearman correlation analysis. Relationships between a continuous variable and a categorical variable were investigated using non-parametrical Mann-Whitney U-tests (unpaired) or using the Wilcoxon signed-rank test (paired). All analyses were performed in R (v3.4.0) and *P*-values < 0.05 were considered significant.

Results

Cell motility following TGFβ1 treatment is disabled in IBC cells

TGFβ signaling is associated with metastatic progression in breast cancer which is a key feature of IBC biology. Given the fact that cell motility is crucial for metastatic dissemination, the effect of TGFβ1 on cell motility was investigated in 3 IBC cell lines, SUM149, SUM190, and KPL4 and in 3 nIBC cell lines, MM231, MM436, and MCF7. Using the xCELLigence system, we noted a 39-fold reduction in the cell motility inducing capacity of TGFβ1 in IBC cells relative to nIBC cells (*P* = 0.003). For comparison, a panel of 10 additional growth factors and cytokines was also screened: none of these ligands induced significant differences in cell motility between IBC and nIBC cells (Fig. 1a). The observations obtained for TGFβ1 were confirmed using classical wound healing assays (Fig. 1b; Additional file 2: Fig. S1). Importantly, the cell motility responses of IBC and nIBC cells in the presence or absence of FBS were similar, indicating that our observations cannot be attributed to differences in the basal migration rates of the 6 evaluated cell lines (Additional file 2: Fig. S1).

Assessment of mRNA expression levels in the same cell lines revealed 1,078 differentially expressed genes between IBC and nIBC at a nominal P-value of 5%, of which 272 remained significant after correction for false discovery (Additional file 2: Table S1-S2). With respect to most canonical TGFβ signaling genes (i.e. TGFBR1, TGFBR2, TGFBR3, SMAD2, SMAD3, SMAD4, SMAD6, SMAD7, TGFB2, and TGFB3), no expression differences were noted. For TGFβ1 and TGFBI, a 10-fold (*P* = 0.039; Q=0.356) and 44-fold (*P* = 0.013; Q=0.242) increased expression level was observed in nIBC and IBC cells respectively. GSEA revealed frequent overexpression of CEBP/ATF

and C/EBPβ transcriptional targets, protein interaction partners and co-expressed genes in IBC (Fig. 2a). But again, no differences with respect to molecular concepts associated with TGFβ signaling were retained. Together, these data demonstrate that cell motility of IBC cells following TGFβ1 treatment is attenuated and that this observation is not related to differences in basal migration rates nor to differences in basal expression levels of key TGFβ signaling mediators amongst all evaluated cell lines.
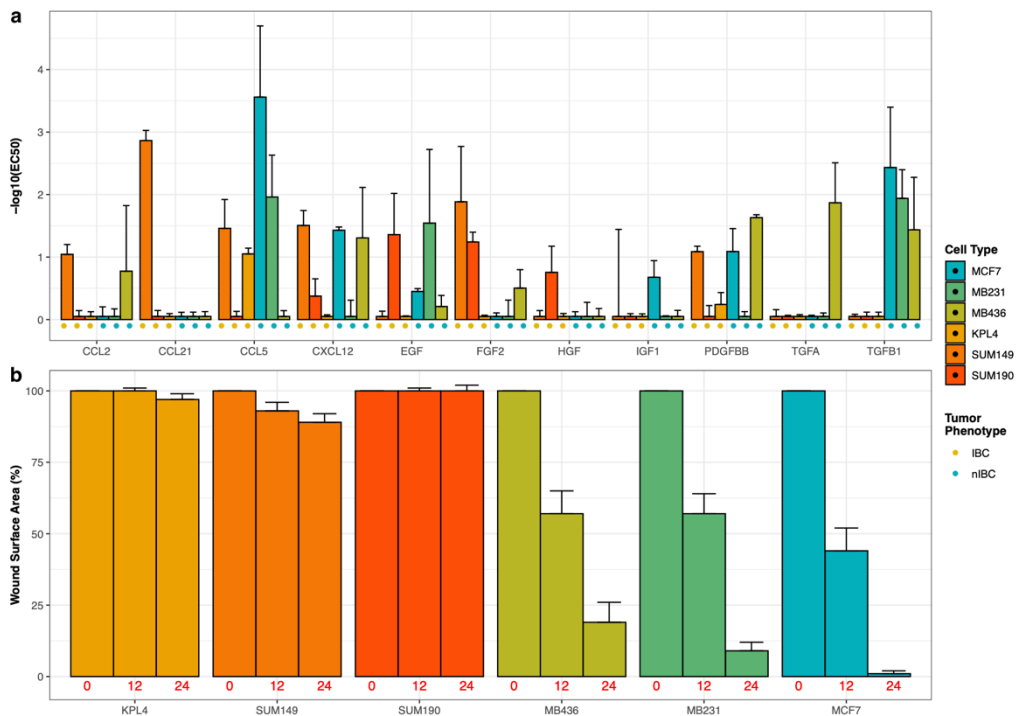

Fig1 a Cell motility-inducing effect of 11 chemokines in three IBC cell lines and three subtype-matched nIBC cell lines. TGFβ1 induces a 38.728-fold reduction in cell motility of IBC cells relative to nIBC cells ($P = 0.003$). **b** Wound healing assays after 12 hours and 24 hours of TGFβ1 treatment in all cell lines. nIBC cells show a near complete closure of the scratch (range scratch surface area reduction: 81-98%) after 24 hours. In IBC cells, the surface area of the scratch remains virtually unchanged (i.e. range: 0-11%).

IBC cells exhibit a SMAD3 deficient response to TGFβ1 treatment

To investigate mechanisms of TGFβ signaling in IBC and nIBC cells, a time course experiment was performed in which IBC and nIBC cells were treated with TGFβ1 for 1hr, 4hrs or 14hrs. To explore global expression differences in the data set, PCA was performed for 15,193 genes. The resulting 2D scatter plot in Fig. 2b shows that only subtle changes to gene expression could be attributed to TGFβ1 treatment and tumor phenotypes, IBC and nIBC. Firstly, the global scattering pattern is cell line specific, indicating that the expression variation within cell lines across different TGFβ1

treatment conditions is smaller than the expression variation between different cell lines. Secondly, the leading principal component is associated with expression differences between luminal KPL4, SUM190 and MCF7 cell lines and mesenchymal SUM149, MM231, MM436 cell lines. This indicates that cell line subtypes are a major source of expression variation. Finally, the second principal component is associated with expression differences between IBC and nIBC cell lines. These results were confirmed using unsupervised hierarchical cluster analysis of the 500 most variable genes measured by standard deviation (Additional file 2: Fig. S2). Together, these data indicate that expression patterns are related most significantly to the intrinsic properties of cell type and subtype.
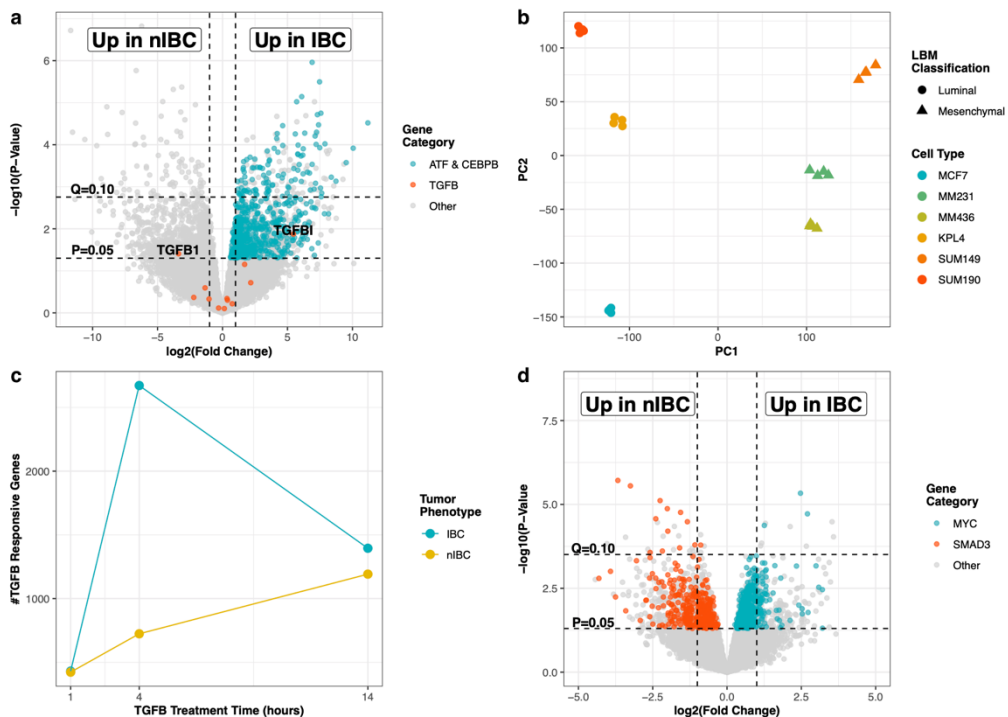
Fig2 a Volcano plot displaying differentially expressed genes between untreated IBC and nIBC cells. The x-axis displays the log2 fold change value, the y-axis corresponds to the mean expression value. Values are considered significant if P>0.5. Negative fold changes represent genes higher expressed in nIBC cells; positive fold changes show upregulated transcripts in IBC cells. A frequent enrichment of CEBP/ATF and C/EBPβ transcriptional targets, protein interaction partners and co-expressed genes amongst the upregulated genes in IBC can be observed (blue dots). No significant expression differences exist for genes involved in TGFβ signaling (red dots), except for a significant 10-fold (P = 0.039; Q = 0.356) and 44-fold (P = 0.013; Q = 0.242) higher expression of TGFB1 in nIBC cells and TGFBI in IBC cells respectively. **b** Expression variation between the cell lines is evident as shown by the global scattering pattern. The leading principal component (PC) classifies cell lines as luminal (i.e. KPL4, SUM190 and MCF7) or mesenchymal (i.e. SUM149, MM231, MM436). The second PC

is associated with expression differences between IBC and nIBC cell lines. **c** Time course-dependent TGFβ1-induced expression changes. The most elaborate gene expression differences are visible after 4 hours of TGFβ1 treatment. **d** Volcano plot displaying 1,820 genes that respond differently in IBC (i.e. 924 genes) and nIBC (i.e. 896 genes) cells after 4 hours of TGFβ1 treatment. These genes are enriched for SMAD3 transcriptional targets, protein interaction partners and co-expressed genes in nIBC cells (red dots), while IBC cells are characterized by a MYC-driven transcriptional response (blue dots).

To investigate specific expression differences between IBC and nIBC cells post TGFβ1 treatment, the following gene sets were identified: TGFβ1-responsive genes in IBC cells; TGFβ1-responsive genes in nIBC cells; and genes that respond differently to TGFβ1 in IBC and nIBC cells. Dominant sources of variation in gene expression, identified through unsupervised analysis (*vide supra*), were accounted for as described in the supplementary methods section.

A clear difference in the dynamics of TGFβ-induced gene expression changes between IBC and nIBC cells was observed (Fig. 2c). Four hours of TGFβ1 treatment induced a spike in the number of differentially expressed genes in IBC cells whereas in nIBC cells a gradual, steady increase in differential gene expression was observed throughout the entire time course. Gene lists are provided in the supplementary data (Additional file 2: Table S1). Since expression differences were most distinct after 4 hours of TGFβ1 treatment, genes that responded differently in IBC and nIBC cells at this time point (N=1,820) were subjected to GSEA. Results are provided in Fig. 2d. TGFβ1-responsive genes in nIBC were enriched for SMAD3 transcriptional targets, protein interaction partners and co-expressed genes, whereas IBC cells were characterized by a MYC-driven transcriptional response. Gene lists are provided in the supplementary data (Additional file 2: Table S3). Given these results, changes in SMAD3 and MYC mRNA levels over time were analyzed in IBC and nIBC cells separately and only MYC expression was found to be upregulated in IBC cells after 1 hour of TGFβ1 treatment (fold-change = 1.659; 95%C.I. = 1.133-2.438; *P* = 0.012).

SMAD3 nuclear expression is weak in cancer cells from patients with IBC
To study TGFβ signaling patterns in IBC and nIBC in a translational setting, nuclear protein expression of SMAD2, SMAD3 and SMAD4 was investigated using IHC on a series of FFPE tissue sections from 76 IBC and 152 nIBC patients. An overview of the clinicopathological variables related to the patient series is provided in Additional file 2: Table S4. Expression levels for SMAD2, SMAD3 and SMAD4 were significantly attenuated in IBC compared to nIBC (all *Ps* < 0.001), with almost no SMAD3 expression in IBC tissue (median score: 0; range: 0 - 270). Data are shown in Fig. 3a. Multivariate analysis demonstrated that these results are not confounded by differences between

IBC and nIBC with respect to classical clinicopathological variables. Additional multivariate analyses revealed that the expression levels of both SMAD3 and SMAD4, but not SMAD2, are independently associated with the IBC phenotype (Additional file 2: Fig. S3). Interestingly, in the few IBC samples with elevated SMAD3 nuclear expression, defined relative to the median nuclear SMAD3 expression level in nIBC samples (N = 9/76; P = 0.021), the nuclear expression of SMAD4 was particularly low. This association was less pronounced in nIBC samples (P = 0.118), suggesting co-operation between SMAD3 and SMAD4 in defining IBC biology.

SMAD3 and SMAD4 staining patterns were evaluated in tumor emboli in a subseries of 19 samples from patients with IBC (Fig. 3b, Additional file 2: Fig. S4). Neither the proportion of stained cancer cells nor the total expression score in tumor emboli was different when compared to cancer cells in the primary tumor. However, we did observe a significant decrease in staining intensity between both compartments (SMAD3: P = 0.019 and SMAD4: P = 0.006). When considering all samples with SMAD3 and/or SMAD4 expression data, decreased SMAD staining intensity was observed in 11/19 (58%) of tumor emboli. In addition, none of the 19 samples demonstrated increased staining intensity in the tumor emboli relative to the primary tumor, suggesting that attenuation of nuclear SMAD3 and SMAD4 expression is integral to the biology of IBC tumor emboli.
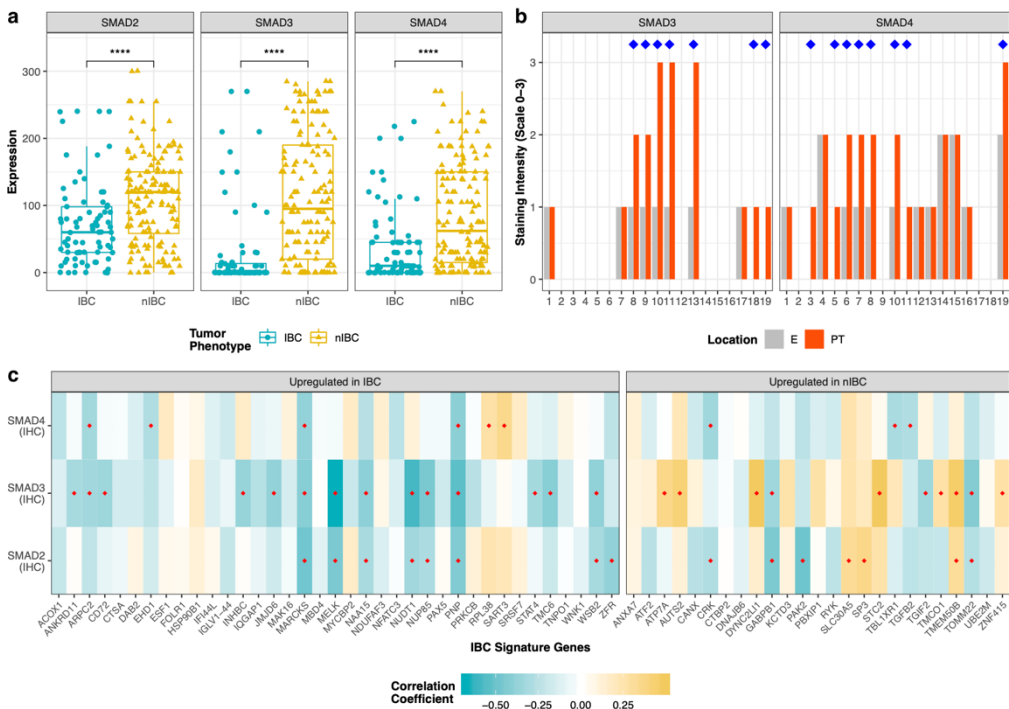

Fig3 a Nuclear protein expression levels for total SMAD2, SMAD3 and SMAD4 in a series of 76 IBC and 152 nIBC patient samples. **b** In 11/19 IBC samples, SMAD3 and/or SMAD4

staining intensity is decreased (resp. $P = 0.019$ and $P = 0.006$) in cells of the tumor emboli relative to cells of the matching primary tumor. **c** Correlation analysis between SMAD protein expression and gene expression of 62/79 genes belonging to a reported IBC signature [4] in 31 IBC and 23 nIBC patient samples. Significant correlations are found for SMAD2, SMAD3, and SMAD4 with respectively 24% (i.e. 15/62), 39% (i.e. 24/62) and 15% (i.e. 9/62) of the IBC signature genes (red dots).

A similar correlation analysis was carried out for 1,107/1,820 genes that responded differently to 4 hours of TGFβ1 treatment in IBC and nIBC cells and that were adequately expressed in the Affymetrix data set (Fig. 4a). In this analysis, 36% (402/1,107) of the correlations with SMAD3 nuclear expression were significant. When analyzing the SMAD3 and MYC related genes identified after GSEA in the time course experiment (*vide supra*), we observed a 1.789-fold enrichment for the SMAD3 related genes (blue dots) amongst the positively correlated genes (yellow) and a 3.588-fold enrichment for the MYC related genes (yellow dots) amongst the negatively correlated genes (light blue). These data show that, also in clinical samples, the expressions of the TGFβ1-responsive genes are primarily associated with SMAD3 and that increased MYC target gene expression coincides with attenuated SMAD3 nuclear expression. In contrast, the percentage of significant correlations with SMAD2 or SMAD4 was respectively 24% (265/1,107) and 12% (129/1,107).

To validate these findings in function of the IBC phenotype, associations between expressions of SMAD3 and MYC related genes and the IBC phenotype were investigated in patient samples. Therefore, GSEA was performed on the Affymetrix data set expanded with an additional 19 IBC and 32 nIBC patient samples for which no SMAD protein expression analysis was performed as well as on a second independent series of samples from patients with and without IBC. In both cohorts, SMAD3 and MYC related genes were significantly overexpressed in nIBC and IBC samples respectively. Results are shown in Fig. 4b and 4c.
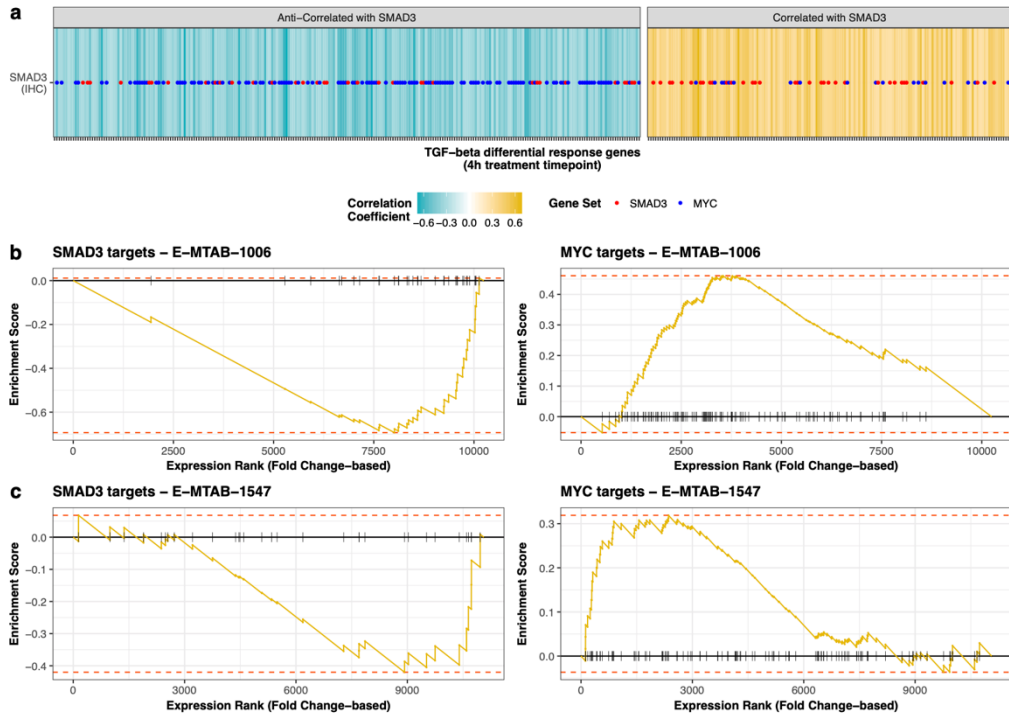
Fig4 a Correlation analysis between SMAD protein expression and gene expression of 1,107/1,820 genes that respond differently after 4 hours of TGFβ1 treatment in IBC and nIBC cells. **b** Enrichment plot comparing gene expression data from 50 IBC and 55 nIBC patient samples (19 IBC and 32 nIBC without SMAD protein expression analysis). The x-axis displays all genes in E-MTAB-1006 ranked according to their log2 fold change value. High fold changes (left) represent genes upregulated in IBC cells, low fold changes (right) shows highly expressed transcripts in nIBC cells. SMAD3 related genes that are positively correlated with SMAD3 protein expression (left graph) demonstrate significant, molecular subtype independent depletion amongst genes overexpressed in IBC (NES = -2.317, $P < 0.001$). MYC related genes that show an anticorrelation with SMAD3 protein expression (right graph) reveal a significant, molecular subtype independent enrichment amongst genes overexpressed in IBC (NES = 1.765, $P < 0.001$). **c** Enrichment plot comparing SMAD3 protein expression data with gene expression data from an independent dataset (E-MTAB-1547) consisting of 74 IBC and 143 nIBC patient samples (SMAD3: NES = -1.335, $P = 0.048$; MYC: NES = 1.479, $P = 0.007$).

Discussion

In 2013, the World IBC Consortium reported a gene signature that differentiated between tissue samples from patients with and without IBC. This gene signature suggested that TGFβ signaling is attenuated in IBC, which was surprising given the importance of TGFβ signaling in metastatic progression across various cancer types [7-9]. In the present study, we further investigate the role of TGFβ1 mediated migration and signaling in IBC cells and extend these observations to patient samples.

First, a chemotactic cell motility experiment showed that the response to TGFβ1 by IBC and nIBC was the only significant difference with cell motility almost completely impaired in all 3 IBC cell lines, extending across luminal and mesenchymal molecular subtypes. TGFβ receptor genes and their downstream transcription factors, SMAD2, SMAD3 and SMAD4 were expressed in all cell lines evaluated and no expression differences for any of these genes were observed between IBC and nIBC cells. Therefore, the inhibited motility of IBC cells cannot be attributed to differential expression of TGFβ signaling genes and thus requires further investigation.

A time course experiment then revealed that in nIBC cells, TGFβ1 induced overexpression of genes related to the transcriptional activity of SMAD3, a transcription factor that features in the TGFβ signal transduction pathways [10]. By contrast, TGFβ1-responsive genes overexpressed in IBC cells were enriched for genes related to the transcriptional activity of MYC, indicating that IBC cells respond to TGFβ1 by activating a MYC response program. This observation is unexpected given that SMAD proteins are natural antagonists of MYC activity [11]. Notably, a SNP in a cis-regulatory enhancer element of MYC was already shown to be associated with major metastatic risk in IBC [12]. This suggests that the mechanisms of TGFβ1-induced SMAD3 transcriptional activity are specifically altered in IBC cells.

In order to link the absence of SMAD3 transcription activity to IBC biology, protein levels were examined in patient samples. Nuclear protein expression levels for all SMAD proteins were reduced in IBC relative to nIBC samples in a molecular subtype independent manner, with a near complete absence of SMAD3 expression in most IBC cases. Comparative analysis of SMAD nuclear protein and gene expression data demonstrated that the expression levels of a substantial number of the 79 IBC signature genes [4] correlated with SMAD3 protein expression levels. Genes overexpressed in IBC were predominantly negatively correlated to nuclear SMAD3 protein expression and vice versa.

Expression levels of many IBC and nIBC specific TGFβ1-responsive genes identified in the time course experiment were also primarily correlated to nuclear SMAD3 protein expression in patient samples, further strengthening the association between a TGFβ response program in IBC cells and SMAD3. Amongst the positively correlated TGFβ1-responsive genes, there was significant enrichment for genes related to the transcriptional activity of SMAD3 and these genes were also highly expressed in nIBC cases in two independent patient series. In contrast, TGFβ1-responsive genes negatively correlated to nuclear SMAD3 protein expression were enriched for genes related to the transcriptional activity of MYC and these genes were highly expressed in

IBC cases from the same independent patient series. Together, these results suggest that the molecular response of IBC cells to TGFβ1 is orchestrated in a SMAD3 independent manner with concomitant MYC transcriptional activity.

The emerging role of abrogated SMAD3 transcriptional activity in IBC biology provides a potential model for the disseminative and metastatic characteristics of IBC cells. In 2009, Giampieri and colleagues reported that TGFβ signaling switches the mode of cancer cell migration from collective to single cell phenotype and that transient TGFβ signaling is essential for blood-borne metastasis [13]. Furthermore, Matise and colleagues corroborated these results and additionally demonstrated that TGFβ-induced single cell motility involves the regulation of epithelial to mesenchymal transition (EMT) [14]. Using genetically modified mammary epithelial cell cultures, Kohn and colleagues revealed that the regulation of EMT through TGFβ signaling depends on expression of SMAD3 but not SMAD2 [15], confirming earlier observations in keratinocyte cultures [16]. In a separate analysis, Kohn and colleagues investigated SMAD3 gene dosage effects on cell biology using mammary epithelial cells and revealed that a 50% reduction of SMAD3 expression (i.e. SMAD3$^{+/-}$ genotype) abrogated the cell motility response but enhanced the invasion response [17]. These observations were attested to the induction of partial EMT in which some molecular changes associated with EMT are observed without the classical morphological changes.

Therefore, the data presented in this study suggest that IBC cells are characterized by partial EMT and collective invasion by means of their reduced SMAD3 expression. The partial EMT in part could explain the ubiquitous but counterintuitive presence of E-cadherin in IBC [4, 18]. In addition, the attenuated cell motility response observed in conjunction with partial EMT is consistent with the reduced cell motility inducing capacity of TGFβ1 observed in IBC cells. Studies suggest that collectively invading cancer cells possess a higher metastatic potential due to an enhanced capacity for extravasation [13, 14, 17, 19], and favor lymphatic over hematogenous dissemination [13]. Collectively migrating cancer cells that disseminate as E-cadherin positive cancer cell clusters through the lymphatic systems is reminiscent of tumor emboli, which are characteristic of IBC. Interestingly, the nuclear protein staining intensity of SMAD3 was never higher in cancer cells residing in tumor emboli as compared to those in the primary tumor, suggesting that the mechanism leading to abrogated SMAD3 transcriptional activity in the primary tumor is even more pronounced in tumor emboli and thus plays a vital role in the dissemination of IBC cells and their metastatic potential.

The majority of the data in this study indicate that SMAD3 is the main determinant of the specific TGFβ response in IBC cells. However, multivariate analysis revealed that attenuated nuclear expression of SMAD4 is also associated with the IBC phenotype but that this expression is independent of SMAD3. In-depth analysis demonstrated that SMAD4 nuclear expression was particularly low in a small fraction of IBC cases with elevated nuclear SMAD3 expression. In addition, SMAD4 staining intensity was further diminished in cancer cells residing in tumor emboli and particularly in some patients where differences in staining intensity for SMAD3 between cancer cells in the primary tumor and tumor emboli were not observed. These observations suggest that SMAD3 and SMAD4 expression is mutually exclusive and reduction of nuclear SMAD4 is an alternative pathway to establish the TGFβ response in IBC cells which is associated with metastatic progression.

Few studies have examined the role of SMAD4 in partial EMT and collective invasion, but it has been reported that increased expression of SMAD4 mediates the TGFβ-dependent switch from cohesive to single cell motility [13]. Furthermore, these data imply that for a thorough understanding of IBC biology in relation to TGFβ signaling, common targets of both SMAD3 and SMAD4 should be considered. Possible targets identified in this study are APRC2, MARCKS, and PNP that are IBC-specific genes [4, 20] of which at least ARPC2 and MARCKS are involved in the regulation of the actin cytoskeleton, which in turn is linked to the formation of metastases through its effect on cell motility and invasion, possibly in an EMT-independent way [21-25].

In this study, IBC and nIBC cell lines of different molecular subtypes and a large series of patient samples were analyzed in order to identify mechanisms of TGFβ signaling that are intrinsic and specific to IBC cells. In order to fully comprehend the role of TGFβ signaling in IBC, concepts not addressed by this study require further investigation. Firstly, the effect of TGFβ signaling in the tumor stroma may be relevant to IBC biology given that fibroblasts are the primary reservoir of TGFβ ligands present in the inflammatory tumor microenvironment. Secondly, the effects of the other TGFβ isoforms, TGFβ2 and TGFβ3, were not considered although literature suggests that distinct TGFβ ligands play unique roles in the biology of breast cancer [26]. Finally, total SMAD nuclear expression was regarded as a read-out of SMAD transcriptional activity, which is corroborated by the fact that SMAD3 transcriptional targets are enriched amongst the genes positively correlated with total nuclear SMAD3 expression. Different phosphorylated SMAD isoforms exist, each with different implication for cell biology [27] and a detailed analysis may provide novel insights into how TGFβ signaling contributes the biology of IBC.

Conclusions

This study has demonstrated that IBC cells are characterized by attenuated SMAD3 or SMAD4 protein expression and transcriptional activity that obliterates the cell motility inducing capacity of TGFβ1. Recent studies revealed an essential role for SMAD3 in TGFβ1-induced cell motility through induction of EMT. In the absence of SMAD3 expression, TGFβ1 induces a partial EMT leading to collectively invading cancer cells which possess a high metastatic potential and the tendency for lymphatic dissemination. The data described in this paper combined with a substantial body of literature on the subject provides an intriguing explanatory model for the biology of IBC, particularly the formation of tumor emboli and the associated metastatic potential, which merits further investment.

References

1. Woodward WA (2015) Inflammatory breast cancer: unique biological and therapeutic considerations. Lancet Oncol 16 (15):e568-576. doi:10.1016/S1470-2045(15)00146-1

2. Arora J, Sauer SJ, Tarpley M, Vermeulen P, Rypens C, Van Laere S, Williams KP, Devi GR, Dewhirst MW (2017) Inflammatory breast cancer tumor emboli express high levels of anti-apoptotic proteins: use of a quantitative high content and high-throughput 3D IBC spheroid assay to identify targeting strategies. Oncotarget 8 (16):25848-25863. doi:10.18632/oncotarget.15667

3. Nath S, Devi GR (2016) Three-dimensional culture systems in cancer research: Focus on tumor spheroid model. Pharmacol Ther 163:94-108. doi:10.1016/j.pharmthera.2016.03.013

4. Van Laere SJ, Ueno NT, Finetti P, Vermeulen P, Lucci A, Robertson FM, Marsan M, Iwamoto T, Krishnamurthy S, Masuda H, van Dam P, Woodward WA, Viens P, Cristofanilli M, Birnbaum D, Dirix L, Reuben JM, Bertucci F (2013) Uncovering the molecular secrets of inflammatory breast cancer biology: an integrated analysis of three distinct affymetrix gene expression datasets. Clin Cancer Res 19 (17):4685-4696. doi:10.1158/1078-0432.CCR-12-2549

5. Kim D, Pertea G, Trapnell C, Pimentel H, Kelley R, Salzberg SL (2013) TopHat2: accurate alignment of transcriptomes in the presence of insertions, deletions and gene fusions. Genome Biol 14 (4):R36. doi:10.1186/gb-2013-14-4-r36

6. Langmead B, Salzberg SL (2012) Fast gapped-read alignment with Bowtie 2. Nat Methods 9 (4):357-359. doi:10.1038/nmeth.1923

7. Ikushima H, Miyazono K (2010) TGFbeta signalling: a complex web in cancer progression. Nat Rev Cancer 10 (6):415-424. doi:10.1038/nrc2853

8. Massague J (2012) TGFbeta signalling in context. Nat Rev Mol Cell Biol 13 (10):616-630. doi:10.1038/nrm3434

9. Wakefield LM, Hill CS (2013) Beyond TGFbeta: roles of other TGFbeta superfamily members in cancer. Nat Rev Cancer 13 (5):328-341. doi:10.1038/nrc3500

10. Moustakas A, Souchelnytskyi S, Heldin CH (2001) Smad regulation in TGF-βeta signal transduction. J Cell Sci 114 (Pt 24):4359-4369

11. Frederick JP, Liberati NT, Waddell DS, Shi Y, Wang XF (2004) Transforming growth factor beta-mediated transcriptional repression of c-myc is dependent on direct binding of Smad3 to a novel repressive Smad binding element. Mol Cell Biol 24 (6):2546-2559

12. Bertucci F, Lagarde A, Ferrari A, Finetti P, Charafe-Jauffret E, Van Laere S, Adelaide J, Viens P, Thomas G, Birnbaum D, Olschwang S (2012) 8q24 Cancer risk allele associated with major metastatic risk in inflammatory breast cancer. PLoS One 7 (5):e37943. doi:10.1371/journal.pone.0037943

13. Giampieri S, Manning C, Hooper S, Jones L, Hill CS, Sahai E (2009) Localized and reversible TGFbeta signalling switches breast cancer cells from cohesive to single cell motility. Nat Cell Biol 11 (11):1287-1296. doi:10.1038/ncb1973

14. Matise LA, Palmer TD, Ashby WJ, Nashabi A, Chytil A, Aakre M, Pickup MW, Gorska AE, Zijlstra A, Moses HL (2012) Lack of transforming growth factor-beta signaling promotes collective cancer cell invasion through tumor-stromal crosstalk. Breast Cancer Res 14 (4):R98. doi:10.1186/bcr3217

15. Kohn EA, Du Z, Sato M, Van Schyndle CM, Welsh MA, Yang YA, Stuelten CH, Tang B, Ju W, Bottinger EP, Wakefield LM (2010) A novel approach for the generation of genetically modified mammary epithelial cell cultures yields new insights into TGFbeta signaling in the mammary gland. Breast Cancer Res 12 (5):R83. doi:10.1186/bcr2728

16. Hoot KE, Lighthall J, Han G, Lu SL, Li A, Ju W, Kulesz-Martin M, Bottinger E, Wang XJ (2008) Keratinocyte-specific Smad2 ablation results in increased epithelial-mesenchymal transition during skin cancer formation and progression. J Clin Invest 118 (8):2722-2732. doi:10.1172/JCI33713

17. Kohn EA, Yang YA, Du Z, Nagano Y, Van Schyndle CM, Herrmann MA, Heldman M, Chen JQ, Stuelten CH, Flanders KC, Wakefield LM (2012) Biological responses to TGF-βeta in the mammary epithelium show a complex dependency on Smad3 gene dosage with important implications for tumor progression. Mol Cancer Res 10 (10):1389-1399. doi:10.1158/1541-7786.MCR-12-0136-T

18. Jolly MK, Boareto M, Debeb BG, Aceto N, Farach-Carson MC, Woodward WA, Levine H (2017) Inflammatory breast cancer: a model for investigating cluster-based dissemination. NPJ Breast Cancer 3:21. doi:10.1038/s41523-017-0023-9

19. Novitskiy SV, Forrester E, Pickup MW, Gorska AE, Chytil A, Aakre M, Polosukhina D, Owens P, Yusupova DR, Zhao Z, Ye F, Shyr Y, Moses HL (2014) Attenuated transforming growth factor beta signaling promotes metastasis in a model of HER2 mammary carcinogenesis. Breast Cancer Res 16 (5):425. doi:10.1186/s13058-014-0425-7

20. Manai M, Thomassin-Piana J, Gamoudi A, Finetti P, Lopez M, Eghozzi R, Ayadi S, Lamine OB, Manai M, Rahal K, Charafe-Jauffret E, Jacquemier J, Viens P, Birnbaum D, Boussen H, Chaffanet M, Bertucci F (2017) MARCKS protein overexpression in inflammatory breast cancer. Oncotarget 8 (4):6246-6257. doi:10.18632/oncotarget.14057

21. Chen CH, Statt S, Chiu CL, Thai P, Arif M, Adler KB, Wu R (2014) Targeting myristoylated alanine-rich C kinase substrate phosphorylation site domain in lung cancer. Mechanisms and therapeutic implications. Am J Respir Crit Care Med 190 (10):1127-1138. doi:10.1164/rccm.201408-1505OC

22. Dorris E, O'Neill A, Hanrahan K, Treacy A, Watson RW (2017) MARCKS promotes invasion and is associated with biochemical recurrence in prostate cancer. Oncotarget 8 (42):72021-72030. doi:10.18632/oncotarget.18894

23. Zhang J, Liu Y, Yu CJ, Dai F, Xiong J, Li HJ, Wu ZS, Ding R, Wang H (2017) Role of ARPC2 in Human Gastric Cancer. Mediators Inflamm 2017:5432818. doi:10.1155/2017/5432818

24. Hanniford D, Segura MF, Zhong J, Philips E, Jirau-Serrano X, Darvishian F, Berman RS, Shapiro RL, Pavlick AC, Brown B, Osman I, Hernando E (2015) Identification of metastasis-suppressive microRNAs in primary melanoma. J Natl Cancer Inst 107 (3). doi:10.1093/jnci/dju494

25. Rauhala HE, Teppo S, Niemela S, Kallioniemi A (2013) Silencing of the ARP2/3 complex disturbs pancreatic cancer cell migration. Anticancer Res 33 (1):45-52

26. Hachim MY, Hachim IY, Dai M, Ali S, Lebrun JJ (2018) Differential expression of TGFbeta isoforms in breast cancer highlights different roles during breast cancer progression. Tumour Biol 40 (1):1010428317748254. doi:10.1177/1010428317748254

27. Matsuzaki K (2013) Smad phospho-isoforms direct context-dependent TGF-βeta signaling. Cytokine Growth Factor Rev 24 (4):385-399. doi:10.1016/j.cytogfr.2013.06.002

Supplementary material

<u>Additional file 1</u>: Supplementary Methods_Rypens.docx
A detailed description of all methods used in the study.
<u>Additional file 2</u>: Supplementary Tables and figure_Rypens.xlsx

- Fig. S1: Wound healing assays showing the effect of TGF-B on the migration IBC and nIBC cell lines
- Fig. S2: Global expression differences between IBC and nIBC cells that were treated with TGFβ1 for 1hr, 4hrs or 14hrs using unsupervised hierarchical cluster analysis of the 500 most variable genes measured by standard deviation
- Fig. S3: Forrest plot showing univariate (A) and multivariate (B) analysis comparing SMAD nuclear expression between IBC and nIBC.
- Fig. S4: Immunohistochemistry images for SMAD staining comparing tumor emboli to primary tumors
- Table S1: Differentially expressed genes in IBC and nIBC cells after four hours of TGFβ1 treatment.
- Table S2: Subset of Table S1; 272 genes that remain significant after correction for false discovery.
- Table S3: Gene lists showing TGFβ1-responsive genes in nIBC an IBC cells after four hours of TGFβ1 treatment.
- Table S4: Overview of the clinicopathological variables related to the patient series (76 IBC and 152 nIBC).

Combined transcriptomic and phosphopeptidomic profiling identifies AMPK and Hippo signaling as potential modulators of TGFβ1 signaling in IBC.

Unpublished data

Introduction

Inflammatory breast cancer (IBC) is an uncommon type of breast cancer that develops rapidly and progresses to metastatic disease in 30% of new diagnoses [1]. The aggressive behavior of IBC is translated into poor survival rates, which are significantly lower compared to non-inflammatory breast cancer patients [2, 3]. Despite therapeutic progresses, IBC is still responsible for a disproportionally high amount of breast-cancer related deaths. Therefore, there is an urgent need to identify biomarkers involved in therapeutic purposes of IBC and to improve patients' outcomes.

The past decades, several efforts have been undertaken to better elucidate the mechanisms of IBC aggressiveness and to identify pathways distinct to IBC [4-12], however many have failed validation in distinct data series. In 2013, a robust signature of 79 probes reporting an IBC-specific and molecular subtype-independent expression profile was published, indicating that TGF-β signaling might be an important driver of IBC biology [13]. Recently, Rypens and colleagues have investigated how TGF-β1 signaling is implicated in IBC biology and demonstrated that IBC cells exhibit a marked inability to engage cell motility following TGF-β1 treatment. This behavior was accompanied by a specific gene expression program following 4 hours of TGF-β1 treatment and characterized by repression and activation of respectively SMAD3 and MYC target genes [14].

The goal of the present study is to combine gene expression and peptide phosphorylation profiles of preclinical models to further unravel the signal transduction mechanisms that orchestrate the differential TGF-β response program in IBC and nIBC cells. Our results show nIBC cells, but not IBC cells, exhibit changes in protein kinase activity following TGF-β1 treatment. In addition, integrative analysis of mRNA and phosphopeptide profiles through protein-protein interaction networks demonstrate that TGF-β signaling in nIBC cells via TGFBR2 leads to activation of SMAD3 and modulators of epithelial-to-mesenchymal transition (i.e. ZEB1, ZEB2, SNAI1, SNAI2) via the non-canonical pathway involving several MAPK proteins (i.e. JNK, p38, TAK1). Moreover, several proteins possibly explaining the blunted TGF-β response in IBC cells were identified including TGIF2, PPP5C, AMPK, epigenetic modifiers, and Hippo signaling molecules.

Materials and Methods

Cell culture

Four nIBC cell lines, i.e. MCF7, SKBR3, MDA-MB-231, and MDA-MB-436 were purchased from ATCC (Manassas, USA) and cultured in respectively DMEM and RPMI

1640 medium supplemented with 10% FBS and antibiotics. Four IBC cell lines, i.e. KPL4, IBC3, SUM149 and SUM190 were a kindly gift from a kindly gift from MD Anderson Cancer Center, TX, USA. The KPL4 cell line is cultured in RPMI 1640 medium supplemented with 10% FBS and antibiotics. The SUM149, the SUM190 and IBC3 cell lines are cultured in Ham's F-12 Nutrient Mix, supplemented with 5% FBS, insulin, hydrocortisone and antibiotics. All cell lines are maintained in a 5% CO_2-humidified atmosphere at 37°C. Mycoplasma testing was performed monthly using the LookOut® Mycoplasma PCR Detection Kit (Sigma Aldrich, Missouri, USA).

Gene expression analysis

Gene expression data were measured using RNA-sequencing as described before [14]. Briefly, three IBC (i.e. SUM149, SUM190, KPL4) and three nIBC (i.e. MCF7, MDA-MB-231, MDA-MB-436) cell lines were treated with 5 ng/ml TGF-β1 for 1h, and 4hs and RNA was extracted using in-house protocols. RNA-sequencing was performed using stranded cDNA libraries on a HiSeq2000 system. Reads were mapped to the reference genome (hg19) using TopHat 2.0 and Bowtie 2.0. Genes with at least 10 reads in at least 10% of the samples were retained for further analysis (N=15.897). To inspect global expression themes, unsupervised hierarchical cluster analysis (UHCA) was performed for 1,000 genes with the strongest variation in gene expression measured by standard deviation. The dissimilarity matrix was calculated using Manhattan distance and clustering was performed using Ward linkage. Results were visualized in heatmap format using the R-package pheatmap.

Differences in gene expression were analyzed using generalized linear models (BioC-package limma). The design matrix was set up using a nested interaction formula with the cell type (i.e. IBC vs. nIBC) as main effect, a second term representing the interaction between cell type and TGF-β1 treatment, and a third term representing dominant clustering pattern as blocking variable. Genes differentially expressed between IBC and nIBC cells, between TGF-β1-treated and untreated IBC or nIBC cells, as well as genes that respond differently to TGF-β1 treatment in IBC and nIBC cell were identified. Genes with a raw P-value inferior to 5% were considered significant. Results are represented in volcano plot format.

To identify master regulators of differential gene expression following TGF-β1 treatment in IBC and nIBC cells, the BioC-package VIPER was used. The VIPER algorithm virtually infers protein activity levels of both transcription factors and signal transduction proteins based on target gene mRNA expression. It considers the mode of action (i.e. activation or suppression), the regulator-target gene interaction confidence and the pleiotropic nature of each target gene regulation. The VIPER algorithm was run without a null model and with lists of breast cancer specific target

genes for 6.053 regulators available through the BioC-package aracne.networks. Prior to analysis, nominal P-values resulting from differential gene expression analysis (vide supra) were Z-transformed. Secondary to the core VIPER analysis, leading edge genes were identified, and a shadow analysis was performed to identify pleiotropic interactions amongst significant regulators. Pleiotropic interactions were visualized as interaction maps using the R-packages igraph, ggraph and tidygraph. Proteins with an in-degree of at least 1, indicative of a shadow effect and identified through topological analysis of the interaction maps, were filtered out. Proteins with a false discovery rate (FDR) corrected P-value inferior to 10% were considered significant.

Kinase activity profiling

Four IBC (i.e. SUM149, SUM190, KPL4 and IBC3) and four nIBC cell lines (i.e. MCF7, SKBR3, MM231, MM436) were serum deprived for 24 hours. At time point 0, cells were harvested (i.e. baseline samples) or treated with 5ng/ml TGF-β1. Harvesting was performed by adding M-PER lysis buffer (Thermo Fisher Scientific), followed by incubation on ice for 15 minutes and finally collecting the cells using a cell scraper. The lysate was then centrifuged for 15 minutes at 16.000 x g at 4°C after which aliquots were snap frozen in liquid nitrogen and stored at -80°C until further use. The treated cells were harvested after 1 and 4 hour(s) of incubation. In parallel, untreated cells were harvested at the same time points to control for time dependent effects (i.e. untreated control samples). For all samples, protein quantification and the PamGene assay were performed in collaboration with the Protein chemistry, Proteomics and Epigenetic Signaling (PPES) lab from the Antwerp University. Using PamChip Tyrosine (PTK) and Serine/Threonine Kinase (STK) Array Chips and a PamStation 12 system according to manufacturer's instructions [15], phosphorylation profiles for respectively 197 and 144 peptides were evaluated.

Data preprocessing was done separately for STK and PTK chips as well as for the different TGF-β1 incubation times as these experiments were done on different time points. Raw S100 values were read into R and log2 transformed. Negative values were considered as missing values and peptides with missing data in more than 50% of the samples were filtered out. In total, 156 (PTK; 1h), 116 (STK; 1h), 152 (PTK; 4h) and 89 (STK; 4h) were retained for further analysis. Finally, data were quantile normalized to account for technical differences between arrays. Differences in peptide phosphorylation between conditions of interest were analyzed using generalized linear models with the same design matrix that was used for analyzing gene expression data (vide supra). Due to the lower number of features, raw p-values were not corrected for multiple testing and were considered significant if inferior to 5%.

Processed peptide phosphorylation data were translated into kinase activity scores, using single sample gene set enrichment analysis (ssGSEA; BioC-package gsva) with a Gaussian kernel to estimate the cumulative distribution function and a list of kinase substrate sets that is recorded in a proprietary database shared by PamGene. In this database, 99 (Y), 238 (T) and 204 (S) unique kinases that can phosphorylate at least one of the peptides retained in the final data set are identified, and most peptides can be phosphorylated by multiple kinases albeit with variable confidence. The confidence of a peptide/kinase interaction is expressed as a kinase rank score, which is a numerical value between 1 and 50 with low values indicating high confidence and vice versa. To define signature substrate sets for each kinase, the kinase rank score can be thresholded resulting in the definition of variably composed substrate sets that are either more or less specific depending on the selected cut-off value. To mitigate the effect of thresholding, kinase activity scores are calculated using substrate sets generated by applying different cut-off levels (i.e. 5, 6, 7, 8, 9, 10, 15, 20, 25, 30, 35, 40, 45, and 50) and resulting scores were compared between conditions of interest using generalized linear models with the same design matrix as described before (vide supra). Kinases for which minimally 5 significant observations are reported of which at least 3 for the lower kinase rank scores (i.e. <20) were retained. Results are visualized in heatmap format.

Pathway and network analysis

Master regulators identified using *VIPER* and differentially activated protein kinases identified using PamGene technology were integrated through protein-protein interaction (PPI) networks to identify signal transduction mechanisms that govern TGF-β in IBC and nIBC cells. Therefore, 3 sets of proteins that respond differently to TGF-β1 treatment in IBC and nIBC cells were identified: 1. Modulators of the TGF-β signaling pathway obtained from WikiPathways and Reactome; 2. Master modulators with an absolute normalized enrichment score of at least 5; and 3. Differentially activated protein kinases. All proteins were mapped onto the PPI network STRING that was downloaded from the website (https://www.string-db.org) and converted into an igraph object for manipulation in R (R-package *igraph*), and shortest paths between each pair or proteins was calculated. To evaluate the significance, the shortest path analysis was repeated for the same set of input proteins on 10 randomized networks with identical node degree distribution. The subgraph connecting all pairs of proteins was used to calculate node degree and centrality statistics and was subjected to louvain clustering to detect communities. For each community as well as for the full subgraph, overrepresentation analysis (ORA – BioC-package *fgsea*) was performed for WikiPathways and Reactome gene sets and results were collapsed to identify parental gene sets. For each of the communities, the 3 lists of TGF-β1 regulated proteins

described above were additionally tested. Enrichment in the full subgraph was tested against all proteins in the STRING network, whereas enrichment in the communities was tested against all proteins in the subgraph. Networks are visualized R-packages *tidygraph*, *ggraph*, and *ggpubr*.

Results

Gene expression analysis

UHCA (Figure 1A) identifies two sample clusters (i.e. downstream of the first bifurcation), aligning with clear differences in gene expression patterns. However, no clear relationship between samples clusters and target variables (i.e. tumor phenotype and TGF-β1 treatment duration) is observed. IBC and nIBC cell lines are represented in both clusters and presumably cluster based on their molecular subtype, as described earlier [14]. Replicate samples of cell lines cluster on terminal branches and the expression profile obtained after 4 hours of TGF-β1 treatment is most dissimilar in all cell lines. These data suggest that an effect of TGF-β1 treatment on gene expression in IBC and nIBC cells will be subtle and can be obscured by confounding variables in the data set.
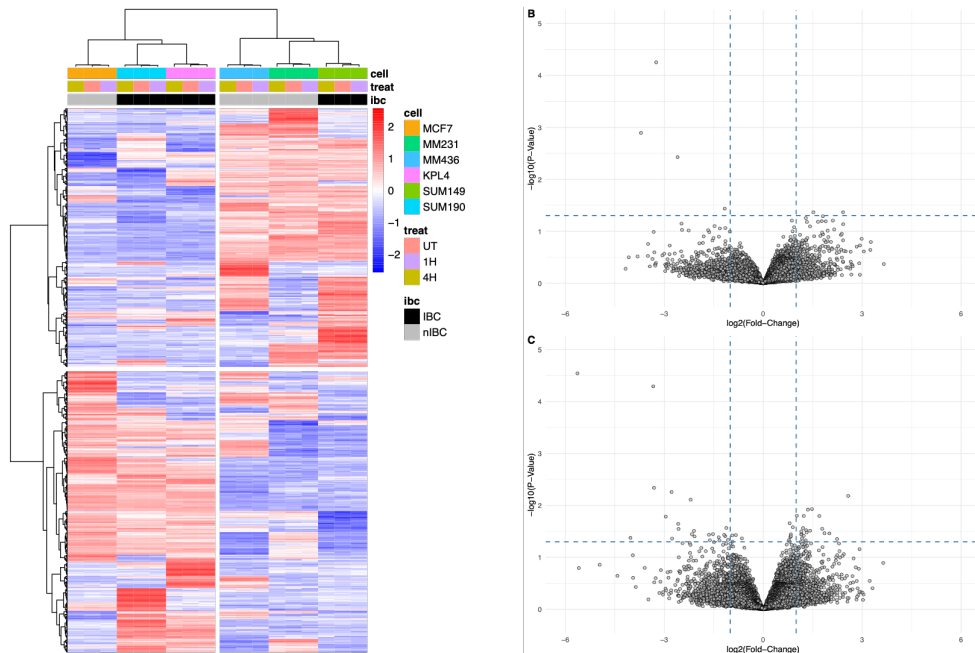

Figure 1. A: Heatmap showing global themes in the mRNA data set in matrix format. Genes and samples are organized in row and columns respectively and are ordered according to the dendrograms shown on top and to the left. Sample annotations are indicated underneath the top dendrogram following the legend shown to the right. Gene expression data are coded according to a blue-red coloring scheme representing under- and overexpression respectively. **B**: Volcano

plot showing genes that respond differently in IBC and nIBC cells following 1h of TGF-β1 treatment. Each gene is represented by a dot. The X-axis denotes to log2-tranformed fold change and 2-fold expression differences are indicated using a vertical dashed line. The –log10 transformed P-value is plotted along the Y-axis with a threshold of 5% indicated using a horizontal dashed line. Genes that have a higher expression change in the treated relative to the control IBC cells as compared to the treated relative to the control nIBC cells have a positive expression fold change and vice versa. **C**: Volcano plots showing genes that respond differently in IBC and nIBC cells follwing 4h of TGF-β1 treatment. Each gene is represented by a dot. The X-axis denotes to log2-tranformed fold change and 2-fold expression differences are indicated using a vertical dashed line. The –log10 tranformed P-value is plotted along the Y-axis with a threshold of 5% indicated using a horizontal dashed line. Genes that have a higher expression change in the treateds relative to the control IBC cells as compared to the treated relative to the control nIBC cells have a positive expression fold change and vice versa.

Differences in gene expression for individual genes between various conditions are shown in volcano plot format in supplementary Figure 1. In line with the results obtained with UHCA (Figure 1A), limited numbers of differentially expressed genes between samples grouped by the target variables were identified: 2,448 genes between IBC and nIBC cells, 5 and 13 genes between TGF-β1-treated and control nIBC cells at 1 and 4 hours respectively, 37 and 275 genes between TGF-β1-treated and control IBC cells at 1 and 4 hours respectively, and 6 and 54 genes that respond differently in IBC and nIBC cells to respectively 1 and 4 hours of TGF-β1 treatment. The latter results are also shown in a rescaled volcano plot format in Figures 1B and 1C. These data reveal that the effect of TGF-β1 on gene expression is most pronounced in IBC cells following 4 hours of treatment.

VIPER analysis was then performed to infer virtual protein activity differences between the conditions of interest. Although differences in gene expression were limited, a more elaborate set of differentially activated proteins was identified with respect to the various contrasts: 1,113 proteins between IBC and nIBC cells, 114 and 540 proteins between TGF-β1-treated and control nIBC cells at 1 and 4 hours respectively, 701 and 654 proteins between TGF-β1-treated and control IBC cells at 1 and 4 hours respectively, and 779 and 663 proteins that respond differently in IBC and nIBC cells to respectively 1 and 4 hours of TGF-β1 treatment. As the aim of the present analysis is to gain insight into the TGF-β signal transduction differences between IBC and nIBC cells, the remainder of the analysis focused on the latter two protein sets. Amongst these, sets of 50 and 53 proteins with a differential TGF-β1 response profile at respectively 1 and 4 hours were identified based on topological analysis of the pleiotropic interaction maps (supplementary Figures 2, 3, 4, and 5) and enrichment statistics (i.e. absolute normalized enrichment score of at least 5). Results are shown in Figure 2 (upper panels). Second, sets of TGF-β signal transduction molecules, obtained from Reactome and WikiPathways, with a differential response profile were identified and include

SMAD3, TGFBR2 and various molecules involved in epithelial-to-mesenchymal transition (i.e. SNAI1, SNAI2, ZEB1, ZEB2). All these proteins are activated at a higher level in nIBC relative to IBC cells following TGF-β1 treatment. Results are shown in Figure 2 (lower panels).
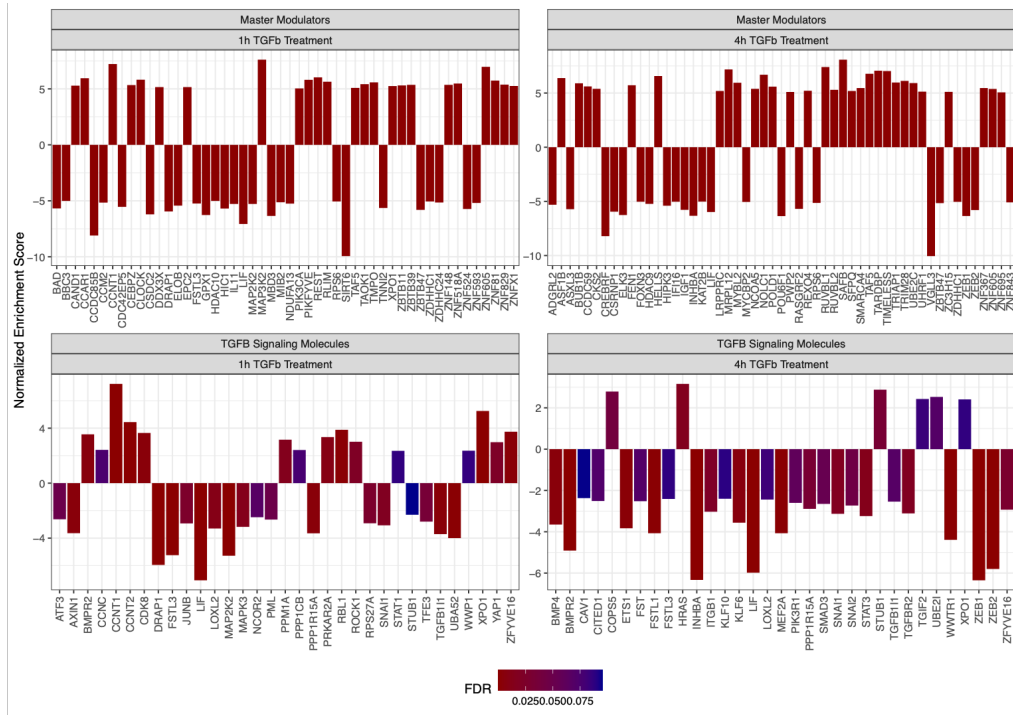

Figure 2. Results of the VIPER analysis are shown in bar plot format. The four panels represent TGF-β signaling proteins (top row) or TGF-β responsive proteins (bottom row) that respond differently in IBC and nIBC cells to 1h (first column) or 4hs (last column) of TGF-β treatment. Genes are plotted along the X-axis, the normalized enrichment score resulting from the VIPER analysis is shown along the Y-axis. Each bar is color-coded according to the significance of the enrichment analysis, following the legend shown underneath the panel.

Kinase activity profiling

Numbers of differentially phosphorylated peptides per condition are visualized in bar plot format in Figure 3A and B. First, the number of differentially phosphorylated peptides is greater after 4hs of TGF-β1 treatment as compared to 1h of TGF-β1 treatment. Second, TGF-β1 treatment of nIBC cells results in larger numbers of differentially phosphorylated peptides as compared to TGF-β1 treatment of IBC cells. Third, differential phosphorylation events between TGF-β1 treated and untreated cells predominantly involve serine or threonine residues. When translating peptide phosphorylation profiles into kinase activity values, these observations are largely recapitulated (Figure 3C), except for a marked increase in tyrosine kinase activity in

nIBC cells following 4hs of TGF-β1 treatment. Interestingly, virtual all these kinases (i.e. CDK2, CDKL1, CDKL2, ERK5, JNK1, JNK2, JNK3, MAP3K5, MAP3K7 and NEK1) also respond differently in IBC and nIBC cells following 4hs of TGF-β1 treatment, suggesting these are involved in the modulation of the TGF-β signaling pathway in IBC cells. In addition, also the serine/threonine kinases CDK9 and CHK2 exhibit a similar profile.
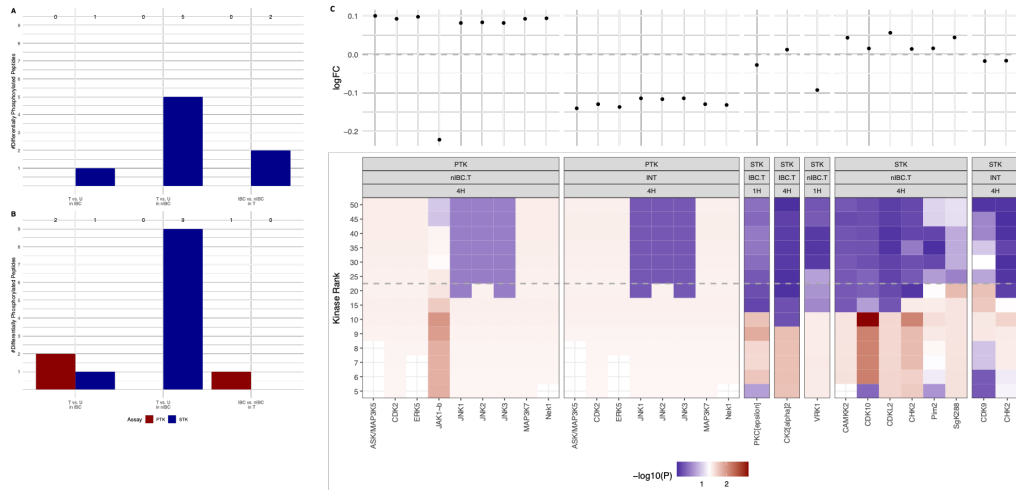
Figure 3. A: Number of differentially phosphorylated peptides (Y-axis) following 1h of TGF-β treatment are shown in bar plot format. Contrasts are listed along the X-axis (T vs U in IBC = TGFB treated vs. untreated in IBC, T vs U in nIBC = treated vs. untreated in nIBC, IBC vs nIBC in T = differentially phosphorylated in IBC and nIBC cells following TGFB treatment). Bars are color-coded according to the used assay following the legend indicated underneath the plot. The exact numbers of differentially phosphorylated peptides are indicated on top of each bar. **B:** Number of differentially phosphorylated peptides (Y-axis) following 4h of TGF-β treatment are shown in bar plot format. Contrasts are listed along the X-axis (T vs U in IBC = TGFB treated vs. untreated in IBC, T vs U in nIBC = treated vs. untreated in nIBC, IBC vs nIBC in T = differentially phosphorylated in IBC and nIBC cells following TGFB treatment). Bars are color-coded according to the used assay following the legend indicated underneath the plot. The exact numbers of differentially phosphorylated peptides are indicated on top of each bar. **C:** Significance values of differentially activated protein kinases according to different kinase rank values are shown in heatmap format. The kinase rank describes how much a peptide-kinase link can be trusted, i.e. a low kinase rank demonstrates a high probability that a peptide is phosphorylated by that kinase, whereas a high kinase rank demonstrates a low probability. In subsequent iterations, a higher kinase rank (5, 6, 7, 8, 9, 10, 15, 20, 25…) was accepted to identify differentially activated protein kinases. The accepted kinase rank is plotted along the Y-axis. This exercise was done for each assay (i.e. PTK and STK), condition (nIBC.T= TGFB treated vs. untreated in nIBC, IBC.T = TGFB treated vs untreated in IBC, INT = differentially phosphorylated in IBC and nIBC cells following TGFB treatment), and time point (4H vs 1H) and is shown in a distinct panel. Within each panel, relevant kinases are listed along the X-axis. Cells are color-coded according to the –log10 transformed P-value following the legend underneath. The kinase rank of 20, which was used in the analysis as cut-off to differentiate

between low and high kinase ranks, is indicated using a vertical dotted line. For each of the identified kinases, at least 3 significant results (i.e. red cells) for lower kinase rank values were observed. On top of the heatmap, the log2-transformed fold change is indicated using a dot plot format with a horizontal dashed lined denoting the threshold of 0. Positive fold changes indicate that the kinase is more active in the TGF-β treated relative to the untreated condition or is stronger activated in IBC treated vs control cells than in nIBC treated vs. control cells. Negative fold changes denote the opposite pattern.

Pathway and network analysis

To identify signal transduction mechanisms that govern TGF-β signaling, 92 proteins (i.e. master modulators identified using VIPER or kinases identified using PamGene) that exibit a different response profile in IBC and nIBC cells following 4hs of TGF-β1 treatment were mapped onto the PPI-network STRING. In total, 30,452 shortest paths between all pairs of proteins (N=4,186 unique combinations) were identified with a median path length of 4 (range: 2-6) and vouching for 1,384 intermediate proteins. On average, each intermediate protein is part of 0.052% (range: 0.013% - 6.200%) of the identified shortest paths. Repeating the same analysis on 10 randomized PPI networks with identical node degree distribution returned on average 5,909 intermediate proteins, which is significantly higher than the number observed using the original STRING network (P<0.001) and indicates that the set 92 seed proteins and 1,384 intermediate proteins constitutes a local community. Furthermore, 97/1,384 intermediate proteins from the original analysis are significantly (P<0.050) more frequently involved any shortest path of the randomized networks, and thus were filtered out due lack of specificity. Furthermore, the set of 1,287 intermediate proteins was significantly enriched for master modulators identified using VIPER that were not part of the original seed list, resulting in a set of 74 additional TGF-β1 responsive proteins that are part of the identified network (OR=2.502; P<0.001). Finally, ORA for gene sets belonging to WikiPathways and Reactome revealed respectively 51 and 83 enriched pathways, including several gene sets associated with TGF-β signaling. Results are shown in supplementary Figure 6 and 7.

The identified subgraph was subjected to clustering, and 6 communities with an average modularity of 0.41 were identified. The largest community, consisting of 528 proteins was subjected to a second clustering step revealing 9 additional communities with an average modularity of 0.42. For each community, ORA was performed for the 3 lists of seed proteins as well as for the list of 74 additional TGF-β1 responsive proteins. Results are shown in Figure 4A. In the full network, 3 communities (i.e. M1, M5 and M6) are enriched for at least one of the target gene sets and contain at least one kinase. Within the first community, based on similar rules, two additional interesting protein clusters were identified (i.e. M1C2 and M1C9). The relative activity changes of the

communities in IBC vs. nIBC cells following TGF-β1 treatment, evaluated by the averaged normalized enrichment scores of the member proteins, are shown in Figure 4B and reveal that M5 and M1C9 are activated in IBC cells whereas the TGF-β-related communities M6 and M1C2 are activated in nIBC cells. Node degree statistics, revealing the importance of the seed and intermediate proteins in their module, are shown in Figure 4C. Network representation of M5, M6, M1C2 and M1C9 are shown in Figure 5.
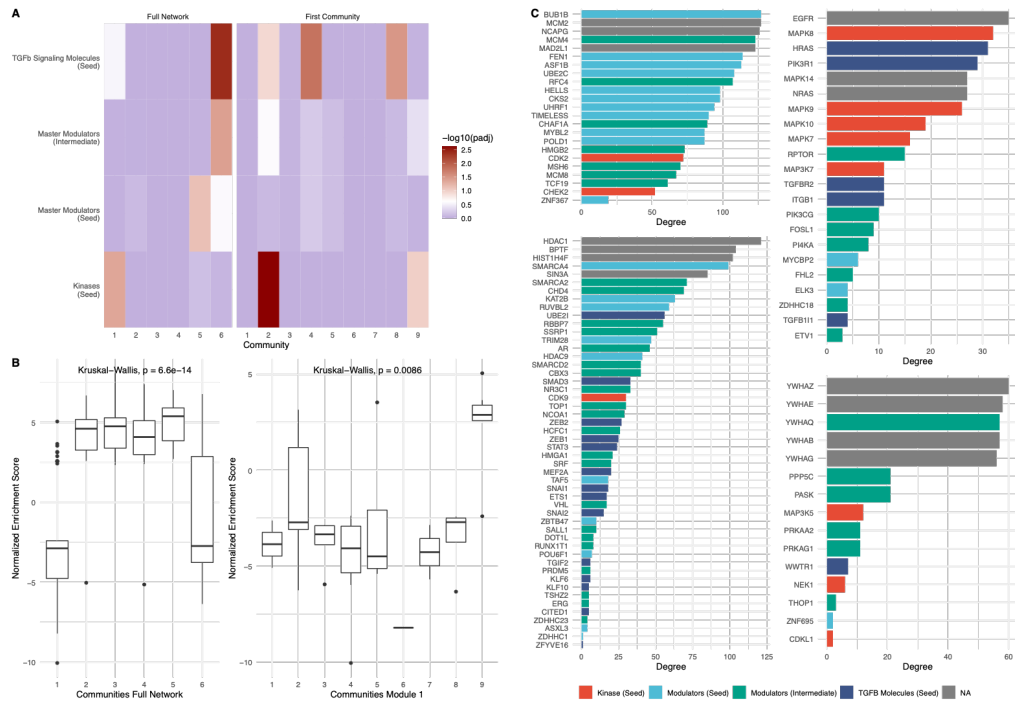
Figure 4. A: Enrichment results of network communities for four lists of TGF-β responsive proteins are shown in heatmap format. The communities are listed along the X-axis, the gene lists of interest are indicated along the Y-axis. Two panels are provided showing the results for the full network (left) and for the first community within that network (right). Cells are color-coded according to the –log10 transformed P-value as indicated in the legend. Red colors denote significant results. **B:** The global activities of each community in IBC relative to nIBC cells following 4hs of TGF-β treatment are shown in boxplot format. The communities are indicated along the X-axis, the averaged normalized enrichment score of the community specific TGF-β-responsive proteins is shown along the Y-axis. Positive normalized enrichment scored indicate communities that are more strongly activated in IBC as compared to nIBC following TGF-β treatment. Negative normalized enrichment scores indicate the opposite pattern. Two panels showing the results of the full network (left) and the first community within that network (right) are provided. P-values resulting from comparing the distributions of the normalized enrichment scores between the different clusters and calculated using Kruskal-Wallis test are shown on top. **C:** Four communities with interesting enrichment patterns were identified. For each of these, the node degree distribution is shown in barplot format with the degree plotted along the X-axis and TGF-β-responsive proteins are plotted along the Y-axis. Bars are color-coded according to

the legend underneath indicating the specific list of TGF-β-responsive proteins the corresponding protein belongs to. In addition, for each community the degree of the top 5 proteins is also provided as a reference. For each community, a different panel is provided: M5, M6, M1C2 and M1C9 from top to bottom and from left to right.

To test for functional enrichment patterns, ORA for gene sets belonging to WikiPathways and Reactome was performed, and results are shown in supplementary Figure 5A and B. Both M6 and M1C2 are enriched for core TGF-β signaling molecules (i.e. SMAD3, TGFBR2) in addition to proteins involved in the modulation of gene expression and epigenetic reprogramming in M6 (i.e. SMARCA2, SMARCA4, SIN3A, KAT2B) and kinases associated with stress and non-canonical TGF-β signaling in M1C2 (i.e. CDK9, MAPK7, MAPK8, MAPK9, MAPK10, MAPK14, MAP3K7). In addition, M6 also contains many proteins involved in epithelial-to-mesenchymal transition (i.e. ZEB1, ZEB2, SNAI1, SNAI). In addition, M6 and M1C2 are linked through MAPK7 suggesting both networks are jointly involved in TGF-β signaling in nIBC cells, primarily via the non-canonical pathway. Importantly, although the M6 and M1C2 communities are globally activated in nIBC relative to IBC cells following TGF-β1 treatment (Figure 4B), not all network members adhere to that pattern (Figure 5). These proteins could explain why the TGF-β pathway in IBC cells operates differently. Finally, the M5 and M1C9 modules that are globally activated in IBC relative to nIBC cells following TGF-β1 treatment are involved in DNA metabolism and cell proliferation (M5) and apoptosis, Hippo and AMPK signaling (M1C9).
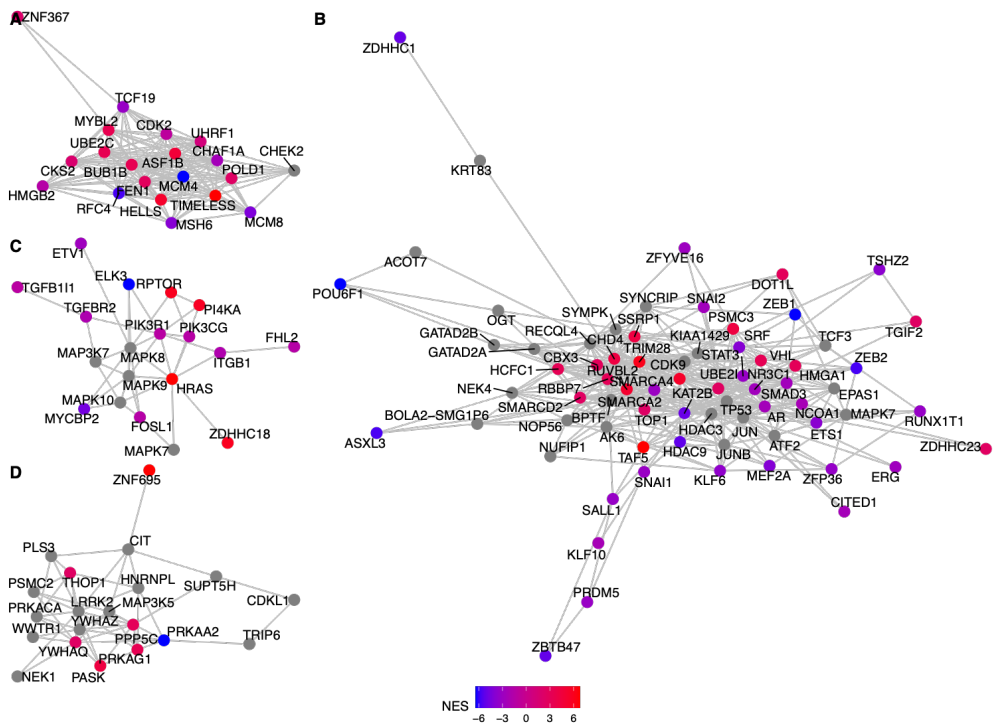
Figure 5. Network representations for each of the identified communities enriched for any of the TGF-β-responsive protein lists: M5 (A), M6 (B), M1C2 (C) and M1C9 (D). Proteins (nodes) are represented as dots and interactions (edges) as grey lines. Each protein for which normalized enrichment scores resulting from the VIPER analysis are available are color-coded according to the legend shown underneath, with red indicating a protein that becomes more active in IBC cells relative to nIBC cells following TGF-β treatments and blue indicating the opposite pattern.

Discussion

In this paper, mRNA and peptide phosphorylation data were integrated using network-based approaches to unravel the molecular mechanisms that are responsible for the apparent differences in TGF-β signaling between IBC and nIBC cells. By combining different layers into a PPI network, 4 modules or clusters of strongly interacting genes were identified containing proteins or kinases that respond differently to TGF-β1 treatment in IBC and nIBC cells. By inspecting the relative activity changes of the proteins of these gene clusters, 2 modules were identified that are globally more active in nIBC relative to IBC following TGF-β1 treatment. Both modules contain many proteins involved in TGF-β/SMAD3 signal transduction pathway, thereby corroborating earlier hypotheses that stimulation of nIBC cells with TGF-β1 augments SMAD3 transcriptional activity via non-canonical TGF-β signaling [14, 16, 17]. In addition, several proteins responsible for epithelial-to-mesenchymal transition (i.e. ZEB1, ZEB2, SNAI1, SNAI2) are also part of these modules, which aligns with the observations that breast cancer cells of the non-inflammatory phenotype activate cell motility by switching to a mesenchymal state upon stimulation with TGF-β1 [18-20].

The same analysis identified 2 modules with globally increased protein activities in IBC relative to nIBC following TGF-β1 treatment. One of these modules is part of a larger gene cluster that also contains one of the modules involved in non-canonical TGF-β/SMAD3 signaling, suggesting strong cross-regulation between both networks. Proteins contained in the module that is activated in IBC are involved in oxidative stress induced apoptosis (i.e. MAP3K5, and PPP5C), AMPK signaling (i.e. PRKAG1, PRKACA, and PRKAA2), and Hippo signaling (i.e WWTR1). Previous studies already revealed that these pathways can modulate the TGF-β signaling, and the present network analysis suggest that these interactions are also relevant in the context of IBC biology. Each of above identified pathways will be further discussed in the following paragraphs.

In the past, reports have shown that AMPK can inhibit TGF-β signaling, SMAD2/3 activation and EMT in breast cancer as well as in other diseases [21-26]. The AMPK pathway is an energy sensing pathway that alters cell metabolism and biology when the ATP:AMP ratio is low. In cancer biology, AMPK signaling has been associated both with tumor suppressive and promoting effects. In general, activation of AMPK inhibits

signaling pathways that promote cell growth and proliferation and activates autophagy when cellular energy levels are low. Oncogenic signaling is an important stimulator of AMPK activity by straining cells from nutrients and energy by vigorously engaging cell proliferation as well as by inducing DNA damage which is sensed by the AMPK upstream activator STK11. In this context, AMPK signaling protects cancer cells under conditions of oncogenic stress, a process that has been documented particularly for the MYC oncogene [27]. In IBC, activation of oncogenes including MYC as well as genomic scars associated with DNA damage have been frequently reported [14, 28-31]. Therefore, alterations in AMPK signaling secondary to MYC-induced DNA damage may contribute to the observed inhibition of TGF-β/SMAD3 signaling in IBC.

In addition to AMPK, also the Hippo pathway is a known modulator of TGF-β signaling. The Hippo pathway operates by inhibiting the YAP and WWTR1/TAZ transcription factors and controls organ size by regulating cell proliferation and apoptosis. Ample evidence exits that both YAP and WWTR1/TAZ are involved in altering the activity of SMAD transcription factors amongst others by regulating their nucleocytoplasmic localization [32-38]. More precisely, Hippo signaling stimulates LATS-dependent phosphorylation and proteasomal degradation of YAP and WWTR1/TAZ thereby inhibiting nuclear localization and transcriptional activation of SMAD proteins. Interestingly, several lines of evidence exist showing that activated AMPK facilitates the phosphorylation and proteasomal degradation of YAP and WWTR1/TAZ [39, 40] also in a MYC-dependent manner [41], suggesting that the inhibition of TGF-β by AMPK mentioned above is mediated by crosstalk with the Hippo signal transduction machinery.

Two proteins involved in oxidative stress mediated apoptosis (i.e. MAP3K5, and PPP5C) were also identified as part of the IBC activated network module. MAP3K5, also known as ASK1, is an important signal transduction protein in the TGF-β pathway that orchestrates TGF-β-dependent cell death responses to oxidative stress [42-44] in conjunction with PPP5C [45, 46]. PPP5C is a protein serine/threonine phosphatase that inactivates a wide range of signal transduction proteins including SMAD3 [47]. PPP5C is also known to alter AMPK signaling, although most of the reports indicate that this interaction is antagonistic [48-50]. In addition, literature has shown that PPP5C is involved in sensing DNA damage by regulation by ATM and ATR mechanisms [51, 52], again suggesting that DNA damage in IBC may be an important driver of intrinsic cancer cell signaling mechanisms. In this context, it is worth mentioning that the second network module enriched with protein activated in IBC is entirely devoted to DNA metabolism and damage repair.

Finally, the present data also support a role for epigenetic chromatin remodeling in suppressing TGF-β signaling in IBC. Several studies have shown that ARID1A, a member of the SWI/SNF chromatin remodeling complex is able to inhibit the TGF-β pathway [53-55], most likely by interfering with chromosome accessibility and denying SMAD transcription factors from binding to the promotors of their target genes. In IBC, ARID1A is often mutated [28, 56] and this study demonstrated that several SMARCA proteins are part of the PPI module that involves SMAD3. In addition, all of them exhibit increased activity levels in IBC cells relative to nIBC cells following TGF-β1 treatment. The role of chromatin remodeling in repression of the TGF-β pathway is also corroborated by the upregulation of TGIF2 in IBC cells after 4h of TGF-β1 treatment. TGIF2 is a TGF-β-inducible gene that is overexpressed in IBC patient samples in a molecular subtype independent manner and is part of the 79 gene model that accurately discriminates between IBC and nIBC tissue samples and preclinical models. Literature has shown that TGIF2 can repress SMAD transcription through interaction with histone deacetylases [57] and polycomb repressor 2 complexes [58]. Expression of EZH2, which is the catalytic subunit of the polycomb repressor complexes, has been documented in more than 75% of IBC patient samples [59]. Lastly, also the Hippo pathway is known to be involved in chromatin remodeling [60] and YAP1 has been shown to regulate SMAD3 activity by altering chromatin accessibility [61].

In conclusion, the present study was undertaken to gain more insight into the biology responsible for the observed difference in TGF-β/SMAD3 responses between IBC and nIBC cells. By integrating gene expression and peptide phosphorylation profiles of preclinical IBC and nIBC models treated with TGF-β1, 4 candidate mechanisms were discovered including AMPK-, Hippo-, PP5/MAP3K5-signaling as well as chromatin remodeling. The exact contribution of these pathways to the establishment of TGF-β resistance in IBC cells remains a matter of debate and requires further investigation, but DNA damage and/or oncogenic stress is a potential driver.

References

1. Wang Z, Chen M, Pan J, Wang X, Chen XS, Shen KW: Pattern of distant metastases in inflammatory breast cancer - A large-cohort retrospective study. J Cancer 2020, 11(2):292-300.

2. Dawood S, Ueno NT, Valero V, Woodward WA, Buchholz TA, Hortobagyi GN, Gonzalez-Angulo AM, Cristofanilli M: Differences in survival among women with stage III inflammatory and noninflammatory locally advanced breast cancer appear early: a large population-based study. Cancer 2011, 117(9):1819-1826.

3. Fouad TM, Kogawa T, Liu DD, Shen Y, Masuda H, El-Zein R, Woodward WA, Chavez-MacGregor M, Alvarez RH, Arun B et al: Overall survival differences between patients with inflammatory and noninflammatory breast cancer presenting with distant metastasis at diagnosis. Breast Cancer Res Treat 2015, 152(2):407-416.

4. Kleer CG, van Golen KL, Braun T, Merajver SD: Persistent E-cadherin expression in inflammatory breast cancer. Mod Pathol 2001, 14(5):458-464.

5. Guerin M, Gabillot M, Mathieu MC, Travagli JP, Spielmann M, Andrieu N, Riou G: Structure and expression of c-erbB-2 and EGF receptor genes in inflammatory and non-inflammatory breast cancer: prognostic significance. Int J Cancer 1989, 43(2):201-208.

6. Cabioglu N, Gong Y, Islam R, Broglio KR, Sneige N, Sahin A, Gonzalez-Angulo AM, Morandi P, Bucana C, Hortobagyi GN et al: Expression of growth factor and chemokine receptors: new insights in the biology of inflammatory breast cancer. Ann Oncol 2007, 18(6):1021-1029.

7. Masuda H, Zhang D, Bartholomeusz C, Doihara H, Hortobagyi GN, Ueno NT: Role of epidermal growth factor receptor in breast cancer. Breast Cancer Res Treat 2012, 136(2):331-345.

8. van Golen KL, Davies S, Wu ZF, Wang Y, Bucana CD, Root H, Chandrasekharappa S, Strawderman M, Ethier SP, Merajver SD: A novel putative low-affinity insulin-like growth factor-binding protein, LIBC (lost in inflammatory breast cancer), and RhoC GTPase correlate with the inflammatory breast cancer phenotype. Clin Cancer Res 1999, 5(9):2511-2519.

9. Shirakawa K, Kobayashi H, Heike Y, Kawamoto S, Brechbiel MW, Kasumi F, Iwanaga T, Konishi F, Terada M, Wakasugi H: Hemodynamics in vasculogenic mimicry and angiogenesis of inflammatory breast cancer xenograft. Cancer Res 2002, 62(2):560-566.

10. Van der Auwera I, Van Laere SJ, Van den Eynden GG, Benoy I, van Dam P, Colpaert CG, Fox SB, Turley H, Harris AL, Van Marck EA et al: Increased angiogenesis and lymphangiogenesis in inflammatory versus noninflammatory breast cancer by real-time reverse transcriptase-PCR gene expression quantification. Clin Cancer Res 2004, 10(23):7965-7971.

11. Silvera D, Arju R, Darvishian F, Levine PH, Zolfaghari L, Goldberg J, Hochman T, Formenti SC, Schneider RJ: Essential role for eIF4GI overexpression in the pathogenesis of inflammatory breast cancer. Nat Cell Biol 2009, 11(7):903-908.

12. Wang X, Saso H, Iwamoto T, Xia W, Gong Y, Pusztai L, Woodward WA, Reuben JM, Warner SL, Bearss DJ et al: TIG1 promotes the development and progression of inflammatory breast cancer through activation of Axl kinase. Cancer Res 2013, 73(21):6516-6525.

13. Van Laere SJ, Ueno NT, Finetti P, Vermeulen P, Lucci A, Robertson FM, Marsan M, Iwamoto T, Krishnamurthy S, Masuda H et al: Uncovering the molecular secrets of inflammatory breast cancer biology: an integrated analysis of three distinct affymetrix gene expression datasets. Clin Cancer Res 2013, 19(17):4685-4696.

14. Rypens C, Marsan M, Van Berckelaer C, Billiet C, Melis K, Lopez SP, van Dam P, Devi GR, Finetti P, Ueno NT et al: Inflammatory breast cancer cells are characterized by abrogated TGFbeta1-dependent cell motility and SMAD3 activity. Breast Cancer Res Treat 2020.

15. Haetscher N, Feuermann Y, Wingert S, Rehage M, Thalheimer FB, Weiser C, Bohnenberger H, Jung K, Schroeder T, Serve H et al: STAT5-regulated microRNA-193b controls haematopoietic stem and progenitor cell expansion by modulating cytokine receptor signalling. Nat Commun 2015, 6:8928.

16. Kohn EA, Yang YA, Du Z, Nagano Y, Van Schyndle CM, Herrmann MA, Heldman M, Chen JQ, Stuelten CH, Flanders KC et al: Biological responses to TGF-beta in the mammary epithelium show a complex dependency on Smad3 gene dosage with important implications for tumor progression. Mol Cancer Res 2012, 10(10):1389-1399.

17. Matise LA, Palmer TD, Ashby WJ, Nashabi A, Chytil A, Aakre M, Pickup MW, Gorska AE, Zijlstra A, Moses HL: Lack of transforming growth factor-beta signaling promotes collective cancer cell invasion through tumor-stromal crosstalk. Breast Cancer Res 2012, 14(4):R98.

18. Piek E, Moustakas A, Kurisaki A, Heldin CH, ten Dijke P: TGF-(beta) type I receptor/ALK-5 and Smad proteins mediate epithelial to mesenchymal transdifferentiation in NMuMG breast epithelial cells. J Cell Sci 1999, 112 (Pt 24):4557-4568.

19. Deckers M, van Dinther M, Buijs J, Que I, Lowik C, van der Pluijm G, ten Dijke P: The tumor suppressor Smad4 is required for transforming growth factor beta-induced epithelial to mesenchymal transition and bone metastasis of breast cancer cells. Cancer Res 2006, 66(4):2202-2209.

20. Zhang J, van Dinther M, Thorikay M, Gourabi BM, Kruithof BPT, Ten Dijke P: Opposing USP19 splice variants in TGF-beta signaling and TGF-beta-induced epithelial-mesenchymal transition of breast cancer cells. Cell Mol Life Sci 2023, 80(2):43.

21. Lin H, Li N, He H, Ying Y, Sunkara S, Luo L, Lv N, Huang D, Luo Z: AMPK Inhibits the Stimulatory Effects of TGF-beta on Smad2/3 Activity, Cell Migration, and Epithelial-to-Mesenchymal Transition. Mol Pharmacol 2015, 88(6):1062-1071.

22. Li NS, Zou JR, Lin H, Ke R, He XL, Xiao L, Huang D, Luo L, Lv N, Luo Z: LKB1/AMPK inhibits TGF-beta1 production and the TGF-beta signaling pathway in breast cancer cells. Tumour Biol 2016, 37(6):8249-8258.

23. Thakur S, Viswanadhapalli S, Kopp JB, Shi Q, Barnes JL, Block K, Gorin Y, Abboud HE: Activation of AMP-activated protein kinase prevents TGF-beta1-induced epithelial-mesenchymal transition and myofibroblast activation. Am J Pathol 2015, 185(8):2168-2180.

24. Zou J, Li C, Jiang S, Luo L, Yan X, Huang D, Luo Z: AMPK inhibits Smad3-mediated autoinduction of TGF-beta1 in gastric cancer cells. J Cell Mol Med 2021, 25(6):2806-2815.

25. Wang L, Tian Y, Shang Z, Zhang B, Hua X, Yuan X: Metformin attenuates the epithelial-mesenchymal transition of lens epithelial cells through the AMPK/TGF-beta/Smad2/3 signalling pathway. Exp Eye Res 2021, 212:108763.

26. Pan Y, Liu L, Li S, Wang K, Ke R, Shi W, Wang J, Yan X, Zhang Q, Wang Q et al: Activation of AMPK inhibits TGF-beta1-induced airway smooth muscle cells proliferation and its potential mechanisms. Sci Rep 2018, 8(1):3624.

27. Haikala HM, Anttila JM, Klefstrom J: MYC and AMPK-Save Energy or Die! Front Cell Dev Biol 2017, 5:38.

28. Bertucci F, Rypens C, Finetti P, Guille A, Adelaide J, Monneur A, Carbuccia N, Garnier S, Dirix P, Goncalves A et al: NOTCH and DNA repair pathways are more frequently targeted by genomic alterations in inflammatory than in non-inflammatory breast cancers. Mol Oncol 2020, 14(3):504-519.

29. Faldoni FLC, Villacis RAR, Canto LM, Fonseca-Alves CE, Cury SS, Larsen SJ, Aagaard MM, Souza CP, Scapulatempo-Neto C, Osorio C et al: Inflammatory Breast Cancer: Clinical Implications of Genomic Alterations and Mutational Profiling. Cancers (Basel) 2020, 12(10).

30. Rypens C, Bertucci F, Finetti P, Robertson F, Fernandez SV, Ueno N, Woodward WA, Van Golen K, Vermeulen P, Dirix L et al: Comparative transcriptional analyses of preclinical models and patient samples reveal MYC and RELA driven expression patterns that define the molecular landscape of IBC. NPJ Breast Cancer 2022, 8(1):12.

31. Li X, Kumar S, Harmanci A, Li S, Kitchen RR, Zhang Y, Wali VB, Reddy SM, Woodward WA, Reuben JM et al: Whole-genome sequencing of phenotypically distinct inflammatory breast cancers reveals similar genomic alterations to non-inflammatory breast cancers. Genome Med 2021, 13(1):70.

32. Qin Z, Xia W, Fisher GJ, Voorhees JJ, Quan T: YAP/TAZ regulates TGF-beta/Smad3 signaling by induction of Smad7 via AP-1 in human skin dermal fibroblasts. Cell Commun Signal 2018, 16(1):18.

33. Labibi B, Bashkurov M, Wrana JL, Attisano L: Modeling the Control of TGF-beta/Smad Nuclear Accumulation by the Hippo Pathway Effectors, Taz/Yap. iScience 2020, 23(8):101416.

34. Pseftogas A, Xanthopoulos K, Poutahidis T, Ainali C, Dafou D, Panteris E, Kern JG, Varelas X, Hardas A, Gonidas C et al: The Tumor Suppressor CYLD Inhibits Mammary Epithelial to Mesenchymal Transition by the Coordinated Inhibition of YAP/TAZ and TGFb Signaling. Cancers (Basel) 2020, 12(8).

35. Gu K, Fu X, Tian H, Zhang Y, Li A, Wang Y, Wen Y, Gu W: TAZ promotes the proliferation and osteogenic differentiation of human periodontal ligament stem cells via the p-SMAD3. J Cell Biochem 2020, 121(2):1101-1113.

36. Speight P, Kofler M, Szaszi K, Kapus A: Context-dependent switch in chemo/mechanotransduction via multilevel crosstalk among cytoskeleton-regulated MRTF and TAZ and TGFbeta-regulated Smad3. Nat Commun 2016, 7:11642.

37. Varelas X, Sakuma R, Samavarchi-Tehrani P, Peerani R, Rao BM, Dembowy J, Yaffe MB, Zandstra PW, Wrana JL: TAZ controls Smad nucleocytoplasmic shuttling and regulates human embryonic stem-cell self-renewal. Nat Cell Biol 2008, 10(7):837-848.

38. Grannas K, Arngarden L, Lonn P, Mazurkiewicz M, Blokzijl A, Zieba A, Soderberg O: Crosstalk between Hippo and TGFbeta: Subcellular Localization of YAP/TAZ/Smad Complexes. J Mol Biol 2015, 427(21):3407-3415.

39. Wang W, Xiao ZD, Li X, Aziz KE, Gan B, Johnson RL, Chen J: AMPK modulates Hippo pathway activity to regulate energy homeostasis. Nat Cell Biol 2015, 17(4):490-499.

40. Mo JS, Meng Z, Kim YC, Park HW, Hansen CG, Kim S, Lim DS, Guan KL: Cellular energy stress induces AMPK-mediated regulation of YAP and the Hippo pathway. Nat Cell Biol 2015, 17(4):500-510.

41. von Eyss B, Jaenicke LA, Kortlever RM, Royla N, Wiese KE, Letschert S, McDuffus LA, Sauer M, Rosenwald A, Evan GI et al: A MYC-Driven Change in Mitochondrial Dynamics Limits YAP/TAZ Function in Mammary Epithelial Cells and Breast Cancer. Cancer Cell 2015, 28(6):743-757.

42. Seong HA, Jung H, Ha H: Murine protein serine/threonine kinase 38 stimulates TGF-beta signaling in a kinase-dependent manner via direct phosphorylation of Smad proteins. J Biol Chem 2010, 285(40):30959-30970.

43. Seong HA, Manoharan R, Ha H: Smad proteins differentially regulate obesity-induced glucose and lipid abnormalities and inflammation via class-specific control of AMPK-related kinase MPK38/MELK activity. Cell Death Dis 2018, 9(5):471.

44. Han Z, Kang D, Joo Y, Lee J, Oh GH, Choi S, Ko S, Je S, Choi HJ, Song JJ: TGF-beta downregulation-induced cancer cell death is finely regulated by the SAPK signaling cascade. Exp Mol Med 2018, 50(12):1-19.

45. Morita K, Saitoh M, Tobiume K, Matsuura H, Enomoto S, Nishitoh H, Ichijo H: Negative feedback regulation of ASK1 by protein phosphatase 5 (PP5) in response to oxidative stress. EMBO J 2001, 20(21):6028-6036.

46. Kutuzov MA, Andreeva AV, Voyno-Yasenetskaya TA: Regulation of apoptosis signal-regulating kinase 1 (ASK1) by polyamine levels via protein phosphatase 5. J Biol Chem 2005, 280(27):25388-25395.

47. Bruce DL, Macartney T, Yong W, Shou W, Sapkota GP: Protein phosphatase 5 modulates SMAD3 function in the transforming growth factor-beta pathway. Cell Signal 2012, 24(11):1999-2006.

48. Hsieh FS, Chen YL, Hung MH, Chu PY, Tsai MH, Chen LJ, Hsiao YJ, Shih CT, Chang MJ, Chao TI et al: Palbociclib induces activation of AMPK and inhibits hepatocellular carcinoma in a CDK4/6-independent manner. Mol Oncol 2017, 11(8):1035-1049.

49. Hsieh FS, Hung MH, Wang CY, Chen YL, Hsiao YJ, Tsai MH, Li JR, Chen LJ, Shih CT, Chao TI et al: Inhibition of protein phosphatase 5 suppresses non-small cell lung cancer through AMP-activated kinase activation. Lung Cancer 2017, 112:81-89.

50. Chen YL, Hung MH, Chu PY, Chao TI, Tsai MH, Chen LJ, Hsiao YJ, Shih CT, Hsieh FS, Chen KF: Protein phosphatase 5 promotes hepatocarcinogenesis through interaction with AMP-activated protein kinase. Biochem Pharmacol 2017, 138:49-60.

51. Kang Y, Cheong HM, Lee JH, Song PI, Lee KH, Kim SY, Jun JY, You HJ: Protein phosphatase 5 is necessary for ATR-mediated DNA repair. Biochem Biophys Res Commun 2011, 404(1):476-481.

52. Ali A, Zhang J, Bao S, Liu I, Otterness D, Dean NM, Abraham RT, Wang XF: Requirement of protein phosphatase 5 in DNA-damage-induced ATM activation. Genes Dev 2004, 18(3):249-254.

53. Guan B, Wang TL, Shih Ie M: ARID1A, a factor that promotes formation of SWI/SNF-mediated chromatin remodeling, is a tumor suppressor in gynecologic cancers. Cancer Res 2011, 71(21):6718-6727.

54. Ren T, Wang J, Tang W, Chen D, Wang S, Zhang X, Yang D: ARID1A has prognostic value in acute myeloid leukemia and promotes cell proliferation via TGF-beta1/SMAD3 signaling. Clin Exp Med 2022.

55. Guo B, Friedland SC, Alexander W, Myers JA, Wang W, O'Dell MR, Getman M, Whitney-Miller CL, Agostini-Vulaj D, Huber AR et al: Arid1a mutation suppresses TGF-beta signaling and induces cholangiocarcinoma. Cell Rep 2022, 40(9):111253.

56. Liang X, Vacher S, Boulai A, Bernard V, Baulande S, Bohec M, Bieche I, Lerebours F, Callens C: Targeted next-generation sequencing identifies clinically relevant somatic mutations in a large cohort of inflammatory breast cancer. Breast Cancer Res 2018, 20(1):88.

57. Melhuish TA, Gallo CM, Wotton D: TGIF2 interacts with histone deacetylase 1 and represses transcription. J Biol Chem 2001, 276(34):32109-32114.

58. Vinchure OS, Sharma V, Tabasum S, Ghosh S, Singh RP, Sarkar C, Kulshreshtha R: Polycomb complex mediated epigenetic reprogramming alters TGF-beta signaling via a novel EZH2/miR-490/TGIF2 axis thereby inducing migration and EMT potential in glioblastomas. Int J Cancer 2019, 145(5):1254-1269.

59. Gong Y, Huo L, Liu P, Sneige N, Sun X, Ueno NT, Lucci A, Buchholz TA, Valero V, Cristofanilli M: Polycomb group protein EZH2 is frequently expressed in inflammatory breast cancer and is predictive of worse clinical outcome. Cancer 2011, 117(24):5476-5484.

60. Hillmer RE, Link BA: The Roles of Hippo Signaling Transducers Yap and Taz in Chromatin Remodeling. Cells 2019, 8(5).

61. Stronati E, Giraldez S, Huang L, Abraham E, McGuire GR, Hsu HT, Jones KA, Estaras C: YAP1 regulates the self-organized fate patterning of hESC-derived gastruloids. Stem Cell Reports 2022, 17(2):211-220.
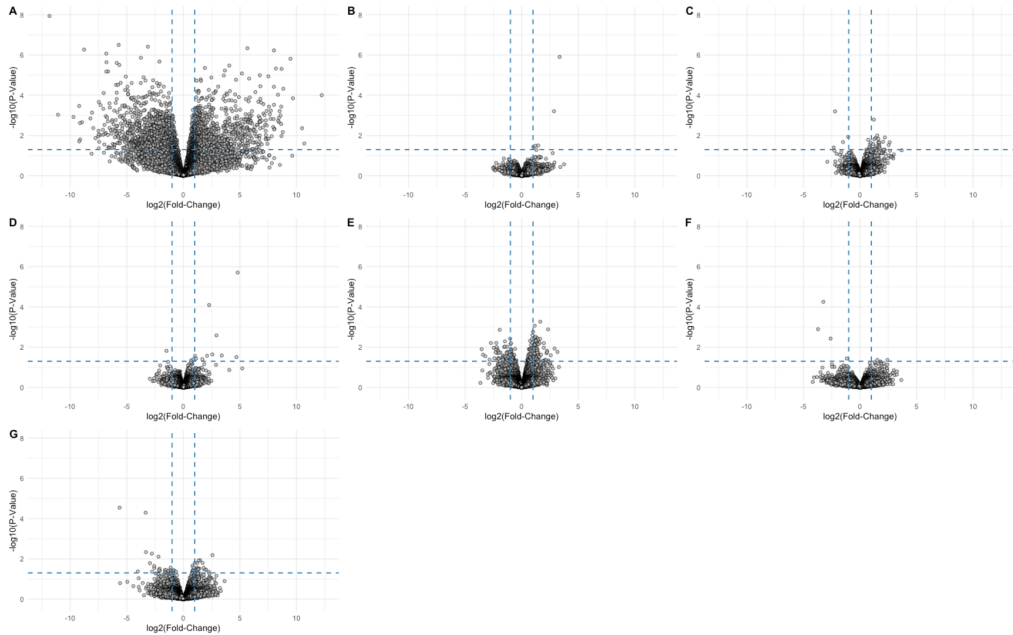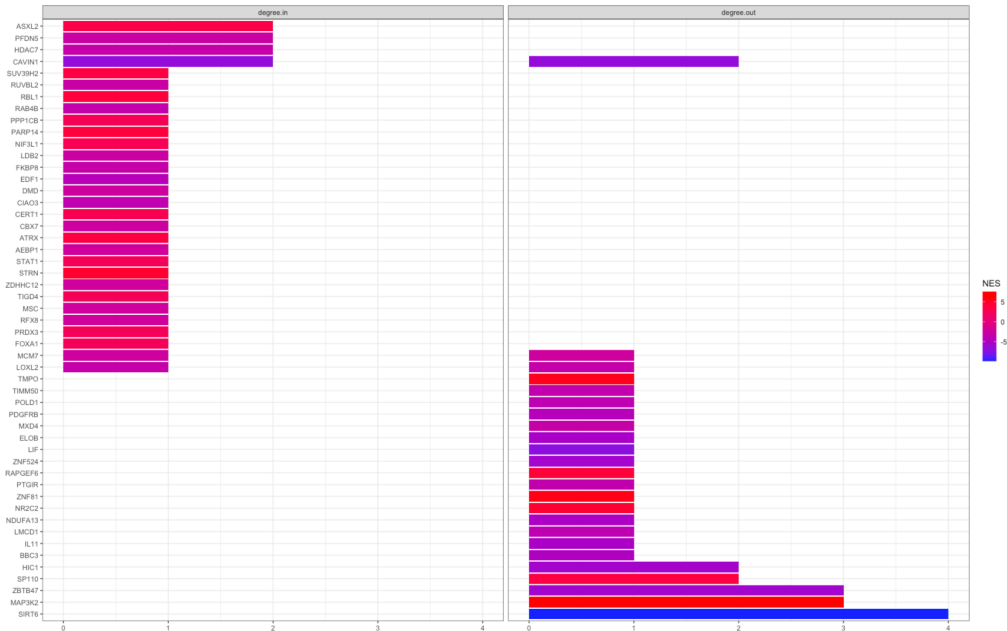
Supplementary Figure 1. Volcano plots showing genes differentially expressed between IBC and nIBC cells (**A**), between treated and control IBC cells at 1hr of TGFb treatment (**B**), between treated and control IBC cells at 4h of TGFb treatment (**C**), between treated and control nIBC cells at 1hr of TGFb treatment (**D**), between treated and control nIBC cells at 4h of TGFb treatment (**E**), genes that respond differently in IBC and nIBC cells following 1h of TGFB1 treatment (**F**) and genes that respond differently in IBC and nIBC cells following 4hs of TGFB1 treatment (**G**). Each gene is represented by a dot. The X-axis denotes to log2-tranformed fold change, and 2-fold expression differences are indicated using a vertical dashed line. The –log10 transformed P-value is plotted along the Y-axis with a threshold of 5% indicated using a horizontal dashed line.
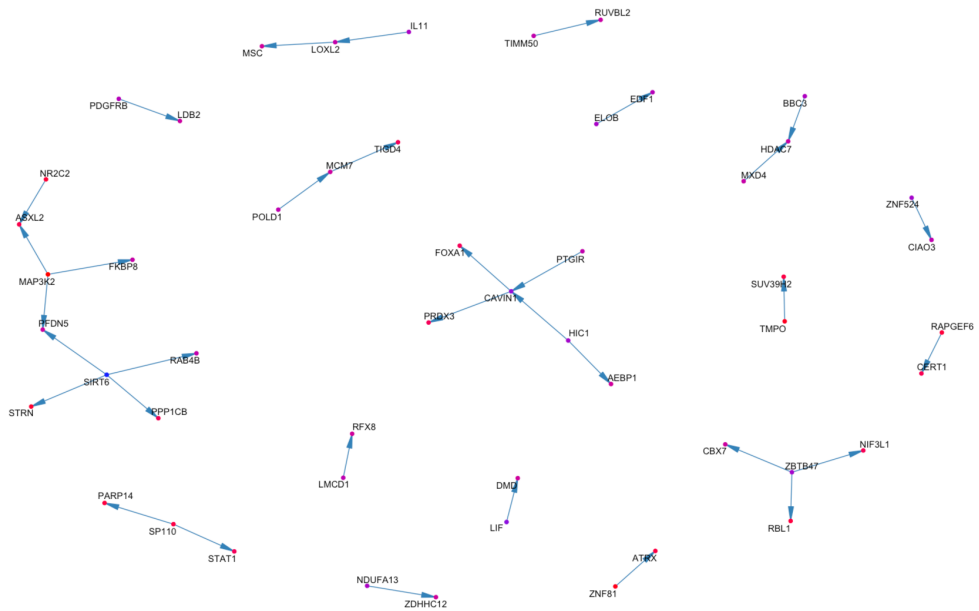
Supplementary Figure 2. Network representing pleiotropic interactions between master modulators identified based on genes that respond differently in IBC and nIBC cells following 1h of TGFB1 treatment. Pleiotropic interactions were identified using shadow analysis (VIPER). Every master modulator for which pleiotropic interactions have been identified is represented by a dot, color-coded according to the normalized enrichment score of the VIPER analysis with red and blue denoting stronger induction of protein activity by TGFB in IBC and nIBC cells respectively. Pleiotropic interactions are indicated using blue edges with arrow heads indicating the direction of the pleiotropic interaction. Master modulators at the left-hand side of the arrow (i.e. arrow pointing away) have inferred protein activity values that are partly attributable to co-regulation of target genes by the master modulators at the right hand side.
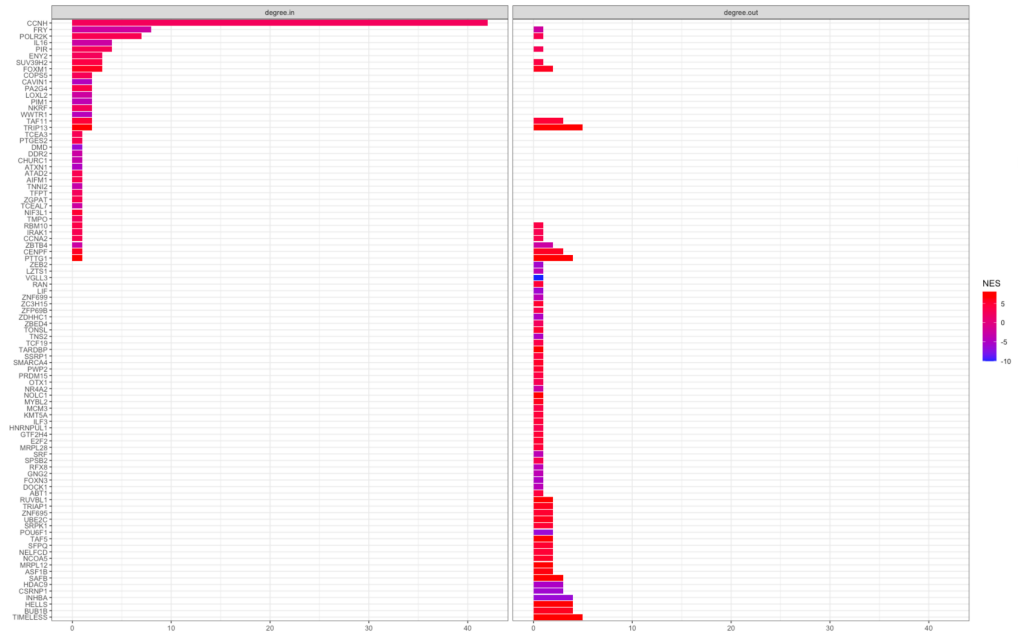
Supplementary Figure 3. Topological analysis of the interaction graph shown in supplementary Figure 2. For each node in the interaction graph, the in- and out-degree was recorded, which is shown in the left and right panel respectively. Each node is represented by a bar, the height of which corresponds to the in- or out-degree and is color-coded according to the normalized enrichment score resulting from the VIPER analysis. Nodes with an in-degree of at least 1, have at least one incoming arrow indicating that their inferred protein activity is at least partly due to co-regulation with other master modulators. These proteins were filtered out for further analysis. Nodes are listed along the Y-axis in order of decreasing in-degree.
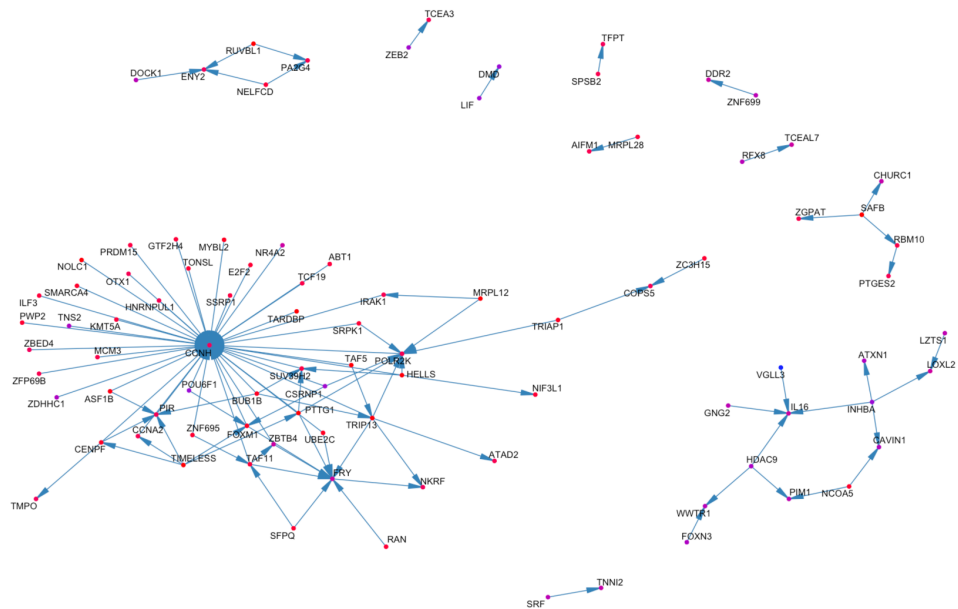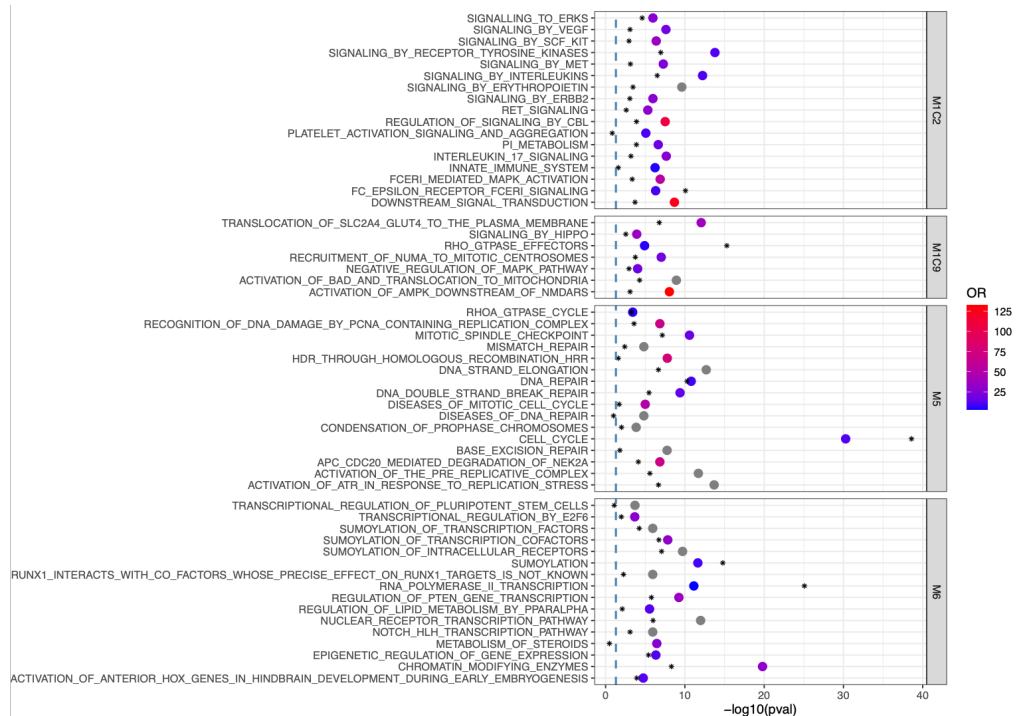
Supplementary Figure 4. Network representing pleiotropic interactions between master modulators identified based on genes that respond differently in IBC and nIBC cells following 4hs of TGFB1 treatment. Pleiotropic interactions were identified using shadow analysis (VIPER). Every master modulator for which pleiotropic interactions have been identified is represented by a dot, color-coded according to the normalized enrichment score of the VIPER analysis with red and blue denoting stronger induction of protein activity by TGFB in IBC and nIBC cells respectively. Pleiotropic interactions are indicated using blue edges with arrow heads indicating the direction of the pleiotropic interaction. Master modulators at the left-hand side of the arrow (i.e. arrow pointing away) have inferred protein activity values that are partly attributable to co-regulation of target genes by the master modulators at the right hand side.

Supplementary Figure 5. Topological analysis of the interaction graph shown in supplementary Figure 4. For each node in the interaction graph, the in- and out-degree was recorded, which is shown in the left and right panel respectively. Each node is represented by a bar, the height of which corresponds to the in- or out-degree and is color-coded according to the normalized enrichment score resulting from the VIPER analysis. Nodes with an in-degree of at least 1, have at least one incoming arrow indicating that their inferred protein activity is at least partly due to co-regulation with other master modulators. These proteins were filtered out for further analysis. Nodes are listed along the Y-axis in order of decreasing in-degree.

Supplementary Figure 6. Overrepresentation analysis for gene sets belonging to the Reactome knowledge base in each of the four modules identified in protein-protein interaction network. Each module is represented by a distinct panel and labelled accordingly. In each panel, collapsed gene sets that are significantly enriched are plotted along the Y-axis. Significance values per gene can be derived from the position of color-coded dots along the X-axis that represents the –log10 transformed P-value. The P-value threshold of 5% is indicated using a blue dashed line. The coloring scheme reflect the odds ratio of the overrepresentation test as shown in the legend to the right. Grey dots represent gene sets with an infinite odds ratio. In addition, for each gene set, a black diamond indicates the enrichment P-value of the same gene set in the full network to which the communities belong. Only gene sets that are more significant in the community as compared to the full network can be considered specific.

Supplementary Figure 7. Overrepresentation analysis for gene sets belonging to the WikiPathways knowledge base in each of the four modules identified in protein-protein interaction network. Each module is represented by a distinct panel, and labelled accordingly, except for M1C9 for which no significant enrichment was retained. In each panel, collapsed gene sets that are significantly enriched are plotted along the Y-axis. Significance values per gene can be derived from the position of color-coded dots along the X-axis that represents the –log10 transformed P-value. The P-value threshold of 5% is indicated using a blue dashed line. The coloring scheme reflect the odds ratio of the overrepresentation test as shown in the legend to the right. Grey dots represent gene sets with an infinite odds ratio. In addition, for each gene set, a black diamond indicates the enrichment P-value of the same gene set in the full network to which the communities belong. Only gene sets that are more significant in the community as compared to the full network can be considered specific.

CHAPTER 2: GENOMIC LANDSCAPE OF IBC

NOTCH and DNA repair pathways are more frequently targeted by genomic alterations in inflammatory than in non-inflammatory breast cancers

Abstract

Inflammatory breast cancer (IBC) is the most pro-metastatic form of breast cancer. Better understanding of its pathophysiology and identification of actionable genetic alterations (AGAs) are crucial to improve systemic treatment. We aimed to define the DNA profiles of IBC versus non-IBC clinical samples in terms of copy-number-alterations (CNAs), mutations, and AGAs. We applied targeted next-generation sequencing (tNGS) and array comparative genomic hybridization (aCGH) to 57 IBC and 50 non-IBC samples and pooled these data with four public datasets profiled using NGS and aCGH, leading to a total of 101 IBC and 2,351 non-IBC untreated primary tumors. The respective percentages of each molecular subtype (HR+/HER2-, HER2+, and TN) were 68%, 15% and 17% in non-IBC versus 25%, 35% and 40% in IBC. The comparisons were adjusted for both the molecular subtypes and the AJCC stage. The 10 most frequently altered genes in IBCs were TP53 (63%), HER2/ERBB2 (30%), MYC (27%), PIK3CA (21%), BRCA2 (14%), CCND1 (13%), GATA3 (13%), NOTCH1 (12%), FGFR1 (11%), and ARID1A (10%). The tumor mutational burden was higher in IBC than in non-IBC. We identified 96 genes with an alteration frequency (p<5% and q<20%) different between IBC and non-IBC, independently from the molecular subtypes and AJCC stage; 95 were more frequently altered in IBC, including TP53, genes involved in the DNA repair (BRCA2) and NOTCH pathways, and one (PIK3CA) was more frequently altered in non-IBC. Ninety-seven percent of IBCs displayed at least one AGA. This percentage was higher than in non-IBC (87%), notably for drugs targeting DNA repair, NOTCH signaling, and CDK4/6, whose pathways were more frequently altered (DNA repair) or activated (NOTCH and CDK4/6) in IBC than in non-IBC. The genomic landscape of IBC is different from that of non-IBC. Enriched AGAs in IBC may explain its aggressiveness and provide clinically relevant targets.

Introduction

Inflammatory breast cancer (IBC) is the most aggressive clinical form of breast cancer (Dawood et al., 2011). Despite therapeutic progresses, ~50% of patients die from metastatic relapse. The distinct clinical presentation and aggressive behavior have not translated in design of differential treatment that remains similar to that of stage 3 non-IBC. Identification of new therapeutic targets and better understanding of the pathophysiology are crucial (Charafe-Jauffret et al., 2008). Because of the scarcity of disease, "omics" studies remain rare in IBC (Bertucci et al., 2014a). The largest series reported to date is the one that we had collected within the International IBC Consortium (Bertucci et al., 2014b; Masuda et al., 2013; Van Laere et al., 2013), in which we notably showed the overrepresentation of aggressive molecular subtypes (basal, HER2-enriched, luminal B) when compared with non-IBC, justifying the need to stratify the IBC/non-IBC comparison upon the molecular subtypes (Van Laere et al., 2013).

During the last decade, next-generation sequencing (NGS) led to identification of driver alterations in non-IBC (Banerji et al., 2012; The Cancer Genome Atlas, 2012; Ellis et al., 2012; Ferrari et al., 2016; Nik-Zainal et al., 2012a; Nik-Zainal et al., 2016; Nik-Zainal et al., 2012b; Shah et al., 2012; Stephens et al., 2012). Precision medicine trials have shown the potential of DNA-based genomics screening to identify clinically actionable genetic alterations (AGAs) for guiding treatment (Andre et al., 2014; Le Tourneau et al., 2015). Regarding IBC, five NGS-based studies have been published since 2015 (Goh et al., 2016; Hamm et al., 2016; Liang et al., 2018; Matsuda et al., 2017; Ross et al., 2015). Except the most recent contribution (Liang et al., 2018), they concerned small series ranging from 19 to 53 IBCs, including both untreated primary tumors (between 16 and 25 cases only) and pre-treated relapses. The number of tested genes varied between 50 to 255 for the studies using targeted NGS (Hamm et al., 2016; Liang et al., 2018; Matsuda et al., 2017; Ross et al., 2015), and whole-exome sequencing (WES) (Goh et al., 2016). Few studies directly compared the genomic portraits of primary IBC and non-IBC, and comparison was never stratified upon the molecular subtypes. However, three of the most recurrently mutated genes (TP53, PIK3CA, and HER2) have clear ties with molecular subtypes (i.e. triple-negative (TN), luminal, and HER2-enriched respectively). The main finding of these studies was an increased tumor mutational burden (TMB) in IBC that translated in the presence of many AGAs with low frequency, but without identification of IBC-specific driver genes.

Here, we present a large comparative study of untreated primary tumors of IBC and non-IBC based on NGS data from Institut Paoli-Calmettes (Marseille, France) and TCRU (Antwerp, Belgium), pooled with publicly available data (The Cancer Genome Atlas, 2012; Hamm et al., 2016; Pereira et al., 2016; Ross et al., 2015). After adjustment upon

both the molecular subtypes and AJCC stage, we compared the genomic profiles of IBC and non-IBC by in terms of DNA mutations and copy number alterations (CNA), TMB, and presence of AGAs.

Material and methods

Patients and samples selection

All clinical samples were pre-treatment diagnostic samples of primary breast cancers. IBC was clinically defined as T4d according to the international consensus criteria (Dawood et al., 2011), and the samples were diagnostic biopsies (American Joint Committee on Cancer AJCC stages 3-4). Non-IBC samples were surgical specimens in case of early-stage disease (stages 1-2) and diagnostic biopsies in case of advanced stage disease (locally advanced: stage 3, and metastatic: stage 4). The whole series included 101 IBCs and 2,351 non-IBCs, collected from six different sources (Supplementary Table 1).

Forty-four IBC and 50 non-IBC samples were from patients consecutively treated at Institut Paoli-Calmettes (IPC), and 13 IBC samples were from patients consecutively treated at the General Hospital Sint-Augustinus (TCRU). Extraction of tumor DNA, quality control and concentration assessment were done as described (Bertucci et al., 2016). Each patient gave written informed consent and the study was approved by the respective institutional review boards. The study methodology conformed to the standards set by the Declaration of Helsinki. The selection criteria included available frozen sample, tumor cellularity assessment to guide DNA extraction (>50%), goodquality extracted tumor DNA, and available clinicopathological data. These samples were pooled with four public series of similarly defined IBC and non-IBC samples profiled by NGS (and array-comparative genomic hybridization (aCGH) for two series). The Ross' (Ross et al., 2015) and Hamm's (Hamm et al., 2016) series included 25 and 17 IBC samples respectively; the TCGA series (Cancer Genome Atlas, 2012) included two IBC and 988 non-IBC samples; the Metabric (Molecular Taxonomy of Breast Cancer International Consortium) series included 1,313 non-IBC samples (Pereira et al., 2016). The molecular subtype of tumors based upon immunohistochemistry was defined as HR+/HER2- when ER and/or PR were positive and HER2 negative, HER2+ when HER2 was positive, and TN when the three receptors were negative.

We also included NGS and aCGH data of metastatic samples from 468 non-IBC patients pooled from our PERMED-01 prospective clinical trial (NCT02342158) (N=174) and from two public sets: Lefebvre et al. (2016) (N=216), and the Metastatic Breast Cancer Project (MBC Project, 2018) (N=78). Moreover, we used the gene expression data from the International IBC Consortium (137 IBC and 252 non-IBC samples) (Van Laere et al.,

2013) to apply gene expression signatures of NOTCH (Villanueva et al., 2012) and E2F4 (Guerrero-Zotano et al., 2018) activation.

DNA copy number profiling

In three series (IPC, TCGA, Metabric), the DNA copy number profiles were established by using whole-genome aCGH: high-resolution 4Å~180K CGH microarrays (SurePrint G3-Human CGH-Microarray, Agilent Technologies, Massy, France) for IPC (Bertucci et al., 2016), and Affymetrix SNP 6.0 arrays (Santa Clara, CA) for TCGA and Metabric. All aCGH probes were mapped according to UCSC Build 37 (hg19). In the other series (TCRU, Ross, Hamm), the DNA copy number of tumors was derived from targeted NGS data generated by Foundation Medicine. The copy number alterations (CNA) results of those public sets were collected as processed data from the GDC Data Portal for the TCGA series, cBioPortal for Metabric, and the journal websites for Ross and Hamm series. Across all series, we used one threshold value (log2 ratio >|1|) to define amplifications and deletions. The HRD score (homologous recombination deficiency) (Marquard et al., 2015) was defined on segmented data processed with circular binary segmentation and considered positive above 10 (Olshen et al., 2004). We searched for chromothripsis in IBC by applying the CTLPScanner (Yang et al., 2016).

Mutational profiling

All series were sequenced using Illumina platforms. Except the TCGA series, which used WES, the other ones used targeted NGS (tNGS). IPC samples were sequenced with a home-made panel of 493 "cancer-associated" genes (CCP-V8 panel, Supplementary Table 2). The DNA-libraries of all coding exons and intron-exon boundaries of all genes were prepared using the HaloPlex Target-Enrichment-System (Agilent, Santa Clara, CA, USA) as described (Bertucci et al., 2016), and sequencing was done using the 2Å~150-bp paired-end technology on the NextSeq500 Illumina platform (Illumina, San Diego, CA, USA). All sequence data were aligned to UCSC hg19 and analyzed as described (Bertucci et al., 2016). Pathogenicity scores for the SNVs were obtained with Annovar. Mutations were classified as "neutral" or "damaging" using the majority rule of predictor softwares (provided by dbnsfp: Sift, Polyphen2, LRT, MutationTaster, MutationAssesor, FATHMM, RadialSVM, LR). The TCRU, Ross's and Hamm's series were sequenced by Foundation Medicine (Cambridge, MA) for respectively 324, 195/255, and 225 genes. The Metabric series (Pereira et al., 2016) was analyzed on a 173-gene panel. Sequencing data of the public sets and TCRU were collected and processed as indicated above. The TMB was defined as the number of non-silent mutations per megabase of genome sequenced (Bertucci et al., 2016).

Definition of actionable gene alterations

We defined the actionable genetic alterations (AGAs) by using the Perera-Bel's algorithm (Perera-Bel et al., 2018), which matches patient-specific genomic alterations to treatment options. The molecular alterations of 312 actionable genes are classified into a six-level system to rank the associations according to their evidence. The system uses two axes representing the cancer-type (axis A/B) and the strength of clinical evidence (axis 1/2/3). Levels A and B mean evidence in the same cancer-type (here breast cancer) and in any other cancer-type, respectively. Level-1 means supported by drug approval organizations/clinical guidelines, level-2 contains clinical evidence, in which late clinical trials are ranked higher followed by early clinical trials and case reports, and level-3 consists of preclinical evidence. The highest level is A1, followed by B1, then A2, B2, A3, and B3. Our analysis was limited to alterations noted as associated with "sensitivity" to drugs or "response".

Statistical analysis

Correlations between tumor classes and clinicopathological and molecular variables were analyzed using the Student t-test or the Fisher's exact test when appropriate. Uni- and multivariate analyses comparisons of the frequency of molecular alterations between the tumor groups adjusted for the molecular subtypes and the AJCC stage were done using Logit link function. Genes with p-value inferior to 0.05 and q-value inferior to 0.2 in uni- and multivariate analyses were considered as significant. Ontology analysis (DAVID database: https://david.ncifcrf.gov/) of the gene list was limited to the Reactome pathways. Hypergeometric test assessed the significance of enrichment of genes common to the different gene lists. The significance of the p-values threshold was set at 5% and analyzes used the R-software (version 2.15.2: http://www.cran.rproject.org/).

Results

Population and genes analyzed

We analyzed 101 IBCs and 2,351 non-IBCs (Table 1). As expected, IBCs were associated with more unfavorable prognostic features than non-IBCs: younger age, prevalent ductal type, higher AJCC stage (including stage 4), higher pathological grade, and more frequent HER2+ and TN subtypes. Forty percent of samples were TN and 60% were non-TN in IBC, versus 17% and 83% respectively in non-IBC. By definition, all IBC were stage 3 or 4, but the precise stage (3 or 4) was available for 59/101 cases, including 33 stage 3 (59%) and 23 stage 4 (41%). Across all six data sets included, there were five different targeted gene panels and one whole-exome. The CCP-V8 panel gene list was

compared with the four other lists retrieved from the Foundation Medicine website for TCRU, Ross and Hamm series, and the journal website for Metabric. Because there were only 41 genes common to all panels, we focused our analysis on 756 different genes defined as being present in at least one targeted panel (Supplementary Table 2).

Table 1. Clinicopathological characteristics of patients and samples.

Characteristics	N	All cases	Type non-IBC	IBC	P-value
Age	2397	59.75 (24–96.29)	60 (26–96.29)	49.5 (24–80)	2.43E-07
Pathological type					
Ductal	1808	1808 (76%)	1763 (75%)	45 (98%)	2.61E-03
Lobular	277	277 (12%)	276 (12%)	1 (2%)	
Other	309	309 (13%)	309 (13%)	0 (0%)	
Pathological grade					
1	146	146 (11%)	146 (11%)	0 (0%)	1.02E-03
2	509	509 (38%)	498 (39%)	11 (25%)	
3	682	682 (51%)	649 (50%)	33 (75%)	
AJCC stage					
1–2	1615	1615 (82%)	1615 (87%)	0 (0%)	< 1.00E-06
3–4	349	349 (18%)	248 (3%)	101 (100%)	
ER status					
Negative	587	587 (25%)	540 (23%)	47 (64%)	3.44E-13
Positive	1791	1791 (75%)	1765 (77%)	26 (36%)	
PR status					
Negative	1069	1069 (45%)	1017 (44%)	52 (72%)	2.94E-06
Positive	1305	1305 (55%)	1285 (56%)	20 (28%)	
ERBB2 status					
Negative	1937	1937 (85%)	1891 (85%)	46 (65%)	3.09E-05
Positive	355	355 (15%)	330 (15%)	25 (35%)	
Molecular subtype					
HR+/HER2−	1520	1520 (66%)	1502 (68%)	18 (25%)	< 1.00E-06
HER2+	355	355 (16%)	330 (15%)	25 (35%)	
TN	415	415 (18%)	387 (17%)	28 (40%)	

Gene alterations in IBC

We identified 1,101 gene alterations through the 101 IBCs, including 228 amplifications (21% of all alterations), 15 deletions (1%), and 857 mutations (78%), comprising 730 single-nucleotide-variants (SNVs: non-synonymous, stop-gains, splice-site; 66%), and 127 indels (12%). They corresponded to 1,013 different alterations involving 331 different genes (Supplementary Table 3). The distribution of alterations of the top 50 genes altered in at least two IBCs is shown in Figure 1. The 10 most frequently altered genes were TP53 (63%), HER2 (30%), MYC (27%), PIK3CA (21%), BRCA2 (14%), CCND1 (13%), GATA3 (13%), NOTCH1 (12%), FGFR1 (11%), and ARID1A (10%). For HER2, there was 93% concordance between the clinical status and the CNA. Ninety-eight percent of IBC samples (99/101) harbored at least one alteration. The mean number of alterations per sample was 11 (CI95, 9-13). The mean TMB was 6 mutations per megabase (CI95, 4-8) (Supplementary Figure 1). Chromothripsis was present in 20 out of 44 tested IBC (45%). The most affected chromosomes were chromosome 17 (8% of samples), followed by chromosomes 11 (5%) and 8 (3%). The presence of chromothripsis tended to be associated with the molecular subtype: 69% of HER2+

samples displayed chromothripsis, versus 35% of HR+/HER2- and 30% of TN (p=0.092; Fisher's exact test).
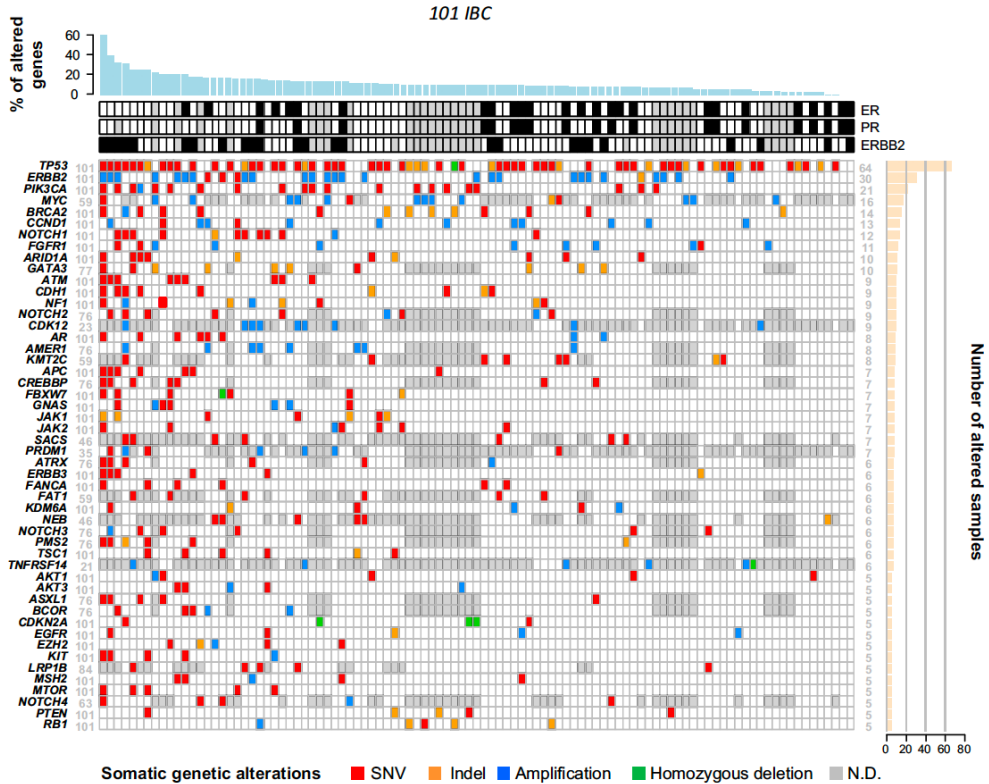
Fig. 1. Distribution of alterations of the top 50 genes altered in IBC. Oncoprint of the top 50 genes altered in at least two IBC samples and analyzed in at least 20 samples. Top: immunohistochemical status for ER, PR, and ERBB2 (white: negative; black: positive; gray: unavailable). Bottom: somatic gene alterations (mutations and CNA) color-coded according to the legend. The genes are ordered from top to bottom by decreasing number of altered tumors (right panel) and the tumors from left to right by decreasing percentage of altered genes (top panel). ND: not defined.

Comparison of gene alterations between IBC and non-IBC

Similar analysis was done in the 2,351 non-IBCs. We identified 22,936 gene alterations, corresponding to 14,448 different alterations (Supplementary Table 3). The distribution of the types of alterations was different from that of IBC (p=1.24E-17, Fisher's exact test) with a lesser percent of mutations (70% vs 78%, corresponding to 62% vs 66% for SNVs, and 8% vs 12% for indels). The gene alterations identified in non-IBC confirmed the literature data (Banerji et al., 2012; Cancer Genome Atlas, 2012; Ellis et al., 2012; Ferrari et al., 2016; Nik-Zainal et al., 2012a; Nik-Zainal et al., 2016; Nik-Zainal et al., 2012b; Shah et al., 2012; Stephens et al., 2012), i.e. the most frequently altered genes including PIK3CA (39%), TP53 (34%), HER2 (13%), GATA3 (13%), KMT2C (11%), CDH1 (10%), and MAP3K1 (10%). The mean TMB for all variants was higher in IBC (6 mutations/Mb; CI95, 4-8) than in non-IBC (2; CI95, 2-2; Student t-test, p=6.29E-

05; Supplementary Figure 1). Sixteen percent of IBC samples presented a TMB >10 versus only 1% of non-IBC samples (p=3.36E-12, Fisher's exact test). The same difference was observed when SNVs and indels were analyzed separately (Supplementary Figure 1), and all those differences persisted in multivariate analysis adjusted for the molecular subtypes, the type of NGS (targeted vs WES), and the AJCC stage.

We then applied similarly adjusted supervised analysis to search for genes with differential frequency of alterations between IBC and non-IBC. Of note, when a sample was not informative for the gene tested, it was excluded from analysis. We identified 96 genes differentially altered (p<0.05 and q<0.20 in both univariate and multivariate analyses), including 95 more frequently altered in IBC and only one (PIK3CA) more frequently altered in non-IBC (Supplementary Table 4).
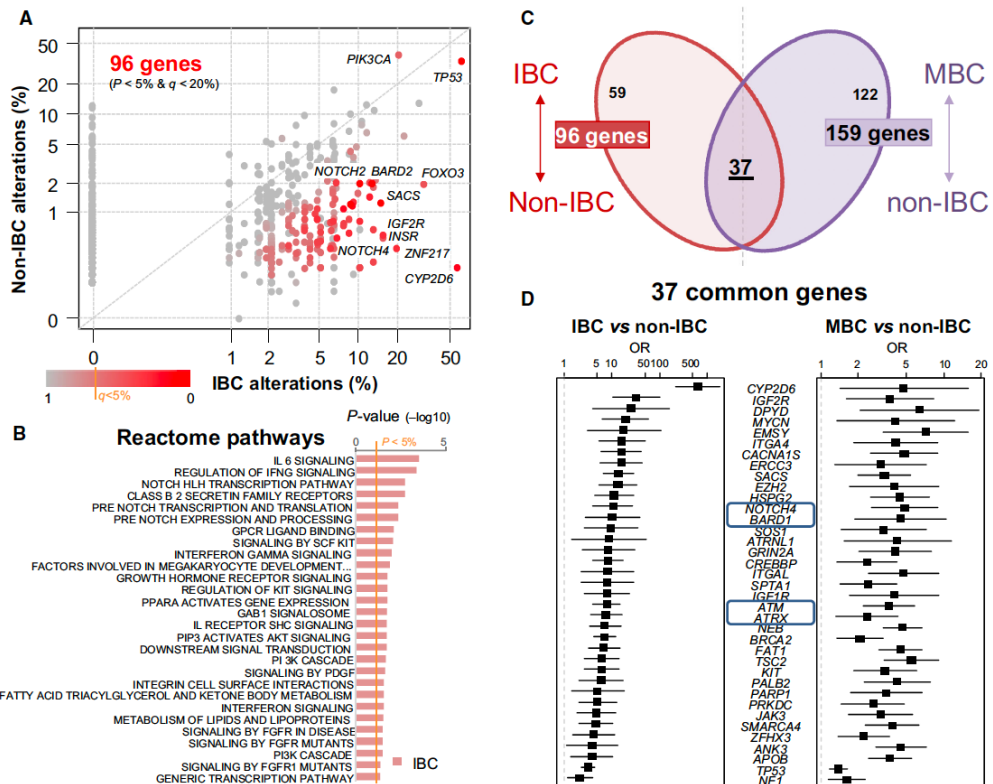
Fig. 2. Identification of genes with differential frequency of alterations between samples. (A) Scatter plot depicting the alteration frequency (% of patients) between IBC and non-IBC. Each dot represents one gene, and dots are color-coded according to the P-values ($-\log_{10}$ P-values) according to the legend below. Significantly mutated genes in either IBC or non-IBC are included. A few genes differentially mutated are labeled. (B) Ontology analysis revealed several Reactome pathways significantly associated with the 95 IBC genes. (C) Crossings of the lists of genes differentially altered in IBC vs non-IBC (96 genes) and of genes differentially altered in metastatic (MBC) vs primary non-IBC (159 genes). (D) List of 37 genes common to the two gene lists. OR: odds ratio of frequencies of alterations in the tumor subgroups.

The most differentially altered gene was CYP2D6. Four genes (CYP2D6, FOXO3, TP53, and ZNF217) were altered in more than 20% of IBCs and 57 genes such as BRCA2, ATM, ATRX, EMSY, NOTCH2, and NOTCH4 were altered in 5 to 20% of cases. Ontology analysis of the 96 differential genes revealed several pathways associated with IBC genes, such as NOTCH-related pathways, interleukins and interferon signal, and KIT signaling (Figure 2B). Genes involved in chromatin remodeling were also more frequently altered in IBC, such as EZH2 and SMARCA4, altered in 5% of IBC, providing a rationale for the evaluation of epigenetic modifiers for the treatment of IBC. Of note, the use of the PAM50-based genomic definition of molecular subtypes and the use of the IHC definition applied to the 1,773 samples (41 IBC and 1,732 non-IBC) informative for both definitions and for the multivariate analysis showed similar results with the two definitions: 54 and 51 genes were identified as differential with the IHC definition and the PAM50 definition respectively, with 49 (91% and 96% respectively) common genes (Supplementary Figure 2).

Supposing that these 96 differentially altered genes might be related to IBC aggressiveness, we tested whether they were also differentially altered in metastatic versus primary non-IBC. We compared the frequency of alterations between 468 metastatic samples of non-IBC patients and the 2,351 non-IBC primary samples. By using the same significance threshold as above, we found 159 differentially altered genes, most of them being more frequently altered in metastatic samples (Supplementary Table 5). The comparison with the above-quoted 96-gene list identified 37 genes more frequently altered in both IBC versus non-IBC samples and in metastatic versus primary non-IBC samples (Figure 2C-D). Such overrepresentation was significant (p=5.58E-06, hypergeometric test), and indirectly validated the association of our 96-gene list with IBC, known for its stronger metastatic potential than non-IBC. These 37 common genes included genes involved in DNA repair (ATM, ATRX, BARD1, BRCA2, EMSY, PALB2) and in NOTCH pathway (NOTCH4). By contrast, the same analysis between the 468 metastatic samples of non-IBC patients and the 101 IBC samples identified only one gene differentially altered (HER2), indicating that IBC and metastatic non-IBC samples are not so different at a genomic level when compared head-on.

Actionable genetic alterations in IBC versus non-IBC

We assessed the distribution of AGAs in IBC, comparatively to non-IBC, using the Perera-Bel's algorithm (Perera-Bel et al., 2018). The percentage of IBC patients with AGAs was high (97%) with 26% of A1 alterations, which corresponded to HER2 amplification, 24% of B1, 18% of A2, and 29% of B2 (Supplementary Table 3). Examples of B1 alterations included BRCA2, JAK2 and EGFR alterations observed in 13 (13%), 5 (5%), and 3 (3%) patients respectively. Examples of A2 alterations included PIK3CA,

FGFR1, and PTEN alterations observed in 21 (21%), 8 (8%), and 4 (4%) patients respectively. Examples of B2 alterations included CCND1 and ATM (9 cases each: 9%), NF1 (7 cases: 7%), MTOR and TSC2 (5 cases each: 5%), AKT1, RB1, and TSC1 (4 cases each: 4%), and ERBB3 (3 cases: 3%). Figure 3 shows the distribution of 44 genes with AGA in at least four IBC samples. The most frequent actionable targets with evidence-level between A1 and B2 were TP53, HER2, PIK3CA, BRCA2, CCND1, FGFR1, ATM, and NF1. Many samples had several AGAs simultaneously. This percentage of patients with AGAs was higher than the one observed in non-IBC (87%; p=4.65E-20, Logit link; Supplementary Figure 3A), and the difference remained significant in multivariate analysis (p=5.65E-14, Logit link). There were significantly more A1 and B1 alterations in IBC and more A2 and A3 alterations in non-IBC (Supplementary Figure 3B).
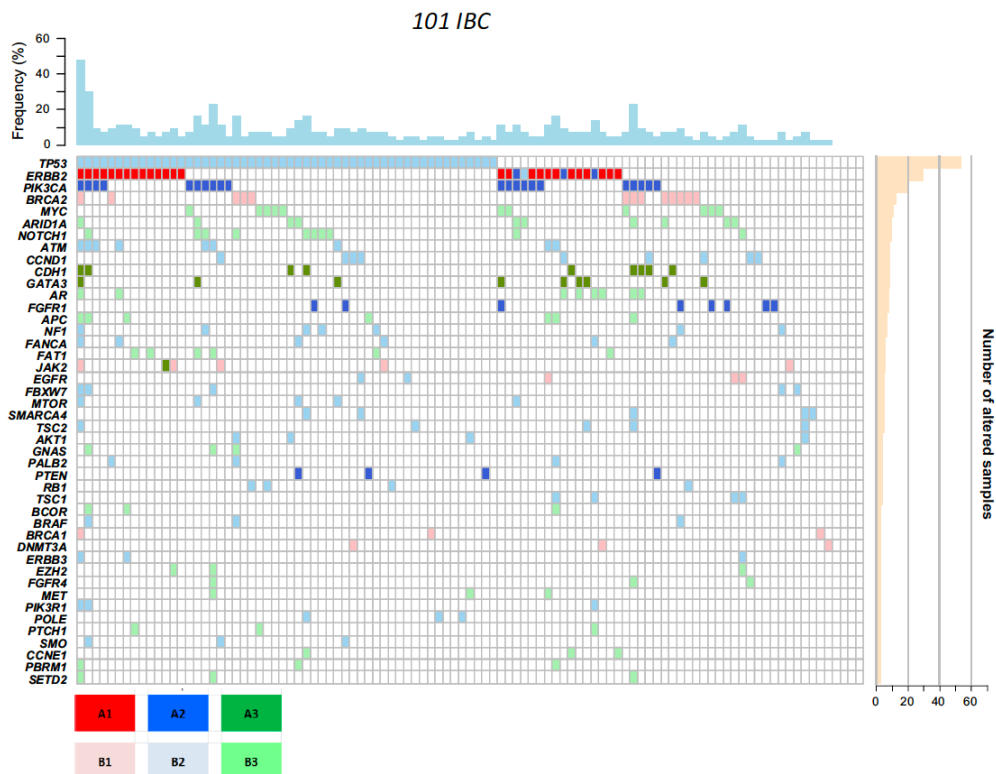

Fig. 3. Distribution of genes with actionable alterations in IBC. The 44 genes with actionable alterations in at least four IBC are shown. The genes are ordered from top to bottom by decreasing frequency of mutations. The degree of evidence of actionable alterations according to the Perera-Bel's algorithm (2018) is color-coded as indicated in the color scale.

Enrichment of actionable genetic alterations for different therapeutic classes

We analyzed whether there was enrichment in patients with AGAs in IBC versus non-IBC in specific drug classes and functional pathways (Supplementary Figure 4). Regarding the class of PI3K/AKT/mTOR inhibitors, the percentage of patients with AGAs

was higher in non-IBC patients (52% vs 40%; p=1.97E-02), but this difference disappeared in multivariate analysis (p=0.185). The percentage of "actionable patients" in the class of HER/EGFR inhibitors was higher in IBC (36% vs. 23% in non-IBC, p=2.68E-03), and tended to be significant in multivariate analysis (p=0.091). This percentage regarding the class of other tyrosine kinase receptors (TKR) inhibitors, higher in IBC (27% vs. 18% in non-IBC) in univariate analysis (p=2.01E-02), but did not remain significant in multivariate analysis (p=0.565). The same was observed regarding the class of CDK inhibitors with higher percentage of patients with AGAs in IBC (29% vs. 15%, p=4.48E-04), not significant in multivariate analysis (p=0.180). We applied an E2F4 activation 24-gene signature associated with sensitivity to the palbociclib CDK4/6 inhibitor and resistance to aromatase inhibitor (Guerrero-Zotano et al., 2018) to the 389 samples of the International IBC Consortium expression dataset (Supplementary Figure 5). The corresponding metagene score was higher in IBC than in non-IBC samples (p=3.68E-04, Student t-test; p=5.93E-03, Fisher's exact test), and this difference remained independent from the molecular subtypes and the AJCC stage (p=0.055, glm; Supplementary Figure 5A). This enrichment concerned the HR+/HER2- subtype, which is currently the subtype candidate for CDK4/6 inhibitors (Supplementary Figure 5B).
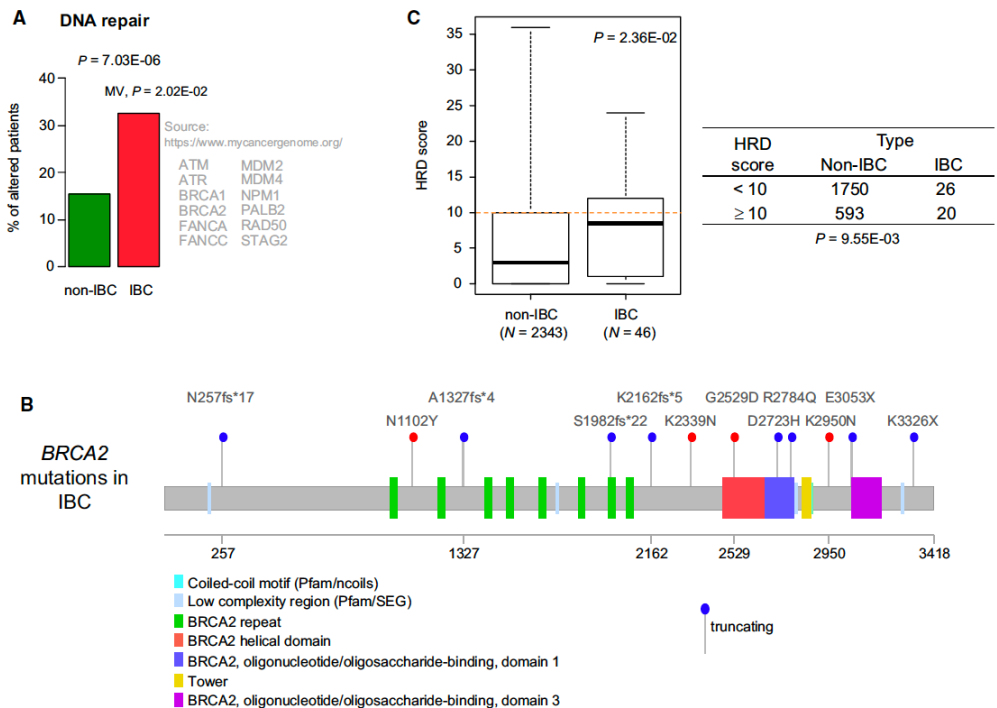
Fig. 4. DNA repair genes are more frequently altered in IBC than in non-IBC. (A) Plot showing the percentage of patients with AGAs in genes involved in DNA repair in IBC *vs* non-IBC patients. The *P*-values are for the logit link in univariate analysis and in MV. Beside the plot, are indicated the 12 genes common to the pathway in the indicated bibliographic source and to our list of 756 genes tested. (B) Lolliplot of *BRCA2* gene showing the 12 mutations identified in IBC (blue: truncating mutation; red: nontruncating mutation). (C) Left: Box-plot of HRD score in non-IBC and IBC samples. Right: Contingency table between HRD score and IBC/non-IBC status.
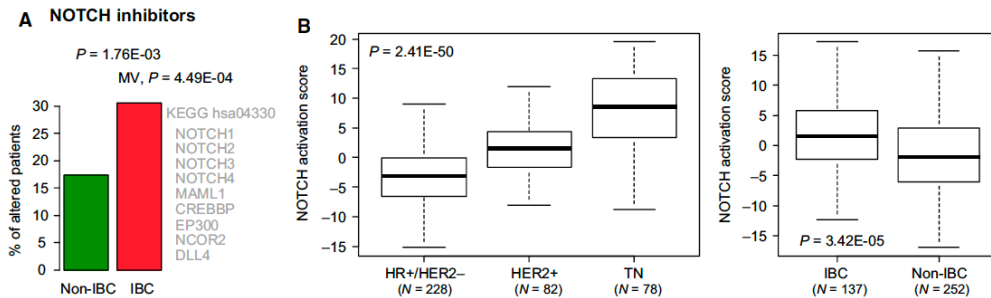
DNA repair more frequently altered in IBC

Several genes more frequently altered in IBC such as ATM, ATRX, BARD1, BRCA2, and EMSY are involved in DNA repair. Pathway analysis confirmed such enrichment: the percentage of patients with alterations of DNA repair genes was 33% in IBC versus 17% in non-IBC (p=7.03E-06, Logit link), even after adjustment in multivariate analysis (p=2.20E-02, Logit link; Figure 4A). BRCA2 was the most frequently altered DNA repair gene in IBC with 13 mutations, including eight truncating mutations (Figure 4B), suggesting possible enrichment in Homologous Recombination Deficiency (HRD) in IBC. This was confirmed with a higher HRD score in IBCs than in non-IBCs (p=2.36E-02, Student t-test). The OR for high HRD score (≥10) was 2.27 (95CI 1.19-4.26) in IBC compared with non-IBC (p=9.45E-03, Fisher's exact test; Figure 4C).

NOTCH pathway more frequently altered in IBC

NOTCH pathway alterations were also enriched in patients with IBC (30% vs 17% in non-IBC patients) in univariate (p=1.76E-03, Logit link) and multivariate analyses (p=4.49E-04, Logit link; Figure 5A). Whereas NOTCH1 was among the most frequently altered genes in IBC (12%), it was not differentially altered compared with non-IBC. By contrast, NOTCH2, and NOTCH4 were significantly more frequently mutated in IBC with a total of 12 mutations, including 9 predicted as damaging in silico. There was a mutual exclusivity in IBC samples between alterations in the three genes (NOTCH2, NOTCH4, and CREBBP) found differentially altered in IBC vs non-IBC, present in the KEGG NOTCH pathway, and tested in at least 30% of samples (Supplementary Figure 6). Other genes involved in the NOTCH pathway and frequently altered in IBC included MAML1 (11%), MED12 (9%), and FBXW7 (8%).

Such enrichment led to search for signs of NOTCH pathway activation in IBC. We applied a 384-gene signature of NOTCH activation (Villanueva et al., 2012) to expression data of the International IBC Consortium set. As expected (Shen et al., 2017), the activation score was higher in the TN samples than in the HR+/HER2- samples (p=2.41E-50, one way ANOVA test Figure 5B), validating its robustness. Interestingly, this score was higher in IBCs than in non-IBCs (p=3.42E-05, Student t-test; Figure 5B), and this difference remained significant in multivariate analysis (Table 2).

Fig. 5. NOTCH pathways genes are more frequently altered in IBC than in non-IBC. (A) Plot showing the percentage of patients with AGAs involved in the NOTCH pathway in IBC *vs* non-IBC patients. The *P*-values are for the logit link in univariate analysis and in MV. Beside the plot, are indicated the nine genes common to the pathway in the indicated bibliographic source and to our list of 756 genes tested. (B) Left: Box-plot of NOTCH activation score in the breast cancer samples of the International IBC Consortium dataset according to the molecular subtypes. The *P*-value is for the one-way ANOVA test. Right: Box-plot of NOTCH activation score in the breast cancer samples of the International IBC Consortium dataset according to the non-IBC and IBC statutes. The *P*-value is for the Student's *t*-test.

Comparison with literature

Finally, we compared our results to those of two tNGS studies for which data, publicly unavailable, were not included in our analysis. The Liang et al. study analyzed 91 genes in a series of non-pretreated primary tumors including 156 IBC and 197 stage 3-4 TCGA non-IBC (Liang et al., 2018): 17 genes were more frequently mutated in IBC than in non-IBC, including TP53, NOTCH2, MYH9, BRCA2, ERBB4, POLE, FGFR3, ROS1, NOTCH4, LAMA2, EGFR, BRCA1, TP53BP1, ESR1, THBS1, CASP8, and NOTCH1, and one gene, CDH1, more frequently mutated in non-IBC. The Matsuda et al. series analyzed 50 genes in non-pretreated primaries and pre-treated relapses of 24 IBC and 376 non-IBC (Matsuda et al., 2017): two genes (TP53, HER2) were more frequently mutated in IBC. In both studies, the comparison was not stratified upon the molecular subtypes. We compared these lists of differential genes with ours (Supplementary Figure 7). Between the Liang et al. list and ours, 84 genes were common to both panels tested, with only five differential genes in common: BRCA2, NOTCH2, NOTCH4, POLE, and TP53. Between the Matsuda et al. list and ours, 50 genes were common to both panels tested, with only one differential gene (TP53) in common. Thirty genes were common to the Matsuda et al. and Liang et al. panels, with only one differential gene in common: TP53. These results revealed low concordance between all three gene lists.

Table 2. Uni- and multivariate analyses for IBC *vs* non-IBC. OR, odds ratio.

	Univariate			Multivariate		
	N	OR (95% CI)	P-value	N	OR (95% CI)	P-value
Villanueva's NOTCH activation score	389	1.06 (1.04–1.09)	9.27E-05	384	1.07 (1.03–1.12)	5.82E-03
Molecular subtype, HER2+ *vs* HR+/HER2−	388	2.81 (1.81–4.36)	1.04E-04	384	1.40 (0.79–2.48)	0.336
TN vs HR+/HER2−	388	1.96 (1.25–3.08)	1.36E-02	384	0.77 (0.39–1.53)	0.532
AJCC stage, 3–4 *vs* 1–2	389	1.06 (1.04–1.09)	9.27E-05	384	4.8E8 (0.00–Inf)	0.981

Discussion

We compared the DNA copy number and mutational profiles of untreated primary tumors of 101 IBCs and 2,351 non-IBCs. Ninety-seven percent of IBCs displayed at least one AGA. This percentage, higher than in non-IBC, suggests that personalized therapy is a relevant approach for this aggressive disease, in particular with drugs targeting the DNA repair and NOTCH pathways.

We focused our study on untreated primary tumors to avoid biases induced by previous systemic treatments that induce changes in mutations and subclonal structure between primary tumor and relapses (Bertucci et al., 2019; McGranahan et al., 2015). The scarcity of IBC and diagnostic samples, and the need to adjust analyses upon the molecular subtypes and AJCC stage because of the unbalance between IBC and non-IBC led us to pool our own bicentric data with available public data. As expected for breast cancers, the genomic profiles were heterogeneous in IBC. We found higher TMB in IBC compared to non-IBC, possibly related to the higher genomic instability and complexity of the disease (Bekhouche et al., 2011), suggesting that immune checkpoint inhibitors warrant further investigation in IBC (Bertucci et al., 2015; Bertucci and Goncalves, 2017; Van Berckelaer et al., 2019; Van Laere et al., 2013). Such difference was independent from the molecular subtypes and the disease stage. Chromothripsis was identified in 45% of 44 tested IBC, a percentage close to that previously reported in a series of 28 non-IBC (Przybytkowski et al., 2014).

The 10 most frequently altered genes in IBC are TP53 (63%), HER2 (30%), MYC (27%), PIK3CA (21%), BRCA2 (14%), CCND1 (13%), GATA3 (13%), NOTCH1 (12%), FGFR1 (11%), and ARID1A (10%), which are also altered in non-IBC. But the comparison with non-IBC identified 95 genes more frequently altered in IBC in a molecular subtype and stage-independent way, including 37 that were also more frequently altered in metastases versus primary tumors of non-IBC patients. This suggests a possible link of these genes with disease aggressiveness and proclivity to metastasize, although functional studies are warranted. Interestingly, the pairwise comparisons of IBC, non-IBC primaries, and non-IBC metastatic samples showed that IBC and metastatic non-IBC are much less different at a genomic level when compared head-on than are IBC versus non-IBC primaries and primary versus metastatic non-IBC. CYP2D6 was the most differentially altered gene (58% of IBC vs 0.2% in non-IBC). This gene codes for the cytochrome P-450 2D6, which oxidizes tamoxifen to its most active metabolite. Many CYP2D6 polymorphisms, such as the one found in our series (435T>S), have been identified, leading to the decrease of CYP2D6 enzymatic activity. Several data suggest that poor metabolizers of CYP2D6 do not benefit as much from tamoxifen therapy as other patients do; however conflicting results were published (Hoskins et al., 2009). Absence

of analysis of constitutional DNA impedes us to conclude on the SNP nature of our variant. However, the large difference in frequency with non-IBC potentially reveals an important role for this variant in the predisposition to IBC and/or the known resistance of the disease to standard hormone therapy. Analysis of a larger series is needed, including both tumor and matched normal DNA.

Several therapeutically actionable targets were frequently altered in IBC, including a few ones more frequently than in non-IBC and independently from the molecular subtypes and AJCC stage. For example, we found frequent alterations in genes involved in DNA repair. ATM, ATRX, BARD1, BRCA2, ERCC3, MSH2, MSH6, PMS2, and POLE were more frequently altered in IBC, in which we found also frequent alterations of TP53, FANCA, and FANCB. This observation confirms recent findings (Liang et al., 2018) of frequent alterations in BRCA1/BRCA2/POLE genes in IBC. It is likely that deficient DNA repair contributes to disease progression, as well as to the high TMB observed in IBC and indirectly to its peculiar immune microenvironment (Bertucci et al., 2015; Van Berckelaer et al., 2019; Van Laere et al., 2013). In addition, IBC showed more frequently a homologous recombination deficiency and alterations in genes involved in mismatch repair, supporting the ongoing development of PARP inhibitors in IBC as radiosensitizers in phase I-II trials with veliparib (Jagsi et al., 2018) and olaparib (NCT03598257) (Michmerhuizen et al., 2019). This observation warrants a deeper NGS study of IBC, using whole-genome sequencing (WGS) to investigate structural variations. A recent study assessed the prevalence of germline variants in cancer predisposition genes in 368 patients with IBC (Rana et al., 2019). Germline mutations were identified in 53 cases (14.4%). BRCA1 or BRCA2 mutations were found in 7.3% of the subjects, 6.3% had a mutation in other breast cancer genes (PALB2, CHEK2, ATM, and BARD1), and 1.6% had mutations in genes not associated with breast cancer.

Alterations in the NOTCH pathway were almost twice as enriched in IBC (30% vs 17% in non-IBC), independently from the molecular subtypes and AJCC stage. NOTCH receptors are transmembrane receptors that play an essential role in cell fate decisions such as proliferation, differentiation, and apoptosis, and in the maintenance of breast cancer stem-like cells (Mollen et al., 2018). NOTCH1 was the most frequently altered NOTCH gene in IBC (12%), whereas NOTCH2, and NOTCH4 were more frequently altered in IBC compared with non-IBC, with a total of 12 mutations including 9 predicted as damaging. Functional studies measuring NOTCH pathway activation, transformation potential, and sensitivity to pathway inhibition are required to better define the relevance of these alterations. Interestingly, we found a mutual exclusivity in IBCs for NOTCH2, NOTCH4, and CREBBP alterations, present in a total of 19 out of 76 (25%) informative samples. Of note, NOTCH2, and NOTCH4 were also reported as more

frequently mutated in IBC in the recent Liang's study (Liang et al., 2018). We also found a NOTCH pathway activation score (Villanueva et al., 2012) higher in IBC than in non-IBC independently from the molecular subtypes and AJCC stage, further supporting a role for the NOTCH pathway in IBC. Several data in literature, based on pre-clinical models, have also related IBC and NOTCH alterations. In the MARY-X model, the lymphovascular emboli of IBC exhibit a NOTCH3 addiction (Xiao et al., 2011). The FC-IBC02 cell line shows NOTCH3 amplification (Fernandez et al., 2013). Pregnant mice expressing higher levels of an activated intracellular form of NOTCH3 develop luminal mammary tumors resembling IBC that frequently metastasize (Ling et al., 2013). Thus, the NOTCH targeting might be an option for IBC treatment. Accordingly, a preclinical study in IBC showed that a gamma-secretase inhibitor, RO4929097, was able to block the NOTCH signaling and to attenuate the stem-like phenotype of IBC cells and regulate the inflammatory environment (Debeb et al., 2012). All this taken together, the NOTCH pathway may constitute the most prominent difference between IBC and non-IBC.

We also analyzed four other classes of targeted therapies approved or tested in breast cancer. Regarding the PI3K/AKT/mTOR inhibitors, even if PIK3CA was the only gene more frequently altered in non-IBC compared to IBC, its frequency of alteration was relatively high in IBC (21%), with many hotspot mutations. Other actionable genes of the PI3K/AKT/mTOR pathway were frequently altered in IBC with likely loss-of-function mutations in PTEN, TSC1, and TSC2 and gain-of-function mutations in AKT1, AKT3, MTOR, RPTOR, and RICTOR. Thus, like non-IBC patients, IBC patients may benefit from inhibition of the pathway with the PI3K/AKT/mTOR inhibitors approved and in development (Kenna et al., 2018).

Regarding the CDK4/6 inhibitors class, we found twice as higher percentage of patients with AGAs in IBC than in non-IBC (29% vs. 15%). The most frequent AGA in this group was CCND1 amplification (10% of IBCs), followed by CDKN2A deletion/mutation (5%). Mutations in the FAT1 and RB1 tumor suppressors, potentially associated with resistance to CDK4/6 inhibitors (Li et al., 2018), were also observed in 10% and 4% of IBC respectively. Interestingly, an E2F4 activation expression signature associated with sensitivity to palbociclib and resistance to aromatase inhibitors (Guerrero-Zotano et al., 2018) was higher in IBC than in non-IBC samples, notably in HR+/HER2- patients. Clearly, CDK4/6 inhibitors deserve to be tested in IBC.

The percentage of "actionable patients" in the class of HER/EGFR inhibitors was higher in IBC (36% vs. 23%), and the difference tended towards significance in multivariate analysis including the molecular subtypes and AJCC stage. As expected, ERBB2 amplification was observed in 26% of IBC, and activating ERBB2 mutations (Petrelli et

al., 2017) were much less frequent. Five IBC patients displayed such mutations, including two with (HER2+ patient) and three without (HER2- patient) simultaneous amplification. Mutations were located in the extracellular domain and the kinase domain and have been associated with sensitivity to ERBB2 tyrosine kinase inhibitors such as neratinib (Bose et al., 2013) with which clinical trials are ongoing. Three IBC patients (3%) displayed an ERBB3 mutation identified as AGA versus 42 non-IBC patients (1.8%). In their small series of cases, Hamm et al. (2016) previously reported frequent co-occurrence of ERBB3 mutations and ERBB2 amplification in IBC and suggested possible contribution to resistance to anti-HER2 therapy. In our larger series, such co-occurrence was found in 2% of IBC and only 0.2% of non-IBC, supporting investigation of ERBB3-inhibitors in combination with ERBB2 inhibitors in IBC.

Conclusions

Our study confirms the hypothesis that IBC is distinct from non-IBC at the genomic level, independently from the molecular subtypes and disease stage. We found higher TMB in IBC than in non-IBC and 95 genes more frequently altered in IBC in a molecular subtype- and stage-independent way. Ninety-seven percent of IBC samples displayed at least one AGA. This percentage, higher than in non-IBC (87%), suggests that precision medicine is a bona fide option in this aggressive disease, notably with drugs targeting DNA repair, NOTCH signaling, and CDK4/6. The strengths of our study are: i) the largest comparison of IBC versus non-IBC samples (total of 2,452 samples), and the largest number of genes tested (756 genes) in such comparison, ii) a consensual uniform case definition for IBC, iii) a homogeneous series of non-pretreated primary tumors, iv) an adjustment upon both the molecular subtypes and AJCC stage, and v) a statistical correction (FDR with q-values) for multiple tests in the gene-by-gene supervised analysis.

To our knowledge, these two last points have never been combined in studies comparing the molecular alterations of IBC and non-IBC. Other strengths include the use of an algorithm to define more objectively the AGAs, the validation of differential activation of potentially targetable pathways (NOTCH, HRD) using transcriptomic and genomic data, and the demonstration that our supervised analysis gave very similar results whatever was the definition of molecular subtypes included in the multivariate analysis, either IHC or PAM-based. However, like most of other studies published in the field, it also displays a few limitations: i) its retrospective nature and associated biases, ii) absence of matched normal DNA sequenced for the targeted NGS-based series and absence of information regarding eventual germline mutations and family and personal histories of cancer, iii) presence of missing data for several genes because of the variation in genes targeted across the cohorts examined, leading to a loss of sensitivity

regarding identification of genes differentially altered, iv) the use of different sequencing platforms including targeted NGS and WES, even if that did not impact our comparative analysis as suggested by the multivariate analysis, and v) no further analysis of structural variations, driver mutations, intra-tumor heterogeneity, and mutational signatures. Of course, analysis of a larger and homogeneous series of untreated primary tumors analyzed with WES, WGS and RNA-Seq is warranted. Such analysis could also reveal etiology of IBC by identifying DNA sequences not matching to the human genome, such as viral or bacterial infection, as suggested (El-Shinawi et al., 2016). But yet, our results suggest targeted therapies that have the potential to bring benefit to IBC patients and encourage prospective clinical trials.

References

Andre, F., Bachelot, T., Commo, F., Campone, M., Arnedos, M., Dieras, V., Lacroix-Triki, M., Lacroix, L., Cohen, P., Gentien, D., Adelaide, J., Dalenc, F., Goncalves, A., Levy, C., Ferrero, J.M., Bonneterre, J., Lefeuvre, C., Jimenez, M., Filleron, T., Bonnefoi, H., 2014. Comparative genomic hybridisation array and DNA sequencing to direct treatment of metastatic breast cancer: a multicentre, prospective trial (SAFIR01/UNICANCER). Lancet Oncol 15, 267-274.

Banerji, S., Cibulskis, K., Rangel-Escareno, C., Brown, K.K., Carter, S.L., Frederick, A.M., Lawrence, M.S., Sivachenko, A.Y., Sougnez, C., Zou, L., Cortes, M.L., Fernandez-Lopez, J.C., Peng, S., Ardlie, K.G., Auclair, D., Bautista-Pina, V., Duke, F., Francis, J., Jung, J., Maffuz-Aziz, A., Onofrio, R.C., Parkin, M., Pho, N.H., Quintanar-Jurado, V., Ramos, A.H., Rebollar-Vega, R., Rodriguez-Cuevas, S., Romero-Cordoba, S.L., Schumacher, S.E., Stransky, N., Thompson, K.M., Uribe-Figueroa, L., Baselga, J., Beroukhim, R., Polyak, K., Sgroi, D.C., Richardson, A.L., Jimenez-Sanchez, G., Lander, E.S., Gabriel, S.B., Garraway, L.A., Golub, T.R., Melendez-Zajgla, J., Toker, A., Getz, G., Hidalgo-Miranda, A., Meyerson, M., 2012. Sequence analysis of mutations and translocations across breast cancer subtypes. Nature 486, 405-409.

Bekhouche, I., Finetti, P., Adelaide, J., Ferrari, A., Tarpin, C., Charafe-Jauffret, E., Charpin, C., Houvenaeghel, G., Jacquemier, J., Bidaut, G., Birnbaum, D., Viens, P., Chaffanet, M., Bertucci, F., 2011. High-resolution comparative genomic hybridization of inflammatory breast cancer and identification of candidate genes. PLoS One 6, e16950.

Bertucci, F., Finetti, P., Colpaert, C., Mamessier, E., Parizel, M., Dirix, L., Viens, P., Birnbaum, D., van Laere, S., 2015. PDL1 expression in inflammatory breast cancer is frequent and predicts for the pathological response to chemotherapy. Oncotarget 6, 13506-13519.

Bertucci, F., Finetti, P., Guille, A., Adelaide, J., Garnier, S., Carbuccia, N., Monneur, A., Charafe-Jauffret, E., Goncalves, A., Viens, P., Birnbaum, D., Chaffanet, M., 2016. Comparative genomic analysis of primary tumors and metastases in breast cancer. Oncotarget 7, 27208-27219.
Bertucci, F., Finetti, P., Vermeulen, P., Van Dam, P., Dirix, L., Birnbaum, D., Viens, P., Van Laere, S., 2014a. Genomic profiling of inflammatory breast cancer: a review. Breast 23, 538-545.

Bertucci, F., Goncalves, A., 2017. Immunotherapy in breast cancer: the emerging role of PD-1 and PD-L1. Curr Oncol Rep 19, 64.

Bertucci, F., Ng, C.K.Y., Patsouris, A., Droin, N., Piscuoglio, S., Carbuccia, N., Soria, J.C., Dien, A.T., Adnani, Y., Kamal, M., Garnier, S., Meurice, G., Jimenez, M., Dogan, S., Verret, B., Chaffanet, M., Bachelot, T., Campone, M., Lefeuvre, C., Bonnefoi, H., Dalenc, F., Jacquet, A., De Filippo, M.R., Babbar, N., Birnbaum, D., Filleron, T., Le Tourneau, C., Andre, F., 2019. Genomic characterization of metastatic breast cancers. Nature 569, 560-564.

Bertucci, F., Ueno, N.T., Finetti, P., Vermeulen, P., Lucci, A., Robertson, F.M., Marsan, M., Iwamoto, T., Krishnamurthy, S., Masuda, H., Van Dam, P., Woodward, W.A., Cristofanilli, M., Reuben, J.M., Dirix, L., Viens, P., Symmans, W.F., Birnbaum, D., Van Laere, S.J., 2014b. Gene expression profiles of inflammatory breast cancer: correlation with response to neoadjuvant chemotherapy and metastasis-free survival. Ann Oncol 25, 358-365.

Bose, R., Kavuri, S.M., Searleman, A.C., Shen, W., Shen, D., Koboldt, D.C., Monsey, J., Goel, N., Aronson, A.B., Li, S., Ma, C.X., Ding, L., Mardis, E.R., Ellis, M.J., 2013. Activating HER2 mutations in HER2 gene amplification negative breast cancer. Cancer Discov 3, 224-237.

Charafe-Jauffret, E., Tarpin, C., Viens, P., Bertucci, F., 2008. Defining the molecular biology of inflammatory breast cancer. Semin Oncol 35, 41-50.
Dawood, S., Merajver, S.D., Viens, P., Vermeulen, P.B., Swain, S.M., Buchholz, T.A., Dirix, L.Y., Levine, P.H., Lucci, A., Krishnamurthy, S., Robertson, F.M., Woodward, W.A., Yang, W.T., Ueno, N.T., Cristofanilli, M., 2011. International expert panel on inflammatory breast cancer: consensus statement for standardized diagnosis and treatment. Ann Oncol 22, 515-523.

Debeb, B.G., Cohen, E.N., Boley, K., Freiter, E.M., Li, L., Robertson, F.M., Reuben, J.M., Cristofanilli, M., Buchholz, T.A., Woodward, W.A., 2012. Pre-clinical studies of Notch signaling inhibitor RO4929097 in inflammatory breast cancer cells. Breast Cancer Res Treat 134, 495-510.

Ellis, M.J., Ding, L., Shen, D., Luo, J., Suman, V.J., Wallis, J.W., Van Tine, B.A., Hoog, J., Goiffon, R.J., Goldstein, T.C., Ng, S., Lin, L., Crowder, R., Snider, J., Ballman, K., Weber, J., Chen, K., Koboldt, D.C., Kandoth, C., Schierding, W.S., McMichael, J.F., Miller, C.A., Lu, C., Harris, C.C., McLellan, M.D., Wendl, M.C., DeSchryver, K., Allred, D.C., Esserman, L., Unzeitig, G., Margenthaler, J., Babiera, G.V., Marcom, P.K., Guenther, J.M., Leitch, M., Hunt, K., Olson, J., Tao, Y., Maher, C.A., Fulton, L.L., Fulton, R.S., Harrison, M., Oberkfell, B., Du, F., Demeter, R., Vickery, T.L., Elhammali, A., Piwnica-Worms, H., McDonald, S., Watson, M., Dooling, D.J., Ota, D., Chang, L.W., Bose, R., Ley, T.J., Piwnica-Worms, D., Stuart, J.M., Wilson, R.K., Mardis, E.R., 2012. Whole-genome analysis informs breast cancer response to aromatase inhibition. Nature 486, 353-360.

El-Shinawi, M., Mohamed, H.T., Abdel-Fattah, H.H., Ibrahim, S.A., El-Halawany, M.S., Nouh; M.A., Schneider, R.J., Mohamed, M.M., 2016. Inflammatory and Noninflammatory Breast Cancer: A Potential Role for Detection of Multiple Viral DNAs in Disease Progression. Ann Surg Oncol 23, 494-502.

Fernandez, S.V., Robertson, F.M., Pei, J., Aburto-Chumpitaz, L., Mu, Z., Chu, K., Alpaugh, R.K., Huang, Y., Cao, Y., Ye, Z., Cai, K.Q., Boley, K.M., Klein-Szanto, A.J., Devarajan, K., Addya, S., Cristofanilli, M., 2013. Inflammatory breast cancer (IBC): clues for targeted therapies. Breast Cancer Res Treat 140, 23-33.

Ferrari, A., Vincent-Salomon, A., Pivot, X., Sertier, A.S., Thomas, E., Tonon, L., Boyault, S., Mulugeta, E., Treilleux, I., MacGrogan, G., Arnould, L., Kielbassa, J., Le Texier, V., Blanche, H., Deleuze, J.F., Jacquemier, J., Mathieu, M.C., Penault-Llorca, F., Bibeau, F., Mariani, O., Mannina, C., Pierga, J.Y., Tredan, O., Bachelot,

T., Bonnefoi, H., Romieu, G., Fumoleau, P., Delaloge, S., Rios, M., Ferrero, J.M., Tarpin, C., Bouteille, C., Calvo, F., Gut, I.G., Gut, M., Martin, S., Nik-Zainal, S., Stratton, M.R., Pauporte, I., Saintigny, P., Birnbaum, D., Viari, A., Thomas, G., 2016. A whole-genome sequence and transcriptome perspective on HER2-positive breast cancers. Nature Commun 7, 12222.

Goh, G., Schmid, R., Guiver, K., Arpornwirat, W., Chitapanarux, I., Ganju, V., Im, S.A., Kim, S.B., Dechaphunkul, A., Maneechavakajorn, J., Spector, N., Yau, T., Afrit, M., Ahmed, S.B., Johnston, S.R., Gibson, N., Uttenreuther-Fischer, M., Herrero, J., Swanton, C., 2016. Clonal Evolutionary Analysis during HER2 Blockade in HER2-Positive Inflammatory Breast Cancer: A Phase II Open-Label Clinical Trial of Afatinib +/-Vinorelbine. PLoS Med 13, e1002136.

Guerrero-Zotano, A.L., Stricker, T.P., Formisano, L., Hutchinson, K.E., Stover, D.G., Lee, K.M., Schwarz, L.J., Giltnane, J.M., Estrada, M.V., Jansen, V.M., Servetto, A., Gavila, J., Perez-Fidalgo, J.A., Lluch, A., Llombart-Cussac, A., Bayar, M.A., Michiels, S., Andre, F., Arnedos, M., Guillem, V., Ruiz-Simon, A., Arteaga, C.L., 2018. ER(+) Breast Cancers Resistant to Prolonged Neoadjuvant Letrozole Exhibit an E2F4 Transcriptional Program Sensitive to CDK4/6 Inhibitors. Clin Cancer Res24, 2517-2529.

Hamm, C.A., Moran, D., Rao, K., Trusk, P.B., Pry, K., Sausen, M., Jones, S., Velculescu, V.E., Cristofanilli, M., Bacus, S., 2016. Genomic and Immunological Tumor Profiling Identifies Targetable Pathways and Extensive CD8+/PDL1+ Immune Infiltration in Inflammatory Breast Cancer Tumors. Mol Cancer Ther 15, 1746-1756.

Hoskins, J.M., Carey, L.A., McLeod, H.L., 2009. CYP2D6 and tamoxifen: DNA matters in breast cancer. Nat Rev Cancer 9, 576-586.

Jagsi, R., Griffith, K.A., Bellon, J.R., Woodward, W.A., Horton, J.K., Ho, A., Feng, F.Y., Speers, C., Overmoyer, B., Sabel, M., Schott, A.F., Pierce, L., Translational Breast Cancer Research, C., 2018. Concurrent Veliparib With Chest Wall and Nodal Radiotherapy in Patients With Inflammatory or Locoregionally Recurrent Breast Cancer: The TBCRC 024 Phase I Multicenter Study. J Clin Oncol 36, 1317-1322.

Kenna, M.M., McGarrigle, S., Pidgeon, G.P., 2018. The next generation of PI3K-AktmTOR pathway inhibitors in breast cancer cohorts. Biochim Biophys Acta Rev Cancer 1870, 185-197.

Le Tourneau, C., Delord, J.P., Goncalves, A., Gavoille, C., Dubot, C., Isambert, N., Campone, M., Tredan, O., Massiani, M.A., Mauborgne, C., Armanet, S., Servant, N., Bieche, I., Bernard, V., Gentien, D., Jezequel, P., Attignon, V., Boyault, S., Vincent-Salomon, A., Servois, V., Sablin, M.P., Kamal, M., Paoletti, X., investigators, S., 2015. Molecularly targeted therapy based on tumour molecular profiling versus conventional therapy for advanced cancer (SHIVA): a multicentre, open-label, proof-of-concept, randomised, controlled phase 2 trial. Lancet Oncol 16, 1324-1334.

Lefebvre, C., Bachelot, T., Filleron, T., Pedrero, M., Campone, M., Soria, J.C., Massard, C., Levy, C., Arnedos, M., Lacroix-Triki, M., Garrabey, J., Boursin, Y., Deloger, M., Fu, Y., Commo, F., Scott, V., Lacroix, L., Dieci, M.V., Kamal, M., Dieras, V., Goncalves, A., Ferrerro, J.M., Romieu, G., Vanlemmens, L., Mouret Reynier, M.A., Thery, J.C., Le Du, F., Guiu, S., Dalenc, F., Clapisson, G., Bonnefoi, H., Jimenez, M., Le Tourneau, C., Andre, F., 2016. Mutational Profile of Metastatic Breast Cancers: A Retrospective Analysis. PLoS Med 13, e1002201.

Li, Z., Razavi, P., Li, Q., Toy, W., Liu, B., Ping, C., Hsieh, W., Sanchez-Vega, F., Brown, D.N., Da Cruz Paula, A.F., Morris, L., Selenica, P., Eichenberger, E., Shen, R., Schultz, N., Rosen, N., Scaltriti, M., Brogi, E., Baselga,

J., Reis-Filho, J.S., Chandarlapaty, S., 2018. Loss of the FAT1 Tumor Suppressor Promotes Resistance to CDK4/6 Inhibitors via the Hippo Pathway. Cancer Cell 34, 893-905 e898.

Liang, X., Vacher, S., Boulai, A., Bernard, V., Baulande, S., Bohec, M., Bieche, I., Lerebours, F., Callens, C., 2018. Targeted next-generation sequencing identifies clinically relevant somatic mutations in a large cohort of inflammatory breast cancer. Breast Cancer Res 20, 88.

Ling, H., Sylvestre, J.R., Jolicoeur, P., 2013. Cyclin D1-dependent induction of luminal inflammatory breast tumors by activated notch3. Cancer Res 73, 5963-5973.

Marquard, A.M., Eklund, A.C., Joshi, T., Krzystanek, M., Favero, F., Wang, Z.C., Richardson, A.L., Silver, D.P., Szallasi, Z., Birkbak, N.J., 2015. Pan-cancer analysis of genomic scar signatures associated with homologous recombination deficiency suggests novel indications for existing cancer drugs. Biomark Res 3, 9.

Masuda, H., Baggerly, K.A., Wang, Y., Iwamoto, T., Brewer, T., Pusztai, L., Kai, K., Kogawa, T., Finetti, P., Birnbaum, D., Dirix, L., Woodward, W.A., Reuben, J.M., Krishnamurthy, S., Symmans, W., Van Laere, S.J., Bertucci, F., Hortobagyi, G.N., Ueno, N.T., 2013. Comparison of molecular subtype distribution in triple-negative inflammatory and non-inflammatory breast cancers. Breast Cancer Res 15, R112.

Matsuda, N., Lim, B., Wang, Y., Krishnamurthy, S., Woodward, W., Alvarez, R.H., Lucci, A., Valero, V., Reuben, J.M., Meric-Bernstam, F., Ueno, N.T., 2017. Identification of frequent somatic mutations in inflammatory breast cancer. Breast Cancer Res Treat 163, 263-272.

Metastatic Breast Cancer Project, 2018.
http://www.cbioportal.org/study?id=brca_mbcproject_wagle_2017. Accessed 20 April 2018.

McGranahan, N., Favero, F., de Bruin, E.C., Birkbak, N.J., Szallasi, Z., Swanton, C., 2015. Clonal status of actionable driver events and the timing of mutational processes in cancer evolution. Sci Transl Med 7, 283ra254.

Michmerhuizen, A.R., Pesch, A.M., Moubadder, L., Chandler, B.C., Wilder-Romans, K., Cameron, M., Olsen, E., Thomas, D.G., Zhang, A., Hirsh, N., Ritter, C.L., Liu, M., Nyati, S., Pierce, L.J., Jagsi, R., Speers, C., 2019. PARP1 Inhibition Radiosensitizes Models of Inflammatory Breast Cancer to Ionizing Radiation. Mol Cancer Ther. 2019 Aug 14

Mollen, E.W.J., Ient, J., Tjan-Heijnen, V.C.G., Boersma, L.J., Miele, L., Smidt, M.L., Vooijs, M., 2018. Moving Breast Cancer Therapy up a Notch. Front Oncol 8, 518.

Nik-Zainal, S., Alexandrov, L.B., Wedge, D.C., Van Loo, P., Greenman, C.D., Raine, K., Jones, D., Hinton, J., Marshall, J., Stebbings, L.A., Menzies, A., Martin, S., Leung, K., Chen, L., Leroy, C., Ramakrishna, M., Rance, R., Lau, K.W., Mudie, L.J., Varela, I., McBride, D.J., Bignell, G.R., Cooke, S.L., Shlien, A., Gamble, J., Whitmore, I., Maddison, M., Tarpey, P.S., Davies, H.R., Papaemmanuil, E., Stephens, P.J., McLaren, S., Butler, A.P., Teague, J.W., Jonsson, G., Garber, J.E., Silver, D., Miron, P., Fatima, A., Boyault, S., Langerod, A., Tutt, A., Martens, J.W., Aparicio, S.A., Borg, A., Salomon, A.V., Thomas, G., Borresen-Dale, A.L., Richardson, A.L., Neuberger, M.S., Futreal, P.A., Campbell, P.J., Stratton, M.R., Breast Cancer Working Group of the International Cancer Genome, C., 2012a. Mutational processes molding the genomes of 21 breast cancers. Cell 149, 979-993.

Nik-Zainal, S., Davies, H., Staaf, J., Ramakrishna, M., Glodzik, D., Zou, X., Martincorena, I., Alexandrov, L.B., Martin, S., Wedge, D.C., Van Loo, P., Ju, Y.S., Smid, M., Brinkman, A.B., Morganella, S., Aure, M.R., Lingjaerde, O.C., Langerod, A., Ringner, M., Ahn, S.M., Boyault, S., Brock, J.E., Broeks, A., Butler, A., Desmedt, C., Dirix, L., Dronov, S., Fatima, A., Foekens, J.A., Gerstung, M., Hooijer, G.K., Jang, S.J., Jones, D.R., Kim, H.Y., King, T.A., Krishnamurthy, S., Lee, H.J., Lee, J.Y., Li, Y., McLaren, S., Menzies, A., Mustonen, V., O'Meara, S., Pauporte, I., Pivot, X., Purdie, C.A., Raine, K., Ramakrishnan, K., Rodriguez-Gonzalez, F.G., Romieu, G., Sieuwerts, A.M., Simpson, P.T., Shepherd, R., Stebbings, L., Stefansson, O.A., Teague, J., Tommasi, S., Treilleux, I., Van den Eynden, G.G., Vermeulen, P., Vincent-Salomon, A., Yates, L., Caldas, C., van't Veer, L., Tutt, A., Knappskog, S., Tan, B.K., Jonkers, J., Borg, A., Ueno, N.T., Sotiriou, C., Viari, A., Futreal, P.A., Campbell, P.J., Span, P.N., Van Laere, S., Lakhani, S.R., Eyfjord, J.E., Thompson, A.M., Birney, E., Stunnenberg, H.G., van de Vijver, M.J., Martens, J.W., Borresen-Dale, A.L., Richardson, A.L., Kong, G., Thomas, G., Stratton, M.R., 2016. Landscape of somatic mutations in 560 breast cancer whole-genome sequences. Nature 534, 47-54.

Nik-Zainal, S., Van Loo, P., Wedge, D.C., Alexandrov, L.B., Greenman, C.D., Lau, K.W., Raine, K., Jones, D., Marshall, J., Ramakrishna, M., Shlien, A., Cooke, S.L., Hinton, J., Menzies, A., Stebbings, L.A., Leroy, C., Jia, M., Rance, R., Mudie, L.J., Gamble, S.J., Stephens, P.J., McLaren, S., Tarpey, P.S., Papaemmanuil, E., Davies, H.R., Varela, I., McBride, D.J., Bignell, G.R., Leung, K., Butler, A.P., Teague, J.W., Martin, S., Jonsson, G., Mariani, O., Boyault, S., Miron, P., Fatima, A., Langerod, A., Aparicio, S.A., Tutt, A., Sieuwerts, A.M., Borg, A., Thomas, G., Salomon, A.V., Richardson, A.L., Borresen-Dale, A.L., Futreal, P.A., Stratton, M.R., Campbell, P.J., Breast Cancer Working Group of the International Cancer Genome, C., 2012b. The life history of 21 breast cancers. Cell 149, 994-1007.

Olshen, A.B., Venkatraman, E.S., Lucito, R., Wigler, M., 2004. Circular binary segmentation for the analysis of array-based DNA copy number data. Biostatistics 5, 557-572.

Pereira, B., Chin, S.F., Rueda, O.M., Vollan, H.K., Provenzano, E., Bardwell, H.A., Pugh, M., Jones, L., Russell, R., Sammut, S.J., Tsui, D.W., Liu, B., Dawson, S.J., Abraham, J., Northen, H., Peden, J.F., Mukherjee, A., Turashvili, G., Green, A.R., McKinney, S., Oloumi, A., Shah, S., Rosenfeld, N., Murphy, L., Bentley, D.R., Ellis, I.O., Purushotham, A., Pinder, S.E., Borresen-Dale, A.L., Earl, H.M., Pharoah, P.D., Ross, M.T., Aparicio, S., Caldas, C., 2016. The somatic mutation profiles of 2,433 breast cancers refines their genomic and transcriptomic landscapes. Nature Commun 7, 11479.

Perera-Bel, J., Hutter, B., Heining, C., Bleckmann, A., Frohlich, M., Frohling, S., Glimm, H., Brors, B., Beissbarth, T., 2018. From somatic variants towards precision oncology: Evidence-driven reporting of treatment options in molecular tumor boards. Genome Med 10, 18.

Petrelli, F., Tomasello, G., Barni, S., Lonati, V., Passalacqua, R., Ghidini, M., 2017. Clinical and pathological characterization of HER2 mutations in human breast cancer: a systematic review of the literature. Breast Cancer Res Treat 166, 339-349.

Przybytkowski, E., Lenkiewicz, E., Barrett, M.T., Klein, K., Nabavi, S., Greenwood, C.M., Basik, M., 2014. Chromosome-breakage genomic instability and chromothripsis in breast cancer. BMC Genomics 15, 579.

Rana, H.Q., Sacca, R., Drogan, C., Gutierrez, S., Schlosnagle, E., Regan, M.M., Speare, V., LaDuca, H., Dolinsky, J., Garber, J.E., Overmoyer, B.A., 2019. Prevalence of germline variants in inflammatory breast cancer. Cancer.

Ross, J.S., Ali, S.M., Wang, K., Khaira, D., Palma, N.A., Chmielecki, J., Palmer, G.A., Morosini, D., Elvin, J.A., Fernandez, S.V., Miller, V.A., Stephens, P.J., Cristofanilli, M., 2015. Comprehensive genomic profiling of inflammatory breast cancer cases reveals a high frequency of clinically relevant genomic alterations. Breast Cancer Res Treat 154, 155-162.

Shah, S.P., Roth, A., Goya, R., Oloumi, A., Ha, G., Zhao, Y., Turashvili, G., Ding, J., Tse, K., Haffari, G., Bashashati, A., Prentice, L.M., Khattra, J., Burleigh, A., Yap, D., Bernard, V., McPherson, A., Shumansky, K., Crisan, A., Giuliany, R., Heravi-Moussavi, A., Rosner, J., Lai, D., Birol, I., Varhol, R., Tam, A., Dhalla, N., Zeng, T., Ma, K., Chan, S.K., Griffith, M., Moradian, A., Cheng, S.W., Morin, G.B., Watson, P., Gelmon, K., Chia, S., Chin, S.F., Curtis, C., Rueda, O.M., Pharoah, P.D., Damaraju, S., Mackey, J., Hoon, K., Harkins, T., Tadigotla, V., Sigaroudinia, M., Gascard, P., Tlsty, T., Costello, J.F., Meyer, I.M., Eaves, C.J., Wasserman, W.W., Jones, S., Huntsman, D., Hirst, M., Caldas, C., Marra, M.A., Aparicio, S., 2012. The clonal and mutational evolution spectrum of primary triple-negative breast cancers. Nature 486, 395-399.

Shen, Q., Cohen, B., Zheng, W., Rahbar, R., Martin, B., Murakami, K., Lamorte, S., Thompson, P., Berman, H., Zuniga-Pflucker, J.C., Ohashi, P.S., Reedijk, M., 2017. Notch Shapes the Innate Immunophenotype in Breast Cancer. Cancer Discov 7, 1320-1335.

Stephens, P.J., Tarpey, P.S., Davies, H., Van Loo, P., Greenman, C., Wedge, D.C., Nik-Zainal, S., Martin, S., Varela, I., Bignell, G.R., Yates, L.R., Papaemmanuil, E., Beare, D., Butler, A., Cheverton, A., Gamble, J., Hinton, J., Jia, M., Jayakumar, A., Jones, D., Latimer, C., Lau, K.W., McLaren, S., McBride, D.J., Menzies, A., Mudie, L., Raine, K., Rad, R., Chapman, M.S., Teague, J., Easton, D., Langerod, A., Oslo Breast Cancer, C., Lee, M.T., Shen, C.Y., Tee, B.T., Huimin, B.W., Broeks, A., Vargas, A.C., Turashvili, G., Martens, J., Fatima, A., Miron, P., Chin, S.F., Thomas, G., Boyault, S., Mariani, O., Lakhani, S.R., van de Vijver, M., van 't Veer, L., Foekens, J., Desmedt, C., Sotiriou, C., Tutt, A., Caldas, C., Reis-Filho, J.S., Aparicio, S.A., Salomon, A.V., Borresen-Dale, A.L., Richardson, A.L., Campbell, P.J., Futreal, P.A., Stratton, M.R., 2012. The landscape of cancer genes and mutational processes in breast cancer. Nature 486, 400-404. The Cancer Genome Atlas, N., 2012. Comprehensive molecular portraits of human breast tumours. Nature 490, 61-70.

Van Berckelaer, C., Rypens, C., van Dam, P., Pouillon, L., Parizel, M., Schats, K.A., Kockx, M., Tjalma, W.A.A., Vermeulen, P., van Laere, S., Bertucci, F., Colpaert, C., Dirix, L., 2019. Infiltrating stromal immune cells in inflammatory breast cancer are associated with an improved outcome and increased PD-L1 expression. Breast Cancer Res 21, 28.

Van Laere, S., Ueno, N.T., Finetti, P., Vermeulen, P.B., Lucci, A., Robertson, F., Marsan, M., Iwamoto, T., Krishnamurthy, S., Masuda, H., van Dam, P., Woodward, W.A., Viens, P., Cristofanilli, M., Birnbaum, D., Dirix, L., Reuben, J., Bertucci, F., 2013. Uncovering the molecular secrets of Inflammatory Breast Cancer biology: An integrated analysis of three distinct Affymetrix gene expression data sets. Clin Cancer Res, 19, 4685-4696.

Villanueva, A., Alsinet, C., Yanger, K., Hoshida, Y., Zong, Y., Toffanin, S., Rodriguez-Carunchio, L., Sole, M., Thung, S., Stanger, B.Z., Llovet, J.M., 2012. Notch signaling is activated in human hepatocellular carcinoma and induces tumor formation in mice. Gastroenterology 143, 1660-1669 e1667.

Xiao, Y., Ye, Y., Zou, X., Jones, S., Yearsley, K., Shetuni, B., Tellez, J., Barsky, S.H., 2011. The lymphovascular embolus of inflammatory breast cancer exhibits a Notch 3 addiction. Oncogene 30, 287-300.

Yang, J., Liu, J., Ouyang, L., Chen, Y., Liu, B., Cai, H., 2016. CTLPScanner: a web server for chromothripsis-like pattern detection. Nucleic Acids Res 44, W252-258.

Supporting information

Additional supporting information may be found online in the Supporting Information section at the end of the article.

Fig. S1. Tumor mutational burden (TMB) in IBC and non-IBC.

Fig. S2. Absence of impact of the definition of molecular subtypes (IHC vs PAM50) on the differentially altered character of our 96 genes.

Fig. S3. Percentage of patients with AGAs along IBC vs non-IBC patients.

Fig. S4. Percentage of patients with actionable alterations in four specific drug classes.

Fig. S5. E2F4 activation signature enriched in IBC vs non-IBC.

Fig. S6. Mutual exclusivity of NOTCH pathway alterations in IBC.

Fig. S7. Comparison of the lists of genes differentially altered in IBC vs non-IBC across three studies.

Table S1. IBC and non-IBC data sets included in the present study.

Table S2. List of 756 genes analyzed in the present study.

Table S3. List of gene alterations identified in the 101 IBC and the 2351 non-IBC.

Table S4. List of 96 genes differentially altered in IBC vs non-IBC in MV.

Table S5. List of 159 genes differentially altered in MBC vs non-IBC.

Table S6. Detailed clinicopathological data and genomic data analyzed in the present study.

CHAPTER 3: PRECLINICAL MODELS OF IBC

Comparative transcriptional analyses of preclinical models and patient samples reveal MYC and RELA driven expression patterns that define the molecular landscape of IBC.

Abstract

Inflammatory breast cancer (IBC) is an aggressive disease for which the spectrum of preclinical models was rather limited in the past. More recently, novel cell lines and xenografts have been developed. This study evaluates the transcriptome of an extended series of IBC preclinical models and performed a comparative analysis with patient samples to determine the extent to which the current models recapitulate the molecular characteristics of IBC observed clinically. We demonstrate that the IBC preclinical models are exclusively estrogen receptor (ER)-negative and of the basal-like subtype, which reflects to some extent the predominance of these subtypes in patient samples. The IBC-specific 79-signature we previously reported was retrained and discriminated between IBC and non-IBC preclinical models, but with a relatively high rate of false positive predictions. Further analyses of gene expression profiles revealed important roles for cell proliferation, MYC transcriptional activity and TNFα/NFκB in the biology of IBC. Patterns of MYC expression and transcriptional activity were further explored in patient samples, which revealed interactions with ESR1 expression that are contrasting in IBC and nIBC and notable given the comparatively poor outcomes of ER+ IBC. Our analyses also suggest important roles for NMYC, MXD3, MAX and MLX in shaping MYC signaling in IBC. Overall, we demonstrate that the IBC preclinical models can be used to unravel cancer cell intrinsic molecular features, and thus constitute valuable research tools. Nevertheless, the current lack of ER-positive IBC models remains a major hurdle, particularly since interactions with the ER pathway appear to be relevant for IBC.

Introduction

Inflammatory Breast Cancer (IBC) is an aggressive and highly metastatic form of breast cancer. At the time of initial diagnosis, virtually all patients have lymph node involvement and 30% present with distant metastases [1]. As a consequence of the rapid onset and early metastasis, patients with IBC display an unfavorable prognosis, with 5-year overall survival rates of 40% despite multimodality treatment [2-4]. IBC is a clinical diagnosis based on the rapid onset of inflammatory symptoms: patients present with a red, enlarged breast associated with shooting pains and warmth. In addition, skin changes (e.g. "peau d'orange") and nipple retraction are often observed and typically, no palpable tumor mass is present [5-7].

In 2008, the Inflammatory Breast Cancer International Consortium (IBC-IC) was established by investigators in this field, with the ultimate aim of accelerating IBC research. The compelling need for this alignment of researches was based on the fact that despite many efforts over decades of research, IBC remained a poorly characterized disease void of specific targets for molecular therapy [8]. The need for better, more efficient, and IBC-specific treatment options is underscored by the fact that there are no significant changes in overall survival of patients up till now. In addition, IBC can be regarded as a human model for aggressive (breast) cancer behavior in general.

The first project of the IBC-IC involved the identification of a molecular profile of IBC using a large multicentric series of clinical samples. A set of 79 probe sets with an IBC-specific and molecular subtype-independent gene expression profile was identified and validated. Translating the IBC signature into pathways and processes indicated that alterations in TGFβ signaling may be an important driver [9], which is confirmed in a more recent study [10]. In addition, a molecular signature predicting pathological complete response to neoadjuvant chemotherapy in IBC was identified [11] and catalogues of genomic alterations were described [12]. In parallel, the role of the tumor microenvironment (TME) in IBC development and progression has been also increasingly emphasized [13-18]. Additionally, efforts were also focused on developing greater numbers of preclinical IBC models of different molecular subtypes, allowing researchers to perform functional validations in more versatile genetic backgrounds. Traditionally, five preclinical models have been used for IBC research: three established cell lines (i.e. KPL4, SUM149, and SUM190) and two xenograft models (i.e. Mary-X and WIBC9). The pre-clinical models of IBC are either triple negative or HER2-amplified, which is reflective of the most prevalent subtypes of this disease [19-30]. Within the last years, novel IBC models have been generated amongst others by researchers at the Fox Chase Cancer Center (i.e. FC-IBC-01 and FC-IBC-02), The University of Texas MD

Anderson Cancer Center (i.e. MDA-IBC-03), the Thomas Jefferson University (i.e. TJ-IBC-04 and TJ-IBC-09), and the GZA Hospital Sint-Augustinus (i.e. UA-IBC-01) [31].

However, the complete molecular characterization and comparative analyses of these cell lines remains to be completed. Therefore, we report here a comprehensive analysis of gene expression data from IBC and non-IBC (nIBC) preclinical models and patient samples. Our primary goal was to gain insight into the molecular characteristics of the above-described IBC preclinical models and to identify features also exhibited by IBC cells in human tissue samples. This set of features will be crucial knowledge when setting up functional validation experiments for data reported in patient samples. In addition, to broaden the clinical perspectives of this panel of IBC preclinical models, their sensitivity profile to a wide range of therapeutic agents was estimated using the CMap dataset of 1.3 million L1000 signatures that reflect transcriptional responses of human cells to chemical and genetic perturbations. It stands to reason that these efforts will also contribute to a more detailed comprehension of biological themes intrinsic to IBC cells.

Results

Cluster analysis and molecular subtyping

To investigate differences between IBC (n = 10) and nIBC (n = 22) preclinical models, we merged expression profile analysis performed in our Institution with external gene expression data from various public resources (Gene Expression Omnibus: GSE12777, GSE16795, and GSE40464; and ArrayExpress: E-MTAB-7). To assess the efficiency of the normalization strategy, unsupervised hierarchical clustering analysis (UHCA) was performed for all 124 profiles and for the 500 most variable genes selected by standard deviation. Results are shown in Fig. 1a. The NbClust algorithm identified four clusters in the data set that were significantly associated with the ER status (P<0.001), the PR status (P<0.001), the HER2 status (P=0.043), the ER/HER2 combined subtypes (P<0.001) and the IBC/nIBC tumor phenotype (P<0.001). Using multinomial regression analyses, we demonstrated that the ER/HER2 combined subtypes were the best predictor of the clustering pattern (AIC=59.881), followed by the ER status (AIC=63.195), the tumor phenotype (AIC=70.293), the PR status (AIC=74.277), and the HER2 status (AIC=82.575). A multivariate model containing the tumor phenotype and the ER/HER2 combined subtypes (AIC=45.589) was significantly better in predicting the clustering pattern as compared to the ER/HER2 combined subtypes alone (Likelihood ratio test; P<0.001). Addition of the PR status to the ER/HER2 combined subtypes did not improve the accuracy of the model in predicting the clustering outcome (AIC= 65.881; (Likelihood ratio test; P=1.000). Given these results and since we observed that all 32 different preclinical models cluster on terminal branches, we argue that the

adopted normalization strategy was effective in removing batch-specific expression variation, that relevant gene expression themes are preserved, and that replicate gene expression profiles (GEPs) can be reliably averaged.
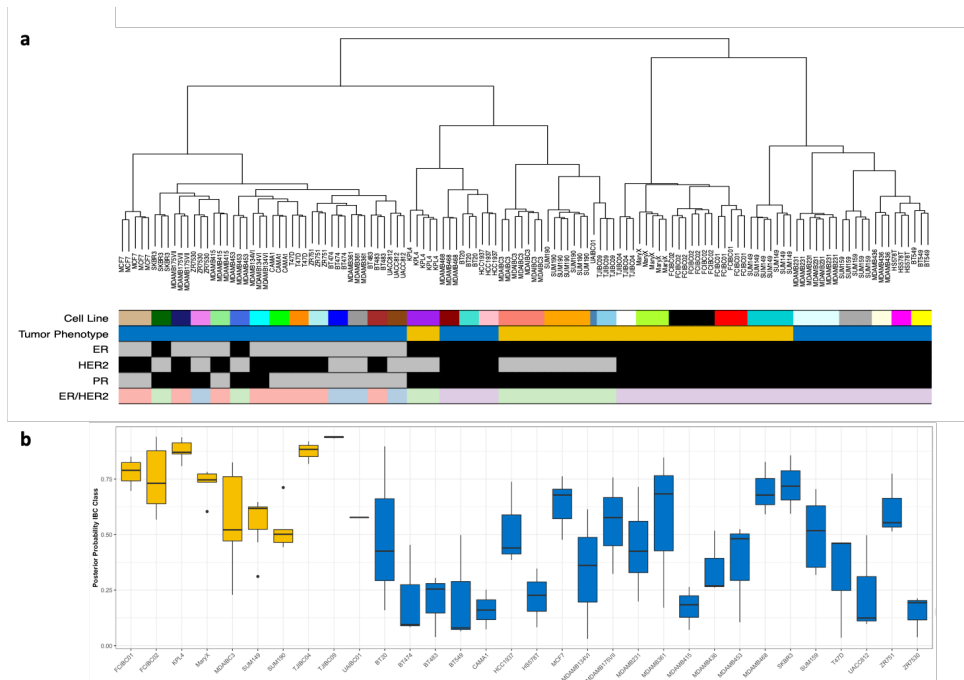
Fig. 1: Molecular characterization and classification of (inflammatory) breast cancer cell lines a Dendrogram resulting from an unsupervised hierarchical cluster analysis performed on the normalized expression data set of preclinical models prior to averaging. The different cell lines are indicated using different colors in the annotation track underneath the dendrogram, in addition to the tumor phenotype (blue=nIBC; yellow=IBC), the ER status (grey=ER+; black=ER-), the HER2 status (grey=HER2-; black=HER2+), the PR status (grey=PR+; black=PR-), and the ER/HER2 combined subtypes (red=ER+/HER2-; green=ER-/HER2+; blue=ER+/HER2+; purple=ER-/HER2-). b The classification scores of the preclinical models are shown in boxplot format. The different preclinical models are shown along the X-axis and the Y-axis represents the posterior probability scores resulting from applying the IBC classification models. Boxes are color coded according to the tumor phenotype: blue=nIBC and yellow=IBC.

Averaged GEPs were then used to classify the IBC preclinical models according to their differentiation status using the differentiation predictor model (DPM), the luminal/basal/mesenchymal classification (LBM) system, and PAM50-subtypes. Results are shown in Table 1 and demonstrated that these cell lines all adhered to the basal-like subtype. The majority of the IBC cell lines exhibited a luminal progenitor phenotype (i.e. 7/10) and with respect to the PAM50 classifications, the ER-negative subtypes predominated (i.e. 9/10 basal-like, HER2-enriched or normal-like). Notably, all

classification distributions, except for the DPM classification (P=0.072) and the HER2 status (P=0.222), are significantly different compared to those obtained in nIBC preclinical models (Table 1).

Table 1: Molecular characteristics of IBC models

IBC model	ER	PR	HER2	ER/HER2	LBM classification	DPM classification	PAM50 subtype
FCIBC01	NEG	NEG	NEG	TN	Basal	Progenitor	Normal
FCIBC02	NEG	NEG	NEG	TN	Basal	Progenitor	Basal
KPL4	NEG	NEG	POS	HER2	Basal	Progenitor	Her2
MaryX	NEG	NEG	NEG	TN	Basal	Progenitor	Basal
MDAIBC3	NEG	NEG	POS	HER2	Basal	Mature	LumA
SUM149	NEG	NEG	NEG	TN	Basal	Progenitor	Basal
SUM190	NEG	NEG	POS	HER2	Basal	Mature	Her2
TJIBC04	NEG	NEG	NEG	TN	Basal	Progenitor	Basal
TJIBC09	NEG	NEG	POS	HER2	Basal	Mature	Her2
UAIBC01	NEG	NEG	POS	HER2	Basal	Progenitor	Her2
P-value (compared to nIBC)	0,011	0,013	0,222	0,001	0,001	0,072	0,006

Then, in order to investigate if the IBC preclinical models recapitulate biological features typical of IBC in clinical samples, we applied the transcriptomic classifier 9 consisting of 79 genes with an IBC-specific expression profile on all 32 preclinical models. An elastic net generalized linear model achieved an accuracy of 82% on an independent series (Supplementary Figure 1). When applied to the series of averaged GEPs of IBC and nIBC preclinical models, an accuracy of 78% was obtained, with a sensitivity and specificity of respectively 100% and 68%. The latter indicated a high rate of false positive predictions amongst the nIBC models (McNemar test; P=0.023), particularly when compared to the patient samples data, where a specificity level of 86% was observed. By consequence, also the positive predictive value was low (i.e. 59%). Another notable observation relates to the fact that when the model was applied onto the replicate GEPs, low posterior probability scores (i.e. close to 0.5) were repeatedly observed for some IBC preclinical models (i.e. SUM149, SUM190 and MDA-IBC-3). All data are shown in Fig. 1b.

To further assess the representativity of the cell lines as models for IBC, the GEPs of UA-IBC-01 and the primary tumor sample it was derived from were directly compared. Both the model and the tumor sample were classified as non-luminal, HER2-enriched according to the PAM50 molecular subtypes despite the use of estrogen pellets during the generation of the UA-IBC-01 PDX-derived cell lines. Gene-wise comparison revealed that both GEPs are strongly correlated (Rs=0.740; P<0.001; Supplementary Figure 2). Out of 12,384 genes expressed above background in both samples, 295 genes were considered overexpressed in the UA-IBC-01 cell line based on expression differences superior to the 97.5th percentile of all gene-wise comparisons. These genes were enriched for hallmark gene sets related to cell proliferation (i.e. E2F target genes: P<0.001; and G2M checkpoint genes: P<0.001). Based on expression differences

inferior to the 2.5th percentile of all gene-wise comparisons, 254 genes were considered overexpressed in the primary tumor sample, and these were enriched for gene sets related to immune response programs (i.e. IFNγ signaling: P=0.007; and TNFα signaling: P=0.003) and epithelial-to-mesenchymal transition (P<0.001), which is consistent with the expected enrichment of stroma and immune cells in the primary tumor sample. Interestingly, hallmarks related to hormone receptor signaling (i.e. early estrogen response genes: P=0.012; late estrogen response genes: P=0.002; and androgen response genes: P=0.003) are also enriched amongst genes overexpressed in the primary tumor sample.

Differential expression and co-expression network analysis

To identify molecular differences between IBC and nIBC preclinical models, two strategies were applied. First, IBC and nIBC cell lines were compared using generalized linear models to identify differentially expressed genes (DEGs). Hence, 931 DEGs were revealed of which 437 (47%) and 494 (53%) were respectively up- and downregulated in IBC at a false discovery rate of 10%. Results are shown in volcano plot format in Fig. 2a. Differential gene expression statistics are provided in Supplementary Data 1. The resulting fold change vector was then used to perform GSEA for the hallmark gene sets. Results are shown in Supplementary Table 1 and reveal that DEGs overexpressed in IBC cell lines were enriched for gene sets related to IL2/STAT5-, KRAS-, or TP53-signalling and MYC target genes, whereas EMT-related genes were enriched amongst downregulated DEGs.

In a second strategy to characterize the IBC preclinical models, weighted gene co-expression network analysis (WGCNA) was applied onto the averaged GEPs. Using data for all available genes, 22 distinct gene co-expression modules were identified with sizes ranging from 104 to 871 genes. Details regarding the network construction and module detection are shown in Supplementary Figure 3 and different co-expression module statistics are summarized in Table 2. The correlation structure of the 22 co-expression modules was investigated and revealed the existence of three co-expression clusters (Fig. 2b). Gene set enrichment analysis (GSEA) of the gene module memberships (GMM) scores (Supplementary Data 2) revealed distinct hallmark enrichment patterns for each of these co-expression clusters (Fig. 2c), suggesting they reflect different biological themes.
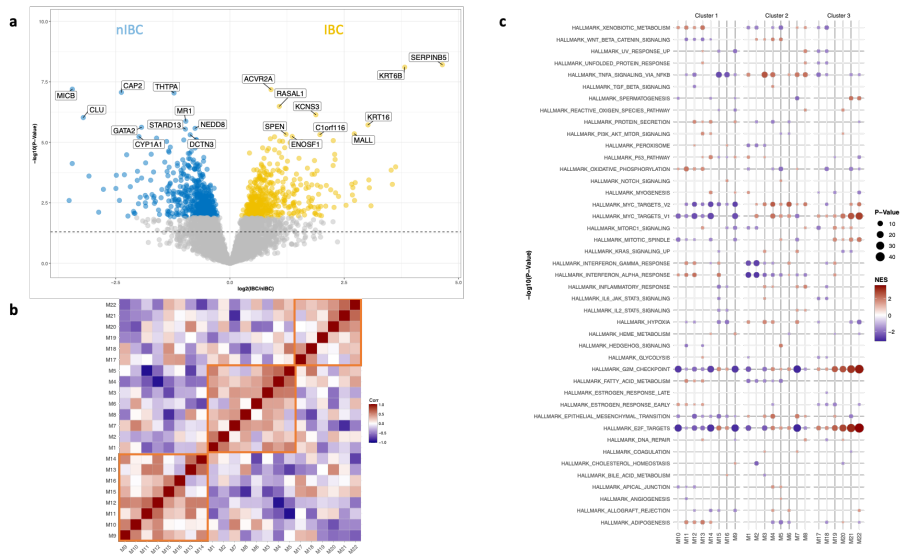
Fig. 2: Identification of molecular differences between IBC and nIBC preclinical models
a Volcano plot representing gene expression differences between IBC and nIBC preclinical models. The X-axis indicates the log2-transformed gene expression fold change in IBC relative to nIBC. The Y-axis represents the –log10-transformed p-value. The horizontal dashed line represents a nominal P-value threshold of 5%. Genes color-coded yellow and blue are overexpressed in IBC and nIBC respectively at a false discovery adjusted p-value of 10%. The top 10 overexpressed genes in IBC and nIBC cell lines are labeled. b Heatmap representing the correlation structure of 22 co-expression modules identified using WGCNA. Pearson correlation coefficients resulting from pairwise comparisons of the eigengenes of the different co-expression modules are coded according to a blue-red color scheme reflecting correlation coefficients ranging from -1 to 1. Row and columns are labeled with the names of the co-expression modules and are ordered according to an unsupervised hierarchical cluster analysis. The three co-expression cluster groups are indicated in orange squares. c Dot plot representing the result of a gene set enrichment analysis (GSEA) obtained by comparing the gene-module membership scores for each co-expression cluster to the hallmark gene sets. The co-expression modules are listed along the X-axis and a different facet is created for each co-expression cluster. Enriched hallmarks per modules are indicated using a dot, the color and size of which vary with respectively the normalized enrichment score (i.e. blue=low; red=high) and the –log10 transformed p-value (i.e. small=less significant; large=more significant) that result from the GSEA.

The extent to which each of the co-expression modules is preserved in the gene expression series of the nIBC preclinical models was investigated (Table 2). The highest preservation score was obtained for the module containing ERBB2 (i.e. M12), most likely reflecting the presence of ERBB2+ cell lines in both IBC and nIBC series. The module containing ESR1 (i.e. M10) was poorly conserved (i.e. preservation score inferior to 2), probably due to the fact that all IBC preclinical models are ER-negative and thus the ER-related expression patterns in IBC preclinical models are weaker than in nIBC.

Table 2: Characteristics of coexpression modules

Module	Cluster	Size	Hallmark	Preservation Z-Score	Enrichment OR	Enrichment P	CS-MYC	CS-RELA	CS-E2F3
M1	C2	240	HALLMARK_TNFA_SIGNALING_VIA_NFKB	0,585	1,861	0,005	1,660	-85,880	96,080
M2	C2	218	HALLMARK_MYC_TARGETS_V1	0,999	1,061	0,457	-97,950	74,690	-1,980
M3	C2	247	HALLMARK_TNFA_SIGNALING_VIA_NFKB	1,302	1,699	0,015	0,000	-85,490	85,200
M4	C2	786	HALLMARK_MYC_TARGETS_V2	14,426	1,238	0,087	-99,920	-48,210	-60,190
M5	C2	301	HALLMARK_HEDGEHOG_SIGNALING	0,789	2,055	0,000	-5,280	-53,350	15,470
M6	C2	261	HALLMARK_MYC_TARGETS_V2	2,265	1,227	0,234	-93,060	-68,860	-4,220
M7	C2	265	HALLMARK_TNFA_SIGNALING_VIA_NFKB	0,499	1,201	0,260	27,110	-97,240	97,920
M8	C2	871	HALLMARK_TNFA_SIGNALING_VIA_NFKB	5,296	0,577	0,999	-91,210	-52,110	95,200
M9	C1	300	HALLMARK_PROTEIN_SECRETION	9,715	1,281	0,166	99,950	-49,330	-23,640
M10	C1	106	HALLMARK_INTERFERON_ALPHA_RESPONSE	1,786	0,935	0,623	63,750	67,590	2,580
M11	C1	584	HALLMARK_OXIDATIVE_PHOSPHORYLATION	2,656	0,441	1,000	1,660	65,330	6,430
M12	C1	558	HALLMARK_INTERFERON_ALPHA_RESPONSE	20,433	0,771	0,919	99,890	42,620	68,760
M13	C1	199	HALLMARK_XENOBIOTIC_METABOLISM	7,593	0,393	0,994	40,460	65,830	57,160
M14	C1	260	HALLMARK_P53_PATHWAY	6,725	1,159	0,312	99,820	-45,060	1,870
M15	C1	680	HALLMARK_E2F_TARGETS	4,575	0,619	0,995	16,280	95,900	-99,870
M16	C1	141	HALLMARK_E2F_TARGETS	0,537	1,882	0,023	0,000	96,340	5,800
M17	C3	104	HALLMARK_E2F_TARGETS	0,255	0,944	0,613	-12,390	96,070	-16,430
M18	C3	238	HALLMARK_E2F_TARGETS	5,279	2,363	0,000	31,780	-15,840	-77,750
M19	C3	157	HALLMARK_G2M_CHECKPOINT	1,118	0,502	0,967	0,000	71,370	-92,310
M20	C3	124	HALLMARK_E2F_TARGETS	3,928	0,644	0,881	-34,090	92,410	-6,250
M21	C3	148	HALLMARK_E2F_TARGETS	0,541	1,121	0,413	-97,320	78,410	-94,160
M22	C3	394	HALLMARK_E2F_TARGETS	15,215	0,728	0,925	-99,580	95,660	-91,000

Module=Gene co-expression module; Cluster=cluster to which the co-expression module belongs; Size=the number of genes in the module; Hallmark=top enriched hallmark in the module; Preservation Z-score=the z-score that defined how significantly a module is conserved in nIBC with values below 2, between 2 and 10 and above 10 indicating respectively poor, moderate and good preservation; Enrichment OR=odds ratio for enrichment of genes differentially expressed between IBC and nIBC cell lines in the module; Enrichment P=p-value corresponding to the Enrichment OR; CS-MYC=connectivity score between transcriptional profile of MYC knock-down and the module specific expression profile; CS-RELA=connectivity score between transcriptional profile of RELA knock-down and the module specific expression profile; CS-E2F3=connectivity score between transcriptional profile of E2F3 knock-down and the module specific expression profile.

Overall, the IBC co-expression modules contained in the 2nd co-expression cluster, which were associated with amongst others MYC, NFκB and Hedgehog signaling (Table 2), were most weakly conserved in nIBC cell lines (i.e. average preservation score per cluster group: C1=6.753; C2=3.270; and C3=4.390), suggesting that these gene clusters reflect biological themes that are more intrinsic to IBC. This is corroborated by the enrichment of genes overexpressed in IBC cell lines (vide supra) in 4/8 of the co-expression modules in the 2nd co-expression cluster (Table 2). Finally, based on the correlation structure of the 22 co-expression modules (Fig. 2b) and their cell line-specific expression levels, a network-based prioritization of the co-expression modules was performed. A minimal set of five co-expression modules connecting all IBC cell lines was identified (i.e. M1, M2, M7, M8 and M9), all but one belonging to the 2nd co-expression cluster (Fig. 3a).
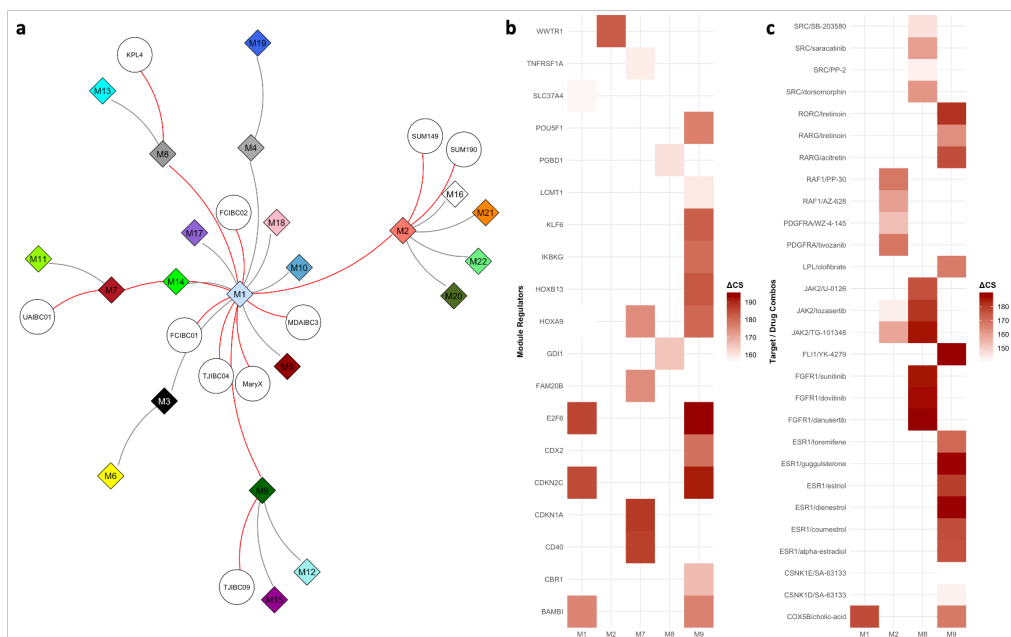
Fig. 3: Identification of co-expression cluster regulators and antagonizing chemical compounds a Network diagram showing the minimal set of edges that connect all co-expression modules and cell lines and that were identified using a minimal spanning tree analysis performed on the binary adjacency matrix representing the full set of interactions between all modules and all cell lines. Co-expression modules and cell lines are indicated respectively as diamonds labeled by module number (i.e. M1 to M22) and circles labeled by cell line name. The edges connecting all cell lines through a minimal set of co-expression modules are indicated in red. b Results identifying upstream regulators (Y-axis) for each of the five co-expression modules that connect all IBC cell lines (X-axis) are shown in heatmap format. At the intersection between rows and columns, cells are color-coded as shown in the legend only when the difference between the co-expression module specific connectivity Scores (CSs) for over-expression and knock-down of the respective genes exceeds 150 (i.e. at least 75 upon overexpression and at most -75 upon knock-down). c Results identifying target/drug combinations (Y-axis) for each

of the five co-expression modules that connect all IBC cell lines (X-axis) are shown in heatmap format. At the intersection between rows and columns, cells are color-coded as shown in the legend only when the difference between the co-expression module specific CSs for over-expression of the drug target and drug treatment exceeds 150 (i.e. at least 75 upon overexpression of the target and at most -75 upon treatment).

Identification of co-expression cluster regulators and antagonizing chemical compounds

Based on the co-expression modules analysis, we then aimed to identify potential modulators of IBC biology as well as potential drug/target combinations for therapy using the CMAP dataset. Connectivity Scores (CSs) are provided in Supplementary Data 3 for all comparisons. As a proof-of-concept, we focused on the CSs of RELA and MYC and demonstrate that knock-down of these transcription factors induced a gene expression profile that was opposite to the characteristic expression profile of the gene co-expression modules enriched for genes involved in NFκB and MYC signaling respectively (Table 2 and Supplementary Figure 4). In addition, we also evaluated all E2F transcription factors (i.e. E2F1 to E2F9) and revealed that particularly the CSs associated with E2F3 knock-down were reduced in those expression modules enriched for E2F target genes. For other E2F transcription factors, no clear association was observed.

We then focused on the set of five co-expression modules (M1, M2, M7, M8, and M9) linking all 10 IBC cell lines to reveal potential regulators and drug/target combinations. According to published literature, several of the identified regulator genes (Fig. 3b) were related to MYC activity (i.e. BAMBI, CD40, CDKN1A, CDKN2C, CDX2, E2F6, HOXA9, HOXB13, KLF6, POU5F1, and WWTR1/TAZ), often in conjunction with WNT signaling, TGFβ signaling or stem cell biology. In addition, 31 potentially effective drug/target combinations were identified involving 13 distinct targets and 26 different drugs (Fig. 3c). Unfortunately, no single target/drug combination was predicted to be effective in all five co-expression modules and no target/drug combination meeting our criteria was identified for M7. Remarkably, for M9 that connects to TJ-IBC-09, our data suggested sensitivity to anti-hormonal drugs.

MYC expression and transcriptional activity in IBC patient samples

Our results in the preclinical models described above suggested that MYC could be an important driver of IBC biology. To corroborate these data, MYC-related molecular changes were evaluated in our series of 146 and 252 expression profiles from IBC and nIBC tissue samples 9. As shown in Fig. 4a, MYC expression was dependent on the ER status defined by stratifying ESR1 mRNA levels into low, moderate, and high expression

categories (P<0.003). When comparing IBC to nIBC, no significant difference in MYC expression was observed (P=0.209). However, when stratifying by ER status, MYC expression was significantly different between IBC and nIBC (P=0.049). Correlation analysis (Fig. 4b) revealed a significant inverse relation between ESR1 and MYC expression in nIBC (Rs=-0.331; P<0.001). Similar correlations were also noted in the TCGA and METABRIC series that primarily consist of nIBC tissue samples (TCGA: Rs=-0.250 – P<0.001; METABRIC: R=-0.222 - P<0.001; data not shown). In IBC however, a different correlation pattern was observed (Rs=0.115; P=0.166), suggesting different interactions between ER and MYC depending on the tumor phenotype. A generalized linear model testing for such interactions, demonstrated that MYC expression in nIBC indeed decreased with increasing ESR1 levels (i.e. decrease with 0.754 and 0.931 expression units in respectively the ER moderate and high categories relative to the ER low category; all Ps<0.001). Results are shown in Fig. 4c, in which the first two columns represent the ER moderate and ER high categories in nIBC. In IBC samples with low ESR1 levels, MYC expression was 0.832 units lower as compared to nIBC samples with similar ESR1 mRNA levels (P<0.001; third column in Fig. 4c) and MYC expression increased by 0.599 and 1.414 expression units in respectively the ER moderate and high categories (P=0.035 and P<0.001 respectively; fourth and fifth column in Fig. 4c). To evaluate differences in MYC transcriptional activity between IBC and nIBC samples, a similar analysis was performed using activation scores calculated using GSVA based on three different published MYC activation signatures [32-34]. Hence, we noticed that differences in MYC transcriptional activity followed the same trends as those described for MYC expression, with the exception that MYC transcriptional activity was not different between IBC and nIBC samples with low ER expression (Fig. 4c).

To evaluate potential confounding effects in the reported observations, MYC expression and transcriptional activation were first compared between samples stratified by tumor stage and the PAM50 subtypes. Significant MYC expression and activation differences according to the strata of both classification systems were observed (Supplementary Figure 5 and Fig.6). Incorporating tumor stage or the PAM50 subtypes separately as blocking variables into each of the generalized linear models described above, revealed that tumor stage did not confound the observed interaction differences of ER and MYC between IBC and nIBC. The PAM50 subtypes on the other hand did account for the overall effect of ER on MYC expression or activation, but the IBC-specific associations between ER and MYC remain significant in 3/4 comparisons. Results, comparing the original with the blocked regression models for each MYC-related feature, are shown in Supplementary Table 2.
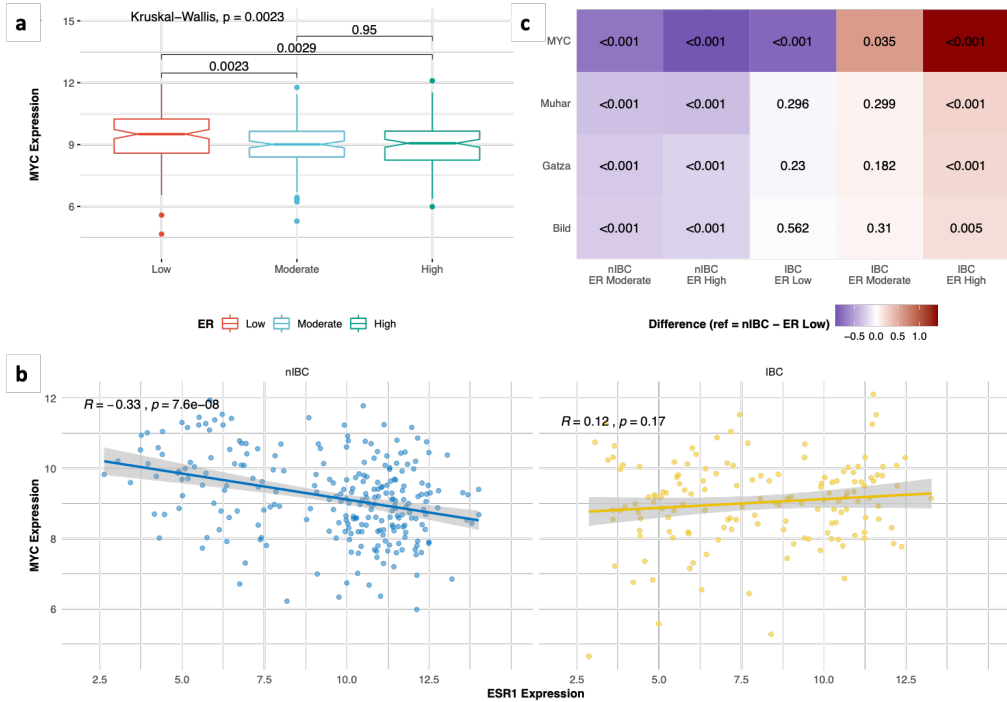
Fig. 4: MYC expression and transcriptional activity in patient samples in function of ESR1
a MYC expression levels (Y-axis) in a data set of 146 IBC and 252 nIBC tissue samples classified according to the ER status, calculated by stratifying ESR1 mRNA levels into low, moderate, and high categories. Data are represented in notched boxplot format and color-coding according to the legend shown underneath the plot. P-values resulting from the pairwise comparison of the MYC expression distributions between the different tumor sample categories are indicated. b Scatter plot comparing ESR1 and MYC expression, represented in the X- and Y-axis respectively, in nIBC (left) and IBC (right) patient series. For each series, a trend line is plotted and the resulting Spearman correlation coefficients are shown in the top left corner. c Heatmap representing the result of a generalized linear regression analysis evaluating MYC expression levels (i.e. top row) and MYC transcriptional activation calculated using the gene sets published by Muhar et al., Gatza et al., and Bild et al. (i.e. bottom 3 rows) in function of the tumor phenotype (i.e. IBC vs. nIBC) and interactions thereof with different strata of ER expression. For each of the resulting categories, shown along the X-axis (i.e. nIBC – ER Moderate, nIBC – ER High, IBC – ER Low, IBC – ER Moderate, and IBC – ER High), regression coefficients representing the change in MYC expression or MYC transcriptional activity in that category relative to nIBC samples with low ER expression, are color-coded as shown in the legend. The heatmap for example shows that MYC expression (i.e. top row) in nIBC samples with high ER levels (i.e. 2nd column) decreases significantly (i.e. blue color) as compared to nIBC samples with low ER expression, whereas relative to the same category the MYC expression in IBC samples with high ER levels increases significantly. P-values evaluating the significance of the changes are indicated in each cell.

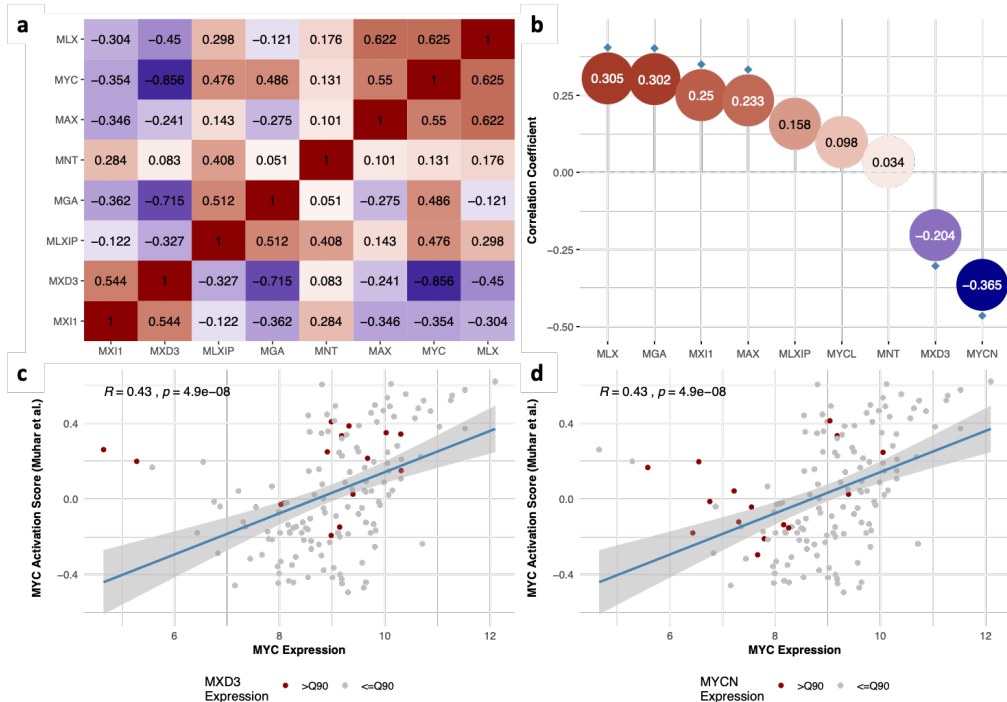*Expression analysis of Proximal MYC Network members*

To provide additional context to the role of MYC in IBC biology, expression levels of genes belonging to the Proximal MYC Network (PMN) and that modulate MYC target gene binding and expression [35], were investigated. With the exception of MYC itself, mRNA levels for only seven members were available in the series of 10 IBC cell lines and the correlation plot is shown in Fig. 5a. This reveals that expression levels MAX (i.e. the primary interaction partner of MYC; P=0.099) and MLX (i.e. MAX-like protein, another dimerization partner of MYC; P=0.053) were positively correlated with MYC, whereas a negative correlation was reported for MXD3 (i.e. MYC competitive MAX dimerization partner; P=0.001). These relationships were recapitulated in a series of 146 samples from patients with IBC (i.e. correlation P-values for MAX: P=0.005, MLX: P<0.001 and MXD3: P=0.027; Fig. 5b). In addition, an inverse relation between MYC and MYCN (i.e. another member of the family of MYC transcription factors) was noted (P=0.016). In general though, the correlation strengths among the PMN members observed in tissue samples were weaker as compared to those obtained in cell lines, possibly owing to confounding effects of ER expression and stromal admixture.

Finally, in the series of IBC patient samples, we demonstrated that MYC transcriptional activation, calculated based on the target gene set published by Muhar and colleagues, was positively associated to MYC (P<0.001), NMYC (P=0.017), MLX (P=0.045) and MXD3 (P<0.001) and negatively to MAX (P<0.001). Identical results were obtained for the MYC transcriptional activation scores calculated using the two remaining gene sets (data not shown). Figs. 5C and 5D show the strong linear relationship between MYC expression and MYC transcriptional activation but also identify a set of outlier samples in which MYC transcriptional activation was associated with elevated mRNA levels of either MXD3 of NMYC rather than MYC itself.

Discussion

The primary goal of the current study was to gain insight into the molecular characteristics of 10 IBC cell lines and to determine to what extent these preclinical models reflect genuine IBC biology. Therefore, gene expression data of IBC preclinical models were integrated with publicly available expression data of nIBC preclinical models. Data set-dependent bias was efficiently removed by normalization as shown by the clustering of replicate samples on terminal branches and by the fact that biologically relevant expression themes, such as those related to the ER and HER2 status of the cell lines, were not compromised. To further limit the effect of gene expression fluctuations associated with passage number, different culture conditions or other stochastic variables, the molecular profile of each preclinical model in this

study was defined as the average of several replicates, except for the UA-IBC-01 cell line for which only one expression profile was available.

Fig. 5: Expression analysis of Proximal MYC Network members a Heatmap showing the correlation structure of the proximal MYC network members in IBC cell lines. The proximal MYC network members are indicated along both X- and Y-axes and ordered similarly based on the output of a Ward clustering analysis. Correlations are coded according to a blue-red coloring scheme representing negative to positive correlation coefficients respectively. Correlation values are provided in the corresponding cells. b MYC correlation analysis for the proximal MYC network members in a series of 146 IBC patient samples. The proximal MYC network members and strength of the correlation between their expression and MYC mRNA levels are shown along the X- and Y-axis respectively. Each correlation coefficient is indicated by a dot, coded according to a blue-red coloring scheme representing negative to positive correlation coefficients respectively and correlation values are provided inside. Significant values are indicated with a blue diamond. c, d Scatter plots comparing MYC expression (X-axis) and MYC transcriptional activity (Y-axis) calculated according to the gene set published by Muhar and colleagues in a series of 146 IBC samples. Each sample is represented by a point, which is colored red if the corresponding sample is characterized by MXD3 (c) or NMYC (d) expression values exceeding the 90th percentile. A regression line depicting the linear relationship between MYC expression and transcriptional activity is indicated and results of the Spearman correlation analysis are provided in the top left corner.

Based on the resulting data set, we observed that all IBC cell lines adhere to the basal-like subtype and 7/10 had a luminal progenitor phenotype. This agrees with the fact that all IBC cell lines are ER-negative and demonstrates that the degree of molecular heterogeneity in the present series of IBC preclinical models is restricted as compared to the nIBC cell lines in which all subtypes and differentiation states are represented. Similar conclusions could be drawn when evaluating the distribution of the PAM50 subtypes, with 8/10 IBC cell lines being either basal-like or HER2-enriched. These results can be explained by the dominance of the basal-like and HER2-enriched subtypes in IBC tissue samples [9,36]. However, they also clearly reveal the paucity in ER+, luminal-type preclinical IBC models despite the fact these subtypes account for roughly 30-40% of the patient samples [14,37]. Another intriguing observation is the absence of the mesenchymal subtype in the panel of IBC cell lines, which is unexpected due to the metastatic potential often associated with this subset of breast cancer cells, but agrees with the reported overexpression of E-Cadherin in IBC cells and thus their presumed epithelial phenotype [38].

Next, we aimed to evaluate to what extend the current series of IBC preclinical models is representative for IBC biology. Therefore, we applied a classification model based on 79 genes with IBC-specific expression patterns [9] onto our preclinical model series. Overall, the prediction accuracy was acceptable (i.e. 78%), but positive predictive value was limited (i.e. 59%) indicating that the model was not reliable in correctly predicting the IBC status of the models or that the models do not fully represent the clinical disease but only limited aspects of it. In an additional analysis, we observed that overexpression patterns in nIBC were maintained between cell lines and tissue samples, but not those from IBC cell lines (data not shown). This result suggests that separation of IBC and nIBC cell lines based on the transcriptomic classifier is mainly driven by the nIBC marker genes. A possible explanation for the lack of predictive power associated with the IBC marker genes in this analysis relates to differences between IBC and nIBC associated with the tumor (immune) microenvironment [13-15,39] that are not recapitulated in the data set of the preclinical models. Indeed, 67% of the IBC marker genes that are part of the IBC-specific transcriptomic signature demonstrate elevated expression in the profiles of immune and endothelial cells of the Human Tissue Compendium relative to those of epithelial cells (data not shown). This conclusion is further corroborated by a direct comparison of the GEPs of the UA-IBC-01 cell line and the primary tumor sample it is obtained from. Although expression differences are limited and cancer cell intrinsic expression themes appear to be preserved in the preclinical model, enrichment of gene sets associated with immune response programs in the primary tumor sample were noted. Together, these data again underscore the importance of the tumor microenvironment in IBC biology, but they do not preclude

the utility of the preclinical models to uncover IBC cell intrinsic features and numerous efforts are underway to incorporate immune features into programs for the development of IBC preclinical models. With respect to the latter, the use of estrogen supplementation should be carefully considered, as modest differences in gene expression of estrogen response genes were noted between UA-IBC-01 and its corresponding primary tissue sample. However, since gene expression changes are not in line with the expected results, this observation requires further investigation.

To further delineate the defining principles of IBC biology, two distinct analysis strategies were undertaken. First, DEGs between IBC and nIBC cell lines were identified. Second, WGCNA was applied to detect modules of co-expressed genes in the series of IBC cell lines only. In both analyses, confounding variables such as ER status and the molecular subtypes were not taken into account for two reasons. First, our data set was too small to perform multivariate analyses. Second, since all the IBC preclinical models are ER-negative and of the basal-like subtype, it is impossible to reliably differentiate between gene expression patterns introduced by the tumor phenotype on the one hand and other sources of latent variation on the other hand. It should be noted that the inability to account for covariates represents a debilitating factor in our analysis. Regardless, both strategies pointed at important roles for cell proliferation (e.g. hallmarks E2F target genes and G2M checkpoint), MYC transcriptional activity and inflammatory response programs (e.g. hallmarks IL2/STAT5 and TNFα/NFκB) in the biology of IBC. Furthermore, the WGCNA approach revealed that several of these processes are jointly regulated. For example, MYC and NFκB target gene expression were the dominant themes in the second co-expression cluster, which suggests an intricate relationship between both transcription factors in shaping IBC biology. NFκB activation in IBC has been reported previously [29,40-42], and MYC and NFκB have been shown to cooperate in breast cancer development and progression [43-46], amongst others by modulating stem cell behavior. By comparing gene co-expression clusters to the L1000 profiles of the CMAP database, we also revealed sets of potential regulators and target/drug combinations. Unfortunately, no single drug with predicted efficacy across all IBC cell lines was identified. This may reflect inherent heterogeneity in the signal transduction networks of the individual IBC cells, limited specificity of the CMAP profiles that are generated using a broad collection of cancer cell lines and thus are not reflective of breast cancer specific transcriptional responses, or the failure to identify robust and highly specific IBC co-expression modules due to the limited size and relative homogeneity (i.e. all ER negative and basal-like samples) of the series of IBC preclinical models. Nevertheless, our results constitute a good starting point to evaluate novel treatment strategies in preclinical IBC research.

The fact that MYC target genes were overexpressed in IBC cell lines and were associated with specific co-expression modules suggests that MYC transcriptional activity is an important characteristic of IBC biology at least in preclinical models. This is corroborated by earlier work of Zhang and colleagues who demonstrated that MYC is a central hub in the signal transduction networks of SUM149 and SUM190 [47]. In addition, we recently showed that MYC mediates the specific response of IBC cells to TGFβ1 treatment [10]. To confirm these observations, MYC expression and transcriptional activation were explored using GEPs from IBC and nIBC tissue biopsies. Our data demonstrate that the levels of MYC expression and transcriptional activation in relation to ESR1 expression exhibit opposite patterns in IBC and nIBC with an ER-dependent decrease and increase in mRNA levels of both MYC and MYC target genes in nIBC and IBC respectively. Particularly the positive association between ER and MYC expression or transcriptional activation in IBC is notable, as it remains significant even when accounting for tumor stage and the PAM50 subtypes and thus cannot be attributed solely by the enrichment of the Luminal B phenotype amongst ER+ IBC tissue biopsies. This observation is in line with earlier results showing that MYC is a common denominator of biological processes active in ER-positive IBC [48]. The induction of MYC activity in ER-positive IBC may provide an explanation for the hormone therapy resistance phenotype often associated with IBC [49]. Miller and colleagues illustrated that a gene signature of breast cancer cells with acquired hormone independence and predictive of resistance to hormonal therapy reflects MYC pathway activation [50]. Importantly, these data re-emphasize the need for ER+ luminal-type preclinical models of IBC. It stands to reason that inclusion of such models in our present analysis would further amplify the here reported MYC-related differences.

Recently, we reported that MYC was frequently affected by genomic alterations in a series of 101 IBC tissue biopsies [12] and Faldoni et al. reported frequent gains covering the MYC gene in IBC, with a concomitant MYC protein overexpression in IBC patient samples [51]. We performed a meta-analysis of published data [12,52-56] and demonstrate that the frequency of MYC genomic alterations in primary IBC is 23% (95%CI: 13-33%) vs. 30% (95%CI: 24-37%) in a subtype matched nIBC series consisting of METABRIC and TCGA samples respectively. This reveals that MYC genomic alterations are not specifically enriched in IBC. Therefore, we hypothesize that other mechanisms of MYC activation in IBC are operational and the present data contribute to earlier observations linking MYC in IBC to signaling pathways involved in developmental biology [12,57]. Here, we show that some co-expression modules associated with MYC target gene expression are additionally related to WNT or Hedgehog signaling, and that many of the upstream regulators for these co-expression clusters are also involved in these pathways (i.e. BAMBI, E2F6, HOXB13, and WWTR1/TAZ) or in plain stem cell biology

(i.e. CDX2, HOXA9, KLF6, and POU5F1). Interestingly, a SNP (rs6983267) located at 8q24 close to the MYC locus, is known to exhibit enhanced binding properties for the WNT effector TCF4 and can be directed to the MYC locus through chromatin loops allowing for WNT/TCF4-dependent MYC expression. In addition, the rs6983267 genotype is associated with metastatic risk in IBC but not in nIBC, suggesting that MYC is also involved in cancer cell dissemination in IBC [58]. In line with this, MYC expression levels are predictive of reduced distant metastasis-free survival in patients with ER-positive IBC [48] and have shown to be associated with metastasis in ER-positive metastatic breast cancer [59,60]. Apart from stem cell signaling pathways, also signals from the tumor microenvironment could be involved in modulating MYC signaling. In this context, MYC has been shown to be a target gene of the NFκB transcription factor RELA [43,61] that orchestrates cellular responses to pro-inflammatory cues. Finally, we want to draw attention to the fact that in a small subset of IBC samples, the activation of the MYC pathway was apparently associated with NMYC and MXD3, which have been shown to jointly regulate cell proliferation in cerebellar granule neuron precursors, downstream of Hedgehog signaling [62]. This indicates that MYC biology in IBC is complex and involves different proximal MYC network members.

In conclusion, in this study we demonstrate that the currently available preclinical models of IBC recapitulate to some extent the molecular features of IBC cells in patient samples, and thus constitute valuable research tools. However, it should be noted that the present panel of IBC models do not fully recapitulate the molecular heterogeneity seen in patient samples. Particularly, the lack of hormone sensitive, luminal-type preclinical models for IBC is worrisome, since data indicate that ER may contribute to IBC biology in a specific manner as shown by the ER-dependency of MYC expression and transcriptional activity in patient samples. By consequence, the lack of ER expressing IBC cell lines represents one of the major limitations associated with the present study, particularly in the comparison of IBC and nIBC cell lines in which the influence ER positivity on differences in gene expression could not be assessed. A second limitation of this study and of the presented series of preclinical models in general relates to the absence of the specific immune contexture, which is now being increasingly accepted as a hallmark of IBC biology. However, it should be noted that signatures of activated immune response pathways prevail in IBC cells as intrinsic properties, possibly reflecting past interactions between IBC cells and an inflamed tumor micro-environment. Finally, the rather limited size of the series of IBC cell lines, which impacts on statistical power, implies that additional and more subtle molecular features of IBC cells may yet be undetermined. We argue that researchers need to be aware of these limitations, allowing their appropriate consideration in the design of

preclinical experiments to maximize the translatability of research results into daily patient care.

Methods

This study was approved by the local review board of the GZA Hospitals and each patient gave written informed consent.

UAIBC01 PDX Model

The UAIBC01 PDX model was generated in collaboration with Oncotest Gmbh (Freiburg, Germany). Briefly, metastatic tumor tissue from a patient with hormone receptor-negative and HER2-amplified IBC was subcutaneously implanted in NOD-SCID mice with estrogen pellets and serially passaged in nude mice. Tissue samples obtained after the fourth passage were processed for molecular analysis. Information on the clinical and pathological characteristics of the patient from which this IBC cell line and the other nine IBC models were derived, can be found in Supplementary Table 3.

Gene expression data from cell lines

We profiled a series of nine IBC (i.e. SUM149, SUM190, KPL4, Mary-X, MDAIBC03, FCIBC01, FCIBC02, TJIBC04, and TJIBC09) and three nIBC (i.e. MCF7, MDAMB231, and SUM159) preclinical models at least in triplicate using Affymetrix HGU133plus2 GeneChips. Using the same platform, an additional gene expression profile (GEP) of our in-house generated PDX model for IBC (i.e UAIBC01) was generated and included in the study, yielding a total of 57 gene expression profiles. The SUM149, SUM190, KPL4 and MDAIBC03 cells were a kindly gift from MD Anderson Cancer Center, TX, USA. The FCIBC01, FCIBC02, TJIBC04, and TJIBC09 cells were a kindly from Dr. Cristofanilli and the Mary-X model from Dr. Barsky. The nIBC cell lines were purchased from ATCC (Manassas, USA).

To expand the group of nIBC preclinical models, four additional gene expression data sets generated using the Affymetrix HGU133 series were retrieved from public resources (Gene Expression Omnibus: GSE12777, GSE16795, and GSE40464; and ArrayExpress: E-MTAB-7). Expression data for 19 extra nIBC models was avalaible, i.e. BT-20, BT-474, BT-483, BT-549, CAMA1, HCC1937, HS578T, MDAMB134VI, MDAMB175VII, MDAMB361, MDAMB415, MDAMB436, MDAMB453, MDAMB468, SKBR3, T47D, UACC812, ZR751, ZR7530. To reduce technical bias due to interlaboratory variability in these data sets, only cell lines that were profiled at least in triplicate were

included. In total, 124 expression profiles of 32 different breast cancer models (i.e. 10 IBC models and 22 nIBC models) from five different data sets were included.

For each individual data set (N=5), expression data were normalized using the Robust Multi-array Averaging algorithm with correction for GC probe content (BioConductor package gcrma – v.2.60.0) and probe sets with a fluorescence intensity above log2(100) in at least two samples were included. The individual data sets were then merged based on the common probe sets (N=10,961) and batch effects were removed using empirical Bayesian methods (i.e. the combat function implemented in the BioConductor-package sva – 3.36.0), with protection of cell line-specific variation in gene expression. The resulting data set was then subjected to quantile normalization and probe set redundancy was removed by retaining the probe set with the highest standard deviation per gene for a total of 7,182 unique genes. As a final step, replicate GEPs were averaged.

Gene expression data from patient samples

Gene expression data from 146 IBC and 252 nIBC tissue samples have been described earlier [9]. However, in this study, raw GEPs were reprocessed using a similar normalization strategy as described for the preclinical models in order to ensure data comparability. Batch effects due to the inclusion of samples from three distinct sites (i.e. MD Anderson, Institut Paoli-Calmettes and GZA Hospitals Sint-Augustinus) were removed using empirical Bayesian methods. The final processed data set contained 12,769 probes sets for 8,086 unique genes. Finally, breast cancer gene expression data from the TCGA (Firehose legacy) and METABRIC series were downloaded from the cBioPortal for cancer genomics (https://www.cbioportal.org) using the R package cgdsr (v.1.3.0).

Unsupervised analysis

Unsupervised hierarchical clustering analysis (UHCA) was performed using Manhattan distance as dissimilarity metric and Ward clustering as the dendrogram drawing method. Prior to cluster analysis, data were centered and scaled to unit variance. The optimal number of clusters, ranging from 2 to 10, was determined by evaluating cluster separability based on 30 distinct indices (BioConductor package NbClust – v.3.0). The clustering scheme that was supported by the majority of these indices was selected.

Classification

Preclinical models and patient samples were classified according to the PAM50 molecular subtypes 63 using the BioConductor package genefu (v.2.20.0). Furthermore, the preclinical models were classified according to the ER status, the PR status, the HER2 status 64, the luminal/basal/mesenchymal classification (LBM) system for breast cancer cell lines 65, the differentiation predictor model (DPM) 66, and the IBC-specific classification model composed of 79 probe sets 9. For the PR status, nIBC cell lines reported to be PR negative by Dai and colleagues were considered as PR negative whereas nIBC cell lines with weak or strong PR expression were classified as PR positive 64. In addition, IBC and nIBC patient samples were stratified into ER low, moderate, and high expression groups based on the 33rd and 66th quantiles of the ESR1 mRNA levels.

To perform the classification according to the signature of 79 IBC-specific probe sets, a model based on elastic net generalized linear regression was optimized on GEPs of the tumor samples using the R package caret (v.6.0-86). This data set was split into a training and validation set according to a 3/1 split ratio. Prior to model construction, the data were centered and scaled to unit variance. Model construction was performed using repeated 10-fold cross-validation against a tuning grid of alpha values ranging from 0 to 1 with 0.1 increments and lambda values ranging from 0.001 to 0.1 with 0.001 increments. The optimal model was selected using ROC statistics and was then applied onto the validation set of tumor samples to define the model accuracy and onto the data set of preclinical models to record posterior probabilities for each breast cancer model. For the latter analysis, the non-averaged GEPs (N=124) were used in order to be able to evaluate the cell line-specific variation of the classification scores and the final call was generated based on the median posterior probability across replicates.

Differential expression analysis

Identification of differentially expressed genes (DEGs) was performed using the BioConductor package limma (v.3.44.3). Resulting p-values were corrected for false discovery using the Benjamini and Hochberg procedure and false discovery rate (FDR)-corrected p-values inferior to 10% were considered significant.
To identify genes presumably differentially expressed between the UA-IBC-01 preclinical models and to primary tumor sample it was derived from, gene-wise differences in expression between both samples were calculated by subtracting the expression levels measured in the cell line from those measure in the tumor sample. Genes overexpressed in the tumor sample and the cell line were then defined based

on respectively the 97.5th and the 2.5th percentile of the global distribution of the gene-wise expression differences.

Weighted gene co-expression network analysis (WGCNA)

To identify gene co-expression modules in the series of 10 IBC preclinical models, WGCNA was performed using the R package WGCNA (v.1.69) and following online instructions (https://horvath.genetics.ucla.edu/). To construct a signed co-expression matrix, pairwise biweight midcorrelation coefficients were calculated between all 7,182 genes. The resulting adjacency matrix was transformed into a weighted network by raising the biweight midcorrelation coefficients to a power that was chosen for the resulting network to adhere to scale-free topology. Detection of co-expression modules was performed using UHCA by subjecting the topological overlap dissimilarity matrix of the network to Ward clustering. The resulting dendrogram was analyzed using an adaptive branch pruning algorithm combined with partitioning around medoids to assign genes to co-expression clusters enforcing a minimum size of 100 genes and co-expression clusters with a similar profile were merged. Then, gene module memberships (GMM) scores were calculated for each gene and each co-expression cluster and represent the Pearson correlation coefficient between their respective expression profiles. The vector of all gene-wise GMM scores per module is considered as the characteristic GEP of that module. The preservation of the IBC co-expression clusters in the series of nIBC preclinical models was investigated using connectivity and density statistics. Finally, network-based prioritization of the co-expression clusters was performed using the R package igraph (v.1.2.5). Therefore, based on the expression levels of the co-expression modules in the cell lines, the correlation structure amongst the co-expression modules was determined and dichotomized relative to 0 (i.e. positive and negative correlation coefficients transformed into 1 and 0 respectively). Then, individual cell lines were linked to the co-expression modules by dichotomizing the cell line specific expression values of the co-expression modules (i.e. positive and negative expression values transformed into 1 and 0 respectively). The resulting binary adjacency matrix, representing both modules and cell lines, was analyzed using a minimal spanning tree algorithm to determine the minimal set of edges that connect all components. The result was visualized using the R package ggnetwork (v.0.5.8).

Systems biology

To translate expression profiles (i.e. vectors of log2-transformed fold changes or GMM scores) into biological themes, gene set enrichment analysis (GSEA) was performed for the hallmark gene sets of the molecular signatures database (https://www.gsea-msigdb.org/gsea/msigdb). Overrepresentation analysis (ORA) of DEGs between IBC and

nIBC cell lines in each of the co-expression modules was performed using the hypergeometric test. Both analyses were performed using the BioConductor package fgsea (v.1.14.0). To assess MYC transcriptional activity in IBC and nIBC tissue samples based on published MYC activation signatures 32-34, GEPs were subjected to gene set variation analysis using the BioConductor package GSVA. Finally, the analysis of the Proximal MYC Network (PMN) was performed based on genes reported by Schaub and colleagues 35.

To identify regulators of IBC biology and potentially effective target/drug combinations for treatment based on the WGCNA results, the GEP of each co-expression module based on 300 marker genes with the highest or lowest GMM scores (i.e. 150 each) was analyzed against 1.3 million L1000 profiles present in the CMAP dataset (https://clue.io/cmap). These L1000 profiles catalogue the transcriptional responses of human cells to a variety of chemical or genetic (i.e. both knock-down and overexpression) perturbations. The resulting connectivity scores (CSs) reflect the level of agreement between the analyzed GEPs and the L1000 profiles and range between -100 to 100 reflecting incongruent or congruent profiles respectively. Then, for each co-expression module, regulators are defined as genes with a CS of at least 75 upon overexpression and at most -75 upon knock-down and drug/target combinations are defined based on a CS smaller than -75 for the drug and greater than 75 upon overexpression of the drug target.

Statistics

To compare the distribution of two categorical variables, Fisher Exact tests, Chi-square tests or multinomial regression analyses were performed. To compare the distribution of a continuous variable in the context of one or more categorical variables, Wilcoxon tests, Kruskal-Wallis tests or generalized linear regression analyses were performed. To compare two continuous variables, Spearman correlation or linear regression analyses were performed. Regression models were performed in uni- or multivariate setting where appropriate. Particularly, to analyze MYC-related parameters in the context of ER expression and the tumor phenotype, a nested interaction model was established to estimate the main effect of the tumor phenotype and ER expression in addition to IBC-specific effects of ER expression on MYC expression levels. Comparison of different regression models was performed using the likelihood ratio test. In all cases, 2-sided tests were performed and p-values inferior to 5% were considered significant. Data analysis was done in R (v.4.0.1) and data visualization was done using the R package ggplot2 (v.3.3.1).

Data availability

The data that support the findings of this study are available from the corresponding author upon reasonable request. The gene expression profiles of the 10 IBC preclinical models and three nIBC preclinical models (i.e. MCF7, MDAMB231, and SUM159) can be accessed on ArrayExpress with accession number E-MTAB-11134.

Code availability

All code generated in part of this publication is available at https://github.com/StevenVanLaere/IBCModels.

Author Contributions

CR and FB are equal first co-authors
Design of the work: SVL, FB, data analysis and interpretation: SVL, FB, CR, manuscript preparation: SVL, CR, manuscript review: all authors

Corresponding Author: Charlotte Rypens, Center for Oncological Research (CORE), Integrated Personalized and Precision Oncology Network (IPPON), University of Antwerp. Phone: 003234433637; E-mail: rypens.charlotte@hotmail.com, steven.vanlaere@uantwerpen.be

Competing Interests

The authors declare no competing interests.

References

1. Robertson, F. M. et al. Inflammatory breast cancer: the disease, the biology, the treatment. CA Cancer J Clin 60, 351-375, doi:10.3322/caac.20082 (2010).

2. Hance, K. W., Anderson, W. F., Devesa, S. S., Young, H. A. & Levine, P. H. Trends in inflammatory breast carcinoma incidence and survival: the surveillance, epidemiology, and end results program at the National Cancer Institute. J Natl Cancer Inst 97, 966-975, doi:10.1093/jnci/dji172 (2005).

3. Schlichting, J. A., Soliman, A. S., Schairer, C., Schottenfeld, D. & Merajver, S. D. Inflammatory and non-inflammatory breast cancer survival by socioeconomic position in the Surveillance, Epidemiology, and End Results database, 1990-2008. Breast Cancer Res Treat 134, 1257-1268, doi:10.1007/s10549-012-2133-2 (2012).

4. Hennessy, B. T. et al. Disease-free and overall survival after pathologic complete disease remission of cytologically proven inflammatory breast carcinoma axillary lymph node metastases after primary systemic chemotherapy. Cancer 106, 1000-1006, doi:10.1002/cncr.21726 (2006).

5. Dawood, S. et al. International expert panel on inflammatory breast cancer: consensus statement for standardized diagnosis and treatment. Ann Oncol 22, 515-523, doi:10.1093/annonc/mdq345 (2011).

6. Cristofanilli, M. et al. Inflammatory breast cancer (IBC) and patterns of recurrence: understanding the biology of a unique disease. Cancer 110, 1436-1444, doi:10.1002/cncr.22927 (2007).

7. Singletary, S. E. & Cristofanilli, M. Defining the clinical diagnosis of inflammatory breast cancer. Semin Oncol 35, 7-10, doi:10.1053/j.seminoncol.2007.11.010 (2008).

8. Mohamed, M. M., Al-Raawi, D., Sabet, S. F. & El-Shinawi, M. Inflammatory breast cancer: New factors contribute to disease etiology: A review. J Adv Res 5, 525-536, doi:10.1016/j.jare.2013.06.004 (2014).

9. Van Laere, S. J. et al. Uncovering the molecular secrets of inflammatory breast cancer biology: an integrated analysis of three distinct affymetrix gene expression datasets. Clin Cancer Res 19, 4685-4696, doi:10.1158/1078-0432.CCR-12-2549 (2013).

10. Rypens, C. et al. Inflammatory breast cancer cells are characterized by abrogated TGFbeta1-dependent cell motility and SMAD3 activity. Breast Cancer Res Treat, doi:10.1007/s10549-020-05571-z (2020).

11. Bertucci, F. et al. Gene expression profiles of inflammatory breast cancer: correlation with response to neoadjuvant chemotherapy and metastasis-free survival. Ann Oncol 25, 358-365, doi:10.1093/annonc/mdt496 (2014).

12. Bertucci, F. et al. NOTCH and DNA repair pathways are more frequently targeted by genomic alterations in inflammatory than in non-inflammatory breast cancers. Mol Oncol, doi:10.1002/1878-0261.12621 (2019).

13. Reddy, J. P. et al. Mammary stem cell and macrophage markers are enriched in normal tissue adjacent to inflammatory breast cancer. Breast Cancer Res Treat 171, 283-293, doi:10.1007/s10549-018-4835-6 (2018).

14. Lim, B., Woodward, W. A., Wang, X., Reuben, J. M. & Ueno, N. T. Inflammatory breast cancer biology: the tumour microenvironment is key. Nat Rev Cancer 18, 485-499, doi:10.1038/s41568-018-0010-y (2018).

15. Huang, A., Cao, S. & Tang, L. The tumor microenvironment and inflammatory breast cancer. J Cancer 8, 1884-1891, doi:10.7150/jca.17595 (2017).

16. Mohamed, M. M. Monocytes conditioned media stimulate fibronectin expression and spreading of inflammatory breast cancer cells in three-dimensional culture: A mechanism mediated by IL-8 signaling pathway. Cell Commun Signal 10, 3, doi:10.1186/1478-811X-10-3 (2012).

17. Mohamed, H. T. et al. IL-10 correlates with the expression of carboxypeptidase B2 and lymphovascular invasion in inflammatory breast cancer: The potential role of tumor infiltrated macrophages. Curr Probl Cancer 42, 215-230, doi:10.1016/j.currproblcancer.2018.01.009 (2018).

18. Mohamed, M. M. et al. Cytokines secreted by macrophages isolated from tumor microenvironment of inflammatory breast cancer patients possess chemotactic properties. Int J Biochem Cell Biol 46, 138-147, doi:10.1016/j.biocel.2013.11.015 (2014).

19. Forozan, F. et al. Molecular cytogenetic analysis of 11 new breast cancer cell lines. Br J Cancer 81, 1328-1334, doi:10.1038/sj.bjc.6695007 (1999).

20. Ignatoski, K. M. & Ethier, S. P. Constitutive activation of pp125fak in newly isolated human breast cancer cell lines. Breast Cancer Res Treat 54, 173-182, doi:10.1023/a:1006135331912 (1999).

21. Kurebayashi, J. Regulation of interleukin-6 secretion from breast cancer cells and its clinical implications. Breast Cancer 7, 124-129, doi:10.1007/bf02967443 (2000).

22. Kurebayashi, J. et al. Isolation and characterization of a new human breast cancer cell line, KPL-4, expressing the Erb B family receptors and interleukin-6. Br J Cancer 79, 707-717, doi:10.1038/sj.bjc.6690114 (1999).

23. Kurebayashi, J., Yamamoto, S., Otsuki, T. & Sonoo, H. Medroxyprogesterone acetate inhibits interleukin 6 secretion from KPL-4 human breast cancer cells both in vitro and in vivo: a possible mechanism of the anticachectic effect. Br J Cancer 79, 631-636, doi:10.1038/sj.bjc.6690099 (1999).

24. Alpaugh, M. L., Tomlinson, J. S., Shao, Z. M. & Barsky, S. H. A novel human xenograft model of inflammatory breast cancer. Cancer Res 59, 5079-5084 (1999).

25. Shirakawa, K. et al. Hemodynamics in vasculogenic mimicry and angiogenesis of inflammatory breast cancer xenograft. Cancer Res 62, 560-566 (2002).

26. Shirakawa, K. et al. Inflammatory breast cancer: vasculogenic mimicry and its hemodynamics of an inflammatory breast cancer xenograft model. Breast Cancer Res 5, 136-139, doi:10.1186/bcr585 (2003).

27. Shirakawa, K. et al. Tumor-infiltrating endothelial cells and endothelial precursor cells in inflammatory breast cancer. Int J Cancer 99, 344-351, doi:10.1002/ijc.10336 (2002).

28. Morales, J. & Alpaugh, M. L. Gain in cellular organization of inflammatory breast cancer: A 3D in vitro model that mimics the in vivo metastasis. BMC Cancer 9, 462, doi:10.1186/1471-2407-9-462 (2009).

29. Arora, J. et al. Inflammatory breast cancer tumor emboli express high levels of anti-apoptotic proteins: use of a quantitative high content and high-throughput 3D IBC spheroid assay to identify targeting strategies. Oncotarget 8, 25848-25863, doi:10.18632/oncotarget.15667 (2017).

30. Williams, K. P. et al. Quantitative high-throughput efficacy profiling of approved oncology drugs in inflammatory breast cancer models of acquired drug resistance and re-sensitization. Cancer Lett 337, 77-89, doi:10.1016/j.canlet.2013.05.017 (2013).

31. Fernandez, S. V. et al. Inflammatory breast cancer (IBC): clues for targeted therapies. Breast Cancer Res Treat 140, 23-33, doi:10.1007/s10549-013-2600-4 (2013).

32. Muhar, M. et al. SLAM-seq defines direct gene-regulatory functions of the BRD4-MYC axis. Science 360, 800-805, doi:10.1126/science.aao2793 (2018).

33. Gatza, M. L. et al. A pathway-based classification of human breast cancer. Proc Natl Acad Sci U S A 107, 6994-6999, doi:10.1073/pnas.0912708107 (2010).

34. Bild, A. H. et al. Oncogenic pathway signatures in human cancers as a guide to targeted therapies. Nature 439, 353-357, doi:10.1038/nature04296 (2006).

35. Schaub, F. X. et al. Pan-cancer Alterations of the MYC Oncogene and Its Proximal Network across the Cancer Genome Atlas. Cell Syst 6, 282-300 e282, doi:10.1016/j.cels.2018.03.003 (2018).

36. Iwamoto, T. et al. Different gene expressions are associated with the different molecular subtypes of inflammatory breast cancer. Breast Cancer Res Treat 125, 785-795, doi:10.1007/s10549-010-1280-6 (2011).

37. Lerebours, F., Bieche, I. & Lidereau, R. Update on inflammatory breast cancer. Breast Cancer Res 7, 52-58, doi:10.1186/bcr997 (2005).

38. Kleer, C. G., van Golen, K. L., Braun, T. & Merajver, S. D. Persistent E-cadherin expression in inflammatory breast cancer. Mod Pathol 14, 458-464, doi:10.1038/modpathol.3880334 (2001).

39. Van Berckelaer, C. et al. Infiltrating stromal immune cells in inflammatory breast cancer are associated with an improved outcome and increased PD-L1 expression. Breast Cancer Res 21, 28, doi:10.1186/s13058-019-1108-1 (2019).

40. Van Laere, S. J. et al. Nuclear factor-kappaB signature of inflammatory breast cancer by cDNA microarray validated by quantitative real-time reverse transcription-PCR, immunohistochemistry, and nuclear factor-kappaB DNA-binding. Clin Cancer Res 12, 3249-3256, doi:10.1158/1078-0432.CCR-05-2800 (2006).

41. Lerebours, F. et al. NF-kappa B genes have a major role in inflammatory breast cancer. BMC Cancer 8, 41, doi:10.1186/1471-2407-8-41 (2008).

42. Evans, M. K. et al. XIAP Regulation by MNK Links MAPK and NFkappaB Signaling to Determine an Aggressive Breast Cancer Phenotype. Cancer Res 78, 1726-1738, doi:10.1158/0008-5472.CAN-17-1667 (2018).

43. Kim, D. W. et al. The RelA NF-kappaB subunit and the aryl hydrocarbon receptor (AhR) cooperate to transactivate the c-myc promoter in mammary cells. Oncogene 19, 5498-5506, doi:10.1038/sj.onc.1203945 (2000).

44. Khan, S., Lopez-Dee, Z., Kumar, R. & Ling, J. Activation of NFkB is a novel mechanism of pro-survival activity of glucocorticoids in breast cancer cells. Cancer Lett 337, 90-95, doi:10.1016/j.canlet.2013.05.020 (2013).

45. Yuan, Y. et al. ANXA1 inhibits miRNA-196a in a negative feedback loop through NF-kB and c-Myc to reduce breast cancer proliferation. Oncotarget 7, 27007-27020, doi:10.18632/oncotarget.8875 (2016).

46. Li, F. et al. Ganoderic acids suppress growth and angiogenesis by modulating the NF-kappaB signaling pathway in breast cancer cells. Int J Clin Pharmacol Ther 50, 712-721, doi:10.5414/CP201663 (2012).

47. Zhang, E. Y. et al. Genome wide proteomics of ERBB2 and EGFR and other oncogenic pathways in inflammatory breast cancer. J Proteome Res 12, 2805-2817, doi:10.1021/pr4001527 (2013).

48. Iwase, T. et al. Quantitative hormone receptor (HR) expression and gene expression analysis in HR+ inflammatory breast cancer (IBC) vs non-IBC. BMC Cancer 20, 430, doi:10.1186/s12885-020-06940-z (2020).

49. Jansen, M. P. et al. Decreased expression of ABAT and STC2 hallmarks ER-positive inflammatory breast cancer and endocrine therapy resistance in advanced disease. Mol Oncol 9, 1218-1233, doi:10.1016/j.molonc.2015.02.006 (2015).

50. Miller, T. W. et al. A gene expression signature from human breast cancer cells with acquired hormone independence identifies MYC as a mediator of antiestrogen resistance. Clin Cancer Res 17, 2024-2034, doi:10.1158/1078-0432.CCR-10-2567 (2011).

51. Faldoni, F. L. C. et al. Inflammatory Breast Cancer: Clinical Implications of Genomic Alterations and Mutational Profiling. Cancers (Basel) 12, doi:10.3390/cancers12102816 (2020).

52. Lerebours, F. et al. Evidence of chromosome regions and gene involvement in inflammatory breast cancer. Int J Cancer 102, 618-622, doi:10.1002/ijc.10729 (2002).

53. Bekhouche, I. et al. High-resolution comparative genomic hybridization of inflammatory breast cancer and identification of candidate genes. PLoS One 6, e16950, doi:10.1371/journal.pone.0016950 (2011).

54. Ross, J. S. et al. Comprehensive genomic profiling of inflammatory breast cancer cases reveals a high frequency of clinically relevant genomic alterations. Breast Cancer Res Treat 154, 155-162, doi:10.1007/s10549-015-3592-z (2015).

55. Hamm, C. A. et al. Genomic and Immunological Tumor Profiling Identifies Targetable Pathways and Extensive CD8+/PDL1+ Immune Infiltration in Inflammatory Breast Cancer Tumors. Mol Cancer Ther 15, 1746-1756, doi:10.1158/1535-7163.MCT-15-0353 (2016).

56. Bingham, C. et al. Mutational studies on single circulating tumor cells isolated from the blood of inflammatory breast cancer patients. Breast Cancer Res Treat 163, 219-230, doi:10.1007/s10549-017-4176-x (2017).

57. Xiao, Y. et al. The lymphovascular embolus of inflammatory breast cancer exhibits a Notch 3 addiction. Oncogene 30, 287-300, doi:10.1038/onc.2010.405 (2011).

58. Bertucci, F. et al. 8q24 Cancer risk allele associated with major metastatic risk in inflammatory breast cancer. PLoS One 7, e37943, doi:10.1371/journal.pone.0037943 (2012).

59. Litviakov, N. V. et al. Breast tumour cell subpopulations with expression of the MYC and OCT4 proteins. J Mol Histol 51, 717-728, doi:10.1007/s10735-020-09917-1 (2020).

60   Gerratana, L. et al. Understanding the organ tropism of metastatic breast cancer through the combination of liquid biopsy tools. Eur J Cancer 143, 147-157, doi:10.1016/j.ejca.2020.11.005 (2021).

61. Chapman, N. R. et al. A novel form of the RelA nuclear factor kappaB subunit is induced by and forms a complex with the proto-oncogene c-Myc. Biochem J 366, 459-469, doi:10.1042/BJ20020444 (2002).

62. Yun, J. S., Rust, J. M., Ishimaru, T. & Diaz, E. A novel role of the Mad family member Mad3 in cerebellar granule neuron precursor proliferation. Mol Cell Biol 27, 8178-8189, doi:10.1128/MCB.00656-06 (2007).

63. Parker, J. S. et al. Supervised risk predictor of breast cancer based on intrinsic subtypes. J Clin Oncol 27, 1160-1167, doi:10.1200/JCO.2008.18.1370 (2009).

64. Dai, X., Cheng, H., Bai, Z. & Li, J. Breast Cancer Cell Line Classification and Its Relevance with Breast Tumor Subtyping. J Cancer 8, 3131-3141, doi:10.7150/jca.18457 (2017).

65. Ross, D. T. & Perou, C. M. A comparison of gene expression signatures from breast tumors and breast tissue derived cell lines. Dis Markers 17, 99-109 (2001).

66. Lim, E. et al. Aberrant luminal progenitors as the candidate target population for basal tumor development in BRCA1 mutation carriers. Nat Med 15, 907-913, doi:10.1038/nm.2000 (2009).

Supplementary data

SUPPLEMENTARY FIGURES
Supplementary Figure 1: Results of the model optimization and application
Supplementary Figure 2: Genome-wide expression levels measured in the UA-IBC-01 cell line in function of those measured in the corresponding primary tumor sample.
Supplementary Figure 3: Network construction and module detection.
Supplementary Figure 4: Connectivity scores for MYC, RELA, and E2F3 knockdown for each of the co-expression clusters
Supplementary Figure 5: Boxplots showing MYC expression and MYC activation according to published gene signatures in function of tumor stage
Supplementary Figure 6: Boxplots showing MYC expression and MYC activation according to published gene signatures in function of the PAM50 subtypes

SUPPLEMENTARY TABLES
Supplementary Table 1: Gene set enrichment analysis to identify hallmark gene sets
Supplementary Table 2: Regression analysis for each MYC-related feature
Supplementary Table 3: Clinical and pathological information of the patients (n=10) from whom the IBC models were derived.

SUPPLEMENTARY DATA
Supplementary Data 1: Differential gene expression data comparing IBC and nIBC models
Supplementary Data 2: Gene set enrichment analysis (GSEA) of the gene module memberships (GMM) scores.
Supplementary Data 3: Connectivity Scores to identify potential modulators of IBC biology as well as potential drug/target combinations for therapy using the CMAP dataset.

GENERAL DISCUSSION

This discussion is partially based on the review 'Deciphering the molecular biology of inflammatory breast cancer through high-throughput profiling technologies.' by Rypens et al. 2023, submitted for publication in International Review of Cell and Molecular Biology (IRCMB).

The IBC signature represents a genuine biomarker and reflects disease biology

In 2013, a signature consisting of 79 genes with an IBC-specific expression pattern was reported [1]. At that time an overall classification accuracy of 71% was observed based on a model using nearest shrunken centroids. In this thesis, we undertook an effort to enhance the original classifier, applied the most optimal model onto an independent validation set, resulting in a test accuracy of 82% with a sensitivity of 75% and a specificity of 86% (McNemar test - P=1.000). Overall, these numbers are well within the range of accuracy values reported for various alternative IBC signatures (i.e. 75%-88%), but all these signatures failed upon external validation [2]. In this thesis, we report to our knowledge, the only expression-based IBC classifier, unbiased by the molecular subtypes, with accuracy levels above 80% in a large independent patient cohort. The fact that the current model with superior accuracy is based on the same gene set as the original classifier, reveals the necessity of investing time and effort in model selection and optimization, in addition to feature selection, for any classification or regression problem at hand.

When the model was applied onto an expression series of preclinical models, an overall acceptable test accuracy of 78% was observed, again indicating that the model is at least partially based on gene expression patterns that reflect genuine (intrinsic) differences in cancer biology of IBC and nIBC cells. However, in this data set, we also observed a marked difference between the sensitivity and the specificity levels (i.e. 100% and 68% respectively; McNemar test - P=0.023), resulting in a limited percentage of accurate IBC calls (i.e. positive predictive value of 59%). More profound analysis of this observation revealed that the subset of classifier genes overexpressed in nIBC tissue samples is also overexpressed in nIBC relative to IBC cell lines. In contrast, the subset of classifier genes overexpressed in IBC tissue samples shows no evidence of differential expression between IBC and nIBC cell lines (data not shown). This result suggests that discrimination of IBC and nIBC cell lines based on the transcriptomic classifier is mainly driven by the nIBC marker genes [3]. Interestingly, in this thesis we have shown that particularly this subset of classifier genes exhibits expression levels that are positively correlated with nuclear SMAD3 protein expression levels [4], suggesting that the cancer cell intrinsic differences of IBC and nIBC cells translate to, amongst others, elevated SMAD3 transcriptional activity.

A possible explanation for the lack of predictive power associated with the IBC marker genes in this analysis relates to differences between IBC and nIBC associated with the tumor (immune) microenvironment [5] that are not recapitulated in the data set of the preclinical models. Indeed, 67% of the IBC marker genes that are part of the IBC-specific transcriptomic signature demonstrate elevated expression in the profiles of immune and endothelial cells of the Human Tissue Compendium relative to those of epithelial cells (data not shown). This conclusion is further corroborated by a direct comparison of the gene expression profiles of the UA-IBC-01 cell line and the primary tumor sample it is obtained from. Although expression differences are limited and cancer cell intrinsic expression themes appear to be preserved in the preclinical model, enrichment of gene sets associated with immune response programs in the primary tumor sample were noted [3]. However, it should also be noted that many of the IBC marker genes are strongly anti-correlated with nuclear SMAD3 protein expression [4], which we consider reflecting cancer cell intrinsic differences between IBC and nIBC cells (vide supra). This implies either that the nature of the IBC marker genes may not be completely stromal, which was shown using immunohistochemical assessment of MARCKS protein expression in IBC [6], or that the IBC marker genes are reflective of crosstalk between stroma and IBC cells resulting in or originating from the suppressed SMAD3 transcriptional activity in the latter. A more profound understanding of these mechanisms will require a detailed analysis of the molecular profiles and cell states of various cell populations in IBC at individual level using single cell technologies.

IBC preclinical models are useful to study IBC biology

Part of this thesis aimed at the molecular characterization of the available IBC cell lines and to determine to what extent these preclinical models reflect genuine IBC biology. Based on our results, all IBC cell lines adhere to the basal-like subtype and the majority adhered to the luminal progenitor phenotype, which agrees with the fact that all IBC cell lines are ER- negative and demonstrates that the degree of molecular heterogeneity in the present series of IBC preclinical models is restricted as compared to the nIBC cell lines in which all subtypes and differentiation states are represented. Similar conclusions could be drawn when evaluating the distribution of the PAM50 subtypes, with 8/10 IBC cell lines being either basal-like or HER2-enriched. These results can be explained by the dominance of the basal-like and HER2-enriched subtypes in IBC tissue samples. However, they also clearly reveal the paucity in ER+, luminal-type preclinical IBC models despite the fact these subtypes account for roughly 30–40% of the patient samples. Therefore, development of ER+ luminal-type preclinical IBC models should be high on the agenda of the IBC research community, particularly as we have shown in this thesis that some features, such as MYC transcriptional activity, show ER dependency in IBC. In this context, the use of estrogen supplementation

should be carefully considered, as we have documented a modest decrease in gene expression of estrogen response genes in the UA-IBC-01 cell line relative to its corresponding primary tissue sample, suggesting that estrogen supplementation may have detrimental or unwanted effects of the ER signaling pathway. Along the same lines, also the incorporation of immune features in the development of IBC preclinical models should be considered, for example using patient-derived organoids co-cultured with autologous immune cells.

When applying the expression-based IBC classifier onto the IBC preclinical models, we noted a limited positive predictive value, indicating that not all cell lines fully represent the clinical disease but only limited aspects of it (as discussed above). In addition, we observed that for some preclinical models, notably SUM149, SUM190, and MDA-IBC-3, low posterior probability scores (i.e. close to 0.5) were repeatedly observed across five replicates, whereas for the other cell lines posterior probability scores are more homogeneously elevated. This may raise some concerns regarding the utility of SUM149, SUM190 and MDA-IBC-3 as genuine IBC preclinical models. Nevertheless, in this thesis we demonstrate that the currently available preclinical models of IBC recapitulate to some extent the molecular intrinsic features of IBC cells in patient samples. For example, the absence of the mesenchymal subtype in the panel of IBC cell lines despite the metastatic potential associated with the disease, is noteworthy and agrees with the reported overexpression of E-Cadherin in IBC cells and thus their presumed epithelial phenotype. Therefore, we argue that the present panel of IBC cell lines constitute valuable research tools, provided that their limitations (e.g. lack of hormone receptor positive models) are adequately addressed in the experimental design by using subtype-matched comparisons as exemplified in the experiments studying the effect of TGFβ1 treatment on gene expression and kinase activation in IBC and nIBC cells reported in this thesis [4, unpublished data – Chapter 2: PamGene].

The molecular profiles suggest that IBC is a MYC-addicted tumor

Within the scope of this thesis, a common theme that emerged across all research chapters relates to the involvement of the MYC oncogene in IBC biology, both in patient samples and in cell lines. In a panel of 10 IBC preclinical models, specific co-expression modules associated with MYC transcriptional activity were identified. More importantly, particularly these co-expression modules were poorly conserved in nIBC preclinical models, suggesting that they represent intrinsic IBC biology. These observations corroborate earlier work of Zhang et al. who demonstrated that MYC is a central hub in the signal transduction networks of SUM149 and SUM190 [7]. In patient samples, Faldoni and colleagues recently revealed MYC nuclear protein expression in 100% of 18 tissue samples from patients with IBC across all molecular subtypes [8]. This

thesis shows that levels of MYC transcriptional activity, measured using three different MYC activation gene sets, are invariably elevated in IBC across various strata of ER expression. This condition is unique to IBC, as an ER-dependent decrease of MYC transcriptional activity was clearly seen in nIBC in various data sets (i.e. METABRIC, TCGA, IBC-IC). These observations are in line with earlier results showing that MYC is a common denominator of biological processes active in ER-positive IBC and may provide an explanation for the hormone therapy resistance phenotype often associated with IBC [9].

To mechanistically explain the elevated levels of MYC activity in IBC, this thesis offers various important insights. First, the analysis of genomic alterations revealed that MYC was the third most frequently altered gene with single nucleotide variants, an indel or amplifications detected in 27% of 101 IBC samples [10]. Of the single nucleotide variants, at least one was predicted to be probably damaging, whereby protein function is affected (Ensemble Variant effect predictor, VarSome Clinical). Also the abundance of MYC amplifications indicate a selective advantage during cell growth. Similar studies looking into the genomic profiles of IBC reported variable alteration rates of MYC ranging from 6-100%, with one study revealing that MYC amplifications and protein overexpression coincide [8]. To formally test the hypothesis that amplification involving the MYC gene are more frequent in IBC as compared to nIBC, a meta-analysis of published data was performed, which demonstrates that the frequency of MYC genomic alterations in primary IBC is 23% (95% CI: 13–33%) vs. 30% (95% CI: 24–37%) in a subtype matched nIBC cohort consisting of METABRIC and TCGA samples. In metastatic IBC, MYC genomic alterations were observed in 25% of the cases (95% CI: 12-38%). These data reveal that MYC genomic alterations are not specifically enriched in IBC.

Given these data, other mechanisms of MYC activation in IBC will be operational. One alternative process was identified when the transcriptional responses of IBC and nIBC cells to TGFβ1 treatment were compared and overexpression of MYC target genes in IBC cells was noted [4]. Since SMAD proteins that operate in the TGFβ signal transduction pathway are antagonists of MYC mRNA expression and transcriptional activity, these observations indicate that MYC is efficiently suppressed in nIBC cells. On the other hand, these results also imply that TGFβ signaling fails to establish similar effects in IBC cells, suggesting that IBC cells are inherently TGFβ resistant. This process has already been described in several epithelial cancers (e.g. ovarian cancer, esophageal cancer) and is associated with the inability to decrease MYC transcription [11, 12]. Further investigations demonstrated that TGFβ-dependent repression of MYC mRNA expression requires degradation of the SKIL (SnoN) or SKI oncoproteins that can

inhibit TGFβ signaling, amongst others by sequestration of SMAD proteins outside the nucleus [13].

A second candidate MYC activation mechanism was identified through weighted gene co-expression network analysis of IBC cell lines that revealed that expression of MYC and NFκB target genes are jointly regulated, suggesting an intricate relationship between both transcription factors in shaping IBC biology. NFκB activation in IBC has been reported previously by us and others [1, 14-16], and NFκB has been shown to cooperate with MYC in breast cancer development and progression by inducing cancer stem cell behavior, amongst others by regulating MYC transcription [17-19]. Importantly, the family of NFκB transcription factors orchestrate cellular responses to pro-inflammatory cues, which suggests that MYC hyperactivation in IBC could be secondary to the inflammatory signals received from the micro-environment.

Within the scope of this thesis, NOTCH signaling emerged as a third candidate pathway that is possibly implicated in the activation of MYC in IBC. Genomic alterations in the NOTCH pathway were almost two-fold enriched in IBC, across all subtypes and tumor stages. Amongst all NOTCH genes, NOTCH1 was most frequently altered in IBC, and both NOTCH2 and NOTCH4 were more frequently altered in IBC compared with nIBC, which corroborates earlier results [20]. Amongst the identified single nucleotide variants, several gain of function or activating mutations were predicted (Ensemble Variant effect predictor, VarSome Clinical). At the pathway level, mutual exclusivity for NOTCH2, NOTCH4, and CREBBP alterations was observed in IBC, which supports a role for the NOTCH pathway in IBC biology. In line with this, a NOTCH pathway activation score [21] is significantly higher in IBC as compared to nIBC, again across all subtypes and tumor stages. Notably, this score is also significantly correlated with scores representing MYC transcriptional activity (unpublished data), suggesting that MYC and NOTCH signaling are entwined. Moreover, the NOTCH transcription factor HEY2 can suppress TGFβ signaling by interfering with SMAD3/4 transcriptional activity [22], thereby providing a point of interaction between TGFβ, MYC and NOTCH signaling with mechanistical implications for IBC cell dissemination as tumor emboli (vide infra). From this perspective, the lymphovascular emboli of the transplantable IBC xenograft MARY-X exhibit an interesting NOTCH3 addiction that is associated with overexpression of MYC mRNA [23]. Also, MYC expression levels have been associated with reduced distant metastasis-free survival in patients with ER positive IBC [24].

In addition to NOTCH, this thesis also indicates that additional pathways implicated in developmental biology could be involved in MYC activation. Some of the co-expression modules associated with MYC target gene expression are additionally related to WNT or Hedgehog signaling, and many of the upstream regulators of these co-expression

clusters, identified through Connectivity Map analysis, are also involved in these pathways (i.e., BAMBI, E2F6, HOXB13, and WWTR1/TAZ) or in plain stem cell biology (i.e., CDX2, HOXA9, KLF6, and POU5F1). In the past, a SNP (rs6983267) located at 8q24 close to the MYC locus, that is known to exhibit enhanced binding properties for the WNT effector TCF4 and that can be directed to the MYC locus through chromatin loops allowing for WNT/ TCF4-dependent MYC expression was reported by Bertucci and colleagues to be associated with metastatic risk in IBC [25]. Also of interest is the observation that in a small subset of IBC patient samples, the activation of the MYC pathway was apparently associated with NMYC or MXD3, which have been shown to jointly regulate cell proliferation in cerebellar granule neuron precursors, downstream of Hedgehog signaling.

Finally, constitutive MYC activation could offer an intriguing explanation for the intrinsic instable nature of the IBC genome, which is exemplified in this thesis by the increased frequency of genomic alterations in DNA repair genes in IBC relative to nIBC, and by the fact that IBC samples are 2.27-fold more likely to exhibit increased homologous recombination deficiency scores. These data are corroborated by Faldoni and colleagues, who reported features of genomic instability in about half of their evaluated IBC patient cohort [8]. In these series, chromothripsis, a single catastrophic event that leads to massive rearrangements with a distinctive cycling pattern of copy number changes, was identified in a staggering 38%-45% across all subtypes. In comparison, in a pan cancer cohort, chromothripsis was only observed in 22.3% of the patients [26]. Bekhouche and colleagues reported a more complex pattern of chromosomal imbalances in IBC indicative of a higher genomic instability [27]. Interestingly, evidence suggests that MYC is an important mediator of genomic instability, chromosome instability and aberrant mitosis and that its deregulated expression results in a mutator phenotype [28-31]. The MYC driven genomic instability may in turn explain the increased hyperinflammatory state in IBC, characterized by increased expression of interferon signaling and immune checkpoint genes (e.g. PD-L1) and elevated tumor inflammation scores [1, 5, 32]. The observation that many of the recurrently mutated genes in IBC reported in this thesis and in other cohorts [8] are enriched for mediators of interferon and interleukin signaling pathways, suggests that genomic alterations of particularly these genes are responsible for one of the hallmarks of IBC biology.

Altered TGFβ signaling shapes IBC cell dissemination

This thesis provides compelling evidence that the TGFβ signaling pathway in IBC is impaired. Treatment of IBC cells, including both luminal and mesenchymal subtypes, with TGFβ1 did not induce a cell motility response in any of the evaluated cell lines,

whereas cell motility was clearly engaged in a comparable panel of nIBC models. Molecular profiling revealed no differences in gene expression for any of the TGFβ receptor genes and their downstream transcription factors (i.e. SMAD2, SMAD3, and SMAD4) between IBC and nIBC cells in untreated conditions, indicating that the inhibited motility of IBC cells cannot be attributed to differential expression of core TGFβ signaling genes. A time-course experiment shows that TGFβ1 induces overexpression SMAD3 target genes in nIBC cells but not in IBC cells (*vide supra*), suggesting that the mechanism of TGFβ1-induced SMAD3 transcriptional activity is altered in IBC cells. In line with this, nuclear protein expression of SMAD3 is nearly absent in tissue sections from patients with IBC, in a molecular subtype independent manner, and comparative analysis of protein and gene expression data reveals that a substantial number of the 79 IBC signature genes show nuclear SMAD3 dependent variation in gene expression. Finally, nuclear protein staining intensity of SMAD3 was never higher in cancer cells residing in tumor emboli as compared to those in the primary tumor of the same patients, suggesting a mechanistic link with cancer cell dissemination in IBC. In line with this, AMPK signaling was brought upfront as a potential candidate pathway explaining the blunted TGF-β response in IBC cells by inhibition of TGFβ signaling and SMAD2/3 activation secondary to MYC-induced DNA damage, supposably by crosstalk with the Hippo signal transduction machinery (unpublished data – Chapter 2: PamGene).

In addition to SMAD3, multivariate analysis showed that attenuated nuclear expression of SMAD4 is also associated with the IBC phenotype. In-depth analysis demonstrated that SMAD4 nuclear expression was particularly low in a small fraction of IBC cases with elevated nuclear SMAD3 expression. In addition, SMAD4 staining intensity was further diminished in cancer cells residing in tumor emboli and particularly in some patients where differences in staining intensity for SMAD3 between cancer cells in the primary tumor and tumor emboli were not observed. These observations suggest that SMAD3 and SMAD4 expression is mutually exclusive and reduction of nuclear SMAD4 is an alternative path to curtail the TGFβ response in IBC cells.

The emerging role of abrogated SMAD transcriptional activity in IBC biology provides a potential model for the disseminative and metastatic characteristics of IBC cells. In 2009, Giampieri and colleagues reported that TGFβ signaling switches the mode of cancer cell migration from collective to single cell phenotype through a transcriptional program involving SMAD4 and that transient TGFβ signaling is essential for blood-borne metastasis [33]. These results were corroborated by Matise and colleagues, who additionally demonstrated that TGFβ-induced single cell motility involves the regulation of epithelial to mesenchymal transition (EMT) [34]. Using genetically modified mammary epithelial cell cultures, Kohn and colleagues revealed that the

regulation of EMT through TGFβ signaling depends on expression of SMAD3 but not SMAD2, confirming earlier observations in keratinocyte cultures [35]. In a separate analysis, Kohn and colleagues investigated SMAD3 gene dosage effects on cell biology using mammary epithelial cells and revealed that a 50% reduction of SMAD3 expression (i.e., SMAD3+/- genotype) abrogated the cell motility response but enhanced the invasion response [36]. This attenuated cell motility response observed in conjunction with loss of SMAD3 expression is consistent with the reduced cell motility-inducing capacity of TGFβ1 observed in IBC cells.

These observations made by Kohn and colleagues on the SMAD3 gene dosage effects were attested to a process coined partial EMT in which cells acquire some molecular changes associated with EMT but not the classical morphological changes. Unfortunately, solid scientific evidence for partial EMT was missing at that time. More recently, Pastushenko and colleagues investigated various stages associated with EMT, including hybrid ones, confirming the existence of partial EMT as well as the role of SMAD proteins particularly in the later, mesenchymal, phase of the process [37]. In addition, Luond and colleagues demonstrated that partial EMT indeed promotes collective invasion and is required for metastasis formation [38]. Therefore, the data presented in this thesis suggest that IBC cells are characterized by partial EMT and collective invasion by means of their reduced SMAD3 expression. Furthermore, partial EMT also explains the ubiquitous but counterintuitive presence of E-cadherin in IBC. Interestingly, Padmanaban and colleagues demonstrated that E-cadherin is required for metastasis in multiple models of breast cancer, and that loss of E-cadherin is associated with upregulation of nuclear SMAD protein expression, reduced seeding of cancer cells in distant organs and metastasis outgrowth as well as reduced number or circulating tumor cells [39]. Along the same lines, Hapach and colleagues demonstrated that weakly migrating breast cancer cells exhibit an epithelial phenotype with overexpression of E-cadherin and enhanced metastatic potential [40]. In addition, the weakly migrating breast cancer cells were present in the circulation as circulating tumor cell clusters, suggestive of collective invasion. Indeed, further molecular analyses indicated that the weakly migrating breast cancer cells exhibited elevated expression of cell-cell adhesion molecules. Notably, Giampieri and colleagues also investigated intravasation in lymph vessels and showed that collectively invading cancer cells favor lymphatic over hematogenous dissemination, which provides a persuasive working hypothesis to explain the presence of the characteristic tumor emboli in IBC through collectively invading and E-cadherin-positive cancer cells clusters disseminating via the lymphatic system [33].

Novel insights into therapeutic options for patient management

Within the scope of this thesis, novel evidence is provided towards potential targeted therapies for IBC patient management. By comparing gene co-expression clusters to the L1000 profiles of the CMAP database, sets of potential target/drug combinations were identified. Unfortunately, no single drug with predicted efficacy across all IBC cell lines was revealed, and therefore this study was not informative. In contrast, the study investigating the genomic profiles of IBC demonstrated that actionable genomic alterations are present in virtually all patient samples, indicating that personalized therapy is indeed a rational approach for this aggressive disease. Amongst all genes tested, the CYP2D6 gene encoding the cytochrome P-450 2D6 subunit, exhibits the strongest difference in the number of genomic alterations between IBC and nIBC. The cytochrome P-450 complex oxidizes tamoxifen to its most active metabolite, and mutations in the genes coding for complex members are known to decrease the enzymatic activity. Several data suggest that patients carrying such mutations do not benefit as much from tamoxifen therapy [41]. The large difference in frequency with nIBC may explain the resistance to standard hormone therapy often associated with IBC.

In this thesis, the elevated number of genomic alterations in DNA repair genes (i.e. ATM, ATRX, BARD1, BRCA2, ERCC3, FANCA, FANCB, MSH2, MSH6, PMS2, POLE, and TP53) was also reported, which is in line with earlier observation [10, 20, 42] and has two implications for personalized precision medicine. First, deficiency in homologous recombination supports the ongoing investigation of PARP inhibition in IBC in phase I–II trials with veliparib [43] and olaparib (NCT03598257) [44]. Second, due to the increased number of mutations in mismatch repair genes as well as the elevated level of genomic instability and complexity, also the tumor mutational burden in IBC is increased. This was already reported in earlier studies [10, 20, 45, 46]. In combination with other data documenting overexpression of immune checkpoints in IBC [5, 32], the elevated number of mutations in IBC underscores that the application of immune therapy in IBC should be further investigated [47].

Apart from the therapeutic implications of alterations in DNA repair genes, this thesis also provides evidence that drugs targeting 4 additional pathways could be effective in treatment of IBC patients. First, as discussed above, NOTCH pathway genes are frequently altered in IBC. Interestingly, a preclinical study in IBC showed that a gamma-secretase inhibitor, RO4929097, was able to block the NOTCH signaling and attenuates the stem-like phenotype of IBC cells and regulates the tumor immune microenvironment [48].

Second, actionable genomic alterations in genes associates with response to CDK4/6 inhibitors were found in a 2-fold higher percentage of patients with IBC with frequent copy number changes of CCND1 and CDKN2A. Furthermore, mutations in FAT1 and RB1, potentially associated with resistance to CDK4/6 inhibitors [49], were also frequently observed. Interestingly, an expression based E2F4 activation score, associated with sensitivity to palbociclib [50], was more elevated in samples from patients with IBC as compared to nIBC suggesting that CDK4/6 is indeed more active in IBC. This observation is in line with the identification of many gene co-expression modules that are associated with E2F signaling in the IBC preclinical models [3], suggesting that the current panel of IBC cell lines are an ideal matrix to test CDK4/6 inhibition.

Third, although PIK3CA was the only gene more frequently altered in nIBC samples, many other genes that operate in the PI3K/AKT pathway (AKT1, AKT3, MTOR, PTEN, RPTOR, RICTOR TSC1, and TSC2) exhibit elevated levels of genomic alterations in IBC, suggesting that also patients with IBC will benefit from PI3K/AKT/mTOR inhibition. In addition, also the PIK3CA gene was mutated in substantial fraction of IBC samples, but this likely reflects the presence of luminal type breast cancer samples in our series.

Finally, the percentage HER/EGFR mutations was higher in IBC, particularly due to elevated numbers of ERBB2 amplifications and mutations. These mutations affect either the extracellular domain or the kinase domain, both of which have been associated with sensitivity to ERBB2 tyrosine kinase inhibitors such as neratinib [51]. In addition, also ERBB3 mutations were observed that often co-occurred with ERBB2 amplifications suggesting that alterations of the ERBB3 gene contribute to anti-HER2 therapy resistance. Unfortunately, our series is too small to draw definitive conclusions and this this observation thus requires further investigation.

Future perspectives

In this doctoral thesis, we aimed to gain a more profound understanding what exactly distinguishes the clinicopathologic manifestations of IBC from non-IBC (nIBC) by studying IBC biology at different "omic" levels. Although it is overall clear that the differences between IBC and nIBC are rather limited, we identified some interesting and valuable insights in the biology of IBC. In particular, the observed difference in TGF-β/SMAD3 responses between IBC and nIBC cells and the contribution of potentially involved pathways to the establishment of TGF-β resistance in IBC cells remains a matter of debate and requires further investigation. We also describe some very specific molecular features associated with IBC such as MYC addiction and increased DNA damage, but all of these remain little unambiguous and thus caution is warranted.

What is becoming more evident, is the undisputed role of the tumor immune microenvironment (TIME) and its significant contribution to the unique biological features associated with IBC. Therefore, it is becoming more and more important to understand the interactions between the TIME and IBC tumor cells. To study this, more recent techniques such as single cell/spatial transcriptomics can be off great value. As such, individual cell types such as immune cells and stromal cells could be identified and in addition, where these cells are localized within the TIME. These insights can help us to understand the communication between the TIME and IBC tumor cells, and to unravel what mechanisms are involved in promoting the aggressive intrinsic features of IBC such as the high metastatic potential. One example of an already well-studied cell type in the TME of IBC are tumor-associated macrophages (TAMs). TAMs have been shown to contribute to the aggressive nature of IBC tumor cells and recently, it was reported that macrophages could influence vascular invasion of IBC tumor emboli [52].

Finally, new information that is obtained from single cell transcriptomics can also be used to further optimize preclinical models for IBC. Although we have shown that the current available models for IBC recapitulate to some extent the molecular intrinsic features of IBC cells in patient samples, they lack a stromal component. By identifying the role of specific cell types in the TIME, preclinical models can be significantly improved by co-culturing of tumor cells and stromal and/or immune cells.

References

1. Van Laere SJ, Ueno NT, Finetti P, Vermeulen P, Lucci A, Robertson FM, Marsan M, Iwamoto T, Krishnamurthy S, Masuda H et al: Uncovering the molecular secrets of inflammatory breast cancer biology: an integrated analysis of three distinct affymetrix gene expression datasets. Clin Cancer Res 2013, 19(17):4685-4696.

2. Chakraborty P, George JT, Woodward WA, Levine H, Jolly MK: Gene expression profiles of inflammatory breast cancer reveal high heterogeneity across the epithelial-hybrid-mesenchymal spectrum. Transl Oncol 2021, 14(4):101026.

3. Rypens C, Bertucci F, Finetti P, Robertson F, Fernandez SV, Ueno N, Woodward WA, Van Golen K, Vermeulen P, Dirix L et al: Comparative transcriptional analyses of preclinical models and patient samples reveal MYC and RELA driven expression patterns that define the molecular landscape of IBC. NPJ Breast Cancer 2022, 8(1):12.

4. Rypens C, Marsan M, Van Berckelaer C, Billiet C, Melis K, Lopez SP, van Dam P, Devi GR, Finetti P, Ueno NT et al: Inflammatory breast cancer cells are characterized by abrogated TGFbeta1-dependent cell motility and SMAD3 activity. Breast Cancer Res Treat 2020.

5. Bertucci F, Boudin L, Finetti P, Van Berckelaer C, Van Dam P, Dirix L, Viens P, Goncalves A, Ueno NT, Van Laere S et al: Immune landscape of inflammatory breast cancer suggests vulnerability to immune checkpoint inhibitors. Oncoimmunology 2021, 10(1):1929724.

6. Manai M, Thomassin-Piana J, Gamoudi A, Finetti P, Lopez M, Eghozzi R, Ayadi S, Lamine OB, Manai M, Rahal K et al: MARCKS protein overexpression in inflammatory breast cancer. Oncotarget 2017, 8(4):6246-6257.

7. Zhang EY, Cristofanilli M, Robertson F, Reuben JM, Mu Z, Beavis RC, Im H, Snyder M, Hofree M, Ideker T et al: Genome wide proteomics of ERBB2 and EGFR and other oncogenic pathways in inflammatory breast cancer. J Proteome Res 2013, 12(6):2805-2817.

8. Faldoni FLC, Villacis RAR, Canto LM, Fonseca-Alves CE, Cury SS, Larsen SJ, Aagaard MM, Souza CP, Scapulatempo-Neto C, Osorio C et al: Inflammatory Breast Cancer: Clinical Implications of Genomic Alterations and Mutational Profiling. Cancers (Basel) 2020, 12(10).

9. Iwase T, Harano K, Masuda H, Kida K, Hess KR, Wang Y, Dirix L, Van Laere SJ, Lucci A, Krishnamurthy S et al: Quantitative hormone receptor (HR) expression and gene expression analysis in HR+ inflammatory breast cancer (IBC) vs non-IBC. BMC Cancer 2020, 20(1):430.

10.Bertucci F, Rypens C, Finetti P, Guille A, Adelaide J, Monneur A, Carbuccia N, Garnier S, Dirix P, Goncalves A et al: NOTCH and DNA repair pathways are more frequently targeted by genomic alterations in inflammatory than in non-inflammatory breast cancers. Mol Oncol 2020, 14(3):504-519.

11. Edmiston JS, Yeudall WA, Chung TD, Lebman DA: Inability of transforming growth factor-beta to cause SnoN degradation leads to resistance to transforming growth factor-beta-induced growth arrest in esophageal cancer cells. Cancer Res 2005, 65(11):4782-4788.

12. Baldwin RL, Tran H, Karlan BY: Loss of c-myc repression coincides with ovarian cancer resistance to transforming growth factor beta growth arrest independent of transforming growth factor beta/Smad signaling. Cancer Res 2003, 63(6):1413-1419.

13. Krakowski AR, Laboureau J, Mauviel A, Bissell MJ, Luo K: Cytoplasmic SnoN in normal tissues and nonmalignant cells antagonizes TGF-beta signaling by sequestration of the Smad proteins. Proc Natl Acad Sci U S A 2005, 102(35):12437-12442.

14. Van Laere SJ, Van der Auwera I, Van den Eynden GG, Elst HJ, Weyler J, Harris AL, van Dam P, Van Marck EA, Vermeulen PB, Dirix LY: Nuclear factor-kappaB signature of inflammatory breast cancer by cDNA microarray validated by quantitative real-time reverse transcription-PCR, immunohistochemistry, and nuclear factor-kappaB DNA-binding. Clin Cancer Res 2006, 12(11 Pt 1):3249-3256.

15. Lerebours F, Vacher S, Andrieu C, Espie M, Marty M, Lidereau R, Bieche I: NF-kappa B genes have a major role in inflammatory breast cancer. BMC Cancer 2008, 8:41.

16. El-Shinawi M, Mohamed HT, El-Ghonaimy EA, Tantawy M, Younis A, Schneider RJ, Mohamed MM: Human cytomegalovirus infection enhances NF-kappaB/p65 signaling in inflammatory breast cancer patients. PLoS One 2013, 8(2):e55755.

17. Khan S, Lopez-Dee Z, Kumar R, Ling J: Activation of NFkB is a novel mechanism of pro-survival activity of glucocorticoids in breast cancer cells. Cancer Lett 2013, 337(1):90-95.

18. Yeh PY, Lu YS, Ou DL, Cheng AL: IkappaB kinases increase Myc protein stability and enhance progression of breast cancer cells. Mol Cancer 2011, 10:53.

19. Kim DW, Gazourian L, Quadri SA, Romieu-Mourez R, Sherr DH, Sonenshein GE: The RelA NF-kappaB subunit and the aryl hydrocarbon receptor (AhR) cooperate to transactivate the c-myc promoter in mammary cells. Oncogene 2000, 19(48):5498-5506.

20. Liang X, Vacher S, Boulai A, Bernard V, Baulande S, Bohec M, Bieche I, Lerebours F, Callens C: Targeted next-generation sequencing identifies clinically relevant somatic mutations in a large cohort of inflammatory breast cancer. Breast Cancer Res 2018, 20(1):88.

21. Villanueva A, Alsinet C, Yanger K, Hoshida Y, Zong Y, Toffanin S, Rodriguez-Carunchio L, Sole M, Thung S, Stanger BZ et al: Notch signaling is activated in human hepatocellular carcinoma and induces tumor formation in mice. Gastroenterology 2012, 143(6):1660-1669 e1667.

22. Wang J, Zhu B, Zhang Y, Saiyin H, Wumaier R, Yu L, Sun L, Xiao Q: HEY2 acting as a co-repressor with smad3 and smad4 interferes with the response of TGF-beta in hepatocellular carcinoma. Am J Transl Res 2019, 11(7):4367-4381.

23. Xiao Y, Ye Y, Zou X, Jones S, Yearsley K, Shetuni B, Tellez J, Barsky SH: The lymphovascular embolus of inflammatory breast cancer exhibits a Notch 3 addiction. Oncogene 2011, 30(3):287-300.

24. Iwase T, Harano K, Masuda H, Kida K, Espinosa Fernandez J, Hess KR, Wang Y, Woodward WA, Layman RM, Dirix L et al: Myc as a poor prognostic marker for ER+ inflammatory breast cancer (IBC): Quantitative estrogen receptor (ER) expression analysis and gene expression analysis in ER+ IBC vs non-IBC. Cancer Res 2019, 79(4).

25. Bertucci F, Lagarde A, Ferrari A, Finetti P, Charafe-Jauffret E, Van Laere S, Adelaide J, Viens P, Thomas G, Birnbaum D et al: 8q24 Cancer risk allele associated with major metastatic risk in inflammatory breast cancer. PLoS One 2012, 7(5):e37943.

26. Consortium ITP-CAoWG: Pan-cancer analysis of whole genomes. Nature 2020, 578(7793):82-93.

27. Bekhouche I, Finetti P, Adelaide J, Ferrari A, Tarpin C, Charafe-Jauffret E, Charpin C, Houvenaeghel G, Jacquemier J, Bidaut G et al: High-resolution comparative genomic hybridization of inflammatory breast cancer and identification of candidate genes. PLoS One 2011, 6(2):e16950.

28. Rohrberg J, Van de Mark D, Amouzgar M, Lee JV, Taileb M, Corella A, Kilinc S, Williams J, Jokisch ML, Camarda R et al: MYC Dysregulates Mitosis, Revealing Cancer Vulnerabilities. Cell Rep 2020, 30(10):3368-3382 e3367.

29. Littler S, Sloss O, Geary B, Pierce A, Whetton AD, Taylor SS: Oncogenic MYC amplifies mitotic perturbations. Open Biol 2019, 9(8):190136.

30. Prochownik EV, Li Y: The ever expanding role for c-Myc in promoting genomic instability. Cell Cycle 2007, 6(9):1024-1029.

31. Garcia-Gutierrez L, Delgado MD, Leon J: MYC Oncogene Contributions to Release of Cell Cycle Brakes. Genes (Basel) 2019, 10(3).

32. Van Berckelaer C, Rypens C, van Dam P, Pouillon L, Parizel M, Schats KA, Kockx M, Tjalma WAA, Vermeulen P, van Laere S et al: Infiltrating stromal immune cells in inflammatory breast cancer are associated with an improved outcome and increased PD-L1 expression. Breast Cancer Res 2019, 21(1):28.

33. Giampieri S, Manning C, Hooper S, Jones L, Hill CS, Sahai E: Localized and reversible TGFbeta signalling switches breast cancer cells from cohesive to single cell motility. Nat Cell Biol 2009, 11(11):1287-1296.

34. Matise LA, Palmer TD, Ashby WJ, Nashabi A, Chytil A, Aakre M, Pickup MW, Gorska AE, Zijlstra A, Moses HL: Lack of transforming growth factor-beta signaling promotes collective cancer cell invasion through tumor-stromal crosstalk. Breast Cancer Res 2012, 14(4):R98.

35. Kohn EA, Du Z, Sato M, Van Schyndle CM, Welsh MA, Yang YA, Stuelten CH, Tang B, Ju W, Bottinger EP et al: A novel approach for the generation of genetically modified mammary epithelial cell cultures yields new insights into TGFbeta signaling in the mammary gland. Breast Cancer Res 2010, 12(5):R83.

36. Kohn EA, Yang YA, Du Z, Nagano Y, Van Schyndle CM, Herrmann MA, Heldman M, Chen JQ, Stuelten CH, Flanders KC et al: Biological responses to TGF-beta in the mammary epithelium show a complex dependency on Smad3 gene dosage with important implications for tumor progression. Mol Cancer Res 2012, 10(10):1389-1399.

37. Pastushenko I, Brisebarre A, Sifrim A, Fioramonti M, Revenco T, Boumahdi S, Van Keymeulen A, Brown D, Moers V, Lemaire S et al: Identification of the tumour transition states occurring during EMT. Nature 2018, 556(7702):463-468.

38. Luond F, Sugiyama N, Bill R, Bornes L, Hager C, Tang F, Santacroce N, Beisel C, Ivanek R, Burglin T et al: Distinct contributions of partial and full EMT to breast cancer malignancy. Dev Cell 2021, 56(23):3203-3221 e3211.

39. Padmanaban V, Krol I, Suhail Y, Szczerba BM, Aceto N, Bader JS, Ewald AJ: E-cadherin is required for metastasis in multiple models of breast cancer. Nature 2019, 573(7774):439-444.

40. Hapach LA, Carey SP, Schwager SC, Taufalele PV, Wang W, Mosier JA, Ortiz-Otero N, McArdle TJ, Goldblatt ZE, Lampi MC et al: Phenotypic Heterogeneity and Metastasis of Breast Cancer Cells. Cancer Res 2021, 81(13):3649-3663.

41. Hoskins JM, Carey LA, McLeod HL: CYP2D6 and tamoxifen: DNA matters in breast cancer. Nat Rev Cancer 2009, 9(8):576-586.

42. Ross JS, Ali SM, Wang K, Khaira D, Palma NA, Chmielecki J, Palmer GA, Morosini D, Elvin JA, Fernandez SV et al: Comprehensive genomic profiling of inflammatory breast cancer cases reveals a high frequency of clinically relevant genomic alterations. Breast Cancer Res Treat 2015, 154(1):155-162.

43. Jagsi R, Griffith KA, Bellon JR, Woodward WA, Horton JK, Ho A, Feng FY, Speers C, Overmoyer B, Sabel M et al: Concurrent Veliparib With Chest Wall and Nodal Radiotherapy in Patients With Inflammatory or Locoregionally Recurrent Breast Cancer: The TBCRC 024 Phase I Multicenter Study. J Clin Oncol 2018, 36(13):1317-1322.

44. Michmerhuizen AR, Pesch AM, Moubadder L, Chandler BC, Wilder-Romans K, Cameron M, Olsen E, Thomas DG, Zhang A, Hirsh N et al: PARP1 Inhibition Radiosensitizes Models of Inflammatory Breast Cancer to Ionizing Radiation. Mol Cancer Ther 2019, 18(11):2063-2073.

45. Hamm CA, Moran D, Rao K, Trusk PB, Pry K, Sausen M, Jones S, Velculescu VE, Cristofanilli M, Bacus S: Genomic and Immunological Tumor Profiling Identifies Targetable Pathways and Extensive CD8+/PDL1+ Immune Infiltration in Inflammatory Breast Cancer Tumors. Mol Cancer Ther 2016, 15(7):1746-1756.

46. Matsuda N, Lim B, Wang Y, Krishnamurthy S, Woodward W, Alvarez RH, Lucci A, Valero V, Reuben JM, Meric-Bernstam F et al: Identification of frequent somatic mutations in inflammatory breast cancer. Breast Cancer Res Treat 2017, 163(2):263-272.

47. Bertucci A, Bertucci F, Zemmour C, Lerebours F, Pierga JY, Levy C, Dalenc F, Grenier J, Petit T, Berline M et al: PELICAN-IPC 2015-016/Oncodistinct-003: A Prospective, Multicenter, Open-Label, Randomized, Non-Comparative, Phase II Study of Pembrolizumab in Combination With Neo Adjuvant EC-Paclitaxel Regimen in HER2-Negative Inflammatory Breast Cancer. Front Oncol 2020, 10:575978.

48. Debeb BG, Cohen EN, Boley K, Freiter EM, Li L, Robertson FM, Reuben JM, Cristofanilli M, Buchholz TA, Woodward WA: Pre-clinical studies of Notch signaling inhibitor RO4929097 in inflammatory breast cancer cells. Breast Cancer Res Treat 2012, 134(2):495-510.

49. Li Z, Razavi P, Li Q, Toy W, Liu B, Ping C, Hsieh W, Sanchez-Vega F, Brown DN, Da Cruz Paula AF et al: Loss of the FAT1 Tumor Suppressor Promotes Resistance to CDK4/6 Inhibitors via the Hippo Pathway. Cancer Cell 2018, 34(6):893-905 e898.

50. Guerrero-Zotano AL, Stricker TP, Formisano L, Hutchinson KE, Stover DG, Lee KM, Schwarz LJ, Giltnane JM, Estrada MV, Jansen VM et al: ER(+) Breast Cancers Resistant to Prolonged Neoadjuvant Letrozole Exhibit an E2F4 Transcriptional Program Sensitive to CDK4/6 Inhibitors. Clin Cancer Res 2018, 24(11):2517-2529.

51. Bose R, Kavuri SM, Searleman AC, Shen W, Shen D, Koboldt DC, Monsey J, Goel N, Aronson AB, Li S et al: Activating HER2 mutations in HER2 gene amplification negative breast cancer. Cancer Discov 2013, 3(2):224-237.

52. Gadde M, Mehrabi-Dehdezi M, Debeb BG, Woodward WA, Rylander MN: Influence of Macrophages on Vascular Invasion of Inflammatory Breast Cancer Emboli Measured Using an In Vitro Microfluidic Multi-Cellular Platform. Cancers (Basel) 2023, 15(19).

SUMMARY

Despite breast cancer being the most frequently diagnosed cancer in women worldwide, inflammatory breast cancer (IBC) is rather a rare and less known subtype. Nonetheless, its aggressive development is responsible for a disproportionally high amount of breast cancer-related deaths. For decades, several efforts have been undertaken to better elucidate the mechanisms of IBC aggressiveness and to identify pathways distinct to IBC, however many have failed validation in distinct data series.

To date, it still remains unclear what exactly distinguishes the clinicopathologic manifestations of IBC from non-IBC (nIBC). To that end, we aimed to gain a more profound understanding of IBC biology at different "omic" levels, i.e. transcriptomic, peptidomic and genomic in the three chapters of this doctoral thesis.

In the first chapter, we investigated the role of the TGF-β pathway in IBC, further building on data published by the inflammatory breast cancer international consortium (IBC-IC) showing that a molecular basis of IBC exists and possibly is shaped by an altered TGF-β signaling in IBC. We have demonstrated that IBC cells are characterized by attenuated SMAD3 or SMAD4 protein expression and transcriptional activity impacting the cell motility inducing capacity of TGFβ1. The data described in this paper combined with a substantial body of literature on the subject provides a potential model for the disseminative and metastatic characteristics of IBC cells. To further unravel the signal transduction mechanisms that orchestrate the differential TGF-β response program in IBC and nIBC cells, we also generated peptide phosphorylation profiles of the same preclinical models treated with TGF-β1 and integrated this data with gene expression data. Four candidate mechanisms were discovered including AMPK-, Hippo-, PP5/MAP3K5-signaling as well as chromatin remodeling. The exact contribution of these pathways to the establishment of TGFβ resistance in IBC cells remains a matter of debate and merits further investigation.

The second chapter of this thesis covers a profound investigation of the differences between IBC and nIBC at the genomic level and confirms that IBC is distinct from non-IBC, independently from the molecular subtypes and disease stage. Higher tumor mutational burden and a large set of genes more frequently altered in IBC are reported. Our data particularly supports a role for the NOTCH and DNA repair pathways in IBC biology. Moreover, a high frequency of actionable genomic alterations in IBC samples was revealed, suggesting that precision medicine is a relevant approach for this aggressive disease, notably with drugs targeting DNA repair, NOTCH signaling, and CDK4/6.

In the third and last chapter of this thesis, we have investigated which tumor-intrinsic factors are responsible for the genuine IBC biology by molecularly characterizing all

available IBC preclinical models. We demonstrated that these preclinical models recapitulate to some extent the molecular features of IBC cells in patient samples, and thus constitute valuable research tools despite the lack of ER+ models. Furthermore, an important role of MYC transcriptional activity, seemingly intrinsic to IBC biology, was further explored and revealed notable interactions with ESR1 expression that are contrasting in IBC and nIBC. The data described in this paper, combined with published literature and various insights collected in this thesis suggests that IBC is a MYC-addicted tumor which warrants further investigation.

Taken together, we have reported valuable new insights in the biology of IBC, which in our opinion, offer important new research opportunities in the run towards a more personalized treatment approach for this aggressive disease.

NEDERLANDSTALIGE SAMENVATTING

Studie naar de biologie van het inflammatoire borstcarcinoom door middel van een multi-omics benadering.

Ondanks dat borstkanker wereldwijd de meest gediagnosticeerde kanker is bij vrouwen, is het inflammatoir borstcarcinoom (IBC) eerder een zeldzaam en minder bekend subtype. Desalniettemin is de agressieve ontwikkeling van IBC verantwoordelijk voor een onevenredig hoog aantal aan borstkanker-gerelateerde sterfgevallen. Decennia lang hebben onderzoekers getracht om de onderliggende mechanismen die deze hoge agressiviteit kunnen verklaren te begrijpen en om pathways te identificeren die afwijken in IBC. Vele van deze onderzoeksresultaten konden echter niet gevalideerd worden in onafhankelijke datasets.

Tot op heden is het nog steeds onduidelijk wat de klinisch-pathologische manifestaties van IBC precies onderscheidt van niet-IBC (nIBC). Daarom trachtten we in de drie hoofdstukken van dit proefschrift een beter begrip te krijgen van de biologie van IBC op transcriptomisch, peptidomisch en genomisch niveau.

In het eerste hoofdstuk hebben we de rol van de TGF-β pathway in IBC onderzocht, waarin we verder bouwen op de resultaten van een grootschalige studie gepubliceerd door het Inflammatory Breast Cancer International Consortium (IBC-IC). Deze studie heeft aangetoond dat er een moleculaire basis voor IBC bestaat die mogelijks gevormd wordt door een afwijkende TGF-β pathway in IBC. Wij hebben aangetoond dat IBC cellen, na behandeling met TGFβ1, gekenmerkt worden door een verminderde SMAD3 of SMAD4 eiwitexpressie en transcriptionele activiteit in vergelijking met nIBC cellen. Deze lagere activiteit bleek dan vervolgens een invloed te hebben op het vermogen van TGFβ1 om celmotiliteit te induceren. De resultaten die in dit artikel worden beschreven, gecombineerd met een aanzienlijke hoeveelheid literatuur over dit onderwerp, bieden een potentieel model voor het verklaren van de metastatische kenmerken die heel eigen zijn aan IBC cellen. Om de signaaltransductiemechanismen die onderliggend zijn aan het verschil in reactie op TGFβ1-behandeling in IBC en nIBC verder te kunnen verklaren, hebben we met behulp van peptidefosforylering (PamGene) profielen gegenereerd van dezelfde preklinische modellen na behandeling met TGF-β1 en deze gegevens vervolgens geïntegreerd met de eerder verworven genexpressiegegevens. Hierbij werden vier kandidaat mechanismen ontdekt en voorgesteld die mogelijks een verklaring kunnen bieden, namelijk de AMPK-, Hippo- en PP5/MAP3K5-signaaltransductie pathways en chromatine remodeling. De exacte bijdrage van deze pathways aan TGFβ-resistentie in IBC cellen blijft een punt van discussie en verdient nader onderzoek.

Het tweede hoofdstuk van dit proefschrift behandelt een diepgaand onderzoek naar de verschillen tussen IBC en nIBC op genomisch niveau en bevestigt dat IBC verschilt van niet-IBC, onafhankelijk van de moleculaire subtypes en het ziektestadium. Wij rapporteren hier een hoge tumor mutational burden en een grote genenset die frequent gemuteerd zijn in IBC. Onze data ondersteunen in het bijzonder een rol voor de NOTCH- en DNA herstel pathways in de biologie van IBC. Bovendien hebben we ook aangetoond dat er frequent genomische veranderingen in IBC voorkomen die in aanmerking komen voor precisiegeneeskunde, met name voor medicijnen gericht op DNA-herstel, NOTCH-signalering en CDK4/6.

In het derde en laatste hoofdstuk van dit proefschrift zijn we verder gaan onderzoeken welke tumor-intrinsieke factoren mede verantwoordelijk zijn voor de biologie van IBC door het moleculair karakteriseren van alle beschikbare preklinische IBC modellen. Deze studie heeft aangetoond dat de huidige preklinische modellen tot op zekere hoogte de moleculaire kenmerken van IBC cellen in patiëntenstalen recapituleren en dus waardevolle onderzoeksinstrumenten zijn. Bovendien werd een belangrijke rol voor MYC-transcriptionele activiteit in de biologie van IBC blootgelegd en verder onderzocht. Hierbij werden opmerkelijk interacties tussen MYC en ESR1 expressie gerapporteerd die verschillend zijn in IBC en nIBC. De resultaten die in dit hoofdstuk worden beschreven, in combinatie met gepubliceerde literatuur en verschillende inzichten verworven doorheen deze thesis, suggereren dat IBC een tumor is die sterk afhankelijk is van MYC. Een belangrijke observatie die verder onderzoek rechtvaardigt.

Samengevat hebben wij in deze thesis een aantal zeer waardevolle nieuwe inzichten in de biologie van IBC verworven die naar onze mening deuren openen naar belangrijke nieuwe onderzoeksmogelijkheden die zouden kunnen bijdragen aan de ontwikkeling van uiteindelijk een meer gepersonaliseerde behandeling voor deze agressieve ziekte.

ACKNOWLEDGEMENTS

"If I have seen further, it is by standing on the shoulders of giants."

- Isaac Newton

Ik zou graag willen starten met bovenstaande quote van Isaac Newton. Ik heb namelijk de kans gehad om samen te werken met heel veel gepassioneerde mensen en onderzoekers waarvan ik stuk voor stuk ongelofelijk veel heb bijgeleerd. Zonder hen was dit boekje nooit tot stand kunnen komen. In dit laatste hoofdstuk van mijn doctoraatsthesis zou ik dan ook graag iedereen willen bedanken die direct of indirect betrokken is geweest bij dit onderzoek.

Eerst en vooral wil ik mijn dank uiten aan mijn promotoren Prof. Steven Van Laere en Dr. Luc Dirix. Zonder hen zou ik natuurlijk nooit aan een doctoraat zijn kunnen beginnen. Steven, jouw interesse en expertise binnen het IBC onderzoek zijn uiteraard van grootste waarde geweest. Ik wil je heel erg bedanken voor jouw onvoorwaardelijke steun en vooral dat je altijd in ons IBC onderzoek, maar ook vooral in mij bent blijven geloven. Zonder jou had ik hier vandaag ook niet gestaan. Dr. Dirix, jouw ongelofelijke kennis binnen het kankeronderzoek, maar ook ver daarbuiten is een inspiratie voor velen. Uw feedback is me dan ook altijd van veel waarde geweest en ik heb heel veel van u geleerd tijdens mijn jaren in het TCRU.

Hierna wil ik heel graag de leden van de jury, Prof. Dr. Bart Loeys, Prof. Dr. Wim Vanden Berghe, Prof. Dr. Carolien Schröder en Prof. Dr. Fedor Berditchevski bedanken die allen tijd hebben vrijgemaakt om deze thesis met veel aandacht te lezen en te bevragen.

En dan wil ik graag een aantal mensen bedanken waar ik dag in dag uit mee hebt samengewerkt. Melike, jij was mijn mentor toen ik in het TCRU startte met mijn masterthesis en nadien toen ik verder ging als doctorandus. Jij bent mee verantwoordelijk voor een deel van de resultaten van deze thesis en zodus ook de start van het verdere onderzoek. Heel erg bedankt dat je mij destijds mee op pad hebt genomen en voor alles wat je me hebt geleerd. Ik zou nooit zo'n goeie en gedreven celcultuur persoon geworden zijn zonder jou! Mijn bijzonder grote dank gaat uit naar onze 'PhDrinking groep'. Bram, Anja, PJ, Steffi en Christophe, jullie zijn goud! Onvergetelijke herinneringen, de leukste feestjes, etentjes enz. Ik heb jullie nooit echt gezien als collega's, maar als vrienden die me altijd door dik en dun gesteund hebben in eender wat! Ik ben jullie zo ontzettend dankbaar en ik hoop, ondanks onze drukke agenda's en uiteenlopende levens, dat we toch af en toe kunnen blijven afspreken om even terug te gaan naar de tijd dat ik jullie meer zag dan mijn eigen man... :) Steffi, wij hebben lief en leed gedeeld in het TCRU, geen geheimen, uren gebabbel, veel gelachen en samen geweend. Ik hoop dat je weet dat je altijd een speciaal plekje zal hebben in mijn hart.

CURRICULUM VITAE

PERSONAL DETAILS

Name: Rypens Charlotte
Date of birth: 11-DEC-1992
E-mail: rypens.charlotte@hotmail.com

EDUCATION AND ACADEMIC CAREER

2004-2010	Modern languages – Mathematics (option: Sciences) – Heilig Hart Instituut Kalmthout
2010-2013	Bachelor Biomedical Sciences - University of Antwerp
2013-2015	Master Biomedical sciences - University of Antwerp

- Major Molecular and Cellular Science, Minor Research
- Graduated the 30th of June 2015 with the mention: Great distinction

Masterthesis: 'The role of TLR4 in inflammatory breast cancer'

Translational Cancer Research Unit – GZA Hospitals
Centre for Oncological Research (CORE) – University of Antwerp
Promotors: Prof. Steven Van Laere, Dr. Luc Dirix
Supervisor: Drs. Melike Marsan, MSc.

2016-2020	PhD in Medical Science – University of Antwerp

"Unraveling the biology of inflammatory breast cancer through multi-omics approaches."

Translational Cancer Research Unit – GZA Hospitals
Centre for Oncological Research (CORE) – University of Antwerp
Promotors: Prof. Steven Van Laere, Dr. Luc Dirix

ADDITIONAL ACADEMIC TRAINING

FELASA Type C Certificate
Writing Academic Papers
Leadership And Teamwork

GRANTS

2017   Research Grant: Emmanuel Van der Schueren (Flemish Liga against Cancer)

PUBLICATIONS

Arora, J., Sauer, S.J., Tarpley, M., Vermeulen, P., **Rypens, C.**, Van Laere, S., et al. Inflammatory breast cancer tumor emboli express high levels of anti-apoptotic proteins: use of a quantitative high content and high-throughput 3D IBC spheroid assay to identify targeting strategies. Oncotarget 8, 25848-25863 (2017).

Van Berckelaer, C., **Rypens, C.**, van Dam, P., Pouillon, L., Parizel, M., Schats, K.A., et al. Infiltrating stromal immune cells in inflammatory breast cancer are associated with an improved outcome and increased PD-L1 expression. Breast Cancer Res 21, 28 (2019).

Bertucci, F., **Rypens, C.**, Finetti, P., Guille, A., Adelaide, J., Monneur, A., et al. NOTCH and DNA repair pathways are more frequently targeted by genomic alterations in inflammatory than in non-inflammatory breast cancers. Mol Oncol (2019).

Rypens, C., Marsan, M., Van Berckelaer, C., Billiet, C., Melis, K., Lopez, S.P., et al. Inflammatory breast cancer cells are characterized by abrogated TGFbeta1-dependent cell motility and SMAD3 activity. Breast Cancer Res Treat (2020).

Van Berckelaer C, Van Geyt M, Linders S, **Rypens C**, Trinh XB, Tjalma WAA et al. A high neutrophil-lymphocyte ratio and platelet-lymphocyte ratio are associated with a worse outcome in inflammatory breast cancer. Breast (2020).

Van Berckelaer C, Vermeiren I, Vercauteren L, **Rypens C**, Oner G, Trinh XB, et al. The Evolution and Prognostic Role of Tumour-Infiltrating Lymphocytes and Peripheral Blood-Based Biomarkers in Inflammatory Breast Cancer Patients Treated with Neoadjuvant Chemotherapy. Cancers (Basel) (2021).

Rypens C, Bertucci F, Finetti P, Robertson F, Fernandez SV, Ueno N, et al. Comparative transcriptional analyses of preclinical models and patient samples reveal MYC and RELA driven expression patterns that define the molecular landscape of IBC. NPJ Breast Cancer (2022).

ORAL PRESENTATIONS

2016   Speaker at The **Belgian Society of Medical Oncology (BSMO)**, Brussels, Belgium
2016   Invited speaker at MIPRO meeting (Department), Antwerp, Belgium
2018   Invited speaker at the **6th International Inflammatory Breast Cancer Symposium,** Madrid, Spain

2019   Invited speaker at the Phosphopeptide Kinome profiling Pamchip-platform Hercules User Meeting, Wilrijk, Belgium.

POSTER PRESENTATIONS

2015   Poster presentation at the **Belgian Association for Cancer Research (BACR)** conference, Belgium. Rypens C, Marsan M, Vermeulen P, Dirix L and Van Laere S. The role of Toll like receptors in inflammatory breast cancer.

2016   Poster presentation at the **Belgian Association for Cancer Research (BACR)** conference, Belgium. Charlotte Rypens, Hanna Nyström, Sara Perez Lopez, Luc Dirix and Steven Van Laere. The use of a new organotypic model to study differences in invasion patterns between IBC and nIBC cell lines.

2017   Poster presentation at the **Belgian Association for Cancer Research (BACR)** conference, Belgium. Charlotte Rypens, Melike Marsan, Patrick Neven, Luc Dirix and Steven Van Laere. Inflammatory breast cancer cells have a specific SMAD3-independent transcriptional program associated with MYC overexpression after TGF-β exposure.

2018   Poster presentation at the **Belgian Association for Cancer Research (BACR)** conference, Belgium. Rypens C, Van Berckelaer C, Van Goethem A, Mercier C, Erven K, De Pooter C, van Dam P, Vermeulen P, Dirix L, Van Laere S. Analysis of inflammatory breast cancer gene expression to identify specific tumor- and stroma-related expression changes.
Poster presentation at the **San Antonio Breast Cancer Symposium (SABCS)**, SA, Texas, USA. Charlotte Rypens, Christophe Van Berckelaer, Charlotte Biliet, Jan Hauspy, François Bertucci, Gayathri Devi, Peter Vermeulen, Luc Dirix, Steven Van Laere. Inflammatory breast cancer cells are characterized by attenuated SMAD dependent TGFβ signaling leading to impaired cell motility responses.

2019   Poster presentation at **ESMO Breast Cancer Congress**, Berlin. Charlotte Rypens, Christophe Van Berckelaer, Charlotte Biliet, Jan Hauspy, François Bertucci, Peter Vermeulen, Luc Dirix, Steven Van Laere. Inflammatory breast cancer cells are characterized by abrogated TGFβ1-dependent cell motility and SMAD3 activity.
Poster presentation at the **San Antonio Breast Cancer Symposium (SABCS)**, SA, Texas, USA. C. Rypens, F. Bertucci, P. Viens, J. W. M. Martens, M. Smid, C. Schröder, N. T. Ueno, M. Cristofanilli, P. Dirix, P. Vermeulen, L. Dirix, S. Van Laere. Inflammatory breast cancer exhibits amplification and transcriptional activation of MYC in conjunction with NOTCH and TGFβ signaling

"Study towards the role of an altered TGF-β signaling pathway in inflammatory breast cancer" by Kirsten Melis, 3rd Bachelor of Biomedical Laboratory Technology - Karel de Grote-Hogeschool, Hoboken, 2017.
Promotors: Rypens C., Van Laere SJ.

"Clinical, cellular and molecular characterization of leptomeningeal metastasis originating from primary breast cancer. Sensitivity and dynamic range of CellSearchTM based DTC enumeration in the CSF in patients with leptomeningeal metastasis" by Alice Van Goethem.
Promotor: Dr. Luc Dirix en Prof. Dr. Pol Specenier.
Co-promotor: Charlotte Rypens en Prof. Steven Van Laere.